The Interactions of Silanes with Nucleophiles

Thesis

THE INTERACTIONS OF SILANES AND NUCLEOPHILES

A Thesis presented for the degree of Doctor of Philosophy

by Timothy Stout.

Department of Chemistry,
Open University.

November, 1984.

Date of submission: November 1984
Date of award: 21 January 1985

ProQuest LLC
789 East Eisenhower Parkway
P.O. Box 1346
Ann Arbor, MI 48106 - 1346

STATEMENT

The work embodied in this thesis was carried out by the author during the period September 1981 to September 1984 in the Chemistry Department of the Open University, under the supervision of Dr. A. R. Bassindale.

Parts of this work have been published in the following papers:-

a) Journal of Organometallic Chemistry, 1982, 238, C41-45

b) Tetrahedron Letters, 1984, Vol. 25, No. 15, 1631-1632

c) Journal of Organometallic Chemistry, 1984, 271, C1-C3

d) J. Chem. Soc., Chemical Communications, 1984, 1387

Signed

November 1984

To my parents

ACKNOWLEDGEMENTS

I would like to thank my supervisor Dr. A. R. Bassindale for his continuous support and encouragement over my three years at the Open University.

I would also like to thank the Open University for financial support.

ABSTRACT

The detailed structural changes resulting from nucleophile-silane interactions are examined, by ^{1}H, ^{13}C and ^{29}Si n.m.r., for a diverse range of nucleophiles (Nu = pyridines, amides, ureas, amines or phosphine oxides) and silanes (R_3SiX, R = H, Me, Et, ^{i}Pr, ^{t}Bu or Ph; X = Cl, Br, I, OSO_2CF_3, ClO_4, imidazolium).

Silylation induces chemical shift changes (^{1}H and ^{13}C) in the nucleophiles that parallel those produced by protonation. Hydrolysis can be ruled out as the cause of these shifts.

In most cases, the dominant species in solution are 1:1 [nucleophile-silane]$^{+}X^{-}$ adducts. These undergo exchange with other nucleophiles and silanes at a rate controlled by the initial attack of the nucleophile or counterion X at a silicon atom in the complex.

The donor strength of each nucleophile, as measured by Beta (Taft), is correlated with the ^{29}Si chemical shift of the [Nu-$SiMe_3$]$^{+}X^{-}$ complex and the relative magnitude of the equilibrium constant for adduct formation, which decreases:-

NMI, DMAP > HMPA > DMI > NMPO, PNO > TPPO > DMPU > 2,4DMP > NMP > DMF > 3,5DMP > DMEU > py > 2,6DMP, quinoline, BIPY and Et_3N.

The lack of evidence for adduct formation at ambient temperature for X=Cl is attributed to a low equilibrium constant. The exothermic nature of these interactions was confirmed by variable temperature n.m.r..

A series of functionalised silyltriflates ($R^1R^2R^3SiOSO_2CF_3$; R=Me, Ph or H) was synthesised and their behaviour with nucleophiles assessed. Novel acyclic, five coordinate $Nu-SiR_3-Nu$ adducts were characterised by ^{29}Si n.m.r. and isolated in some cases. The ability to a given nucleophile for forming five coordinate nucleophile-silane adducts decreases:-

$H_3SiOTf > HMe_2SiX$ (X=OTf > X=Cl); $PhMeHSiOTf >> Ph_3SiX$ (X=I, Br); $Ph_2MeSiBr > Me_3SiX$ (X=Cl, Br, I, OTf, ClO_4); Et_3SiOTf; $^tBuMe_2SiOTf$; $^iPr_3SiOTf$.

The results are consistent with the mechanism of nucleophile assisted solvolysis proposed by Chojnowski, involving rapid pre-equilibrium formation of $[Nu-SiR_3]^+X^-$ adducts followed by slow attack of a second nucleophile.

Contents

Abbreviations

A	acceptor
br	broad
β	Beta (a scale of hydrogen bonding acceptor basicities)
BIPY	2,2-bipyridyl
^{t}Bu	tert-butyl
BTMSIm	N,N'-bistrimethylsilylimidazolium
C	complex
d	doublet
D	donor
DN	Gutmann donor number
DMF	N,N-dimethylformamide
DMI	1,2-dimethylimidazole
2,4DMP	2,4-dimethylpyridine
3,5DMP	3,5-dimethylpyridine
2,6DMP	2,6-dimethylpyridine
DMAP	4-dimethylaminopyridine
DMPU	1,3-dimethyl-3,4,5,6-tetrahydro-2(1H)-pyrimidinone (dimethylpropyleneurea)
DMEU	1,3-dimethyl-2-imidazolidinone (dimethylethyleneurea)
DMSO	dimethylsulphoxide
DMS	dimethylsilyl
DNMR	dynamic nuclear magnetic resonance
γ	gyromagnetic ratio
HMPA	hexamethylphosphoramide (hexamethylphosphoric triamide)
HMDSO	hexamethyldisiloxane
HOMO	Highest Occupied Molecular Orbital
Im	imidazole
J	coupling constant

K	equilibrium constant
k	rate constant
LUMO	Lowest Unoccupied Molecular Obital
Me_4Si	tetramethylsilane
no	not observed
nr	not recorded
NMI	N-methylimidazole (1-methylimidazole)
NMP	1-methyl-2-pyrrolidone (N-methylpyrrolidinone)
NMPO	1-methyl-2-pyridone
Nu	nucleophile
Np	naphthyl
obsc	obscured owing to complex coupling
OTf	trifluoromethanesulphonate (triflate, $CF_3SO_3^-$)
P	perchlorate, ClO_4
py	pyridine
PNO	pyridine N-oxide
q	quartet
qn	quintet
R	alkyl group
s	singlet
sbr	slightly broadened
s.d.	standard deviation
t	triplet
TMS	trimethylsilyl
TMU	1,1,3,3-tetramethylurea
TPPO	triphenylphosphine oxide
TBP	trigonal bipyramidal
TfOH	trifluoromethanesulphonic acid (triflic acid, CF_3SO_3H)
U.V.	ultra violet
vbr	very broad
v	i.r. frequency or chemical shift

CHAPTER 1

INTRODUCTION

1.1 Introduction

Organosilicon reagents are widely used in modern organic chemistry, often in conjunction with nucleophiles[1,2,3].

In many applications, for example the derivatization of amines, amides, alcohols and other functional groups, it is important that the process be both clean and efficient. Similarly, chemists working with minute quantities of material in multistep syntheses require easy, high yielding reactions; silicon reagents can often provide such a facile route, for an otherwise difficult transformation. An extensive array of silicon-based reagents and conditions is already available, but inevitably there is a demand for more effective reagents.

It is essential to have a detailed understanding of the mechanistic processes involved, so that reagents can be tailored to suit specific requirements. At present however the precise mode of action of silylation reagents is not well defined. In particular there appears to be little rationale for the choice of nucleophile to be used in a given reaction. This is not entirely surprising since their role in the silylation mechanism has not been fully resolved. For instance, the information supplied by the manufacturers of silylating agents[4,5] suggests that their products should be used in combination with various nucleophiles such as pyridine (py), triethylamine (Et_3N), 4-dimethylaminopyridine (DMAP), imidazole (Im) and others. Their role is often believed to be simply that of acid scavenger but this assumption has been questioned by Chaudhary and Hernandez[6] who proved that promotion by nucleophiles was not merely a function of basicity, although a base is required in silylation reactions, such as that shown in Scheme 1.1.

$$R_3SiX + R'OH + Nu \rightleftharpoons R_3SiOR' + NuH^+X^-$$

Scheme 1.1

Mechanistic proposals can only be put into perspective when the nature of the species actually present in solution is known. However, at present, the precise nature of these species has not been established conclusively.

Chojnowski[7] isolated and characterised crystalline adducts between trimethylsilyl species TMSX (X=I, Br) and hexamethylphosphoramide (HMPA, hexamethylphosphoric triamide). He proposed an ionic structure [TMS-nucleophile]$^+X^-$ (Figure 1.1) for these adducts and suggested that such species are actively involved in silylation reactions.

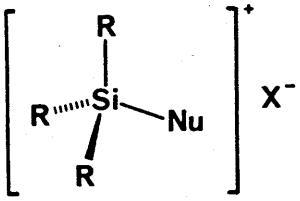

Figure 1.1

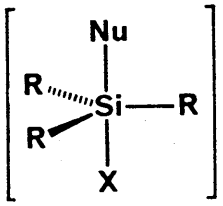

Figure 1.2

Corriu[8] disputed the evidence for ionic species, suggesting that these are just a special case found only for labile Si-X bonds. The mechanism proposed by Corriu also involves nucleophilic activation but it invokes five coordinate (Figure 1.2) rather than four coordinate intermediates. A more detailed discussion on the evidence concerning the various proposals is presented below (Section 1.3).

It is also important to obtain an overall view of the structural and electronic factors controlling the interactions between diverse nucleophiles and silanes. This will enable predictions to be made and hopefully the design of more effective silylation reagents.

The aim of this study is to investigate the relatively neglected aspects of silylation, namely, the structure of nucleophile/silane mixtures. Many of the earlier mechanistic studies[1,9,10,11,12] based their conclusions upon chlorosilanes. The trend in recent years has been towards the use of more efficient and highly electrophilic silylating reagents such as trimethylsilyl trifluoromethanesulphonate[13,14,15] ($Me_3SiOSO_2CF_3$, TMSOTf, TMStriflate), iodotrimethylsilane[16,17] (Me_3SiI, TMSI) and to a lesser extent bromotrimethylsilane[17] (Me_3SiBr, TMSBr). Therefore it is important to determine whether similar mechanisms occur with these species.

This work is divided into two sections. The first part concentrates upon examining the nature of the interactions between a range of nucleophiles and the most commonly used class of silylating agents - the trimethylsilyl derivatives (TMSX, X=Cl, Br, I, OSO_2CF_3 and ClO_4). The relative ability, of each nucleophile, for adduct formation (Scheme 1.2) is assessed together with their kinetic behaviour, and the detailed structural changes in both donor and acceptor are examined.

$$Nu + Me_3SiX \rightleftharpoons [Nu\text{-}SiMe_3]^+X^- \qquad (X=Cl,\ Br,\ I,\ OTf,\ ClO_4)$$

Scheme 1.2

In the second section, a series of functionalised silyl species is synthesised, and a preliminary investigation on the nature of the interactions between these compounds and nucleophiles is carried out.

Multinuclear n.m.r. was chosen as the method of study, since the technique gives easy access to structural as well as dynamic information. In particular silicon-29 n.m.r. is a widely used, very sensitive probe[18,19] giving easy access to otherwise obscure information such as the coordination number of silicon. Furthermore it will be shown that it is also of considerable value for investigating the dynamic processes occurring in nucleophile/silane mixtures. Its use, in conjunction with ^{13}C and ^{1}H n.m.r., provides an extremely powerful tool for studying the intimate structural changes in both donor and acceptor molecules.

1.2 Structure-Reactivity Principles for Silicon

The majority of silicon compounds in use today are carbon functional, thus it is important to understand the interactions between the two elements and to compare their respective chemistries.

Numerous parallels can be drawn between the behaviour of the two elements; nevertheless it is also possible to find significant differences[11]. This dual role is responsible, in part, for the extensive and increasingly popular use of silicon in organic synthesis[3]. A striking example of this difference is the hydrolysis of each element's tetrachloride. Silicon tetrachloride reacts violently with water whilst the carbon analogue is practically inert to hydrolysis. This is not just an isolated example; silicon compounds generally exhibit a higher susceptibility towards nucleophilic attack[11].

The covalent radii of the elements tend to increase, going down each group of the periodic table, owing to the increasing number of electrons. However this trend is not a uniform one; comparison of the covalent radii of the first three Group IV elements shows the size difference between carbon and silicon to be far greater than that between silicon and germanium (C, 77 pm; Si, 117 pm; Ge, 122 pm[20]).

Dewar[21] has suggested, somewhat controversially, that carbon is essentially a small silicon atom. Carbon's relatively inert chemistry (and therefore life itself) results from the unwillingness of this element to expand its coordination shell to accommodate more than four ligands. Thus during nucleophilic substitutions at carbon, the bond to the leaving group must be broken, at least partially, before the nucleophile can enter; a restriction which is not generally observed in silicon chemistry. The reduced steric strain due to the larger size of silicon stabilizes extra-covalent silicon, therefore contributing to reactivity by lowering activation energies.

Extravalent carbon compounds are known from the field of organometallic chemistry[22] but they are not common. Only one compound, resembling the highly energetic S_N2 transition state has so far been isolated[23,24]. In contrast, many hundreds of five or six coordinate silicon species have been proposed, of which many have been fully characterised by X-ray analysis[25]. Their nature, and involvement in reaction mechanisms at silicon will be discussed below.

Explanations of structure-reactivity concepts in organosilicon chemistry have frequently relied upon the inclusion of d-orbitals. This effect, often termed (p-d)π interaction, is shown below for $^{-}CH_2$-$SiMe_3$.

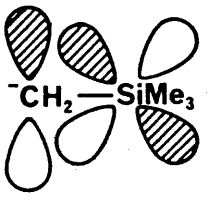

Figure 1.3

Pitt[26,27] showed in the early 1970's, using semiempirical CNDO calculations, that the electronic properties of phenylsilane could be fully explained without reference to d-orbital participation. His hyperconjugation or σ-σ conjugation hypothesis was not new however; Dewar[28] and Traylor[29] have reviewed this subject.

The arguments relating to bonding in silicon compounds will not be analysed in detail here, but Ponec[30] has recently presented a detailed analysis of the theoretical aspects of bonding in these compounds. In this review, he concludes that neither the d-orbital participation hypothesis nor the hyperconjugation model have much physical meaning; in fact he suggests that both should be regarded as simplistic models. However his alternative explanation is not very well defined. He proposes that the higher polarizability of silicon is the decisive factor differentiating the chemistries of carbon and silicon, but no attempt is made at finding a unified orbital description encompassing both elements, which could explain and moreover predict the experimental behaviour of organosilicon compounds.

The participation of d-orbitals in the bonding of silicon to more than four ligands has been questioned by Ebsworth[20], who pointed out that σ orbitals can be used with equal success for rationalising multicentre bonding.

A full description of the bonding in silicon compounds may require detailed quantum mechanical calculations, nonetheless the d-orbital and/or hyperconjugation arguments remain as useful approximations.

Ebsworth has questioned[20] the classical concept of electronegativity but it is nevertheless useful as a qualitative tool for rationalising trends. Silicon is less electronegative than carbon (C, 2.35; Si, 1.64), whichever scale of electronegativity is chosen, which results in polarisation of the $Si^{\delta+}-C^{\delta-}$ bond. Therefore silicon has an enhanced susceptibility towards nucleophilic attack, although other electronic effects such as electron supplying (+I) substituents may offset this effect.

Table 1.1 Bond Strengths of some Silicon Compounds[a]

Bond	Compound	Dissociation energy (kJ mol^{-1})
Si-H	Me_3SiH	376, 325, 343
Si-C	Me_4Si	318, 271, 286
Si-Si	$Me_3SiSiMe_3$	280, 337, 284
Si-N	Me_3SiNMe_2	305-330
Si-O	Me_3SiOMe	530
Si-F	Me_3SiF	590
Si-Cl	Me_3SiCl	380, 426, 410
Si-Br	Me_3SiBr	310-320, 334
Si-I	Me_3SiI	235-245

[a] In most cases, different values of dissociation energy were obtained for the same Si-X bond by various authors, see reference 31.

Another major influence on the reactivity of organosilicon compounds comes from the strength of its bonds to other atoms, which are summarised in Table 1.1[31].

Single bonds between silicon and the electronegative elements - oxygen, chlorine and fluorine are markedly stronger than their carbon counterparts. In fact the Si-F bond is one of the strongest single bonds known. Thermodynamic factors such as these can play a crucial role in determining reaction pathways and are therefore very significant. Despite the considerable strength of these bonds they may be cleaved relatively easily, although Si-F is comparatively inert to hydrolysis. Si-X bonds are always more polarisable than their corresponding C-X bonds[30], thus allowing the attacking species to induce charge separation more easily in the Si-X bond.

1.3 Cations containing Silicon

It is important to distinguish two extremes within this heading, namely, those species in which the positive charge rests on the silicon atom and those in which various substituents bear that charge.

Olah proposed[32] that, by analogy with carbon, all silicon species bearing a positive charge be called silicocations (C^+ equivalents, carbocations). This group is further subdivided into:

i) trivalent (classical) R_3Si^+ - silicenium ions (R_3C^+, carbenium ion)

ii) tetra- or pentacovalent (non-classical) R_4Si^+ or R_5Si^+ are called siliconium ions.

Some confusion is apparent in the literature since Sommer initially

referred to the R_3Si^+ species as a siliconium ion[12]. Olah's terminology will be used throughout this work, as the majority of publication dealing with R_5Si^+ use the term 'siliconium ion'. On the other hand if the charge resides on the ligand, then that species should bear an 'onium' designation, e.g. $[R_3SiN^+R'_3X^-]$ is a silyl ammonium compound.

This distinction is important since in many cases the location of charge is uncertain. The electrical conductivity of a compound in solution is often taken as evidence for the formation of such ionic species[7,33,34]. However great care should be exercised in making deductions from such studies, since even a weakly coordinating solvent such as acetonitrile may assist in the dissociation of an otherwise non-ionic species [refer to Section 1.6(c)]. Furthermore, the possibility of acidic impurities generated by hydrolysis is a major problem for certain classes of compounds. These difficulties can normally be overcome by using confirmatory spectroscopic evidence such as silicon-29 n.m.r. (see Section 1.5).

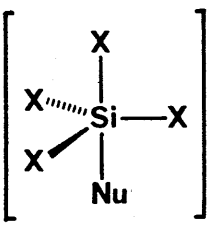

(a) Five coordinate trigonal bipyramidal

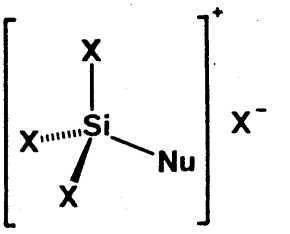

(b) Four coordinate ionic tetrahedral

Figure 1.4

Many adducts have been isolated between nucleophiles and silanes, but a significant proportion of these may have been assigned an incorrect structure. Confusion about the coordination number can easily result, even for a compound of known molecular composition, for instance a number of structures can be conceived for an X_4SiNu complex (Figure 1.4).

Similarly X_4SiNu_2 species can exist in at least three different geometries.

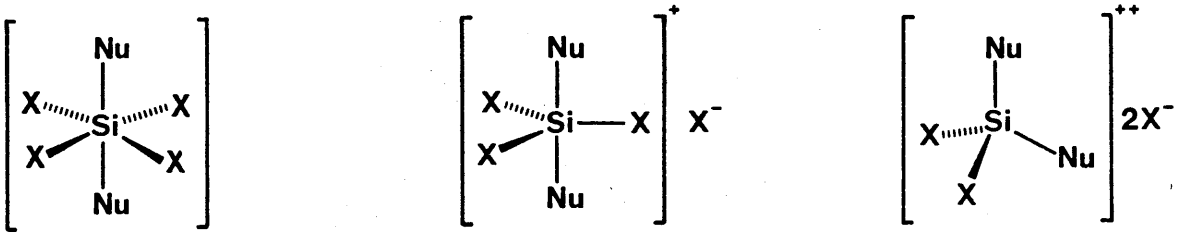

(a) octahedral (b) trigonal bipyramidal ionic (c) tetrahedral ionic

Figure 1.5

Species such as $[R_3SiNu]^+ X^-$ have been postulated for a wide variety of nucleophile-silane combinations. MacDiarmid has presented an interesting discussion on this subject[33].

Chojnowski isolated and characterised 1:1 adducts between TMSX (X=I, Br) and HMPA[7] (Figure 1.6). Very similar ^{31}P n.m.r. chemical shifts were recorded, irrespective of counterion, suggesting that the Si-X bond had been broken to form an ionic complex. In addition Chojnowski analysed the conductiometric behaviour of TMSX (X=Cl, Br, I) mixtures with HMPA. The

moderately high conductivity observed for the bromo- and iodo-silane/HMPA mixtures was attributed to the formation of 1:1 ionic adducts, whilst the low conductivity found for similar chlorosilane/HMPA mixtures was interpreted in terms of a low equilibrium concentration of the [HMPA-TMS]$^{+}Cl^{-}$ adduct.

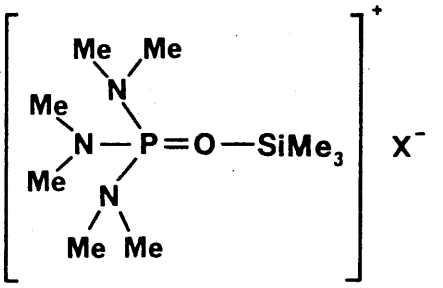

Figure 1.6

These findings were subsequently disputed by Corriu[8] who stated that the conductivity of mixtures of DMF or HMPA with TMSBr or TMSCl in CH_2Cl_2 was below that of HBr or HCl respectively, therefore implying that the observed behaviour was caused by hydrolysis. This explanation could also account for the similarity between the chemical shifts of the bromo- and iodo-silane-HMPA complexes in the ^{31}P n.m.r. i.e. that $[(Me_2N)_3P=O^{+}H]\ X^{-}$ was being formed.

Barton and Tully could not distinguish between a four coordinate ionic and a five coordinate structure for their Me_3SiClO_4-pyridine adduct on the basis of proton n.m.r. studies[35].

The argument concerning the solid state structure of Nu-TMSX complexes was resolved recently by Hensen et al.[36] who demonstrated, using X-ray analysis, that the pyridine-TMSX adducts (X=I, Br) were four coordinate ionic species with no Si-X bonds. The structure in solution remains the subject of some controversy.

1.4 Five and Six Coordinate Silicon

Silicon's ability to form extracoordinate compounds is far greater than that of carbon. This is illustrated by the large number of penta- and hexacovalent silicon complexes identified[25,37], compared to the few proposed in carbon chemistry[22].

A large proportion of these silicon species have been prepared by coordination of an aliphatic or heterocyclic amine, nitrile or other nitrogen containing species to neutral tetravalent silicon. Both monodentate and chelating ligands are common for nitrogen donor species, but there does not appear to be any preference for chelating species, in contrast to the situation concerning oxygen donor ligands. The majority of complexes, involving oxygen bound to silicon, require at least one chelating ligand to confer stability. Most hypervalent silicon compounds contain one or more electronegative ligands such as F, Cl, Br, O or N.

A selection of five coordinate silicon adducts that have been characterised by X-ray crystallography are presented in Figure 1.7[25] (see also Table 1.2).

The predominant stereochemistry for five coordinate silicon is trigonal bipyramidal (TBP), although Holmes has recently demonstrated[25] the presence of a complete series of five coordinate structures intermediate between TBP and square pyramidal. An interesting feature of trigonal bipyramidal molecules is the possibility of internal exchange or pseudorotation of their ligands. This process was first described by Berry[38] and is shown in Scheme 1.3.

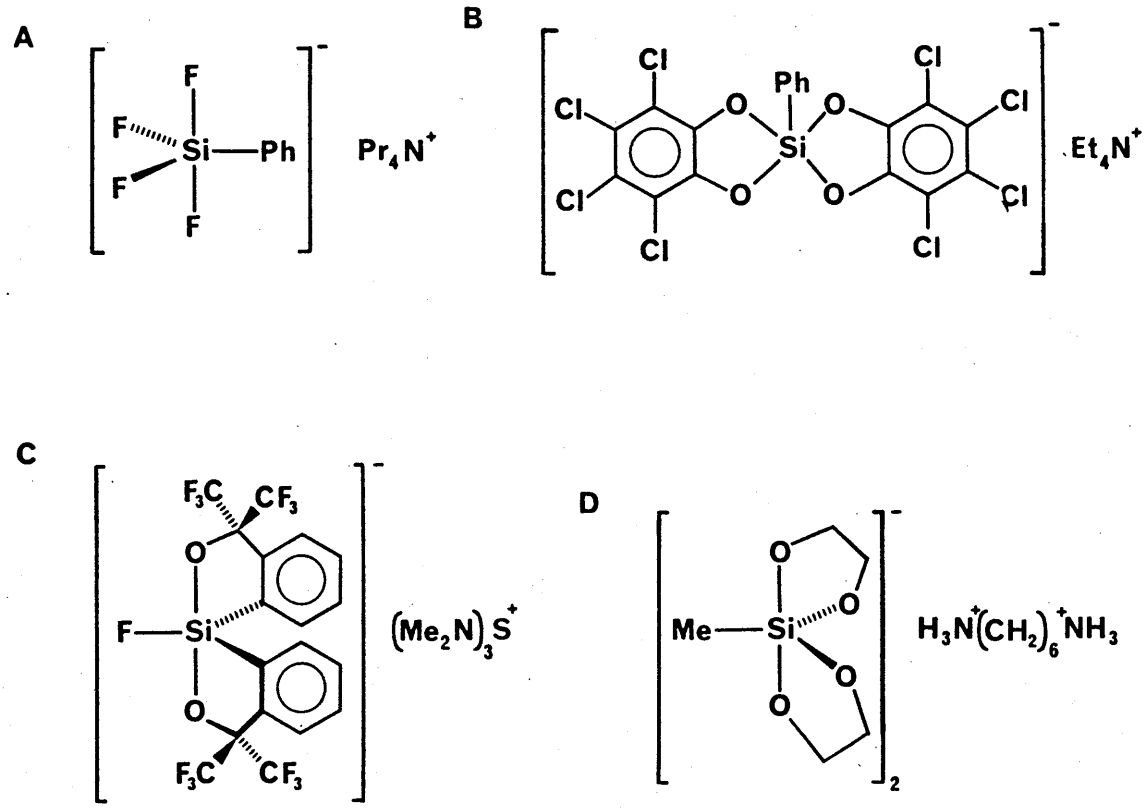

Figure 1.7

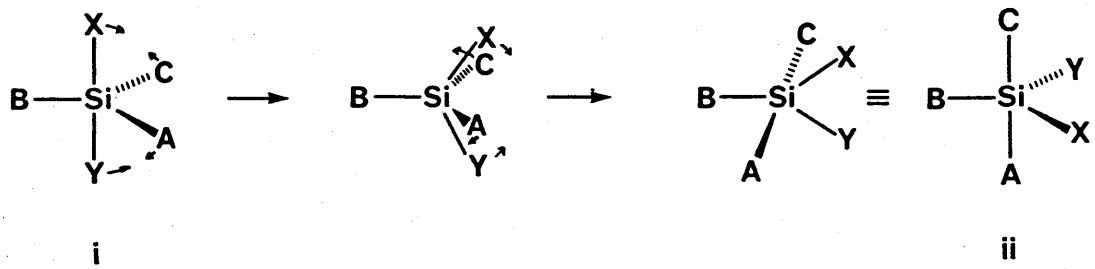

Scheme 1.3

A pseudorotation converts i) to ii) keeping one substituent, called the pivot ligand (B in this case), in an equatorial position. A and C become axial whereas X and Y, originally axial, become equatorial. Thus the X and Y groups, initially in apical positions, are converted to equatorial ligands by one pseudorotation. Hence the observation by Holmes of a

series of geometries ranging from TBP to square pyramidal is particularly relevant to the question of whether this process occurs at silicon (see discussion in Section 1.7).

Six coordinate silicon compounds are only known for species where the silicon atom is bonded to several electronegative atoms. Two typical hexacoordinate silicon compounds are shown in Figure 1.8[18].

Figure 1.8

1.5 Silicon-29 N.M.R.

The use of silicon-29 n.m.r. as a major tool for structure elucidation in silanes only became recognised during the early 1970's, although pioneering studies had been carried out as early as 1956[39]. The expansion of activity in the field resulted in part from the availability of multinuclear Fourier transform spectrometers, which made the study of more dilute systems a practical proposition. Several reviews[18,19,40,41] are available covering both chemical shift data and general trends.

In recent years, the design of special pulse sequences[42] has provided methods of greatly increased sensitivity. In particular the polarization transfer techniques, first proposed by Morris and Freeman[43], are proving to be very useful.

For a two spin system consisting of a sensitive nucleus such as ^{1}H and an insensitive one e.g. ^{29}Si, the population difference between the ground and excited states is determined by γ, the gyromagnetic ratio. Thus the sensitive nuclei, having a large value of γ, experiences a larger increase in the population of its upper energy level upon excitation than does the less sensitive nuclei (low value of γ).

In the INEPT[43] (Insensitive Nuclei Enhanced by Polarisation Transfer) experiment, the full polarization induced in the sensitive nucleus (in this case ^{1}H) is transferred to the insensitive nucleus (^{29}Si). Enhancement of the silicon signal results to a degree which is dependent upon the number of coupled protons[44]. An additional gain ensues from the short relaxation time of the proton nuclei, which allows for faster pulsing. The combined effect of these two factors can reduce the time taken to accumulate a ^{29}Si n.m.r. spectrum by between 30 and 300 times[45].

The technique is not without certain disadvantages however. A resolvable coupling to one or more protons is necessary; but more seriously the enhancement factor is a sine function of the pulse parameters. Improper choice of these parameters, which can only be determined from the silicon-proton coupling constant, can result in signal cancellation in certain unfavourable cases.

Shiftless paramagnetic relaxation reagents such as chromium or iron acetylacetonates (acac) are often employed in low concentration (ca. 1%) to enable faster pulsing, especially if the nuclei have excessively long relaxation times. Their disadvantages are that they contaminate the

sample, undesirable side reactions are possible particularly with reactive species and they can seriously affect the resolution of proton n.m.r. spectra.

To date the known chemical shift range of ^{29}Si is greater than 500 ppm, although the vast majority of species can be found within 250 ppm[18,19]. A number of compounds have been suggested as the reference point for silicon-29 chemical shifts but tetramethylsilane (Me_4Si) has become the generally accepted standard.

Prediction, even approximately, of ^{29}Si chemical shifts from substituent parameters is not straightforward for silicon. A plot of the total substituent electronegativity for all silanes versus their chemical shift shows a U-shaped curve[18,19]. Thus, for example, the successive substitution of methyl groups by chloride shows an initial increase in chemical shift, followed by a decrease to below the initial value (Me_4Si, 0.0 ppm; Me_3SiCl, +30 ppm; Me_2SiCl_2, +32 ppm; $MeSiCl_3$, +12.5 ppm; $SiCl_4$, -20 ppm).

As yet no comprehensive theory has been advanced to explain all of the observed trends. Earlier theories[40] proposed that there were two opposing effects in operation. On the one hand, the inductive effect of substituents caused a decrease in nuclear shielding, whilst a $(p-d)\pi$ interaction resulted in back donation and thus increased shielding around silicon. Other explanations must now be sought since the involvement of d-orbitals in silicon chemistry as a whole is disputed (see above). Additional influences on shielding may come from polarization of Si-X bonds, steric effects, electric fields or magnetic anisotropy of neighbouring groups.

Attempts to correlate silicon-29 chemical shifts with substituent parameters have been fairly successful especially when the changes occurred at positions remote from silicon.

McFarlane and Seaby[46] studied the chemical shifts of substituted methylsilyl carboxylates [$Me_{4-n}Si(OCOR)_n$], and found a good linear correlation of chemical shift with the pKa of the parent carboxylic acid within each particular series. Furthermore the slope of the line, i.e. the magnitude of the shifts' dependence upon substituent effects, decreases as the number of carboxyl substituents increases.

A similar but somewhat more dramatic effect is observed for arylsilanes, where the slope of the Hammett σ value vs. ^{29}Si chemical shift correlation reverses, on changing the substituents from $ArSiF_3$ to $ArSiH_3$[47]. This is a further manifestation of the aforementioned U-curve relationship observed for ^{29}Si chemical shifts generally. Hammett σ^* constants have been used successfully to correlate the $^1J_{Si-H}$ coupling constant in R_3SiH (R=Ph, Me, H)[19].

Pronounced solvent shifts are not normally a problem in ^{29}Si n.m.r., but significant shifts have been encountered for specific classes of compounds. Williams and Cargioli et al.[48] have found an excellent linear correlation between the chemical shift of a series of silanols and silylamines against the Gutmann donor number[49,50] (see Section 1.6) of the solvent. Shift changes were normally restricted to a maximum of 5 ppm between solvents of widely different donicity and were suggested to result from interactions of the type $R_3Si-O-H\longleftarrow$:Donor. Repulsion of the

OH group's bonding electrons may result in increased electron density on the silicon. In the extreme case, very strong bases such as NaOEt/EtOH remove the proton entirely and the resulting $Si-O^-$ species exhibits a pronounced upfield shift of -12 ppm.

The problem, mentioned above, of defining the precise environment around silicon can often be considerably simplified by access to silicon-29 n.m.r. information. In particular, the number of ligands surrounding silicon can often be determined simply by reference to the ^{29}Si chemical shift. Care must be exercised however, since considerable overlap is observed between the chemical shift ranges of each coordination number.

A more useful factor than chemical shifts alone is the large upfield shift, experienced when an extra ligand is added to the coordination shell of the nuclei. This point is illustrated by the comparison between the chemical shifts of a series of substituted silatranes and their analogous triethoxy compounds (Table 1.2)[19].

In most cases a marked increase in shielding of between 20 and 30 ppm is observed upon formation of the silatranes. The lower shift differences of the electronegative substituents (fluoro, ethoxy and phenoxy) may result from increased Si-N distances, but further studies are required to confirm this point. Replacement of one of the bridging oxygen atoms results in a weakened Si-N interaction, whilst carbon functional substituents on the rings or replacement of an oxygen by nitrogen results in a strengthened Si-N interaction.

Table 1.2

^{29}Si Chemical Shifts for some Silatranes and their analogous Triethoxysilanes[a]

Silatrane 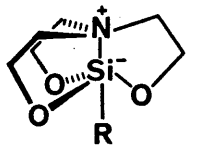

R	$RSi(OCH_2CH_2)_3N$ A	$RSi(OEt)_3$ B	(A-B)
H	-83.6	-59.5	-24.1
Me	-64.8	-44.2	-20.6
Et	-66.5	-45.4	-21.1
Vi	-81.0	-59.5	-21.5
Ph	-81.7	-58.4	-23.3
PhC≡C	-94.7	-69.5	-25.2
F	-101.1	-84.5	-16.6
PhO	-98.4	-86.6	-11.8
EtO	-94.7	-82.4	-12.3

[a] In ppm relative to Me_4Si.

Currently the accepted chemical shift range for five coordinate silicon species extends from -176 ppm (low frequency) to -53 ppm (high frequency). The high frequency end is represented by species such as that shown in Figure 1.9, with chelating ligands, which was among the first five coordinate compound to be studied by silicon-29 n.m.r.. Subsequent studies have tended to extend the higher frequency limit, and it seems likely that this limit will be extended by future work.

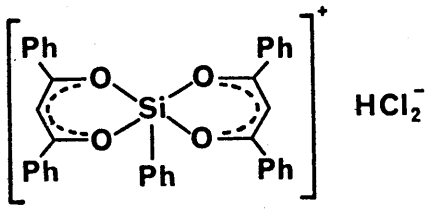

176 ppm

Figure 1.9

X-ray studies have provided perhaps the most conclusive proof for the existence of extracoordinate silicon species, but the nature of the technique effectively limits its scope to the study of solids. Therefore it is important to determine whether significant differences exist between the solid and solution states. To address this point, Hensen and Klebe[51] studied a series of silyl phenanthroline derivatives (Figure 1.10) in solution by ^{29}Si n.m.r., and in the solid state by crystallographic analysis. A crossover from 4- to 5-coordination was observed in both solution and solid phases, by progressively substituting methyl groups on silicon with chloro or other halo species. Again a careful comparison between the observed chemical shift and those of analogous 4-coordinate species proved invaluable for confirming that extracoordination was indeed being observed.

R_3 = Me_3, Me_2Cl, $MeCl_2$, F_3

Figure 1.10

The advent of solid state n.m.r. has provided an additional method for studying structures of solids. The chemical shift (-87 ppm) of the five coordinate species shown in Figure 1.11 was found to differ by only 1 ppm between solution and solid states[19].

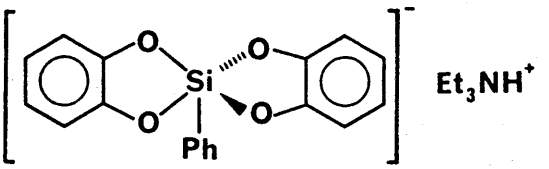

Figure 1.11

The chemical shift range for hexacoordinate silicon species is ca. -120 ppm to -200 ppm[19]. The high frequency end of the chemical shift range is represented by highly deshielded species, the structure of which is often the subject of some controversy.

Olah has attempted to predict the likely chemical shift of a silicenium ion R_3Si^+ by drawing analogies between ^{13}C n.m.r., where such species have been characterised, and ^{29}Si n.m.r.. He compiled all the available ^{13}C and ^{29}Si chemical shift data for $R_1R_2R_3R_4M$ compounds (M=C, Si) and found a reasonable correlation between them[52]. Using this he predicted that the likely chemical shift for a Me_3Si^+ species would lie in the range 225-275 ppm (by analogy with $^tBu_3C$ at 330 ppm in the ^{13}C n.m.r.) and a Ph_3Si^+ species between 100 and 150 ppm. The available data suggest that no long lived trivalent silicon cation has yet been observed by ^{29}Si, although Olah's [R_3Si-X---AlX_3] species at 76 ppm must be considerably deshielded.

An additional factor which should be considered, when assessing ^{29}Si spectra or indeed those of any other nuclei, is whether the species under investigation is undergoing chemical exchange. This branch of n.m.r. spectroscopy, often known as "Dynamic N.M.R." (DNMR)[53], has the advantage that a wide range of rate constants are accessible to it: 10^{-1} to $10^{-6}s^{-1}$ in favourable cases (first or pseudo-first order processes). Furthermore, the technique gives direct information about the nuclei being studied in a non-intrusive manner. The study of degenerate systems at thermodynamic equilibrium is often feasible which would be very difficult using other methods. A more detailed analysis of DNMR processes, including some calculated lineshapes, is included in Appendix 1, together with a brief discussion concerning the methods used for evaluating equilibrium constants from n.m.r. data.

1.6 Factors affecting the outcome of Nucleophilic Substitution at Silicon

a) Structure of the silane

In general, the rate of nucleophilic substitution at silicon is susceptible to steric hindrance. As with S_N2 reactions at carbon, the more highly hindered molecules react more slowly, but electronic effects are also important. For example in the alkyl series - methyl, ethyl, ^{i}propyl and ^{t}butyl, a very large decrease in the rate of substitution is observed[54]. Electron release to silicon tends to slow down nucleophilic substitution, but the large reduction in reactivity observed here is too great to be attributed solely to the positive inductive effect of the alkyl substituents.

Cartledge[55] has used steric parameters, derived from the reactivities of

organic carbonyl compounds, and found them to be moderately successful in describing steric effects for reactions taking place at silicon. Additionally he defined a set of parameters specifically for silicon and showed that steric effects in $R_1R_2R_3SiX$ compounds are often additive.

b) Influence of leaving group

The reactivity of silanes e.g. R_3SiX towards nucleophiles decreases in the order:-

$$X=I > Br > Cl > F >> OR > CR_3, H.$$

Furthermore Corriu[56] has observed that the ability of silanes to be cleaved with inversion and the tendency of halosilanes to be racemised also follow the same order. The extension of this order to include bifunctional and/or cyclic silanes appears to be justified by the results of several other studies. Explanations of this trend by factors such as polarizability, electronegativity or basicity of the leaving group fail to account, satisfactorily, for all cases.

The relative ability for a leaving group X to form a pentacoordinated structure has been examined by Corriu[56] using the system shown in Scheme 1.4.

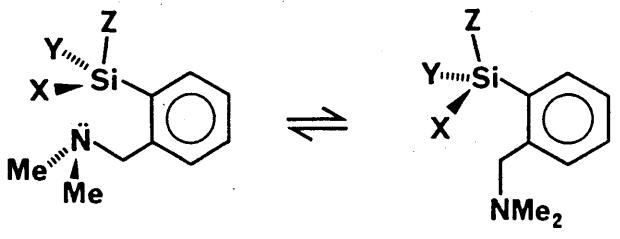

Scheme 1.4

Coordination of the nitrogen to silicon induces diastereotopy in the two methyl groups. By finding the temperatures required to coalesce the two methyl signals (^{1}H n.m.r.) for various leaving groups, he assessed the relative ease of extracoordination which was stated to be:-

Br, Cl, OAc > SR, F > OR, H.

Variable temperature ^{29}Si n.m.r. data[56] was used to confirm the presence of pentacoordinate species in these studies. In addition, Corriu defined a scale of apicophilicity for silicon: as the ability of the ligands on silicon to adopt an apical position relative to the nucleophile.

Axial and equatorial fluorine substituents on silicon can be distinguished by ^{19}F n.m.r. studies which enable the relative apicophilicity of various substituents to be determined. The fluorine substituent in derivatives of $(2\text{-}Me_2NCH_2C_6H_4)SiXYZ$ (Scheme 1.4) (Y=Me, Z=F) was apical when X=H, OR or NR_2 but equatorial for X=Cl. A mixture of the two configurations is found for $X=p\text{-}YC_6H_4CO_2$, the F_{ax}/F_{eq} ratio depends on the nature of the para-substituent Y[56]. It is interesting to note that both the orders of ease of pentacoordination and of increasing apicophilicity are closely parallel to the orders of increasing rate of racemisation and that of increasing proportion of inversion.

These studies suggest that electronegativity is not the controlling factor in determining the stability of extracoordinate complexes, although its influence cannot be discounted entirely. Corriu has proposed[56] that the tendency of the Si-X bond to be stretched by an incoming nucleophile is the major factor in determining the ability of

silanes to form a pentacoordinated structure. However the concept has not yet been quantified, and it is not easy to predict the ability of a different bond, for instance the Si-O bond in silyltriflates, to be "stretched". It would be interesting to correlate the capability for complex formation with a known physical property of each bond to quantify this concept.

c) The influence of the nucleophile and the solvent

The roles of nucleophile and solvent are interrelated since in some cases the solvent can act as the nucleophile and in others it modifies the character of the nucleophile.

Two important properties of a solvent can be distinguished, namely, its donicity or nucleophilicity and its dielectric constant. The latter property results essentially from dipoles within the molecule, whilst donicity is a measure of the solvent's nucleophilicity or Lewis base strength. The relative importance of these two properties depends upon the system under examination, often both are necessary to account for certain phenomena. The process of forming a pair of separated solvated ions is a two step reaction as shown below.

$$\underset{\text{solvent}}{S:} + A:X \rightleftharpoons \underset{\text{ion pair}}{(SA)^{+}(:X)^{-}} \rightleftharpoons \underset{\text{separated solvated ions}}{(SA)^{+} + (:X)^{-}}$$

Scheme 1.5

A distinction must be made between the two processes involved: ionisation (ion formation) and ion dissociation (the dissociation of ion

associates). The first step cannot be induced merely by a solvent which has a high dielectric constant; it depends upon its donicity. The dielectric constant of the medium is important in the second step and therefore the concentration of fully dissociated ions (as measured by the solution's electric conductivity) is a function of both properties. Conductivity studies are often used to determine whether ionic species are present, but the results must be interpreted with some care. Whilst a highly conducting solution must be composed of dissociated ions, a non-conducting solution may consist of ion pairs or indeed no ions at all.

Several attempts have been made to quantify solvent properties:-

i) Gutmann[49,50] introduced his donor number (DN) which is defined by the negative enthalpy of reaction between the solvent and antimony pentachloride ($SbCl_5$) in 1,2-dichloroethane. It is assumed here (and in most other solvent scales) that entropy effects are constant so that the measured enthalpy reflects the strength of the solvent-$SbCl_5$ bond.

ii) Gutmann also introduced an acceptor number (AN)[49,50] which was designed to correlate solute-solvent interaction in acidic solvents. Phosphorus-31 chemical shifts of triethylphosphine oxide ($Et_3P{=}O$), dissolved in the chosen solvent, are normalised to an arbitrary value of 100, chosen as the shift produced by the $SbCl_5$-$Et_3P{=}O$ adduct in dichloroethane.

iii) Drago and Wayland[57,58] proposed their E and C scale for predicting acid-base reaction enthalpies in poorly coordinating solvents (or the gas phase).

$$-\Delta H_{AB} = E_A E_B + C_A C_B \quad \text{..... equation 1.1}$$

Both the acid and the base are characterised by two parameters; E is a measure of their ability to participate in electrostatic bonding and C measures the ability to form covalent bonds.

iv) Linear solvation energy relationships have been used, notably by Taft and co-workers[59,60], to provide a unified scale of solvent effects. Their scale of hydrogen bond acceptor basicities (Beta) is a measure of the solvent's ability to donate an electron pair (or accept a proton) in a solute-solvent hydrogen bond.

Additional parameters have been defined such as:-

(1) the coordinate covalency parameter (for different functional groups);

(2) δ_H, the Hildebrand solubility parameter (a measure of the solvent-solvent interactions that are interrupted in creating a suitably sized cavity for the solute in the solvent);

(3) π^*, the solvent dipolarity/polarizability (related to the solvent's ability to stabilize a charge or dipole as a result of its dielectric effect);

(4) α, the hydrogen bond donor acidity is related to the ability of the solvent to donate a proton in a solute-solvent hydrogen bond.

These parameters have been obtained by "averaging multiple, normalized solvent effects on a wide variety of properties involving many diverse types of indicators"[60]. Good linear relationships with properties as diverse as pKa, ΔG_f (aq BH^+), ^{19}F n.m.r. chemical shifts of 5-fluoro-indole-base complexes in CCl_4 and Gutmann donor number have been obtained using these parameters.

In nucleophilic substitution at silicon, good leaving groups such as chloride react with inversion except with very hard nucleophiles.

Conversely poor leaving groups such as H almost always react to give retention, except with Ph_2CHLi[56]. For moderately good leaving groups such as SR, F or OMe, the stereochemical outcome is decided by the nature of the nucleophile. For a given leaving group, hard nucleophiles give retention whilst softer nucleophiles give inversion. Thus species with a highly localised negative charge such as Ar^-, $PhC{\equiv}C^-$, and RLi produce retention. Inversion is only found with the best leaving groups such as chloride or bromide. In such species, the reactivity can be modified by altering the solvent to one which allows greater solvation of the charged centre, or by changing the metal counterion. Grignard reagents show a tendency towards inversion compared to organolithium reagents, presumably because the more covalent C-Mg bond provides a softer nucleophile. Allyl or benzyl species in which the charge is more delocalized (softer nucleophile) react to give inversion unless the leaving group is exceptionally poor.

An example is provided by the substitution of Si-OMe, Si-F or Si-SMe bonds by lithium or sodium alkoxides. A gradual change of solvent from benzene to alcohol results in increased solvation of the negative charge on oxygen, changing it from a hard anion to a much softer one[56]. A corresponding change in the product stereochemistry from inversion to retention is observed. Further support for the relationship between product stereochemistry and the hardness/softness of the attacking species comes from studies on phenoxides, where the electronic character of the negative charge on oxygen can be varied by altering the substituents on the phenyl ring[56].

The role of solvent in predicting the stereochemical outcome is a crucial one. In the reaction between chlorosilanes and methanol, the course of

reaction can be altered completely from one giving inversion to one producing retention, by changing the solvent from carbon tetrachloride, hexane etc. to HMPA, DMSO or DMF. This may be due either to the nucleophilicity of these species or to the change in dielectric constant of the medium. To distinguish between these two possibilities, Corriu[56] showed that solvents of very low dielectric constant (ϵ=15), but moderate donicity, were capable of causing racemisation of chlorosilanes. This implies that solvent nucleophilicity is the dominant factor rather than the ability of the medium to stabilise a charged intermediate.

The factors controlling the outcome of nucleophilic substitution at silicon can be summarised as follows:-

Soft nucleophile		Hard nucleophile
OTs, OCOR, Br	> Cl >> SR, F >>	OMe > H
Inversion		Retention
Ease of racemisation		
Reactivity		
Ease of pentacoordination		

1.7 Reaction Mechanisms for Nucleophilic Substitution process at Silicon:- a brief survey

A comprehensive coverage of organosilicon chemistry was provided in 1959 by Eaborn[11], who reported that relatively little work had been carried out into the mechanism of organosilicon reactions. However by 1964, in an important monograph, Sommer gave a detailed account of the mechanisms and stereochemical outcome for many silicon-centred reactions[12]. His studies

showed, for the first time, that many nucleophilic displacements at silicon were highly stereospecific, and moreover that retention of configuration is a commonly observed stereochemical outcome in contrast to analogous processes at carbon. The subject has been extensively reviewed since then, notably by Prince[61], Fleming[62], Armitage[31], Sommer[63], and Corriu[56].

The vast array of mechanistic studies (and conclusions) prevents a full discussion here. Nonetheless it is important to review some of the underlying arguments in relation to the role of nucleophiles in substitution processes at silicon.

It is generally agreed that the stereochemical outcome is determined by the site of attack of the nucleophile, i.e. attack at 180° to the leaving group produces inversion (analogous to inversion processes at carbon) whilst equatorial attack gives retention. The disagreement concentrates on the detailed intermediate steps which take place between attack of nucleophile and departure of the leaving group.

It is possible, very crudely, to separate the diverse conclusions reached by various authors into four mechanistic viewpoints:-

Viewpoint (1) - a concerted substitution process, changing to one involving extracoordinate silicon intermediates, depending on the nature of the silane.

Sommer[63] proposed that the dominant mechanism leading to inversion at silicon was an S_N2-Si process resembling that observed in carbon

chemistry. He further subdivided this mechanism into S_N2^*-Si and S_N2^{**}-Si depending upon the nature of the reaction coordinate and the rate determining step. The energy profiles for these processes are summarised in Figure 1.12, together with their corresponding rate laws. The S_N2^*-Si and S_N2^{**}-Si mechanisms become progressively more important in the series $R_3SiX < R_2SiX_2 < RSiX_3 < SiX_4$ (where X is a highly electronegative group). The transition state for the S_N2-Si process matches that for the comparable carbon process, except that stabilizing factors inherent to silicon reduce the activation energy.

Retention of configuration was described by Sommer as involving a quasicyclic S_Ni-Si transition state (or intermediate in some cases) (Figure 1.13).

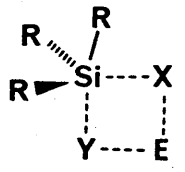

X - leaving group

E - electrophilic part of attacking species EY

Figure 1.13

Corriu has presented data which he uses to argue against the process on several grounds[56]. The S_Ni-Si mechanism involves electrophilic assistance to the leaving group by the M^+ counterion, therefore factors which tend to increase the solvation of M^+ should decrease the proportion of retention. In coupling reactions between silanes and organolithium compounds, addition of Li^+ complexing agents results in an increase in the proportion of retention. The evidence is not conclusive for all reactions however; Sommer has presented a detailed argument in favour of the S_Ni-Si mechanism[63].

Figure 1.12 Reaction profiles for nucleophilic substitution processes at silicon.

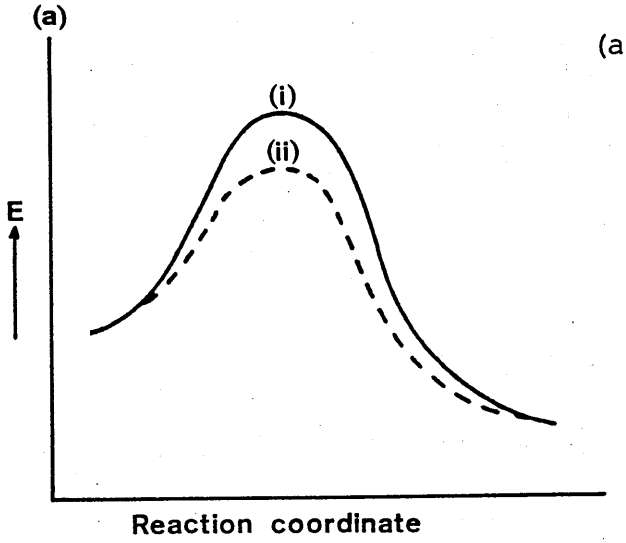

(a) (i) S_N2-Carbon

(ii) S_N2-Silicon

transition state

Rate $\propto [R_3SiX]\ [Nu]$

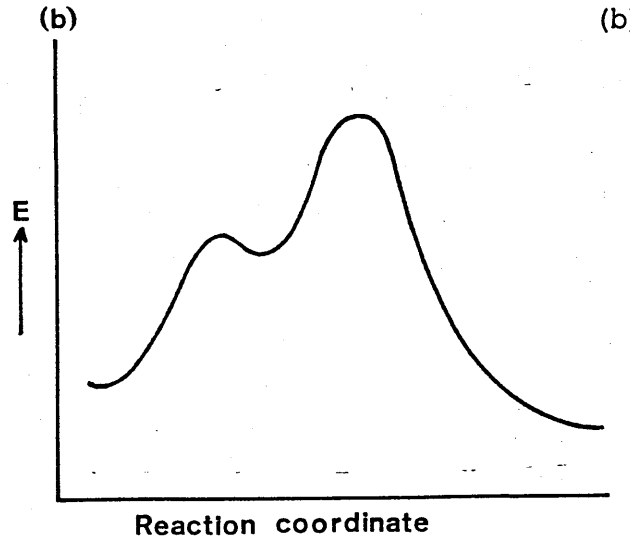

(b) S_N2^*-Si

Rapid pre-equilibrium formation of a five coordinate intermediate, followed by rate limiting conversion to products

$$\text{Rate} = \frac{k_1}{k_{-1}}\ k_2\ [R_3SiX]\ [Nu]$$

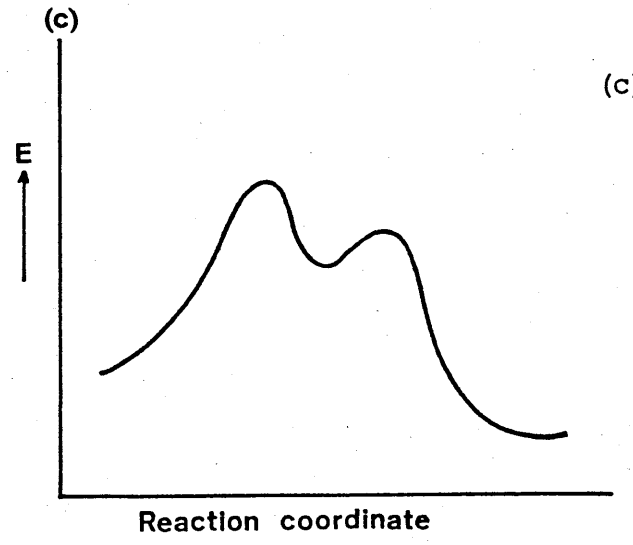

(c) S_N2^{**}-Si

Rate limiting formation of intermediates, followed by rapid dissociation to products

Rate $= k_1 [R_3SiX]\ [Nu]$

Viewpoint (2) - involving pseudorotation.

Prince[61] presented a detailed discussion of the pseudorotation processes in relation to silicon mechanisms, although the pseudorotation hypothesis has been applied to phosphorus mechanisms for some time[64]. This approach has also been used by Fleming in his review of organosilicon chemistry[62], which was subsequently rephrased by Armitage[31]. Pseudorotation (see Section 1.4) is considered to be an important factor controlling the stereochemical outcome. This process is well established as a mechanistic process in phosphorus chemistry, and a number of rules have been formulated to enable the stereochemical outcome to be predicted:-

i) entry of nucleophiles and departure of leaving groups occurs in the apical position;

ii) electronegative substituents prefer apical positions;

iii) four and five membered rings are constrained to span one apical and one equatorial positions.

Equatorial attack of the nucleophile on the phosphorus atom places the leaving group in an equatorial position. A pseudorotation is then required, according to these rules, so that the leaving group can depart from an apical position.

Muetterties[65] showed that rapid isomerisation was taking place in SiF_5^-, $RSiF_4$ and $R_2SiF_3^-$ (R=Me or Ph) by ^{19}F n.m.r.. He proposed that pseudorotation was taking place in a similar manner to that observed for PF_5, however subsequent studies by Janzen[66], Corriu[56] and co-workers proved that the ligand exchange could be rationalized using other mechanisms. Similarly, a ^{19}F n.m.r. study of the isomerisation of

pentacoordinated spirosiliconate anions[67] by Farnham and Harlow suggested that the observed behaviour could be attributed to either pseudorotation or a Si-O bond dissociation-reassociation process. Martin et al.[68,69] have also discussed this subject.

The isolation of the somewhat exotic, square pyramidal silicon compounds such as those characterised by Holmes et al.[25](Section 1.4) does not mean, a priori, that such geometries can be applied to other silicon compounds. The square pyramidal complexes are stabilized by large electron withdrawing aromatic rings which allow stabilization of the negative charge on oxygen, thus minimizing the repulsion between bonding electrons. No definitive evidence has yet been presented for the pseudorotation process at silicon. It is possible that the process may be masked by other, faster, isomerisation pathways. Corriu[56] has pointed out that the pseudorotation process at silicon may have a higher activation energy; and moreover that the relative apicophilicity of ligands in the five coordinate compounds of the two elements is different for silicon.

Viewpoint (3)[56]

The pseudorotation process is not entirely ruled out by Corriu, but he considers that the leaving group can depart from an equatorial position, thus making pseudorotation unnecessary. It is also conceivable that edge attack of the nucleophile could occur during the nucleophilic substitution to give retention products. This process produces a square pyramidal transition state, which then reverts to the more stable trigonal bipyramidal conformation (Scheme 1.6). According to the rule of microscopic reversibility, the reverse process can also proceed via this pathway. Therefore it is not necessary to invoke pseudorotation.

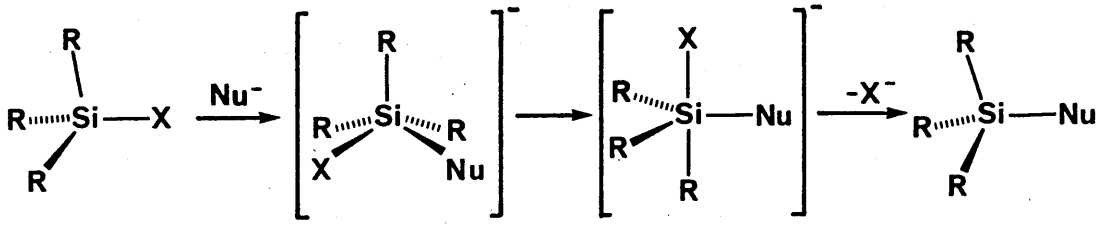

Scheme 1.6

The factors controlling the geometry of approach of the nucleophile have been rationalised by Anh and Minot[70] who applied the Frontier Orbital Approximation[71] to silicon. It is assumed that the dominant interaction during a reaction occurs between the HOMO (Highest Occupied Molecular Orbital) of the nucleophile and the LUMO (Lowest Unoccupied Molecular Orbital) of the silane σ^*_{Si-X} (Figure 1.14).

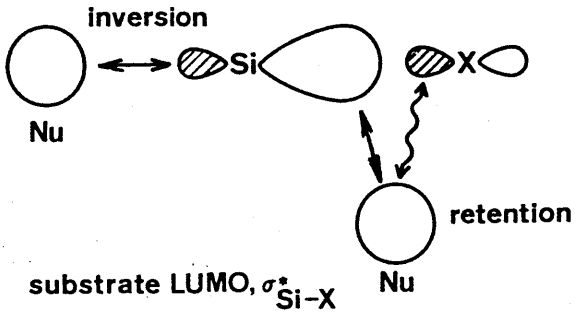

Figure 1.14

The sizes of the LUMO and HOMO orbitals are very sensitive to changes in leaving group and nature of the nucleophile respectively. The relative amounts of in-phase or out-of-phase overlap between the nucleophile and the LUMO of the silane σ^*_{Si-X} controls the site of attack. A detailed account of the Frontier Orbital hypothesis is presented in Corriu's recent reviews[56].

The reaction profiles presented in Figure 1.12 apply equally well to this mechanism. However Corriu has proposed, on the basis of kinetic studies[56], that the formation of a pentacoordinate intermediate is rate determining [S_N2^{**}-Si process, Figure 1.12(c)] and that the S_N2-Si process [Figure 1.12(a)] is rare for silicon.

Chlorosilanes normally react with alcohols or water to give products with inversion of configuration. However, in the presence of nucleophilic agents such as DMSO, DMF, or HMPA, a rate acceleration is produced together with retention of configuration. This aspect of the mechanism of nucleophilic substitution at silicon was initially observed by Corriu et al., who proposed a mechanism involving reversible nucleophilic backside attack on the silane to give a pentacoordinate intermediate, followed by attack of the water (or ROH) in a rate determining step (Scheme 1.7).

Racemisation can be accounted for by a reversible formation of a pentacoordinate silicon intermediate, followed by attack of a second molecule of the nucleophile to give either a hexavalent octahedral species or a pentavalent siliconium ion (Scheme 1.7).

Viewpoint (4)

The formation of ionic adducts between TMSX (X=I, Br) and HMPA led Chojnowski to propose[7] the mechanism shown in Scheme 1.8.

Two consecutive inversions are postulated to account for the retention observed in hydrolysis catalysed by nucleophiles. Racemisation results from attack of a second molecule of nucleophile on the $[R_3Si\text{-}Nu]^+X^-$

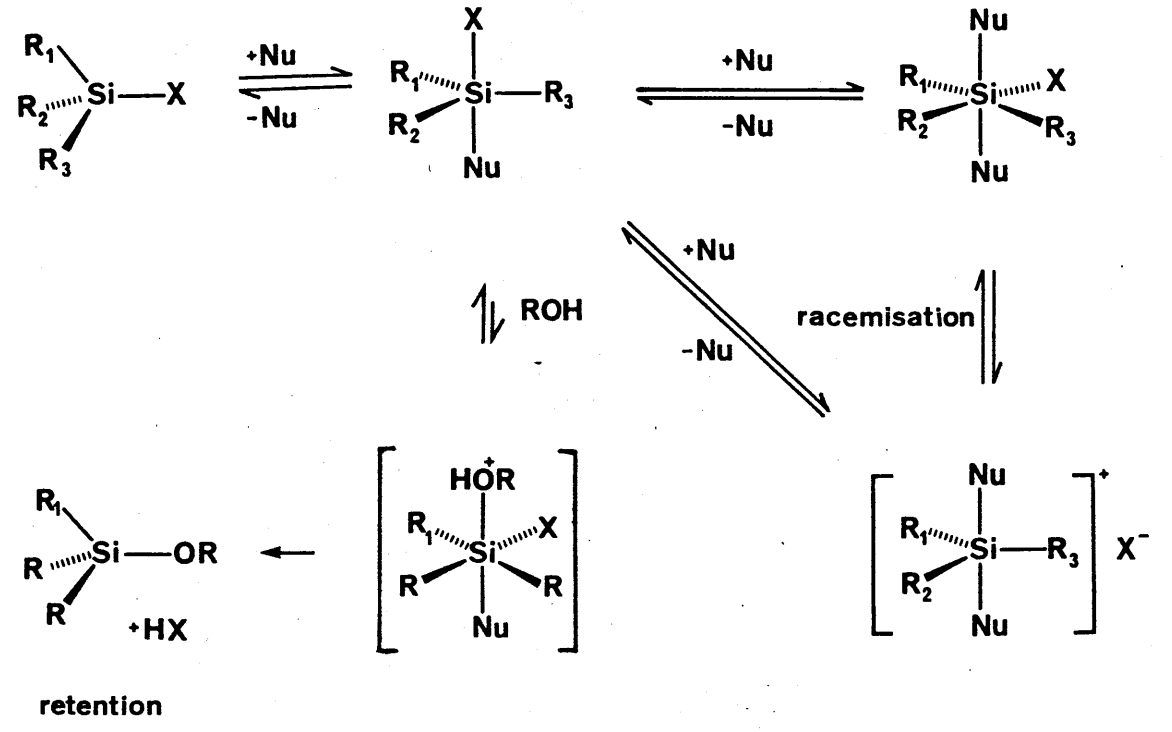

Scheme 1.7

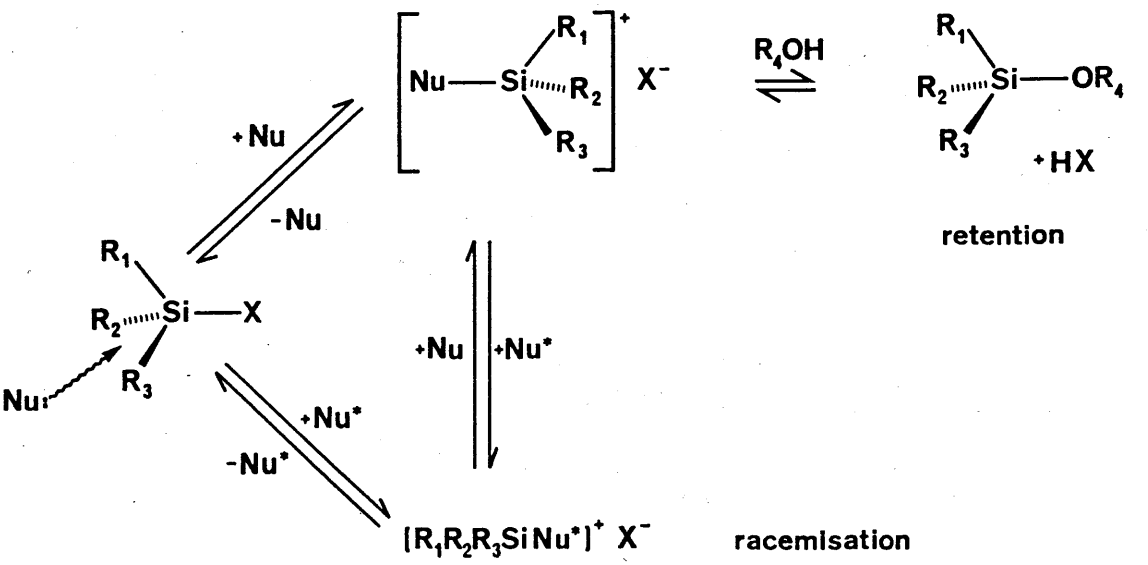

Scheme 1.8

adduct. Corriu has stated that this mechanism cannot explain the low or negative enthalpy of activation for racemisation and hydrolysis, or the nucleophile induced epimerization of chlorosilacyclobutanes. However, this behaviour is to be expected if the ionic adducts are formed in a pre-equilibrium step, in which the forward process is exothermic. Similar behaviour was observed[72] for the hydrolysis or alcoholysis of aminosilanes catalysed by acid (Scheme 1.9).

$$R_2NSiR'_3 + H^+ \rightleftharpoons R_2N^+H\text{-}SiR'_3 \xrightarrow{R''OH\ (r.d.s.)} R_2NH + R''OSiR'_3 + H^+$$

Scheme 1.9

Both mechanisms presented in Schemes 1.7 and 1.8 are in accord with the experimentally observed rate law,

<u>i.e.</u> racemisation rate $\propto$ [silane][nucleophile]^2.

PART I

THE INTERACTIONS BETWEEN NUCLEOPHILES AND TRIMETHYLSILYL SPECIES

CHAPTER 2

STRUCTURAL CHANGES RESULTING FROM NUCLEOPHILE-SILANE INTERACTIONS

2.1 Introduction

Prior to investigating the thermodynamic and kinetic factors governing nucleophile-silane interactions, it is important to define the nature of the dominant species present in solution. The detailed changes induced in both donor and acceptor have been studied by examining mixtures containing:-

i) an excess of nucleophile over silane;

ii) equimolar quantities of nucleophile and silane; and

iii) an excess of silane over nucleophile.

In some systems the interaction was studied in greater detail by chemical shift titrations, low temperature n.m.r. studies and/or conductivity experiments on various mixtures of nucleophiles and silanes. In many cases it was not considered necessary to isolate and characterise the various nucleophile-silane adducts, as this study concentrated particularly on solution state structures, and since, in several cases this has already been done *i.e.* for hexamethylphosphoramide[7] (HMPA)/TMSX (X=I, Br), triphenylphosphine oxide[7] (TPPO)/TMSX (X=I, Br), amides with TMSOTf[13] and pyridine[36] (py)/TMSX (X=I, Br). The choice of nucleophiles was limited to those species which did not undergo significant amounts of silylation[3] *e.g.*:-

$$R_2NH + Me_3SiX \rightleftharpoons R_2N\text{-}SiMe_3 + HX$$

Scheme 2.1

since processes such as these would mask any nucleophile-silane (donor-

acceptor) type interactions. The reactivity of various functional groups, towards silylating agents generally, has been reviewed by Pierce[1], Weber[2] and Colvin[3]. The synthetic utility of individual trimethylsilyl species has also been reviewed for i) TMSI by Olah[16] and ii) TMSOTf by Emde et al.[13] and Noyori[14].

The subsequent discussion is divided into six sub-sections, each dealing with a particular class of donor species.

i) amides

ii) ureas

iii) substituted pyridines

iv) pyridine N-oxide

v) phosphine oxides

vi) amines including the imidazoles

2.2 Amides

Amides such as DMF are frequently used in combination with silylating agents, or sometimes as solvents, and they have been shown to be efficient racemisation agents. The work of Emde et al.[13] has suggested that ionic adducts can be formed between amides and TMSOTf, whereas Corriu concluded that the predominant structural type for DMF-TMSX (X=Cl, Br) adducts was a five coordinate non-ionic one; the ionic nature of the DMF-TMSI adduct being attributed to a specific phenomenon caused by the lability of the Si-I bond, and the affinity of silicon for oxygen[8,56]. Therefore it was necessary to reinvestigate the nature of the interaction between amides, in particular DMF, and several TMSX species, using ^{1}H, ^{13}C and ^{29}Si n.m.r. spectroscopy.

The spectral data obtained for various mixtures of DMF with TMSX (X=Cl, Br, I, OTf) in chloroform-d_1 or dichloromethane-d_2 are presented in Tables 2.1, 2.2 and 2.3. Comparison of the data for the 1:1 nucleophile/silane mixtures with those of the isolated TMSX species (see Appendix 3) shows a pronounced downfield shift for the iodide and bromide, but not for the chloride or triflate. Except for the TMSBr/DMF mixture, no large shifts are observed upon addition of further quantities of DMF to these solutions. These shifts are consistent with the formation of a single type of complex with chemical shift of ca. 44 ppm for all silanes except the chloride.

The different behaviour of the TMSX species can be accounted for by assuming an increasingly large equilibrium constant in the order Cl << Br < I. Thus addition of a large excess of DMF is required to drive the equilibrium in favour of complex formation for the bromide, but the iodide complex is essentially fully formed at 1:1 stoicheiometry. The approach towards a single chemical shift for species with widely different shielding factors suggests that the Si-X bond has been cleaved to form a 1:1 ionic complex $[DMF\text{-}TMS]^+X^-$ (X=Br, I, OSO_2CF_3). This is in accord with the conclusions of Chojnowski[7].

$$DMF + Me_3SiX \rightleftharpoons [DMF\text{-}SiMe_3]^+X^- \qquad (X=Br,\ I,\ OSO_2CF_3)$$

Scheme 2.2

The ^{29}Si chemical shift of this complex is characteristic of a 4-coordinate trimethylsilicon compound, with one very deshielding ligand. Yoder[73] has characterised a 5-coordinate tri-organosilicon species

Table 2.1

Interaction between N,N-Dimethylformamide (DMF) and Trimethylsilyl species (TMSX) : N.M.R. Data

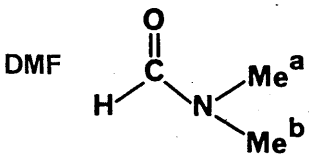

		DMF	DMF + TMSCl 1:1	DMF + TMSCl 10:1	DMF + TMSBr 1:1	DMF + TMSBr 10:1	DMF + TMSI 1:1	DMF + TMSOTf 1:1
δ(ppm)								
^{1}H	H-C=O	8.01	8.04	8.11	8.85	8.18	9.35	8.46
	$N-(CH_3)^b$	2.87	3.00	2.89	3.03	2.87	3.3	3.23
	$N-(CH_3)^a$	2.94	3.25	2.92	3.29	3.05	3.69	3.46
	(a-b)	7.8Hz	9.8Hz	9.8Hz	23.9Hz	16.1Hz	34.4Hz	21.0Hz
	$Si-(CH_3)_3$	-	0.43	0.43	0.58	0.57	0.69	0.50
^{13}C	C=O	162.4	162.3	162.4	163.2	162.4	163.0	164.5
	$N-(CH_3)^b$	31.3	31.2	31.3	33.4	31.2	37.1	35.8
	$N-(CH_3)^a$	36.4	36.2	36.3	38.5	36.4	42.0	41.1
	(a-b)	115Hz	114Hz	114Hz	115Hz	116Hz	110Hz	120Hz
	$Si-(CH_3)_3$	-	3.2	3.2	2.6	1.6	1.8br	-0.63
^{29}Si	$Si-(CH_3)_3$	-	31.0	31.4	33.6	42.1	43.9	44.0
quantities used:								
DMF (mmoles)		2.2	3.6	36.0	1.4	14.0	3.8	2.2
TMSX (mmoles)		-	3.6	3.6	1.4	1.4	3.8	2.2
solvent: CD_2Cl_2, 2.0 ml								

Table 2.2

Interaction between N,N-Dimethylformamide (DMF) and Iodotrimethylsilane (TMSI) : N.M.R. Data

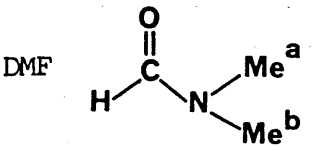

δ(ppm)		Ratio of DMF : TMSI 1:0.5	1:1	1:1.5	1:2.0
^{1}H	H-C=O	9.05	9.35	9.38	9.38
	$N-(CH_3)^b$	3.2	3.3	3.3d	3.3
	$N-(CH_3)^a$	3.5	3.69	3.68d	3.68
	(a-b)	27.7Hz	34.4Hz	34.7Hz	34.7Hz
	$Si-(CH_3)_3$	0.64	0.69	0.73	0.75
^{13}C	C=O	163.1	163.0	163.0	163.0
	$N-(CH_3)^b$	35.7	37.1	37.1	37.1
	$N-(CH_3)^a$	40.6	42.0	42.0	42.0
	(a-b)	110Hz	110Hz	109Hz	109Hz
	$Si-(CH_3)_3$	0.57	1.8(br)	3.4(br)	5.4(br)
^{17}O[a]	C=O	-	-	-	219.0(vbr)
^{29}Si	$Si-(CH_3)_3$	43.9	43.9(sbr)	no	11.0(vbr)
quantities used:					
DMF (mmoles)		7.34	3.8	3.8	3.8
TMSI (mmoles)		3.67	3.8	5.7	7.6
solvent: CD_2Cl_2, 2.0 ml					

[a] Referenced to external D_2O (DMF, 326 ppm).

Table 2.3

Interaction between N,N-Dimethylformamide (DMF) and Trimethylsilyl triflate (TMSOTf) : N.M.R. Data

DMF 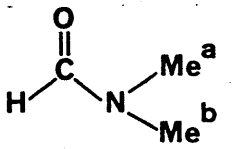

		Ratio of DMF : TMSOTf			
δ(ppm)		5:0	5:1	1:1	1:5
^{1}H	H-C=O	8.02	8.13	8.46	8.55
	$N-(CH_3)^a$	2.97d	3.08	3.46	3.48
	$^{4}J_{HH}$	0.49Hz	no	no	no
	$N-(CH_3)^b$	2.89d	2.93d	3.23d	3.22d
	$^{4}J_{HH}$	0.73Hz	1.0Hz	0.98Hz	0.73Hz
	(a-b)	7.8Hz	12.9Hz	21.0Hz	23.8Hz
	$Si-(CH_3)_3$	-	0.51	0.50	0.50
^{13}C	C=O	162.5	162.9	163.4	163.8
	CF_3	-	120.9q	120.7q	118.8q
	$^{1}J_{CF}$	-	321Hz	321Hz	317Hz
	$N-(CH_3)^a$	36.4	37.3	41.1	41.3
	$N-(CH_3)^b$	31.3	32.1	35.8	35.8
	(a-b)	115.2Hz	117.8Hz	120.4Hz	123.0Hz
	$Si-(CH_3)_3$	-	-0.69	-0.63	-0.20
^{29}Si	$Si-(CH_3)_3$	-	43.3	44.0	43.7
quantities used:					
DMF (mmoles)		2.75	13.77	2.75	0.55
TMSOTf (mmoles)		-	2.75	2.75	2.75
solvent: $CDCl_3$, 2.0 ml					

(Scheme 2.3C) which is essentially analogous to the species expected, if DMF coordinated to TMSCl without Si-Cl bond fission.

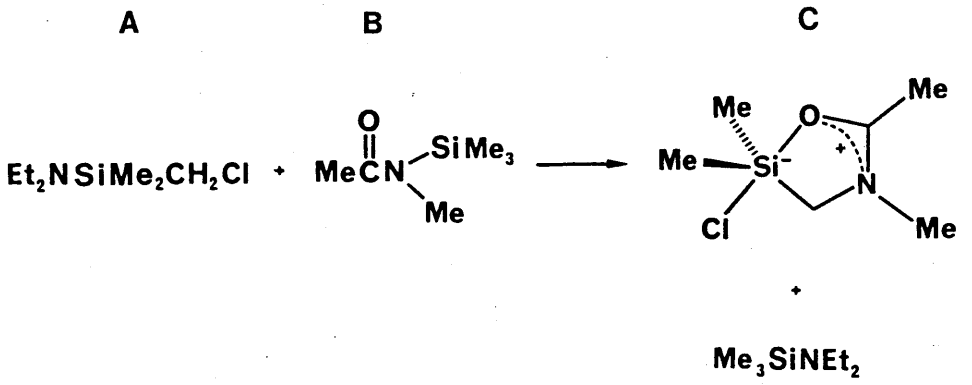

Scheme 2.3

The silicon-29 chemical shift of this species at -30 ppm (CD_2Cl_2[74]) confirms that the concentration of any five coordinate DMF-TMSCl adduct is not significant.

The small upfield chemical shift changes observed for the DMF/TMSCl mixture may indicate a very small equilibrium concentration of an adduct but it is not possible to characterise this species unequivocally. The ^{29}Si n.m.r. data is not conclusive for the triflate, but it will be shown below that the ^{1}H, ^{13}C chemical shift changes in DMF are consistent with complex formation for X=OTf, I and Br. The similarity observed between the chemical shifts of TMSOTf and its DMF complex probably results from accidental coincidence.

Additional information can be deduced from the silicon-29 chemical shift changes at various DMF:TMSI ratios and the corresponding line shapes. Successive additions of DMF to a solution of TMSI cause, at first, slight line broadening accompanied by a small downfield shift. This is followed

by disappearance of the signal owing to excessive line broadening and later reappearance at 43.9 ppm as a slightly broadened singlet. The line shapes presented in Figures A1.1 and A1.2 (Appendix 1) were calculated for an equal population system, but the frequency difference between exchanging sites is very similar to the separation between the DMF-TMSI complex and isolated TMSI (a difference of 34 ppm is equal to 606 Hz at 17.76 MHz). Derivation of the kinetic parameters for the system is theoretically possible by line shape analysis, but the very poor signal to noise ratio for the 1:1.5 mixture makes this impractical.

Sharp resonances of approximately natural linewidth (ca. 0.5 Hz) were observed in the ^{29}Si spectra for all DMF:TMSBr ratios. An approximate calculation using equation A1.5 shows that for equivalent rates of exchange, the peak for the exchange between TMSI and the DMF-TMSI complex should be ca. 4 times broader than the peak for the analogous TMSBr exchange. The observed peaks in the iodide exchange are considerably broader than the bromide ones, indicating that the exchange shown in Scheme 2.4 is slower when X=I. The rationale behind this difference will be discussed in Chapter 4.

$$Me_3Si^*X + [Me_3Si\text{-}DMF]^+X^- \rightleftharpoons Me_3SiX + [Me_3Si^*\text{-}DMF]^+X^-$$

Scheme 2.4

To rule out hydrolysis as the cause of these chemical shifts, enough water (0.5 times the number of moles of silane) was added to completely hydrolyse the silane. The ^{29}Si n.m.r. spectrum taken immediately after the addition showed only one peak at 7.4 ppm, characteristic of

hexamethyldisiloxane (HMDSO). The ^{1}H, ^{13}C and ^{29}Si n.m.r. resonances of HMDSO are given in the summary of trimethylsilyl n.m.r. data in Appendix 3. Care was taken to exclude water from these and all subsequent experiments. Any experiment that showed significant amounts of hydrolysis (as monitored by the appearance of HMDSO peak) was repeated.

The structure of DMF, and that of amides in general, raises the question of whether the oxygen or the nitrogen (or both) acts as the donor atom in complexing with silanes. This dual nature of the amides, sometimes referred to as ambidentate nucleophilicity[75,76], has been extensively studied in connection to the site of protonation in these species. The normally greater basicity of nitrogen nucleophiles suggests intuitively that this site would be preferred. However, extensive investigations by a number of authors[77] have shown that the oxygen-site is generally the preferred site for protonation. This can be rationalized by considering the extra stability conferred on the O-protonated species by resonance, as shown in Scheme 2.5 for DMF. Protonation on nitrogen does not allow delocalisation of the resulting positive charge on the nitrogen. A detailed discussion of the arguments relating to the site of protonation has been presented by Homer and Johnson[77].

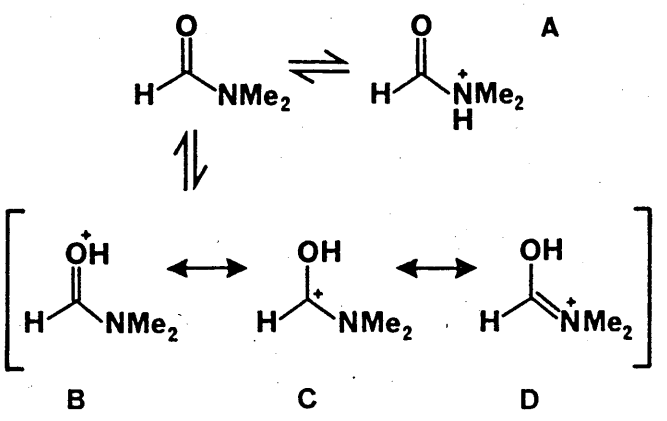

Scheme 2.5

It is interesting to ascertain whether the sites of silylation and protonation are the same. The two singlets observed for the N-methyl carbon and proton atoms result from hindered rotation about the amide $(C=O)-NR_2$ bond, which has partial double bond character. Total line shape analysis of variable temperature n.m.r. data provides an estimate for the barrier to rotation (about 80 kJ mol^{-1}) for this bond in DMF, compared with 270 kJ mol^{-1} for rotation about dideuteroethylene[78]. The magnetic non-equivalence of the two methyl groups results from differential shielding by the adjacent carbonyl group. The deshielding effects of C=O are thought to arise from either magnetic anisotropy, electric dipole effects (C^+-O^-) or paramagnetism centred on the carbon atom[78]. Nuclear Overhauser effects have been used to assign the chemical shifts of each methyl groups[78].

The separation, in Hertz, between the two methyl resonances is shown for all DMF/TMSX mixtures in Tables 2.1, 2.2 and 2.3 for both carbon and proton n.m.r. data. This separation increases in both nuclei as the proportion of silane increases for X=Br, I, OSO_2CF_3. O-silylation is expected to increase the $OC-NMe_2$ bond strength by increasing the proportion of resonance form D (Scheme 2.5) and thus heighten the barrier to rotation. This may explain the observed increase in separation of the methyls, although it should not be taken as evidence, <u>a priori</u>, since silylation on nitrogen could conceivably restrict rotation due to the additional steric bulk created on nitrogen. The latter argument may not be a valid one however, in view of the studies by Hausman and Yoder on the structure and dynamics of N-^{t}butyldimethylsilyl-, N-methylamides[79]. These authors showed that the barriers to rotation about the $OC-NR_2$ bond are lower in those species with highly hindered nitrogen than in the

analogous N-trimethylsilyl derivatives. Similar findings were obtained by Stewart and Siddall using N-alkyl, N-methylformamides[80]. These compounds are not strictly analogous to those studied here, but the results do suggest that steric effects on nitrogen are probably not very important in the DMF/TMSX case.

McClelland and Reynolds[81] attributed the general deshielding of the two methyl groups to the positive charge on nitrogen resulting from O-protonation; quoting the studies of Pugmire and Grant[82], who concluded that direct protonation on N causes upfield shifts in attached methyls. The shift changes observed here are consistent with McClelland and Reynolds's protonation data except that i) small downfield shifts, instead of upfield shifts, of the carbonyl carbon and formyl proton were found in this study; and ii) the methyl closest to the carbonyl experienced greater downfield shifts than its neighbour. The anomalous behaviour could conceivably be taken as evidence for N-silylation since this would increase the carbonyl character of the C=O bond and thus deshield the carbon. O-silylation on the other hand is expected to make the carbon and the formyl proton more like an amidate species $H\text{-}C(\text{-}O\text{-})=N^{+}R_2$ (chemical shifts ca. 7-8 ppm for ^{1}H, ca. 150-160 ppm for ^{13}C)[83]. However N-silylation should not cause differential deshielding of the N-methyls, thus if O-silylation is occurring it must be causing the increased deshielding in nuclei adjacent to C=O. Other arguments can be envisaged but it is clear that neither the ^{1}H nor the ^{13}C data can be interpreted unambiguously.

A preliminary investigation of the DMF/TMSI system was undertaken, using oxygen-17 n.m.r., in order to clarify the situation. Oxygen-17 nuclei are

not so easy to observe as silicon-29 nuclei owing to low receptivity, although relaxation times are generally very fast. The chemical shift range from +900 to -50 ppm (water as reference) encompasses most ^{17}O nuclei, with the more highly deshielded species at higher frequencies[84]. A good correlation is found between the formal π bond order of a particular species and the degree of deshielding in ^{17}O [84], hence C=O groups are considerably deshielded with respect to C-O-. Silicon is known to cause shielding in adjacent oxygen, ethoxysilanes $[Si(CH_3)_{4-n}(OEt)_n]$ show an increased shielding of between -33 (n=1) and -48 (n=4) when compared with the analogous ethoxyalkanes.

The addition of a 2 molar excess of TMSI to DMF in CD_2Cl_2 caused an upfield shift of 107 ppm, consistent with O-silylation. Solvent effects are unlikely to be responsible for such a large shielding increase; water for instance experiences maximum solvent shifts of -10 to +20 ppm due to hydrogen bonding.

The very broad nature of the silylated DMF ^{17}O peak suggests that moderately fast exchange is taking place between free and silylated DMF. This conclusion agrees very well with the broad peak observed in the ^{29}Si n.m.r. for a similar DMF:TMSI ratio.

The cyclic amide, 1-methyl-2-pyrrolidone (NMP, N-methylpyrrolidinone), exhibits very similar chemical shift trends in the carbon and proton n.m.r. spectra of NMP/TMSX (X=I, OTf) mixtures, compared with those observed for DMF. The data are presented in Tables 2.4 and 2.5. In NMP itself the C_4-H and C_5-H protons are present as a complicated multiplet. Silylation reveals the C_4-H quintet and the C_5-H triplet owing

Table 2.4

Interaction between 1-Methyl-2-pyrrolidone (NMP) and Trimethylsilyl triflate (TMSOTf) : N.M.R. Data

NMP

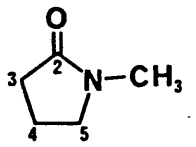

δ(ppm)		Ratio of NMP : TMSOTf 5:0	5:1	1:1	1:5
^{1}H	$C_3(H)-C=O$	3.40t	3.52t	3.89t	3.93t
	$^{3}J_{HH}$	6.8Hz	7.1Hz	7.8Hz	7.3Hz
	$N-CH_3$	2.84	2.88	3.11	3.14
	$C_5(H)-N$	1.94-2.43m	1.98-2.54m	2.97t	3.02t
	$^{3}J_{HH}$	obscured[a]	obscured[a]	7.8Hz	7.8Hz
	C_4-H	1.94-2.43m	1.98-2.54m	2.32qn	2.36qn
	$^{3}J_{HH}$	obscured[a]	obscured[a]	7.1Hz	7.1Hz
	$Si-(CH_3)_3$	-	0.51	0.49	0.49
^{13}C	C=O	174.8	174.8	175.8	176.3
	$N-CH_3$	49.3	50.0	52.9	53.4
	C_3	30.6	30.8	32.2	32.7
	C_5	29.4	29.9	31.4	31.7
	C_4	17.7	17.5	17.1	17.2
	CF_3	-	nr	120.9q	120.0q
	$^{1}J_{CF}$	-	nr	320Hz	319Hz
	$Si-(CH_3)_3$	-	0.0	0.0	0.29
^{29}Si	$Si-(CH_3)_3$	-	39.2	39.4	43.0
quantities used:					
NMP (mmoles)		2.2	11.0	2.2	0.44
TMSOTf (mmoles)		-	2.2	2.2	2.2
solvent: $CDCl_3$, 2.0 ml					

[a] complex coupling, not resolved.

Table 2.5

Interaction between 1-Methyl-2-pyrrolidone (NMP) and Iodotrimethylsilane (TMSI) : N.M.R. Data

NMP 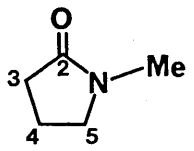

		Ratio of NMP : TMSI			
δ(ppm)		5:0	5:1	1:1	1:5
^{1}H	$C_3(H)-C=O$	3.40t	3.56t	4.11t	4.08t
	$^{3}J_{HH}$	6.8Hz	7.2Hz	7.6Hz	7.6Hz
	$N-CH_3$	2.84	2.92	3.23	3.20
	$C_5(H)-N$	1.94-2.43m	2.04-2.63m	3.3m[a]	3.3m[a]
	C_4-H	1.94-2.43m	2.04-2.63m	2.45qn	2.42qn
	$^{3}J_{HH}$	obscured[b]	obscured[b]	7.0Hz	7.4Hz
	$Si-(CH_3)_3$	-	0.58	0.60	0.76
^{13}C	C=O	174.8	175.3	176.0	175.9
	$N-CH_3$	49.3	50.4	53.9	53.8
	C_3	30.6	31.1	33.8	33.7
	C_5	29.4	30.4	33.1	33.0
	C_4	17.7	17.6	17.3	17.1
	$Si-(CH_3)_3$	-	1.0	1.3	4.9
^{29}Si	$Si-(CH_3)_3$	-	39.7	38.9(sbr)	9.8
quantities used:					
NMP (mmoles)		2.2	11.0	2.2	0.44
TMSI (mmoles)		-	2.2	2.2	2.2
solvent: $CDCl_3$, 2.0 ml					

[a] obscured by the $N-CH_3$ peak.

[b] complex coupling, not resolved.

to the downfield shift of the C_5-H protons. The C_4-H carbon and proton are the only nuclei not to be significantly deshielded because they are remote from the site of silylation. The larger downfield shifts of those nuclei close to the carbonyl group are consistent with the earlier hypothesis that silylation on oxygen causes enhanced deshielding of adjacent nuclei. Rotation about the C(O)-N bond is not possible in this case.

Shielding changes are comparable between the iodide and triflate counterions, although the former may have a slightly higher equilibrium constant for adduct formation. This can be deduced from a detailed comparison of the silylation shifts; the iodide generally requires a smaller amount of NMP to induce a certain shift change. A trend comparable to that observed in DMF, towards a single chemical shift irrespective of counterion, is again observed in the silicon-29 n.m.r. data, although the limiting value is some 4.5 ppm upfield in the case of NMP.

1-methyl-2-pyridinone (N-methylpyridone, NMPO or 1,2-dihydro-1-methyl-2-oxopyridine) can be thought of as a cyclic amide or as an N-substituted pyridine. It can exist in two tautomeric forms (Scheme 2.6) although the oxo tautomer (Scheme 2.6A) is the predominant one[85].

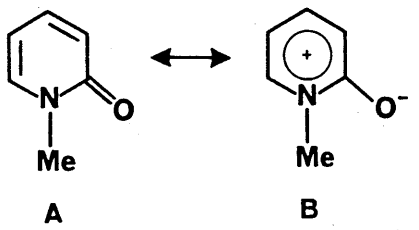

Scheme 2.6

The proton and carbon-13 n.m.r. chemical shift changes that occur in NMPO, as a result of silylation by TMSOTf, (Table 2.6) are somewhat complex. A general deshielding is apparent in the proton and carbon spectra except for C_5 and C=O (Figure 2.1).

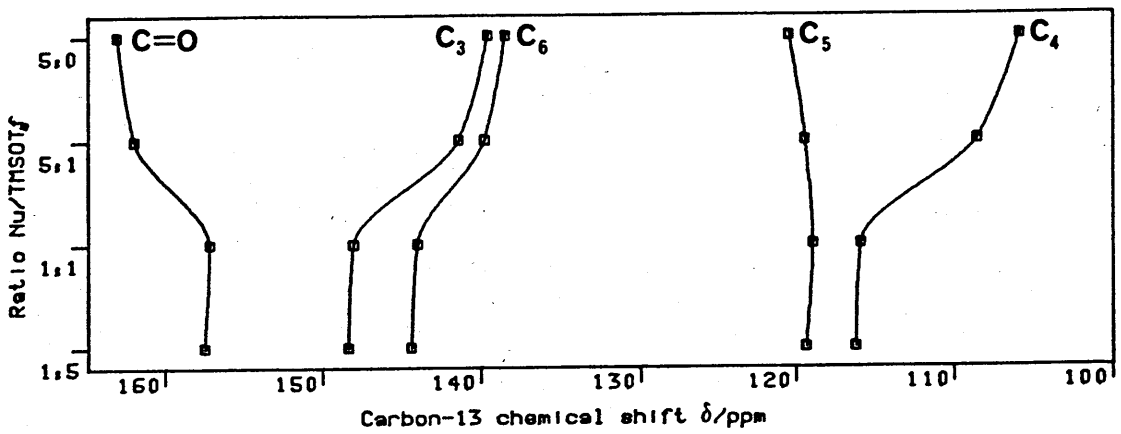

Figure 2.1 Carbon-13 chemical shift changes resulting from silylation of NMPO.

The complexity of the chemical shift changes makes the assignment uncertain, nonetheless the trends are consistent with silylation on the oxygen atom. The carbonyl carbon is substantially shifted to lower frequency in the silylated species, implying that the double bond character of carbonyl group has been reduced, and the changes in C_3 and $N-CH_3$ are the same as was observed above for NMP/TMSX (X=I, OTf). The variation of the chemical shift observed in the remaining carbons may be rationalised by assuming that the positive charge produced by silylation is delocalised, mesomerically and inductively, into the ring system, the inductive effect being more pronounced at those carbon atoms which are closer to the amide moiety.

Table 2.6

Interaction between 1-Methyl-2-pyridone (NMPO) and Trimethylsilyl triflate (TMSOTf) : N.M.R. Data

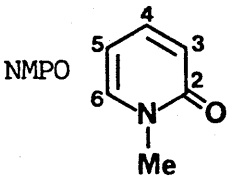

		Ratio of NMPO : TMSOTf			
δ(ppm)		5:0	5:1	1:1	1:5
^{1}H	$C_{5,6}$-H	7.25-7.44m	7.45-7.65m	8.32-8.56m	8.28-8.54m
	C_3-H	6.55d,d	6.68d	7.33-7.50m[a]	7.32-7.48m[a]
	J_{HH}	9.8Hz,1.4Hz	8.8Hz	no	no
	C_4-H	6.15t,d	6.42t,d	7.33-7.50m[a]	7.32-7.48m[a]
	J_{HH}	6.8Hz,1.4Hz	6.6Hz,1.2Hz	no	no
	N-CH_3	3.54	3.65	4.07	4.05
	Si-$(CH_3)_3$	-	0.55	0.54	0.48
^{13}C	C=O	163.1	162.0	157.2	157.5
	C_3	139.6	141.4	148.1	148.4
	C_6	138.5	139.8	144.0	144.4
	C_5	120.5	119.5	119.0	119.4
	C_4	105.9	108.6	116.0	116.3
	CF_3	-	nr	120.8q	119.1q
	$^{1}J_{CF}$	-	nr	321Hz	317Hz
	N-CH_3	37.6	38.4	41.6	41.8
	Si-$(CH_3)_3$	-	0.0	-0.23	0.0
^{29}Si	Si-$(CH_3)_3$	-	35.9	35.8	44.0(br)
quantities used:					
NMPO (mmoles)		2.2	11.0	2.2	0.44
TMSOTf (mmoles)		-	2.2	2.2	2.2
solvent: $CDCl_3$, 2.0 ml					

[a] multiplet, not resolved.

Despite some minor anomalies, the evidence for O-silylation in amides is very strong. This is not unexpected in view of the results from protonation studies, and the very strong Si-O bond which confers additional thermodynamic stability on the O-silylated adducts (Scheme 2.7). The formation of 1:1 ionic adducts between amides and TMSX (X=Br, I, OTf) appears to be a general phenomenon for this class of nucleophiles. The lack of significant complexation in the amide/TMSCl systems can be attributed to a low equilibrium constant for adduct formation, though the investigations carried out here are uninformative about the nature of any amide-TMSCl complex.

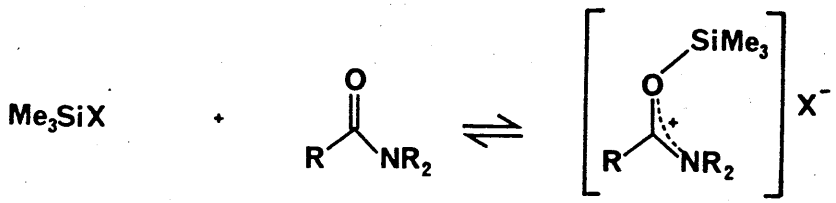

Scheme 2.7

2.3 Ureas

The interactions between TMSOTf and three ureas were studied.

i) 1,1,3,3-tetramethylurea (TMU, Table 2.7)

ii) 1,3-dimethyl-2-imidazolidinone (DMEU, Table 2.8)

iii) 1,3-dimethyl-3,4,5,6-tetrahydro-2(1H)-pyrimidinone (DMPU, Table 2.9)

Stabilization of the charge induced by silylation is more efficient in ureas than in similar amides since the delocalisation of charge can be extended to the additional nitrogen. Apart from the C_5 carbon in DMPU (compare with the C_4 carbon in NMP), a general deshielding of the

Table 2.7

Interaction between 1,1,3,3-Tetramethylurea (TMU) and Trimethylsilyl triflate (TMSOTf) : N.M.R. Data

TMU 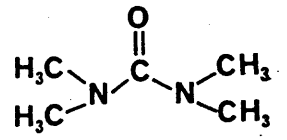

δ(ppm)		Ratio of TMU : TMSOTf 5:0	5:1	1:1	1:5
^{1}H	$N-CH_3$	2.81	2.88	3.14	3.13
	$Si-(CH_3)_3$	-	0.49	0.48	0.49
^{13}C	C=O	165.7	164.8	159.9	160.5
	CF_3	-	121.4q	121.0q	119.2q
	$^{1}J_{CF}$	-	321Hz	320Hz	317Hz
	$N-CH_3$	38.5	38.9	40.3	40.4
	$Si-(CH_3)_3$	-	0.4	0.3	0.0
^{29}Si	$Si-(CH_3)_3$	-	36.2	36.5	43.0
quantities used:					
TMU (mmoles)		2.93	2.93	2.93	2.93
TMSOTf (mmoles)		-	0.59	2.93	14.65
solvent: $CDCl_3$, 2.0 ml					

Table 2.8

Interaction between 1,3-Dimethyl-2-imidazolidinone (DMEU) and Trimethylsilyl triflate (TMSOTf) : N.M.R. Data

DMEU

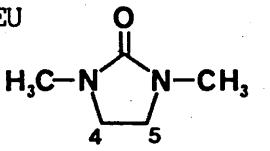

		Ratio of DMEU : TMSOTf			
δ(ppm)		5:0	5:1	1:1	1:5
^{1}H	$N-CH_3$	3.27	3.40	3.84	3.88
	$C_{4,5}-H$	2.78	2.80	2.96	2.97
	$Si-(CH_3)_3$	-	0.53	0.51	0.50
^{13}C	C=O	162.0	161.4	159.0	159.0
	CF_3	-	nr	120.1q	118.9q
	$^{1}J_{CF}$	-	nr	321Hz	317Hz
	$N-CH_3$	45.1	45.3	46.3	46.5
	$C_{4,5}$	31.5	31.5	32.2	32.3
	$Si-(CH_3)_3$	-	0.57	0.69	0.34
^{29}Si	$Si-(CH_3)_3$	-	40.0	40.1	43.1
quantities used:					
DMEU (mmoles)		2.2	11.0	2.2	0.44
TMSOTf (mmoles)		-	2.2	2.2	2.2
solvent: $CDCl_3$, 2.0 ml					

Table 2.9

Interaction between 1,3-Dimethyl-3,4,5,6-tetrahydro-2(1H)-pyrimidinone (DMPU) and Trimethylsilyl triflate (TMSOTf) : N.M.R. Data

DMPU

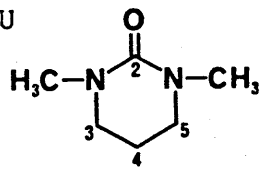

		Ratio of DMPU : TMSOTf			
δ(ppm)		5:0	5:1	1:1	1:5
^{1}H	$C_{4,6}$-H	3.25t	3.33t	3.60t	3.58t
	$^{2}J_{HH}$	6.0Hz	6.0Hz	6.0Hz	6.0Hz
	N-CH_3	2.92	2.95	3.11	3.10
	C_5-H	1.98qn	2.01qn	2.13qn	2.12qn
	$^{3}J_{HH}$	6.0Hz	5.9Hz	5.9Hz	5.8Hz
	Si-$(CH_3)_3$	-	0.50	0.48	0.50
^{13}C	C=O	156.8	156.4	154.4	154.7
	CF_3	-	nr	120.9q	119.1q
	$^{1}J_{CF}$	-	nr	321Hz	318Hz
	N-CH_3	47.9	48.0	48.3	48.3
	$C_{4,6}$	35.6	36.0	38.1	38.0
	C_5	22.2	21.7	19.7	19.8
	Si-$(CH_3)_3$	-	0.4	0.4	0.0
^{29}Si	Si-$(CH_3)_3$	-	36.5	36.6	43.1
quantities used:					
DMPU (mmoles)		2.2	2.2	2.2	2.2
TMSOTf (mmoles)		-	0.44	2.2	11.0
solvent: $CDCl_3$, 2.0 ml					

saturated carbons and their associated protons is observed upon silylation. In contrast to the amides however, a marked decrease in the chemical shift of the carbonyl carbon is observed on silylation. This difference in behaviour may be caused by two opposing trends, namely, the extra deshielding resulting from silylation and the shift towards an amidinium type carbon ($O-C=N^{+}-$). The latter effect is dominant in ureas since these molecules have extra canonical forms (Scheme 2.8).

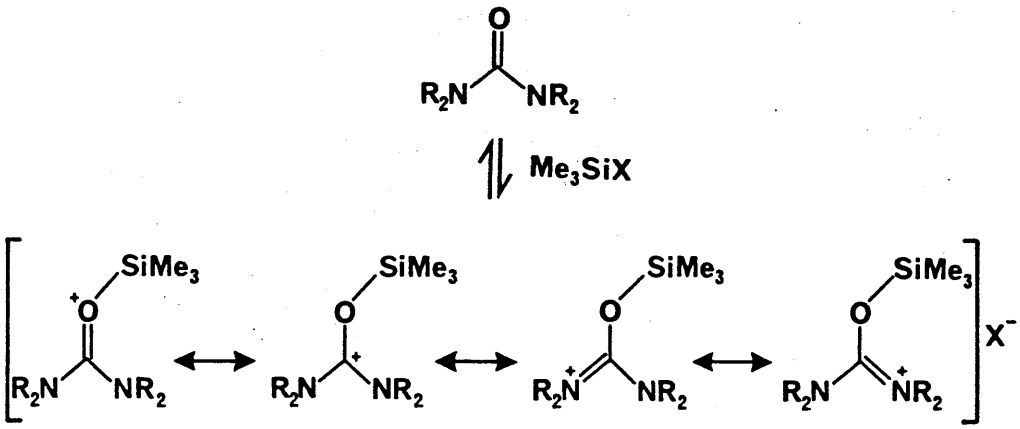

Scheme 2.8

Another interesting feature of the silyl interactions with both amides and ureas is the gradually decreasing silicon-29 n.m.r. value of the [nucleophile-TMS]$^{+}$OTf^{-} complex in the order DMF (44.0), DMEU (40.0), NMP (39.2), DMPU (36.5), TMU (36.2) and NMPO (35.9). The trend towards a single chemical shift, irrespective of counterion, shows that this is not simply due to different equilibrium constants for salt formation. Furthermore, in all nucleophile/TMSOTf interactions, the complex is almost fully formed at 1:1, ruling out any significant contributions from a secondary equilibrium with a highly shielded 5-coordinate species. Similarly, hydrolysis can be ruled out as a cause for the chemical shifts because (a) analytically pure salts have been isolated for numerous

amide/TMSOTf interactions by Simchen and co-workers[13]; and (b) the amount of hydrolysis, as monitored by the appearance of peaks attributable to hexamethyldisiloxane (HMDSO, ^{1}H, 0.06 ppm; ^{13}C, 1.95 ppm; ^{29}Si, 7.8 ppm) was not significant.

Comparisons between the electronic structure of each nucleophile show that, in general, those species which are better at stabilizing the positive charge produced by silylation also give lower frequency ^{29}Si n.m.r. chemical shifts for complex formation. Alternatively this effect can be stated as the ability of nucleophiles to donate an electron pair to form a donor-acceptor bond. A compilation of the relevant solvent properties for all nucleophiles and solvents used in this study is shown in the table in Appendix 4. Gutmann[49,50] only detailed donor numbers (DN) for two of the amides used in this study (DMF, 26.6 and NMP, 27.3) so a correlation would not be justified.

A more significant correlation (Figure 2.2) can be made between Taft's Beta value[60] and the ^{29}Si chemical shift of TMSOTf in the presence of a 5 molar excess of each nucleophile. The 1:1 value has been used for DMF since the 5:1 value appears to be an anomalous one. The limited number of points and the spread of data suggest that not too much significance should be placed on the relationship. Nevertheless there is a clear trend between the electronic factors mentioned above and the chemical shift. Calculation of the two unknown Beta values is possible from equation 2.1, for DMEU (0.75 ± 0.02) and DMPU (0.795 ± 0.02). The Beta/^{29}Si trends in relation to other nucleophiles will be discussed below.

$$^{29}Si[Nu\text{-}TMS]^{+}X^{-} = 95.5 - 74.6\ Beta(Nu) \quad .... \quad \text{equation 2.1}$$

Figure 2.2 Beta vs. Silicon-29 chemical shift correlation for TMSOTf complexes with amides and ureas.

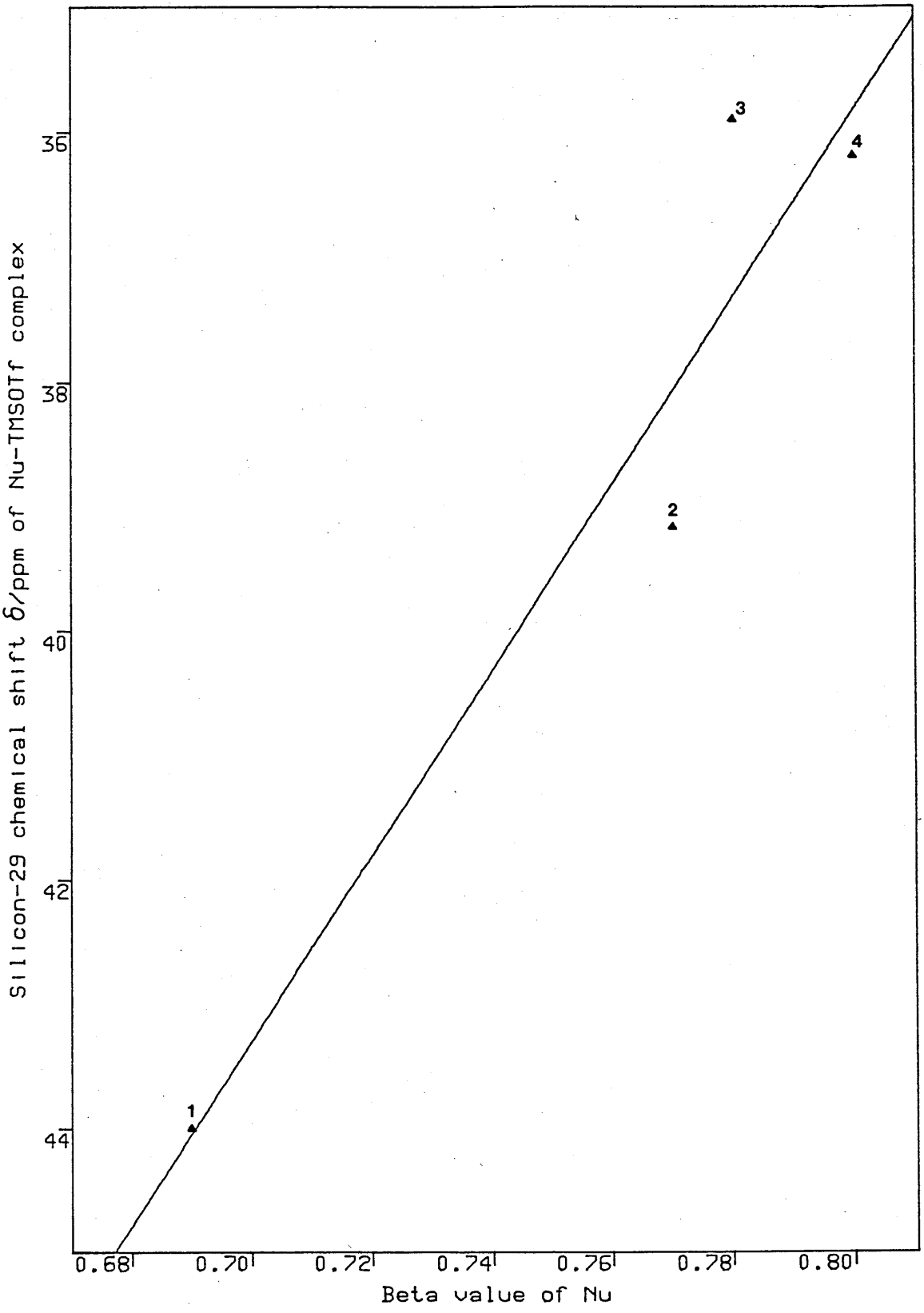

Nucleophiles: 1, DMF; 2, NMP; 3, NMPO; 4, TMU.

Solvent: chloroform. Variance = 1.1

Slope= -74.61 (s.d.= 12.7), intercept= 95.5 (s.d.= 9.6)

Figure 2.3 Chemical shift changes in amides and ureas resulting from silylation by TMSOTf (δ/ppm).

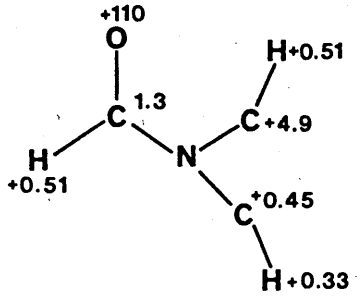

DMF

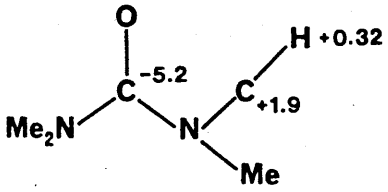

TMU

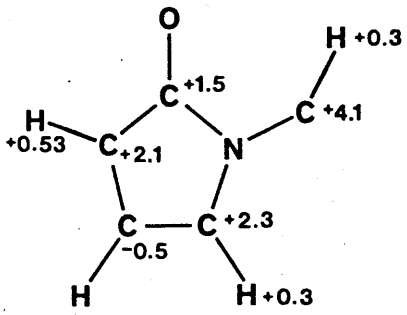

NMP

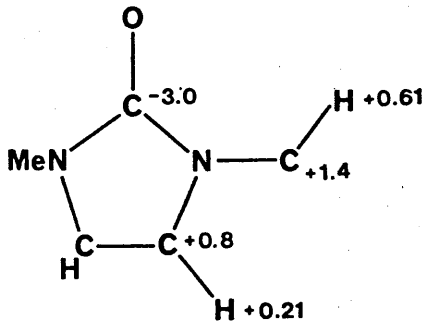

DMEU

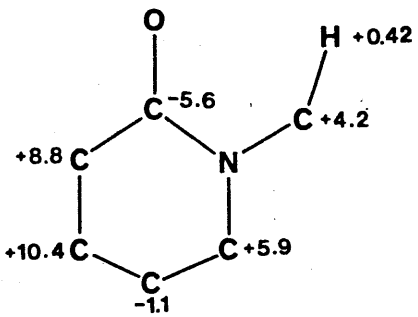

NMPO

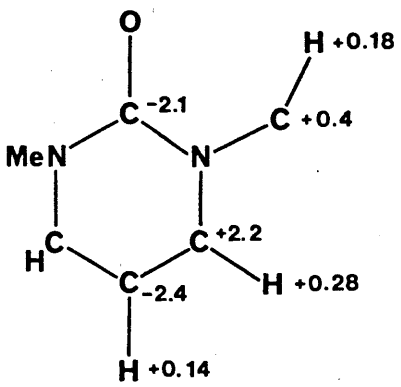

DMPU

In conclusion, the analysis of the urea/TMSOTf data shows that analogous considerations concerning complex formation with TMSX (X=Br, I, OTf) can be applied to the ureas as well as to the amides, not unexpectedly, since these two classes of nucleophiles are structurally similar. A summary of the ^{1}H and ^{13}C chemical shift changes that are produced by the silylation with TMSX is presented in Figure 2.3.

2.4 Pyridines

Breitmaier and Spohn[86] monitored the pH dependence of the carbon-13 chemical shifts of pyridine. The shielding trends for the C_4 and $C_{3,5}$ carbons followed the expected direction towards low field, as the pyridine ring became progressively more cationic due to protonation on nitrogen. However the $C_{2,6}$ carbons shifted to higher field in the protonated species. This apparently anomalous behaviour can be attributed to the utilization of the lone pair on nitrogen in forming the N-H bond, therefore destroying the magnetic anisotropy of the nitrogen[87] and causing decreased deshielding (i.e. increased shielding) of adjacent nuclei. Analogous changes were observed in quinoline and isoquinoline.

Perkampus and Kruger[88] found similar trends in the proton n.m.r. spectra of pyridine-Lewis acid complexes. The authors proposed that three factors were in operation:-

i) donation of nitrogen's lone pair to the Lewis acid resulting in a reduction in electron density, an effect which decreases rapidly with increasing distance from nitrogen;

ii) a small reduction in the ring current - felt equally by all protons;

iii) destruction of the shielding effects of nitrogen resulting in a deshielding of protons close to nitrogen.

The deshielding effect caused by the magnetic anisotropy of the nitrogen is manifested more strongly by the proton nuclei, because they only have one electron each to shield their nuclei from external fields, whereas a carbon atom has six.

A ^{1}H, ^{13}C and ^{29}Si chemical shift titration was carried out for the pyridine/TMSOTf system (Table 2.10) to investigate the effect of silylation on pyridine. The carbon-13 chemical shift trends presented in Figure 2.4 show that the effects on pyridine are similar for silylation and protonation. The titration was carried out in acetonitrile-d_3 because the resulting 1:1 complex is insoluble in chloroform. Simchen[13] has reported that silylation of acetonitrile by pyridine/TMSOTf mixtures is facile in diethylether (2 hours at 5 ^{o}C, 75% yield of silylated products) giving a mixture of products as illustrated in Scheme 2.9.

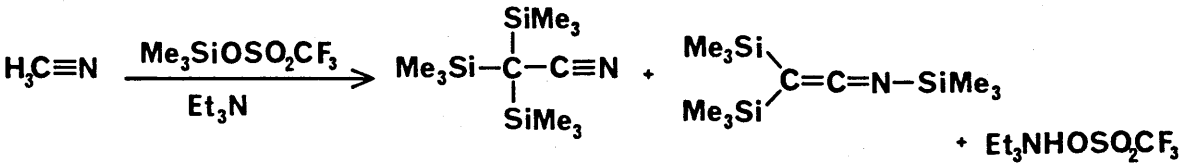

Scheme 2.9

This is surprising since detailed examination of the spectra from the pyridine/TMSOTf titration did not reveal any anomalous peaks. Simchen reported three peaks in the proton n.m.r. spectrum and assigned them to silylated acetonitrile (Scheme 2.9, 0.055, 0.14 and 0.17 ppm). An insignificant peak at 0.06 ppm was observed in this study, but this is attributed to very small amounts of hexamethyldisiloxane (HMDSO) produced by hydrolysis of TMSOTf. Moreover the intensity of the peak remained constant (in relation to both TMSOTf and the reference Me_4Si) throughout

Figure 2.4 Carbon-13 n.m.r. chemical shift titration: pyridine against TMSOTf.

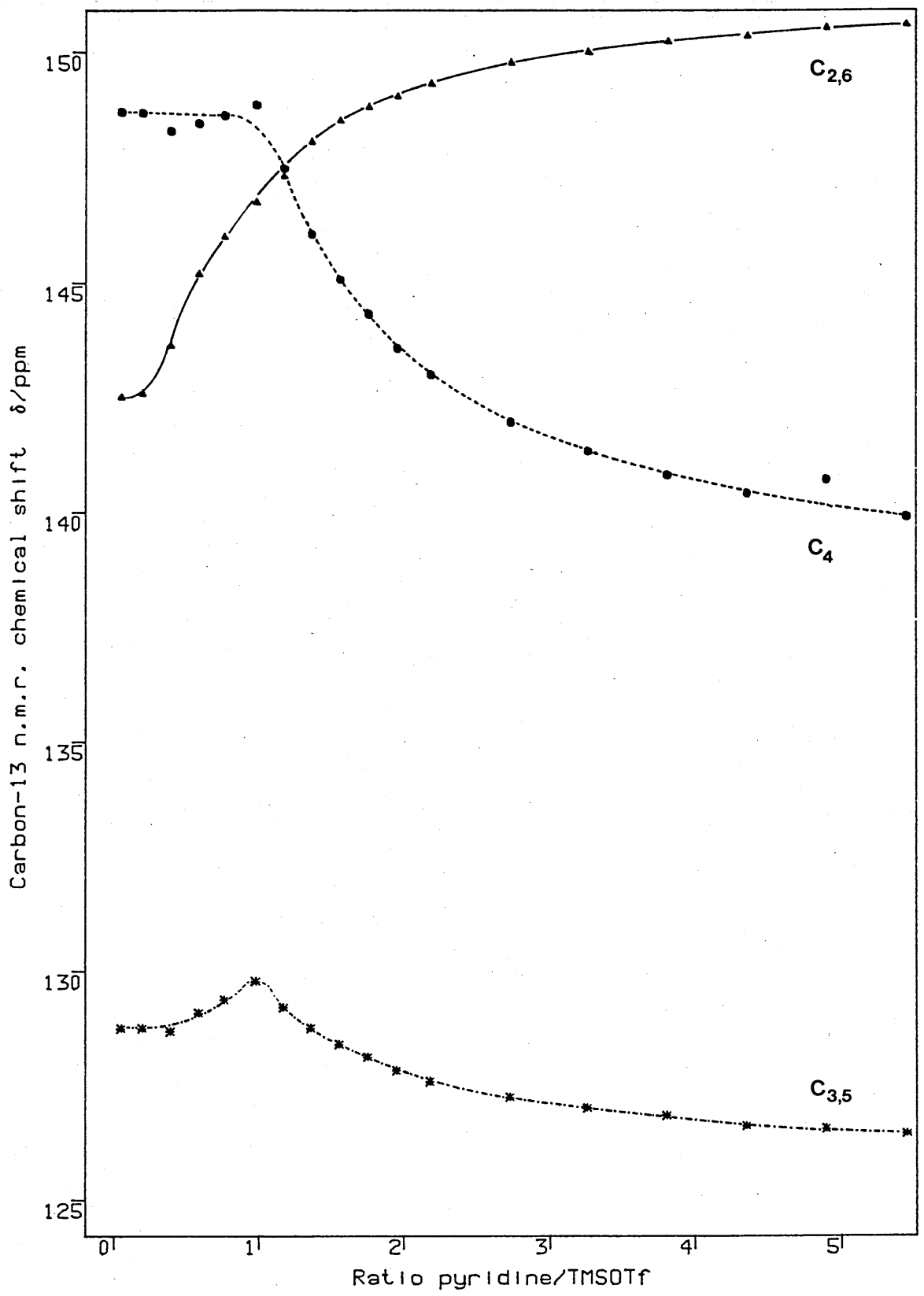

Solvent: acetonitrile-d3

Table 2.10

N.M.R chemical shift titration (^{1}H, ^{13}C, ^{29}Si): Trimethylsilyl triflate (TMSOTf) against Pyridine (py)

Volume py (ml)	Ratio TMSOTf:py	^{1}H	^{13}C			^{29}Si
		$Si(CH_3)_3$	$C_{2,6}$	C_4	$C_{3,5}$	$Si(CH_3)_3$
0.009	20.44:1	0.44	148.7	142.5	128.7	45.7
0.036	5.11:1	0.44	148.7	142.6	128.7	45.3
0.072	2.55:1	0.52	148.3	143.6	128.7	45.7
0.108	1.70:1	0.59	148.4	145.2	129.0	44.6
0.140	1.31:1	0.65	148.6	146.0	129.4	43.6
0.180	1.02:1	0.73	148.8	146.7	129.8	42.4
0.215	1:1.17	0.74	147.5	147.3	129.2	42.2
0.250	1:1.36	0.74	146.0	148.0	128.7	42.3
0.286	1:1.55	0.74	145.0	148.5	128.4	42.2
0.322	1:1.75	0.74	144.3	148.8	128.1	42.2
0.358	1:1.95	0.74	143.6	149.0	127.8	42.2
0.400	1:2.17	0.74	143.0	149.3	127.6	42.2
0.500	1:2.73	0.74	141.9	149.8	127.2	42.2
0.600	1:3.26	0.74	141.3	145.0	127.0	42.2
0.700	1:3.80	0.75	140.8	150.2	126.8	42.1
0.800	1:4.35	0.75	140.4	150.3	126.6	42.2
0.900	1:4.89	0.75	140.7	150.5	126.5	42.1
1.000	1:5.44	0.75	139.9	150.6	126.4	42.1

Solvent: acetonitrile-d_3

the titration (ca. 12 hours). It is difficult to rationalize the differences in behaviour observed between these two studies since the only significant difference appears to be the choice of solvent.

In order to rule out the possibility of hydrolysis and to ascertain that the chemical shift changes were reversible, a variable temperature ^{29}Si and ^{13}C n.m.r. study was undertaken for a pyridine/TMSBr system (1:1 stoicheiometry) in dichloromethane-d_2 (Table 2.11). At ambient probe temperature (300 K) this mixture displays chemical shifts characteristic of uncomplexed pyridine and TMSBr. A progressive temperature decrease, down to 180 K, induces chemical shift changes (displayed in Figures 2.5 and 2.6) which parallel those observed for the pyridine/TMSOTf system (Figure 2.4).

A small, solvent related, shift difference can be anticipated between the limiting silicon-29 chemical shifts of the two py-TMSX complexes and possibly a slight temperature dependence. However these effects are probably insufficient to completely account for the observed difference between the silicon-29 chemical shifts of the two adducts (X=OTf, 42.3 ppm; X=Br, 40.7 ppm at 180 K), which can be attributed to incomplete complexation of the py/TMSBr mixture at 180 K. The slightly broad nature of the silicon and carbon signals at this temperature confirms that this is the case. Furthermore, this explains why the chemical shifts of the $C_{2,6}$ and C_4 carbon nuclei fail to crossover in a similar manner to that observed in the py/TMSOTf system and protonation[86], although the same trends are apparent in each case. The silicon-29 n.m.r. spectrum of the mixture taken after warming back to ambient probe temperature (300 K)

Figure 2.5 Variable temperature carbon-13 n.m.r. data for a 1:1 mixture of Bromotrimethylsilane and Pyridine.

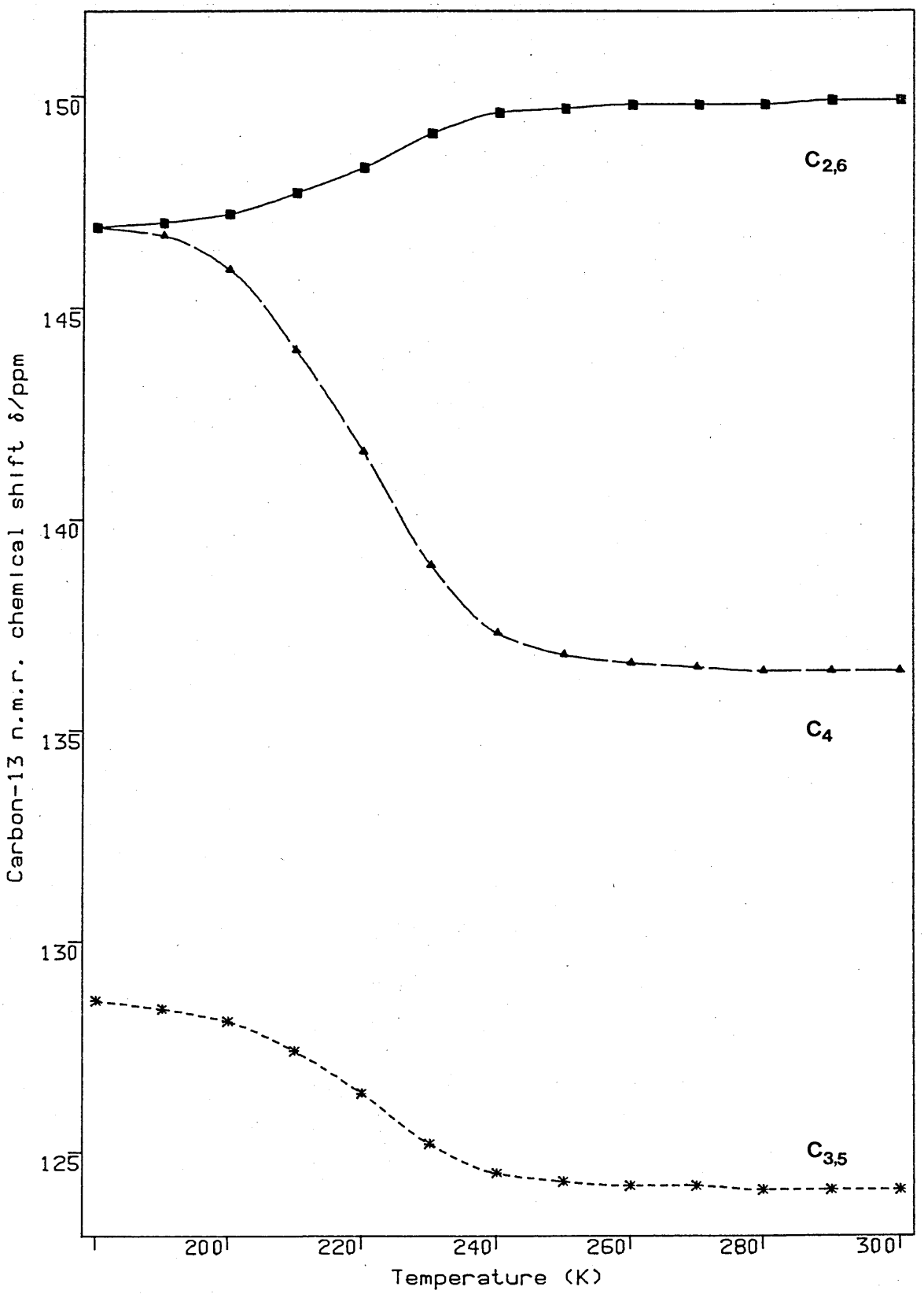

Figure 2.6 Variable temperature silicon-29 n.m.r. data for a 1:1 mixture of Bromotrimethylsilane and Pyridine.

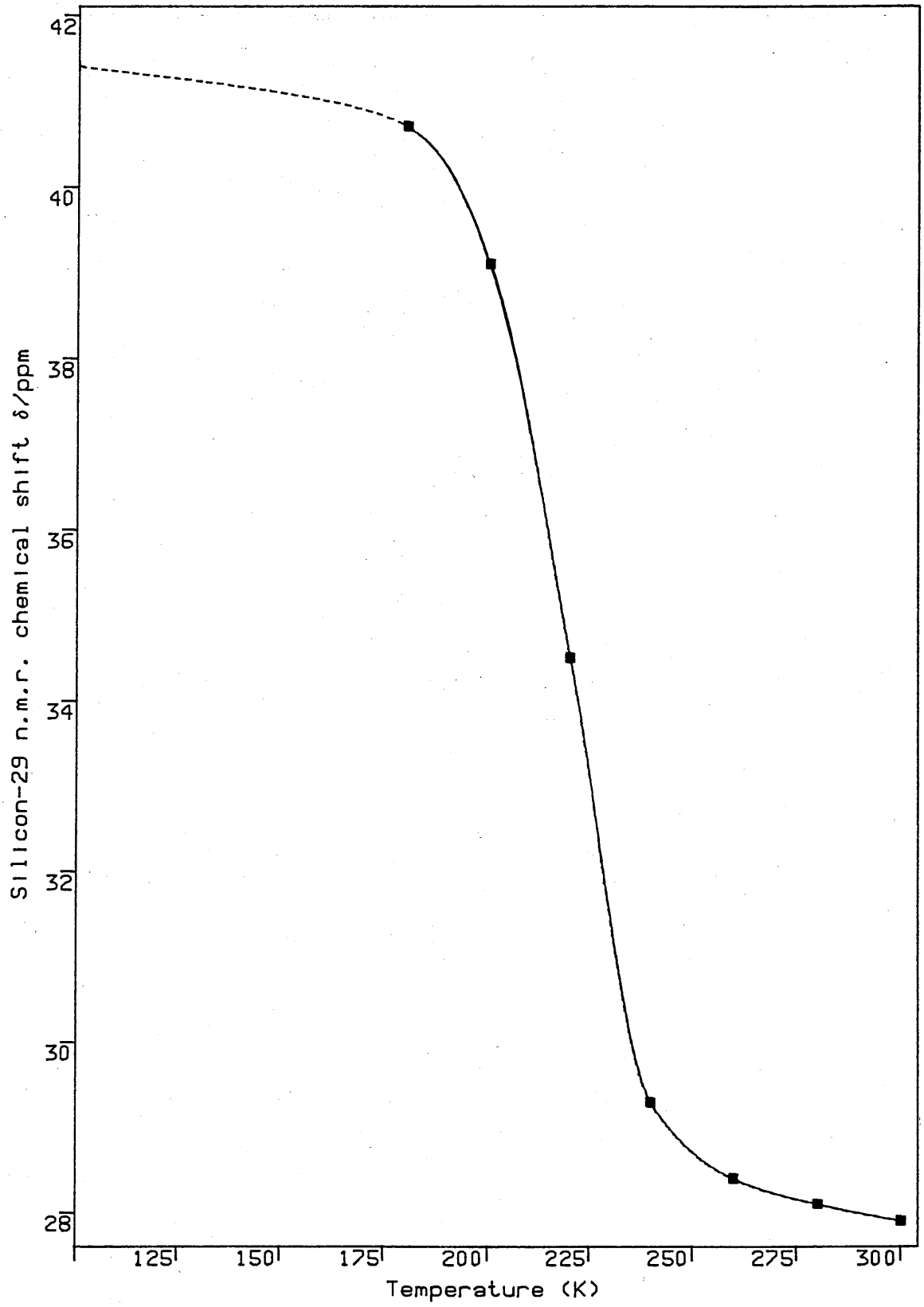

Solvent: dichloromethane-d2

..... Extrapolated curve.

Table 2.11

Variable Temperature N.M.R. Data for a 1:1 mixture of Pyridine (py) and Bromotrimethylsilane (TMSBr)

Temperature (K)	δ(ppm) ^{13}C				^{29}Si
	$C_{2,6}$	C_4	$C_{3,5}$	$Si-(CH_3)_3$	$Si-(CH_3)_3$
180	146.9	146.9	128.6	0.0	40.7
190	147.0	146.7	128.5	0.17	-
200	147.2	145.9	128.1	0.57	39.11
210	147.7	144.0	127.4	1.26	-
220	148.3	141.6	126.4	2.18	34.38
230	149.1	138.9	125.2	3.27	-
240	149.6	137.4	124.5	3.85	29.32
250	149.7	136.8	124.3	4.02	-
260	149.8	136.6	124.2	4.08	28.39
270	149.8	136.6	124.2	4.14	-
280	149.8	136.4	124.1	4.14	28.11
290	149.9	136.4	124.1	4.19	27.92[a]
300	149.9	136.4	124.9	4.19	27.92
py	150.2	136.0	124.0	-	-
TMSBr	-	-	-	4.2	27.6

quantities used: 1.1 mmoles of each component; solvent: CD_2Cl_2, 2.0 ml

[a] Recorded at 296K when warming back to ambient temperature.

confirmed that the chemical shift changes are fully reversible. An enthalpy change of -38 kJ mol^{-1} ($\pm$10 kJ mol^{-1}) and an entropy change of -160 ($\pm$40) J K^{-1} mol^{-1} can be calculated from a $\ln K_{eq}$ *vs.* 1/T plot (see Appendix 2).

Cooling a similar equimolar mixture of chlorotrimethylsilane and pyridine (in CD_2Cl_2) down to 180 K caused only a one ppm downfield shift in the silicon n.m.r. spectrum, and very small changes in the chemical shifts of the carbon nuclei (Table 2.12). Nevertheless these trends are fully consistent with a slight shift towards complex formation.

The structures of the adducts observed here between pyridine and TMSX (X=OTf, Br) are suggested to be identical to those of the analogous bromo- and iodo- complexes characterised by X-ray analysis[36] (Scheme 2.10).

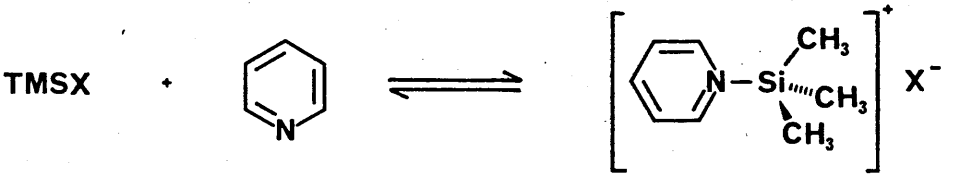

Scheme 2.10

The effect of silylation by TMSOTf was also studied for the following compounds:-

2,4-dimethylpyridine (2,4DMP or 2,4-lutidine, Table 2.13);

3,5-dimethylpyridine (3,5DMP, Table 2.14);

2,6-dimethylpyridine (2,6DMP, Table 2.15);

4-dimethylaminopyridine (DMAP, Table 2.17);

quinoline (Table 2.18); and

2,2-bipyridyl (BIPY, Table 2.19).

Table 2.12

Variable Temperature N.M.R. Data for a 1:1 mixture of Pyridine (py) and Chlorotrimethylsilane (TMSCl)

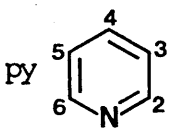

δ(ppm)		TMSCl	py	Temperature (K) 300	180
^{1}H	aromatic C-H	-	8.52-8.62m	8.50-8.63m	8.60-8.65m
		-	7.50-7.75m	7.50-7.76m	7.35-7.74m
		-	7.16-7.32m	7.20-7.30m	7.18-7.30m
	$Si-(CH_3)_3$	0.42	-	0.41	0.44(sbr)
^{13}C	$C_{2,6}$	-	150.2	150.1	150.0
	C_4	-	136.0	136.1	136.6
	$C_{3,5}$	-	124.0	124.0	124.3
	$Si-(CH_3)_3$	3.3	-	3.3	3.3
^{29}Si	$Si-(CH_3)_3$	31.1	-	31.3[a]	32.2
quantities used: 2.2 mmoles of each component; solvent: CD_2Cl_2, 2.0 ml					

[a] Recorded before lowering temperature and after warming back to ambient temperature.

Table 2.13

Interaction between 2,4-Dimethylpyridine (2,4DMP) and Trimethylsilyl triflate (TMSOTf) : N.M.R. Data

2,4DMP 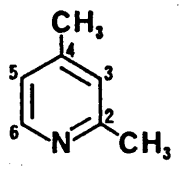

		Ratio of 2,4DMP : TMSOTf			
δ(ppm)		5:0	5:1	1:1	1:5
^{1}H	C_6-H	8.33d	8.35d	8.49d	8.44d
	$^{3}J_{56}$	5.1Hz	5.1Hz	5.6Hz	6.1Hz
	C_3-H	6.93	7.06	7.43	7.28
	C_5-H	6.87d	7.02d	7.39d	7.24d
	$^{3}J_{56}$	5.1Hz	5.1Hz	5.6Hz	6.1Hz
	C_2-CH_3	2.49	2.53	2.72	2.65
	C_4-CH_3	2.26	2.29	2.47	2.43
	Si-$(CH_3)_3$	-	0.80	0.70	0.52
^{13}C	C_2	158.0	157.7	154.9	153.0
	C_6	148.8	148.3	147.1	147.4
	C_4	147.2	149.5	157.4	157.5
	C_3	124.1	125.3	128.2	127.0
	C_5	121.7	122.6	124.5	123.8
	CF_3	-	117.0q	118.0q	118.7q
	$^{1}J_{CF}$	-	318Hz	318Hz	317Hz
	C_2-$\underline{C}H_3$	24.2	23.9	23.3	23.4
	C_4-$\underline{C}H_3$	20.9	20.9	21.4	21.4
	Si-$(CH_3)_3$	-	0.75	0.69	0.34
^{29}Si	Si-$(CH_3)_3$	-	39.1	40.8	43.3
quantities used:					
2,4DMP (mmoles)		2.2	11.0	2.2	0.44
TMSOTf (mmoles)		-	2.2	2.2	2.2
solvent: $CDCl_3$, 2.0 ml					

Table 2.14

Interaction between 3,5-Dimethylpyridine (3,5DMP) and Trimethylsilyl triflate (TMSOTf) : N.M.R. Data

3,5DMP 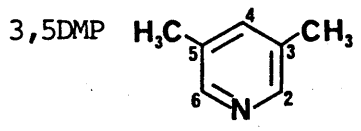

		Ratio of 3,5DMP : TMSOTf			
δ(ppm)		5:0	5:1	1:1	1:5
^{1}H	$C_{2,6}$-H	8.22	8.30	8.53	8.52
	C_4-H	7.21	7.43	8.11	8.12
	$C_{3,5}$-CH_3	2.22	2.30	2.56	2.58
	Si-$(CH_3)_3$	-	0.80	0.77	0.56
^{13}C	$C_{2,6}$	147.4	146.4	142.9	142.5
	C_4	137.0	139.3	147.3	147.9
	$C_{3,5}$	132.4	133.9	138.7	139.1
	CF_3	-	nr	120.8q	118.9q
	$^{1}J_{CF}$	-	nr	321Hz	317Hz
	$C_{3,5}$-CH_3	18.1	18.2	18.3	18.4
	Si-$(CH_3)_3$	-	-1.0	-0.92	0.0
^{29}Si	Si-$(CH_3)_3$	-	41.0	41.2	43.3
quantities used:					
3,5DMP (mmoles)		2.2	11.0	2.2	0.44
TMSOTf (mmoles)		-	2.2	2.2	2.2
solvent: $CDCl_3$, 2.0 ml					

Table 2.15

Interaction between 2,6-Dimethylpyridine (2,6DMP) and Trimethylsilyl triflate (TMSOTf) : N.M.R. Data

2,6DMP 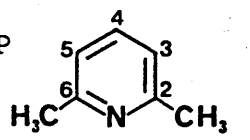

		Ratio of 2,6DMP : TMSOTf			
δ(ppm)		5:0	5:1	1:1	1:5
^{1}H	C_4-H	7.41t	7.42t	7.43t	7.59t
	$^{3}J_{4(5,3)}$	7.8Hz	7.7Hz	7.8Hz	7.8Hz
	C_3-H	6.90d	6.91d	6.92d	6.98d
	$^{3}J_{(3,4)(4,5)}$	7.8Hz	7.8Hz	7.8Hz	7.8Hz
	$C_{2,6}$-CH_3	2.50	2.51	2.50	2.52
	Si-$(CH_3)_3$	-	0.48	0.48	0.50
^{13}C	$C_{2,6}$	157.6	157.6	157.7	157.8
	C_4	136.4	136.6	136.7	137.8
	$C_{3,5}$	120.1	120.2	120.3	120.9
	CF_3	-	nr	118.7q	118.4q
	$^{1}J_{CF}$	-	nr	317Hz	317Hz
	$C_{2,6}$-CH_3	24.5	24.4	24.4	23.9
	Si-$(CH_3)_3$	-	0.23	0.23	0.29
^{29}Si	Si-$(CH_3)_3$	-	43.1	43.4	43.5
quantities used:					
2,6DMP (mmoles)		2.2	11.0	2.2	0.44
TMSOTf (mmoles)		-	2.2	2.2	2.2
solvent: $CDCl_3$, 2.0 ml					

Table 2.16

Interaction between 2,6-Dimethylpyridine (2,6DMP) and Iodotrimethylsilane (TMSI) : N.M.R. Data

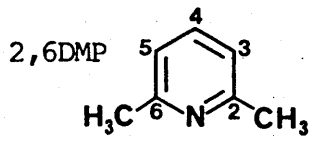

		Ratio of 2,6DMP : TMSI			
δ(ppm)		5:0	5:1	1:1	1:5
^1H	C_4-H	7.41t	7.35t	7.45t	7.60t
	$^3J_{4(5,3)}$	7.8Hz	7.7Hz	7.1Hz	7.6Hz
	C_3-H	6.90d	6.85d	6.93d	7.05d
	$^3J_{(3,4)(4,5)}$	7.8Hz	7.3Hz	7.1Hz	7.6Hz
	$C_{2,6}$-CH_3	2.50	2.46	2.51	2.62
	Si-$(CH_3)_3$	-	0.73	0.78	0.80
^{13}C	$C_{2,6}$	157.6	157.4	157.3	156.8
	C_4	136.4	136.3	136.7	138.0
	$C_{3,5}$	120.1	119.9	120.2	121.0
	$C_{2,6}$-CH_3	24.5	24.4	24.2	23.5
	CF_3	-	nr	nr	nr
	Si-$(CH_3)_3$	-	5.5	5.6	5.6
^{29}Si	Si-$(CH_3)_3$	-	9.1	9.3	9.7
quantities used:					
2,6DMP(mmoles)		2.2	11.0	2.2	0.44
TMSI (mmoles)		-	2.2	2.2	2.2
solvent: $CDCl_3$, 2.0 ml					

Table 2.17

Interaction between 4-Dimethylaminopyridine (DMAP) and Trimethylsilyl triflate (TMSOTf) : N.M.R. Data

DMAP 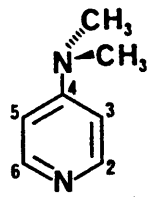

δ(ppm)		Ratio of DMAP : TMSOTf 5:0	5:1	1:1	1:5
^{1}H	$C_{2,6}$-H	8.20d,d	8.17d	8.15d	8.16d
	$C_{3,5}$-H	6.53d,d	6.58d,d	7.05d	7.05d
	$^{5}J_{HH}$	1.7Hz	1.5Hz	no	no
	$^{3}J_{HH}$	5.1Hz	5.4Hz	7.8Hz	7.8Hz
	N-CH_3	3.04	3.02	3.28	3.26
	Si-$(CH_3)_3$	-	0.60	0.63	0.62[a]
	Si-$(CH_3)_3$*	-	no	no	0.51[b]
^{13}C	C_4	154.8	154.7	156.9	157.5
	$C_{2,6}$	147.9	148.2	143.3(br)	142.9(br)
	$C_{3,5}$	106.6	107.0	108.4(br)	108.9(br)
	CF_3	-	nr	120.9q	120.4q
	$^{1}J_{CF}$	-	nr	321Hz	318Hz
	N-CH_3	39.2	39.1	40.0	40.1(sbr)
	Si-$(CH_3)_3$	-	-1.0	-1.1	-1.1[a]
	Si-$(CH_3)_3$*	-	no	no	0.26[b]
^{29}Si	Si-$(CH_3)_3$	-	31.7	31.7	31.8[a]
	Si-$(CH_3)_3$*	-	no	no	44.5[b]
quantities used:					
DMAP (mmoles)		2.51	2.51	2.51	2.51
TMSOTf (mmoles)		-	0.50	2.51	12.55
solvent: $CDCl_3$, 2.0 ml					

Intensity of peak[a] is ca. 20% that of peak[b].

Table 2.18

Interaction between Quinoline and Trimethylsilyl triflate (TMSOTf) :

N.M.R. Data

Quinoline 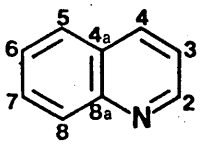

		Ratio of Quinoline : TMSOTf			
δ(ppm)		5:0	5:1	1:1	1:5
^{1}H	aromatic C-H	8.82-8.89m	8.83-8.88m	8.88-8.94m	8.95-9.00m
		7.16-8.17m	7.22-8.10m	7.31-8.21m	7.51-8.45m
	$Si-(CH_3)_3$	-	0.63	0.49	0.50
^{13}C	C_2	150.3	150.3	150.1	150.2
	C_{8a}	148.3	148.0	147.6	147.1
	C_4	135.8	136.4	136.6	139.4
	C_8	130.1	129.6	129.6	130.9
	C_7	129.3	129.2	128.7	128.6
	C_{4a}	128.5	128.3	128.2	no
	C_5	127.7	127.9	127.8	127.3
	C_6	126.4	126.7	126.6	126.9
	C_3	120.9	121.1	121.0	121.4
	CF_3	-	nr	118.4q	118.2q
	$^{1}J_{CF}$	-	nr	317Hz	318Hz
	$Si-(CH_3)_3$	-	0.0	-0.23	-0.29
^{29}Si	$Si-(CH_3)_3$	-	41.9	43.5	43.5
quantities used:					
Quinoline (mmoles)		2.2	11.0	2.2	0.44
TMSOTf (mmoles)		-	2.2	2.2	2.2
solvent: $CDCl_3$, 2.0 ml					

Table 2.19

Interaction between 2,2-Bipyridyl (BIPY) and Trimethylsilyl triflate (TMSOTf) : N.M.R. Data

BIPY 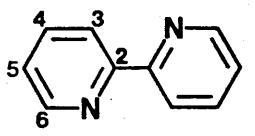

		Ratio of BIPY : TMSOTf			
δ(ppm)		5:0	5:1	1:1	1:5
^{1}H	aromatic C-H	8.64-8.72m	8.63-8.71m	8.65-8.70m	8.63-8.68m
		8.35-8.46m	8.36-8.45m	8.36-8.45m	8.37-8.45m
		7.81-7.90m	7.69-7.89m	7.70-7.89m	7.70-7.89m
		7.21-7.79m	7.20-7.35m	7.20-7.35m	7.21-7.35m
	$Si-(CH_3)_3$	-	0.47	0.47	0.47
^{13}C	C_2	156.2	156.1	156.1	156.0
	C_6	149.2	149.2	149.2	149.1
	C_4	136.9	136.9	137.0	137.0
	C_3	123.7	123.7	123.8	123.8
	C_5	121.1	121.1	121.1	121.1
	CF_3	-	nr	nr	118.4q
	$^{1}J_{CF}$	-	nr	nr	317Hz
	$Si-(CH_3)_3$	-	0.29	0.23	0.0
^{29}Si	$Si-(CH_3)_3$	-	43.5	43.4	43.7
quantities used:					
BIPY (mmoles)		1.31	1.31	1.31	1.31
TMSOTf (mmoles)		-	0.26	1.31	6.55
solvent: $CDCl_3$, 2.0 ml					

The carbon-13 chemical shift trends resulting from silylation of 2,4DMP, 3,5DMP and DMAP were entirely in accord with those observed in the pyridine/TMSX (X=Br, OTf) mixtures. Chemical shift assignments of the isolated nucleophiles are those of Batterham[85]. The different carbon-13 n.m.r. peak heights of the various substituted pyridines confirmed the assignments in the silylated species. The carbon silylation shifts are presented in Figure 2.7 for 2,4DMP, 3,5DMP, DMAP and pyridine N-oxide (PNO) (see subsequent discussion concerning PNO).

The silicon-29 chemical shifts of the various substituted pyridines can be correlated with Beta (cf. discussion on amides and ureas). The resulting plot is presented in Figure 2.8. Taft did not quote a Beta value for 3,5DMP in his latest compilation of solvochromatic parameters[60] so a value for 3,5DMP (Beta = 0.70 calculated from a pKa value of 6.14) was calculated from equation 2.2, which was derived from the Beta vs. pKa correlation plot shown in Figure 2.9.

$$\text{Beta} = 0.352 + 0.0561\ \text{pKa} \qquad \ldots\ldots \qquad \text{equation 2.2}$$

A fairly good correlation was also observed between the silicon-29 chemical shift of each complex and the pKa of the parent pyridine (Figure 2.10). The silicon-29 n.m.r. chemical shift of the respective $[\text{Nu-TMS}]^{+}X^{-}$ adduct can be calculated using equations 2.3 and 2.4, which were derived from the two previous correlations.

$$^{29}\text{Si (Nu-TMSOTf)} = 73.4 - 47.27\ \text{Beta(Nu)} \qquad \ldots \qquad \text{equation 2.3}$$

$$^{29}\text{Si (Nu-TMSOTf)} = 55.4 - 2.45\ \text{pKa(Nu)} \qquad \ldots \qquad \text{equation 2.4}$$

Figure 2.7

Carbon-13 n.m.r. chemical shift changes of some substituted pyridines resulting from silylation of TMSOTf

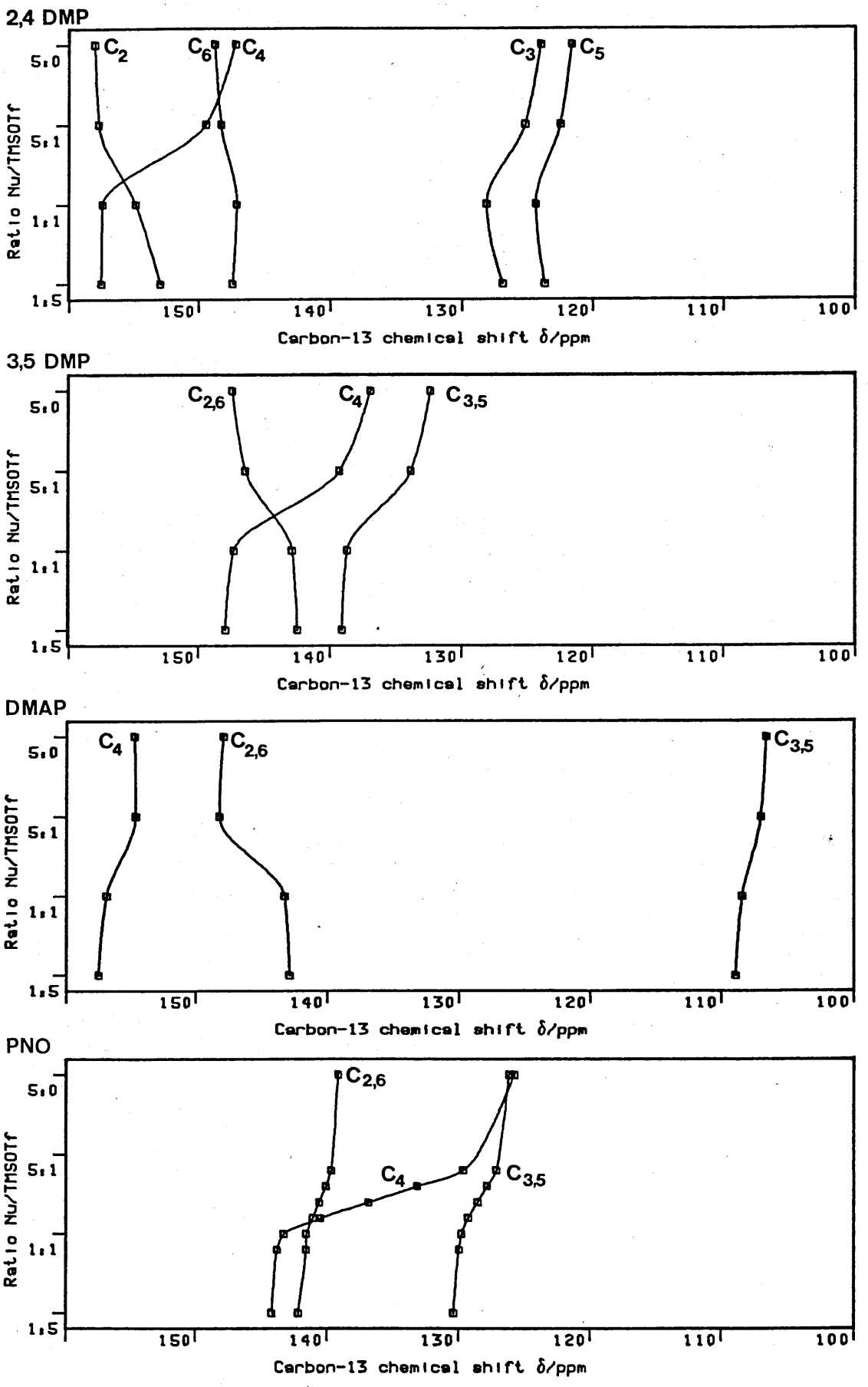

Figure 2.8 Silicon-29 chemical shift vs. Beta correlation for four [substituted pyridine-TMSOTf] complexes.

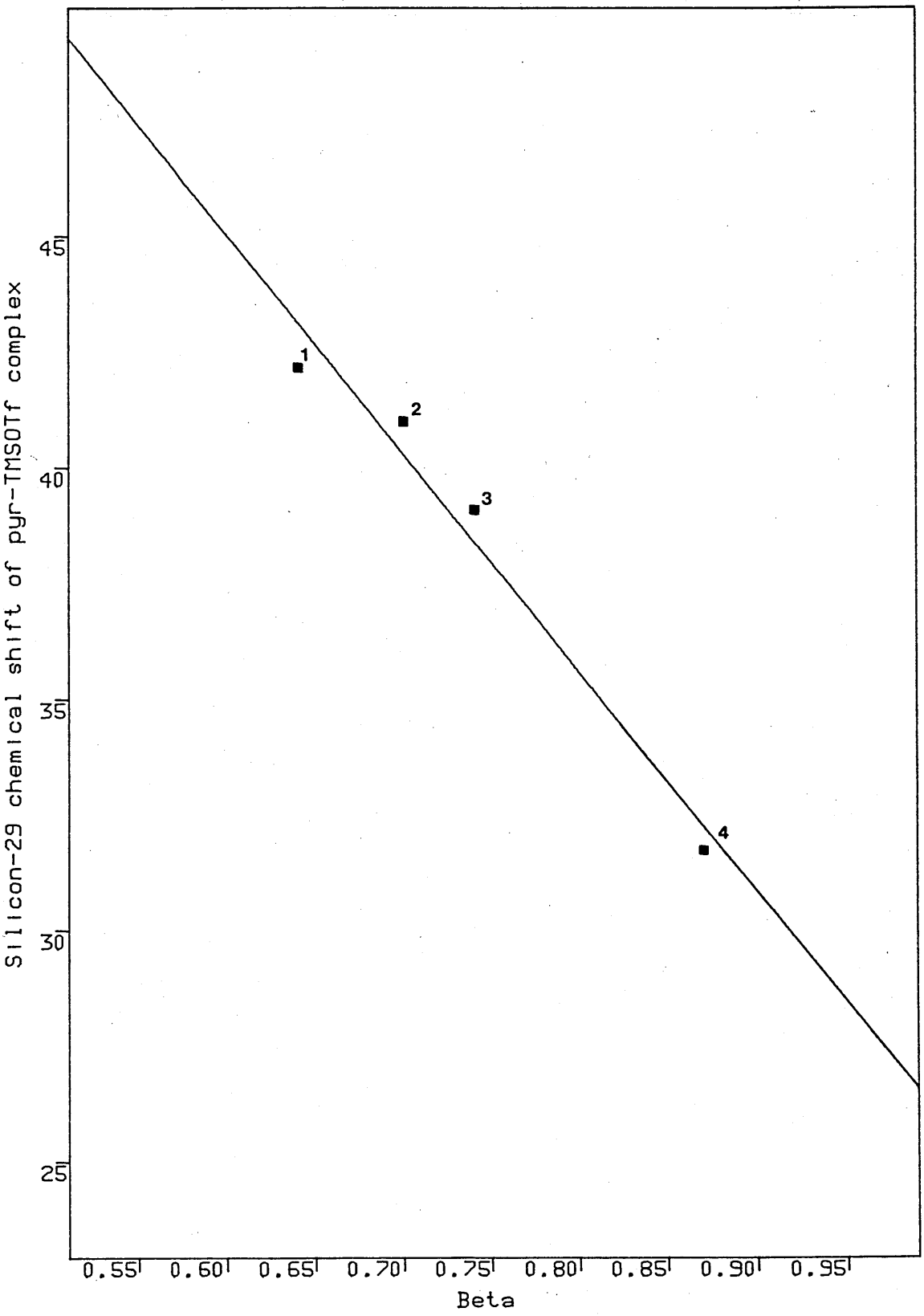

Solvent: chloroform-d1, except py (acetonitrile-d3).

1, py; 2, 3,5DMP; 3, 2,4DMP; 4, DMAP. Variance = 0.23

Slope= -47.3 (s.d.= 5.1), intercept= 73.4 (s.d.= 3.8)

Figure 2.9 pKa vs. Beta correlation.

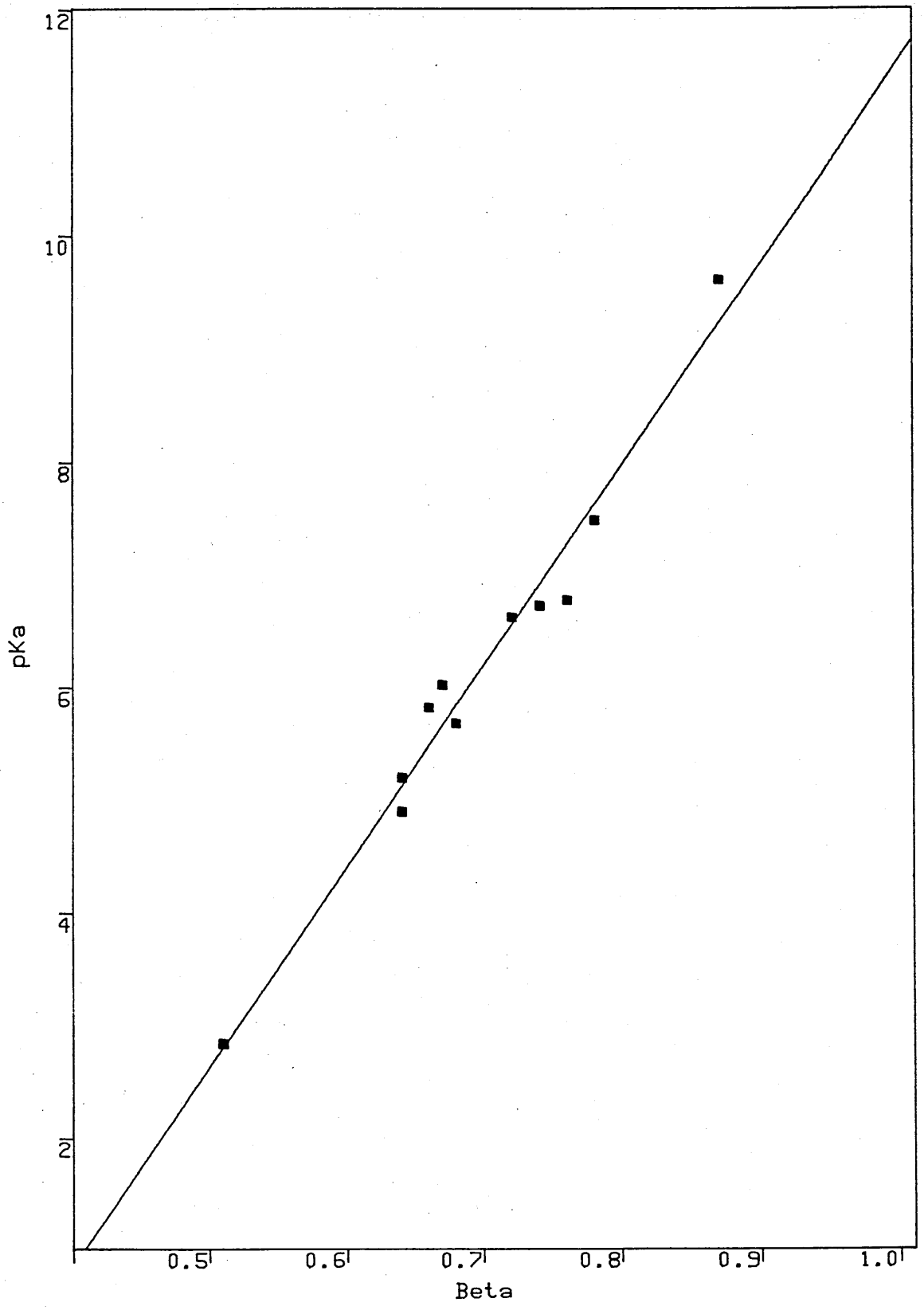

Slope = 17.83 (s.d. = 0.95)

Intercept = -6.28 (s.d. = 0.665)

Variance = 0.078

Figure 2.10 pKa vs. Silicon-29 chemical shift correlation for [substituted pyridine-TMSOTf] complexes.

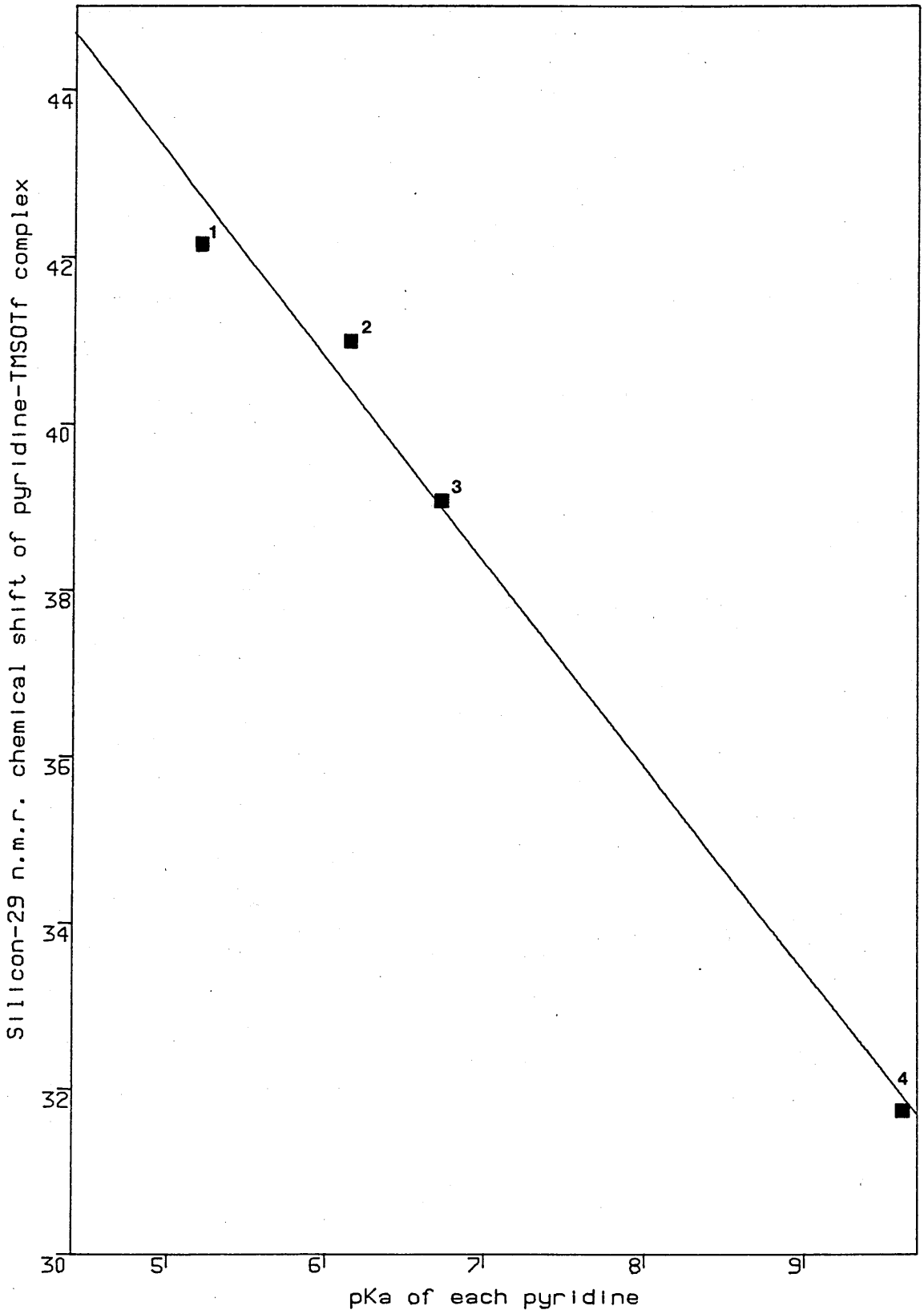

Solvent: chloroform, except py (acetonitrile-d3)

1, py; 2, 3,5DMP; 3, 2,4DMP; 4, DMAP. Variance = 0.23

Slope= -2.45 (s.d.= 0.15), intercept= 55.45 (s.d.= 1.0)

No significant amounts of complex formation could be detected for mixtures of TMSOTf with 2,6DMP, quinoline or BIPY. The likely chemical shifts of TMSOTf complexes with these three pyridines can be predicted from equations 2.3 and 2.4, thus ^{29}Si (2,6DMP-TMSOTf) = 37.5 ppm from a beta value of 0.76 or 38.8 ppm from a pKa value of 6.77. The lack of complex formation for 2,6DMP was confirmed by examining the TMSI/2,6DMP system (Table 2.16), which is particularly surprising in view of the 3,5DMP and 2,4DMP results. The similarity between the donor properties of the three methyl substituted pyridines (pKa = 6.77, 6.14 and 6.72; Beta = 0.76, 0.70 and 0.74 for 2,6DMP, 3,5DMP and 2,4DMP respectively) suggests that the effect is largely steric in origin for 2,6DMP. A similar explanation[89] was used to account for the analogous result observed by Brown et al.[90], who formed BMe_3 complexes with pyridine but failed to observe BMe_3 complexes with 2,6DMP. Barton and Tully reported[35] adduct formation between ^{t}butyldimethylsilyl perchlorate and 2,6-di^{t}butyl-4-methylpyridine. The authors themselves found this surprising because of the extremely hindered nature of the base, but they reported no supporting data for such complex formation. However, it will be shown later that silyl perchlorates are more effective complexing agents than either TMSI or TMSOTf.

No such steric explanation can be advanced to account for the quinoline result, which is sterically very similar to 2,4DMP with respect to silylation on N. The slight ^{29}Si shift may be significant but no major changes were observed for the ring carbons, suggesting that the equilibrium constant for adduct formation is very small. The slightly lower nucleophilicity (as evidenced by the lower pKa and Beta values) may be enough to prevent complexation. If this hypothesis is correct, adduct

formation between TMSX species and BIPY is even less likely since BIPY has a lower pKa than quinoline. In addition there is significantly more steric hindrance in BIPY. However 2,2-bipyridyl is a special case since it presents the possibility of formation of a chelated structure involving 5-coordinated silicon. Therefore it was interesting to study the interaction further, especially in view of the observations of Corey and West who proposed a five coordinate structure for their BIPY-Ph_3SiX (X=I, Br) adduct[91].

Two distinct trends can be deduced from the variable temperature ^{13}C and ^{29}Si n.m.r. data for a 1:1 mixture of 2,2-BIPY and TMSI presented in Table 2.20. This silane was chosen since the predicted chemical shift of the 4-coordinate BIPY-TMSOTf species (44.5 ppm using equation 2.4 and a pKa value of 4.44) is close to that of the isolated TMSOTf. Lowering the temperature, down to 220 K, does not induce any large chemical shift changes in either the carbon or silicon spectra, although the moderate shifts observed are fully consistent with a very small equilibrium proportion of a four coordinate ionic adduct. This trend is accentuated further by cooling below 220 K, but the situation is complicated by the appearance of a new set of peaks in the spectra of both nuclei. The intensity of these new resonances gradually increases at lower temperature with a proportionate decrease in the heights of the bipyridyl and TMSI peaks (Figures 2.11 and 2.12). The late appearance of the new ^{29}Si peak may be the result of it being hidden underneath the spectral noise, owing to exchange broadening and its low population.

Assignment of the new peaks (labelled C_{2b}, C_{3b} *etc.*) is by analogy with those of bipyridyl, bearing in mind the likely shifts resulting from

Table 2.20 Variable Temperature N.M.R. Data for a 1:1 mixture of Bipyridyl (BIPY) and Iodotrimethylsilane (TMSI)

δ (ppm)		BIPY[a]	Temperature (K)				
			300	230	220	210	200	180
^{1}H	aromatic C-H	8.64-8.72m	8.48-8.66m	-	-	-	-	-
		8.35-8.46m	8.37-8.47m	-	-	-	-	-
		7.71-7.90m	7.65-7.84m	-	-	-	-	-
		7.21-7.36m	7.16-7.31m	-	-	-	-	-
	$Si-(CH_3)_3$	-	0.75	-	-	-	-	-
^{13}C	C_2	-	156.2	155.5	155.3	155.3	154.9	154.6[b]
	C_6	-	149.2	149.1	149.1	149.1	149.2	148.9[b]
	C_4	-	136.9	137.1	137.2	137.4	137.6	137.9[b]
	C_3	-	123.7	124.0	124.1	124.2	124.4	124.7[b]
	C_5	-	121.1	120.8	120.7	120.7	120.7	120.8[b]
	C_{2a}	-	no	no	no	149.7	149.6	149.3[b]
	C_{6b}	-	no	no	148.2	148.3	148.6	148.8[b]
	C_{4b}	-	no	no	143.4	143.5	143.7	143.9[b]
	C_{3b}	-	no	no	127.6	127.6	127.9	128.2[b]
	C_{5b}	-	no	no	125.7	125.7	125.8	125.9[b]
	$Si-(CH_3)_3$	-	-	5.4	5.4	5.4	5.4	5.4
	$Si-(CH_3)_3$*	-	-	-	-	5.7	6.0	6.2
^{29}Si	$Si-(CH_3)_3$	-	10.3[c]	-[d]	11.4	11.7	11.8	12.6
	$Si-(CH_3)_3$*	-	-	-	-	-	21.3	18.0
quantities used: 3.31 mmoles of each component; solvent: CD_2Cl_2, 2.0 ml								

[a] Recorded in chloroform-d_3. [b] slightly broadened signals.

[c] Recorded before lowering temperature and after warming back to ambient temperature.

[d] ^{29}Si spectra also recorded at the following temperatures:

273K, 10.6 ppm; 258K, 10.8 ppm; 240K, 11.0 ppm; 215K, 11.5 ppm

Figure 2.11 Variable temperature n.m.r. silicon-29 chemical shifts for a 1:1 BIPY/TMSI mixture.

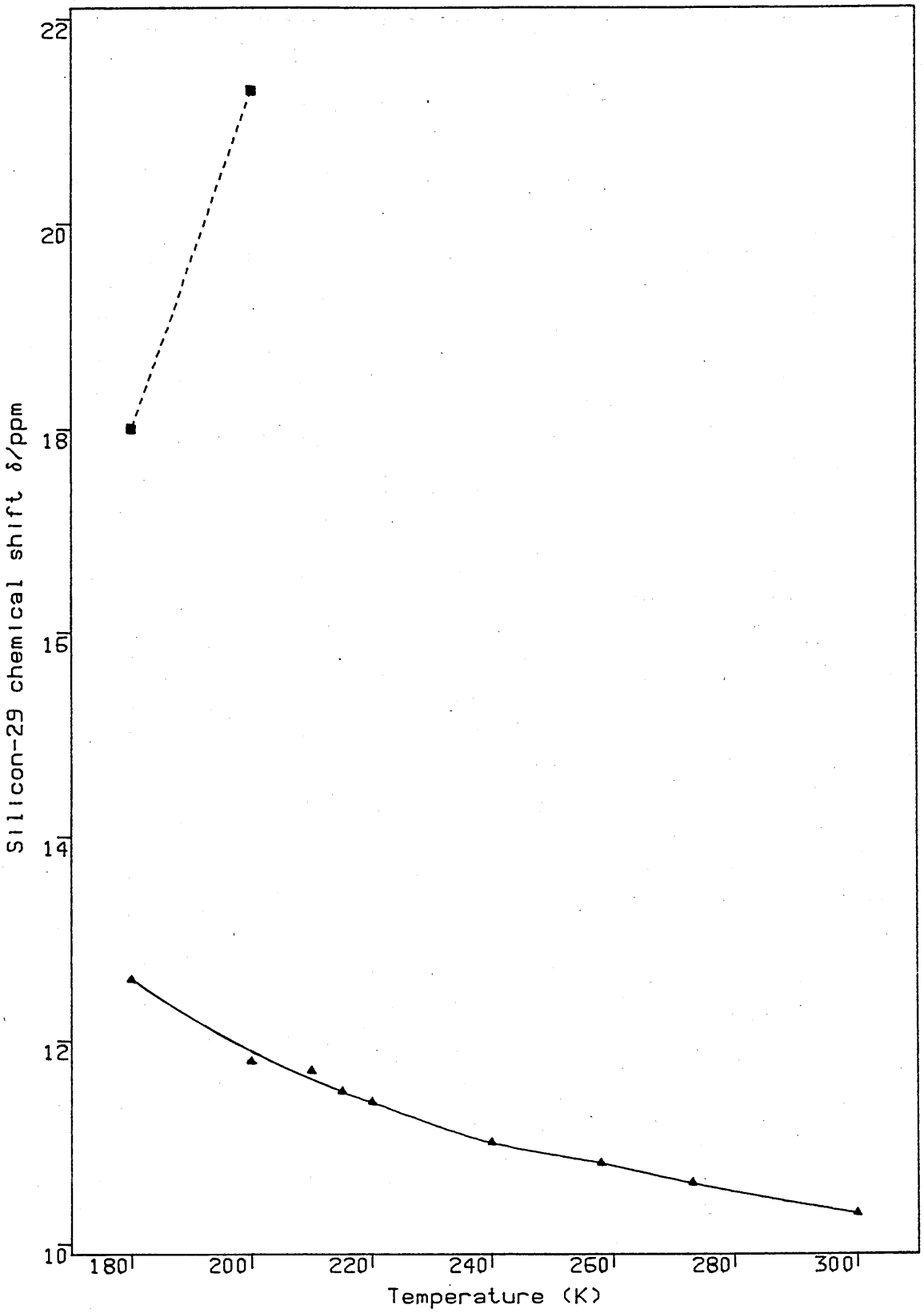

Solvent: dichloromethane-d2 (2.0 ml)

3.31 mmoles of each component.

Figure 2.12 Variable temperature n.m.r. carbon-13 chemical shifts for a 1:1 BIPY/TMSI mixture.

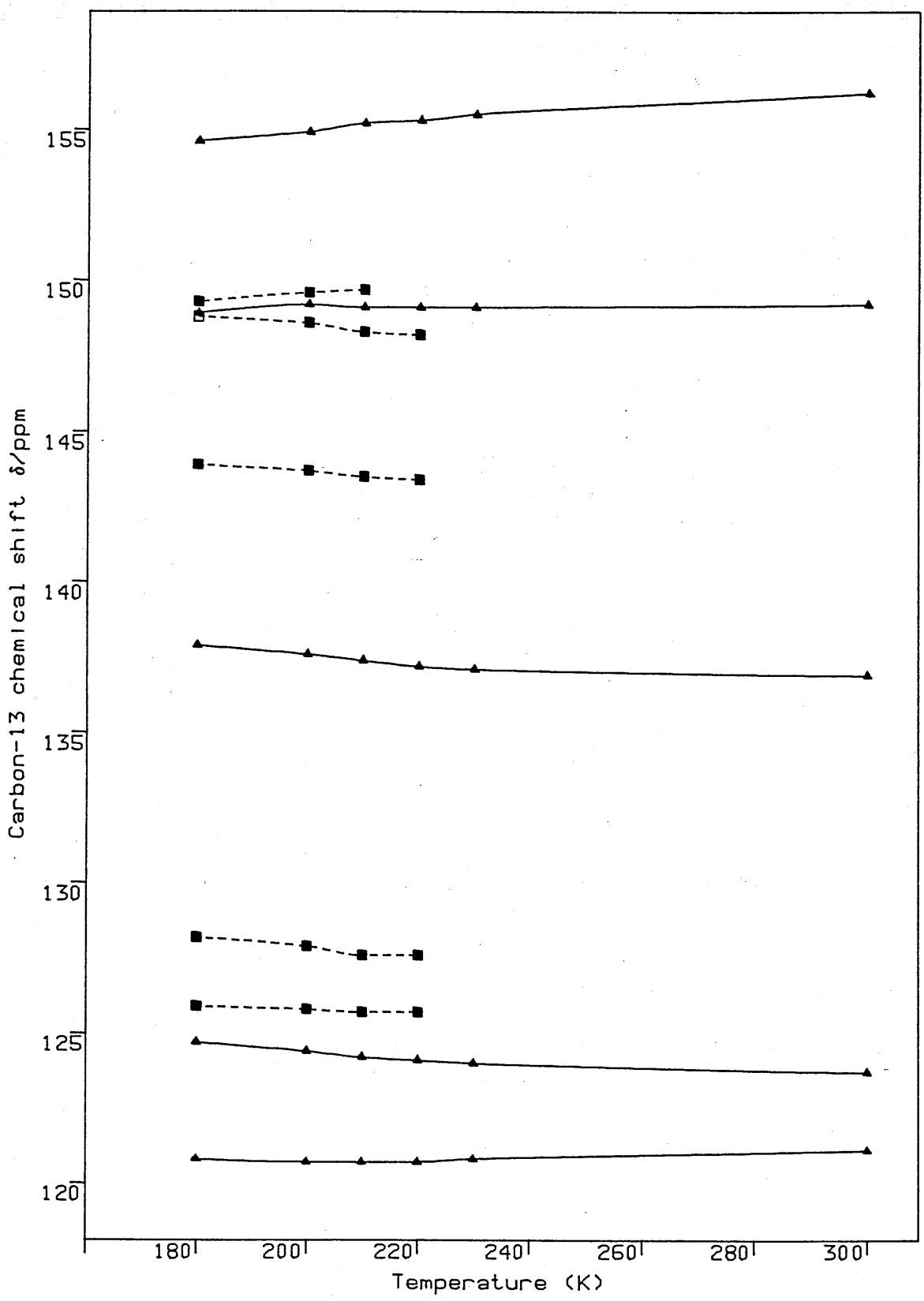

Solvent: dichloromethane-d2 (2.0 ml).

3.31 mmoles of each component.

silylation. These peaks also shift in accord with complex formation, though only to a slight extent. Coordination of silicon to one nitrogen should induce asymmetry into the bipyridyl system and lead to the observation of 10 peaks. This cannot be used as an explanation however, since the relative heights of the peaks are temperature dependent, implying that the 10 peaks are actually two sets of 5 peaks. Therefore the observed degeneracy of the 10 BIPY carbons suggests that either rapid silyl exchange is occurring between the two nitrogens or some degree of symmetry is present in the system. The exact structure of the low temperature adduct is difficult to determine, but the appearance of a new silicon peak which moves to higher field upon cooling strongly suggests a shift towards a 5-coordinate species, since the predicted chemical shift of the BIPY-TMSX ionic adduct is at lower field (ca. 44 ppm). The upfield shift, normally ascribed to valence shell expansion, is between 30 and 40 ppm (see discussion in Chapter 1). Thus, using the predicted value of ca. 44 ppm for the 4-coordinate BIPY complex, a value of between 14 and 4 ppm seems likely for the 5-coordinate silicon species (2.11H) as shown in Scheme 2.11. However this value must be regarded as the upper limit of the chemical shift for this species, since in many cases an increase in coordination number is accompanied by a substantially larger upfield shift (-90 ppm in some cases; see Chapter 5).

The relative exchange rates can be deduced from the observed line shapes and chemical shift trends of the two silicon peaks. Their sharpness indicates either very fast or very slow exchange. Assuming that the observed shifts are not the result of temperature dependent chemical shifts of the isolated species, it can be further implied that the two peaks are actually undergoing fast exchange. Furthermore, examination of

Scheme 2.11 Exchange processes between isolated 2,2-Bipyridyl (BIPY) and Trimethylsilyl X species (X= I), to give four- or five-coordinate $[BIPY\text{-}TMS]^{+}X^{-}$ adducts.

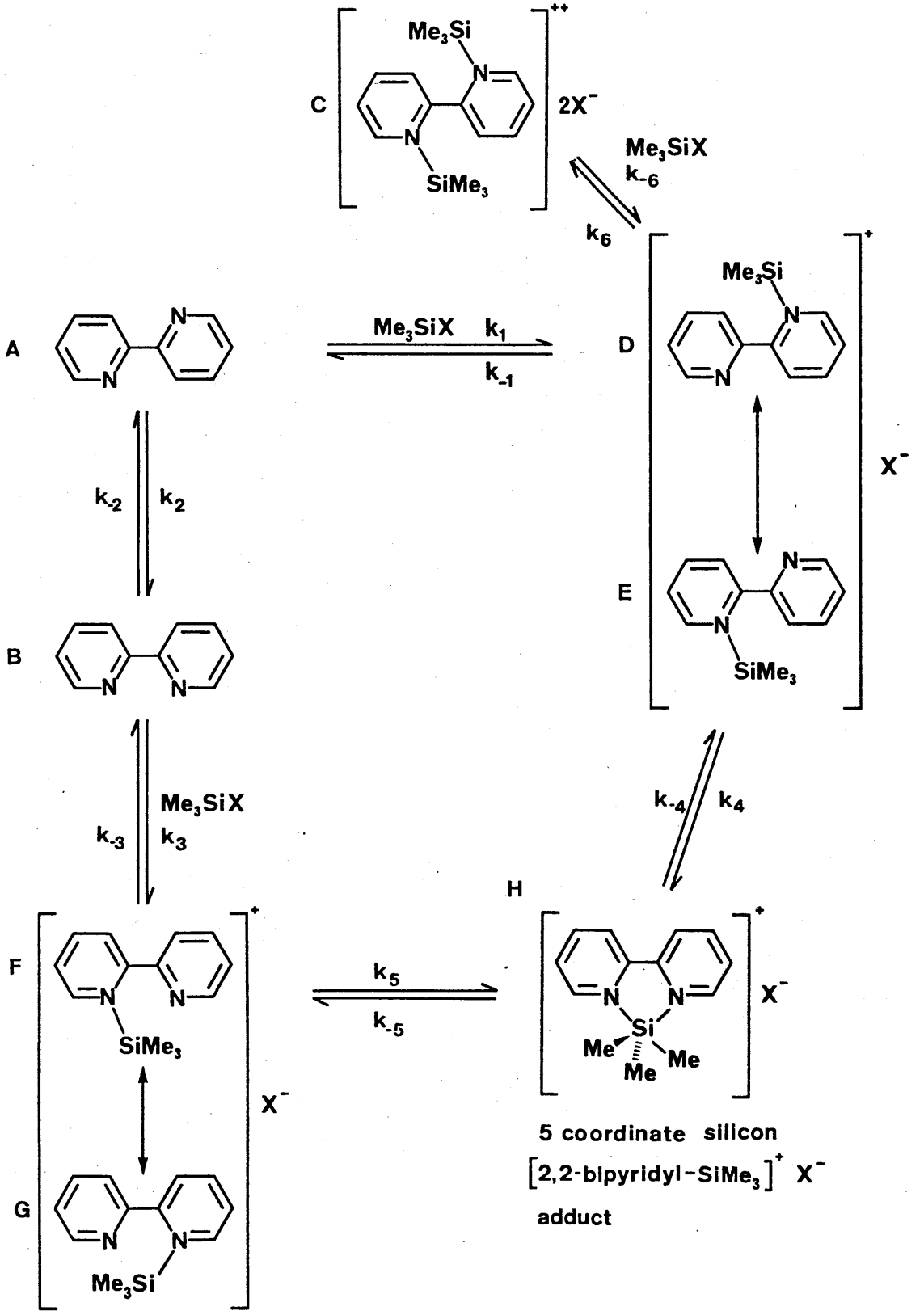

the chemical shift trends shows that the two peaks cannot be exchanging with each other because the nuclear spin with lower population is always shifted by a far greater degree than the nuclear spin with higher population. This fact is confirmed by theoretical line shape calculations[92]. In this case opposite behaviour is observed; the proportion of the new Si peak increases at low temperatures at the expense of bipyridyl and TMSI, but the silicon-29 n.m.r. shows a larger chemical shift change for the new peak than for TMSI. This is confirmed by the relative peak heights in both carbon-13 and silicon-29 n.m.r. spectra. Thus the observed shifts are consistent with two distinct effects; the TMSI peak is in equilibrium with a four coordinate species (2.11D or E), which has a predicted chemical shift of 44 ppm, and the new Si-29 peak is the result of an exchange between a four coordinate BIPY-TMSI adduct of different conformation (2.11F or G) and a five coordinate adduct (2.11H), which has a chemical shift of ca. 14-4 ppm.

Bipyridyl exists in solution predominantly in the anti conformation[85] (2.11A), which is a more stable form because the repulsion between the lone pairs on the two nitrogen atoms is minimised. The slow exchange between the four and the five coordinate species indicates that the four coordinate species (2.11D or E) has to undergo a conformational change, via either conversion back to bipyridyl (route 1 via structures A and B) or direct conversion (route 2), to produce the cis conformer (2.11F or G) as illustrated in Scheme 2.11, before establishing a dynamic equilibrium with the five coordinate species.

The equilibrium k_5/k_{-5} is expected to be very fast, and indeed it seems probable that 2.11F or G represents an intermediate step in the formation

of the 5-coordinate species 2.11H. It is interesting to compare these results with the observation by Corey and West[91] of a 5-coordinate bipyridyl-Ph_3SiI species. This aspect will be discussed more fully in Chapter 5.

On basis of U.V. and conductiometric studies, Tanaka et al.[93] have stated that TMSCl forms a 1:1 adduct with bipyridyl. The earlier observation that no significant amounts of complex formation could be detected between TMSCl and DMF or pyridine even at low temperatures, nor between bipyridyl and TMSX (X=I, OTf) at ambient temperature, strongly suggests that their conclusions were wrong. The authors stated that they carefully purified both solvent (acetonitrile) and chlorotrimethylsilane, but used reagent grade BIPY without purification. The dryness of their BIPY sample cannot be assessed here, but it seems likely that it contained substantial amounts of water. It has been found in this study that commercial BIPY is pure, except for the inclusion of water. This is not surprising because bases such as these are highly hygroscopic. Furthermore their U.V. studies were carried out at silane concentrations of between 9x and $15x10^{-6}$ molar and at a BIPY concentration of $30x10^{-6}$ molar. At such low concentrations of silane only $3x10^{-7}$ g of water is required for complete hydrolysis (assuming 2 ml of CH_3CN in their U.V. cell), so the solvent would have to contain less than 10^{-5}% of water, even if the BIPY was 100% pure. Similarly, the presence of HCl seems a likely reason for the observed conductance in acetonitrile ($1x10^{-3}$ molar in silane). In common with the amides and ureas, the pyridines display marked similarities between the chemical shift trends resulting from silylation and protonation. However in the pyridines, adduct formation with TMSOTf is very susceptible to steric hindrance at the nitrogen donor

site. In addition the equilibrium constant for 1:1 $[py\text{-}TMS]^{+}OTf^{-}$ adduct formation appears to decrease sharply below a certain donicity value. Thus with Beta values of ca. 0.6 or pKa values of ca. 5, the equilibrium constant for complex formation (Scheme 2.12) will be very small.

$$Me_3SiX + \text{substituted pyridine} \rightleftharpoons [\text{substituted pyridine-}SiMe_3]^{+}X^{-}$$

Scheme 2.12

2.5 Pyridine N-oxide

The chemical shift trends produced by titrating pyridine N-oxide (PNO) with TMSOTf in chloroform (Table 2.21) are different from those observed in the various pyridines (refer to Figure 2.7). The 3,5 carbon atoms shift in a similar manner to that observed in other pyridines. However the C_4 carbon experiences a dramatic shielding decrease whilst the $C_{2,6}$ carbons are deshielded, thus all carbons are deshielded (in contrast to the extra shielding observed at the $C_{2,6}$ positions of pyridines). This difference occurs because the nitrogen is already coordinated to the oxygen and thus it has already lost the shielding effect characteristic of the isolated pyridyl nitrogen. There is considerable negative charge associated with the oxygen, much of which will be removed upon coordination to silicon, and this may explain the rather large deshielding of the pyridyl carbons. The carbon-13 n.m.r. of PNO itself shows C_4 to be shielded, compared with C_4 of pyridine, which may indicate a greater contribution of resonance forms A and B[94] (Scheme 2.13).

Table 2.21

Interaction between Pyridine N-oxide (PNO) and Trimethylsilyl triflate (TMSOTf) : N.M.R. Data

PNO 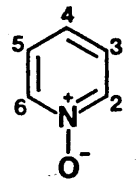

δ(ppm)		Ratio of PNO : TMSOTf 5:0	5:1	5:2	5:3	5:4	1:1	5:6	1:5
^{1}H	aromatic	8.24-	8.41-	-	-	-	9.03-	-	9.00-
	C-H	8.33m	8.50m	-	-	-	9.10m[a]	-	9.07m
		7.33-	7.54-	-	-	-	8.15-	-	8.18-
		7.42m	7.68m	-	-	-	8.63m	-	8.66m
	$Si-(CH_3)_3$	-	0.49	-	-	-	0.50	-	0.51[b]
^{13}C	$C_{2,6}$	139.2	139.7	140.1	140.6	141.1	141.6	141.6	142.2
	$C_{3,5}$	126.3	127.2	127.9	128.6	129.3	129.8	130.0	130.4
	C_4	125.9	129.7	133.2	136.9	140.5	143.3	143.8	144.2
	$Si-(CH_3)_3$	-	-1.3	-1.4	-1.4	-1.4	-1.4	-1.4	-1.4
^{29}Si	$Si-(CH_3)_3$	-	49.1	-	-	-	49.4	-	44.9br
quantities used									
PNO (mmoles)		5.27	5.27	5.27	5.27	5.27	5.27	5.27	5.27
TMSOTf (mmoles)		-	1.05	2.11	3.16	4.22	5.27	6.32	26.35
solvent: $CDCl_3$, 2.0 ml									

[a] complex coupling, not resolved.

[b] slightly broadened signal.

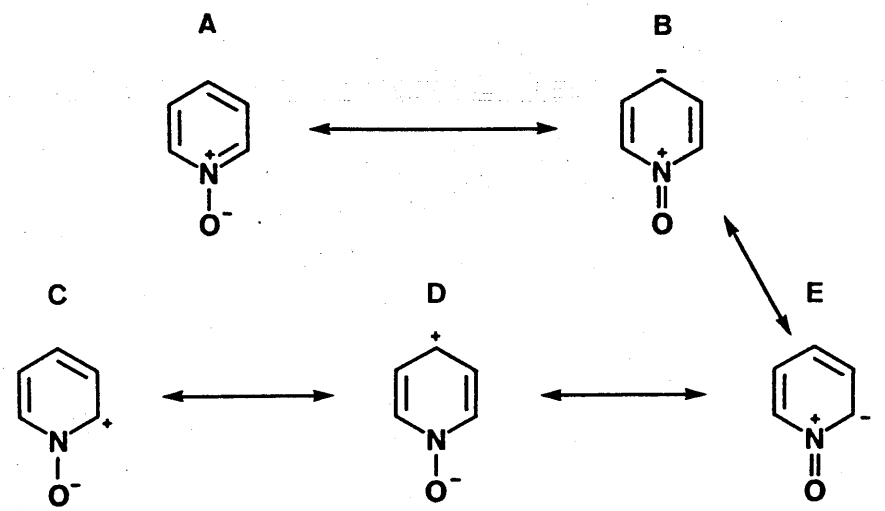

Scheme 2.13

The silicon-29 chemical shift of the PNO complex is unexpectedly high, indicating considerable deshielding of the silicon nucleus in the [PNO-TMS]$^{+}$OTf^{-} adduct (Scheme 2.14).

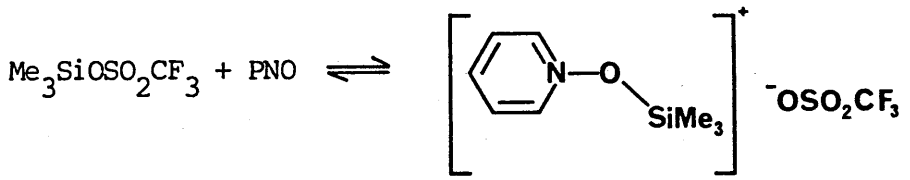

Scheme 2.14

2.6 Phosphine oxides

Chojnowski isolated and characterised the TMSI and TMSBr complexes with hexamethylphosphoramide (HMPA) by analysis, conductiometry and ^{31}P n.m.r., and the triphenylphosphine oxide (TPPO)-TMSI by ^{31}P n.m.r. alone[7]. These interactions have also been studied using conductiometry by Corriu but the two authors disagree over the structure of the resulting complex (refer to previous discussion in Chapter 1.3).

The interactions of trimethylsilyl triflate with both HMPA and TPPO have been studied here. The chemical shift data are presented in Tables 2.22 and 2.23 respectively. At a HMPA:TMSOTf ratio of 1:1 the silicon-29 resonance is split into a doublet, which is indicative of coupling to phosphorus and therefore complex formation. Addition of further quantities of HMPA pushes the equilibrium, shown in Scheme 2.15, very slightly over to the right hand side, as expected (evidenced by the ^{29}Si chemical shift), but this change is also accompanied by the collapse of the doublet to a singlet. This behaviour can be rationalized if the first step of the exchange between HMPA* and HMPA-TMSOTf adduct (Scheme 2.16) involves attack of HMPA* on the 1:1 adduct rather than dissociation, followed by subsequent reassociation (Scheme 2.17).

$$HMPA + Me_3SiOTf \rightleftharpoons [HMPA\text{-}SiMe_3]^+OTf^-$$

Scheme 2.15

$$[HMPA\text{-}SiMe_3]^+OTf^- + HMPA^* \rightleftharpoons [HMPA^*\text{-}SiMe_3]^+OTf^- + HMPA$$

Scheme 2.16

$$[HMPA\text{-}SiMe_3]^+OTf^- \longrightarrow HMPA + Me_3SiOTf$$

$$HMPA^* \quad \rightleftharpoons$$

$$HMPA + [HMPA^*\text{-}SiMe_3]^+OTf^-$$

Scheme 2.17

Table 2.22

Interaction between Hexamethylphosphoramide (HMPA) and Trimethylsilyl triflate (TMSOTf) : N.M.R. Data

HMPA

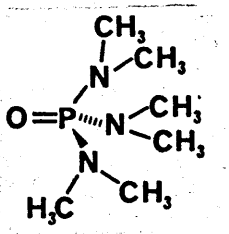

		Ratio of HMPA : TMSOTf			
δ(ppm)		5:0	5:1	1:1	1:5
^{1}H	$N-CH_3$	2.76d	2.67d	2.77d	2.75d
	$^{3}J_{PH}$	9.3Hz	9.5Hz	9.8Hz	9.8Hz
	$Si-(CH_3)_3$	-	0.43	0.43	0.49
^{13}C	CF_3	-	121.1q	121.1q	118.9q
	$^{1}J_{CF}$	-	321Hz	321Hz	317Hz
	$N-CH_3$	36.7d	36.7d	36.6d	36.7d
	$^{2}J_{PC}$	3.9Hz	3.9Hz	5.2Hz	5.2Hz
	$Si-(CH_3)_3$	-	0.63	0.69	0.23
^{29}Si	$Si-(CH_3)_3$	-	28.6[a,b]	28.8d[c]	43.9
	$^{3}J_{PSi}$	-	no	10.2Hz	no
quantities used:					
HMPA (mmoles)		2.2	11.0	2.2	0.44
TMSOTf (mmoles)		-	2.2	2.2	2.2
solvent: $CDCl_3$, 2.0 ml					

[a] The silicon-29 n.m.r. chemical shift for a 2:1 HMPA:TMSOTf mixture is 28.6.

[b] 5:1 HMPA:TMSI, 28.5 ppm.

[c] 1:1 HMPA:TMSI, 28.7 ppm.

Table 2.23

Interaction between Triphenylphosphine oxide (TPPO) and Trimethylsilyl triflate (TMSOTf) : N.M.R. Data

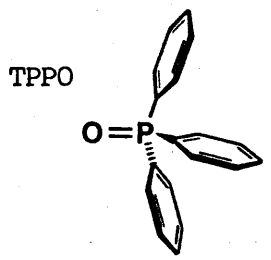

		Ratio of TPPO : TMSOTf			
δ(ppm)		5:0	5:1	1:1	1:5
^{1}H	aromatic C-H	7.4-7.8m	7.33-7.81m	7.67-7.87m	7.60-7.84m
	$Si-(CH_3)_3$	-	0.34	0.35	0.47
^{13}C	C_{para}	131.9	132.7d	136.2d	136.5d
	$^{4}J_{PC}$	no	2.6Hz	2.3Hz	2.6Hz
	C_{meta}	132.1d	132.0d	132.6d	133.0d
	$^{3}J_{PC}$	10.4Hz	10.4Hz	12.9Hz	13.0Hz
	C_{ortho}	128.5d	128.9d	130.4d	130.7d
	$^{2}J_{PC}$	13.0Hz	12.9Hz	12.9Hz	13.0Hz
	C_{ipso}	132.7d	no[a]	121.6d	121.7d
	$^{1}J_{PC}$	113.0Hz	no	111.3Hz	111.3Hz
	CF_3	-	117.2q	117.3q	118.6q
	$^{1}J_{CF}$	-	318Hz	318Hz	318Hz
	$Si-(CH_3)_3$	-	1.1	1.1	0.46
^{29}Si	$Si-(CH_3)_3$	-	37.4	37.5	43.0
quantities used:					
TPPO (mmoles)		0.826	0.826	0.826	0.826
TMSOTf (mmoles)		-	0.165	0.826	4.13
solvent: $CDCl_3$, 2.0 ml					

[a] ipso carbon resonance obscured.

This is in accord with the expected behaviour since HMPA is considerably more nucleophilic than the triflate anion. Moreover in the absence of the nucleophilic attack exchange mechanism, the addition of HMPA* is expected to drive the equilibrium towards complex formation. The ^{29}Si chemical shift, characteristic of four coordinate silicon, together with the absence of a 1:2:1 triplet for the silicon resonance at a 2:1 HMPA:TMSOTf ratio, indicate that the equilibrium concentration of any five coordinate adduct (Figure 2.13) is not significant.

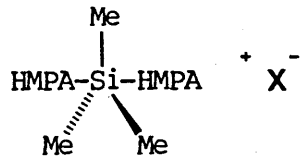

Figure 2.13

The formation of a single type of complex with different counterions was confirmed by the silicon-29 chemical shift of HMPA/TMSI mixtures (1:1 and 5:1 stoicheiometries) also shown in Table 2.22.

The proton atoms of HMPA are deshielded as a result of silylation by TMSOTf, which is in accord with the ^{1}H n.m.r. data presented by Chojnowski for mixtures of HMPA with TMSBr or TMSI[7]. No such shielding decrease is observed for the methyl carbon nuclei in HMPA/TMSOTf mixtures, although the carbon-phosphorus coupling constant shows a slight increase.

The assignment of the phenyl carbons in TPPO is complicated by their similar chemical shifts and the presence of phosphorus-carbon couplings.

It has been assumed here that the magnitude of this coupling constant decreases with increasing distance of each carbon atom from the phosphorus atom. The proton resonances have not been individually assigned since they are present as a complicated multiplet, which shows slight deshielding upon silylation. The chemical shift changes of the carbon nuclei are presented in Figure 2.14 (degenerate atoms are omitted for clarity).

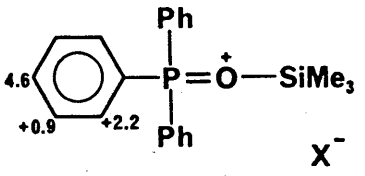

Figure 2.14

These changes are consistent with the operation of two effects:- i) a general inductive withdrawal of electrons from the phenyl ring felt by all carbons, but to a greater degree by those atoms close to phosphorus; and ii) deshielding by mesomeric electron withdrawal (Scheme 2.18).

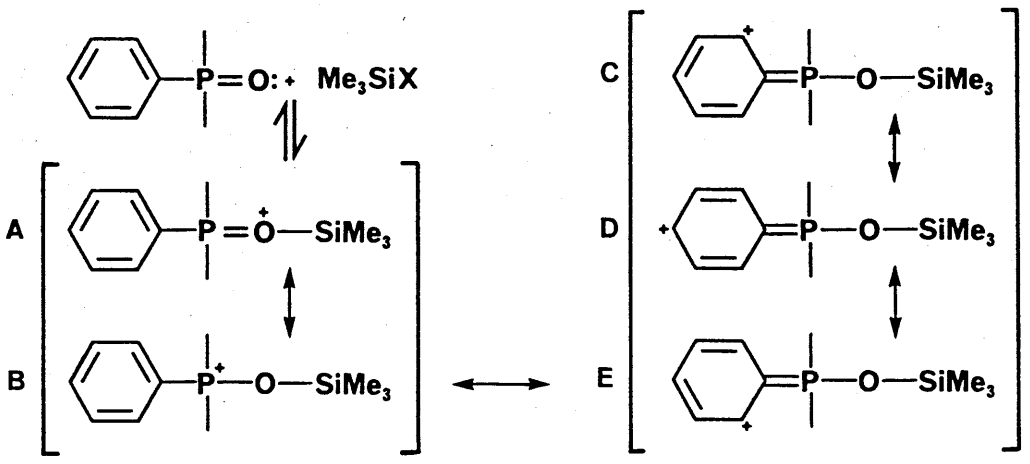

Scheme 2.18

The larger downfield shift experienced by the para carbon suggests that the resonance form D makes a major contribution to the electron distribution in the silylated species. The shift change of the ipso carbon is anomalous assuming that the assignment of the resonance due to this nucleus is correct (low intensity and the proximity of the other carbon resonances makes this difficult). This behaviour may result from shielding changes associated with the P=O bond.

2.7 Amines

Mixtures of triethylamine (Et_3N) with both TMSOTf (Table 2.24) and TMSI (Table 2.25) failed to show any significant changes attributable to adduct formation. The small downfield shifts of 0.9 and 0.5 ppm in the silicon-29 n.m.r., for the iodide and triflate respectively, could be attributed simply to medium effects. This result was somewhat surprising in view of the results of Simchen[13] who isolated and characterised adducts between trialkylamines (including triethylamine) and TMSOTf.

Therefore a low temperature study was undertaken for an equimolar mixture of TMSI and Et_3N. Cooling a solution containing 2.5 mmoles of each component in dichloromethane (2 ml) down to -70 °C (acetone/CO_2) produced a copious white precipitate. Cooling a similar but less concentrated solution down to 180 K induced a downfield shift of 36 ppm from a value of 10.2 ppm for the isolated iodide, which is consistent with adduct formation at the lower temperature (Table 2.26). The intensity of the silicon-29 peak at 11.0 ppm at 240 K was considerably reduced suggesting that it was undergoing chemical exchange with the four coordinate 1:1 salt (at ca. 46 ppm). The presence of two sets of peaks in the carbon-13

Table 2.24

Interaction between Triethylamine (Et_3N) and Trimethylsilyl triflate (TMSOTf) : N.M.R. Data

		Ratio of Et_3N : TMSOTf			
δ(ppm)		5:0	5:1	1:1	1:5
^1H	CH_2	2.52q	2.48q	2.52q	2.56q
	$^3J_{HH}$	7.3Hz	7.3Hz	7.1Hz	7.1Hz
	CH_3	1.02t	0.98t	1.00t	1.03t
	$^3J_{HH}$	7.3Hz	7.3Hz	7.1Hz	7.1Hz
	$Si-(CH_3)_3$	-	0.49	0.50	0.49
^{13}C	CH_2	46.4	46.6	46.6	46.6
	CH_3	11.8	11.8	11.7	11.4
	CF_3	-	118.8q	118.8q	118.6q
	$^1J_{CF}$	-	317Hz	317Hz	317Hz
	$Si-(CH_3)_3$	-	-0.29	-0.34	-0.34
^{29}Si	$Si-(CH_3)_3$	-	43.6	44.1	44.1
quantities used:					
Et_3N (mmoles)		2.2	11.0	2.2	0.44
TMSOTf (mmoles)		-	2.2	2.2	2.2
solvent: CD_2Cl_2, 2.0 ml					

Table 2.25

Interaction between Triethylamine (Et_3N) and Iodotrimethylsilane (TMSI) :

N.M.R. Data

		Ratio of Et_3N : TMSI			
δ(ppm)		5:0	5:1	1:1	1:5
^1H	CH_2	2.52q	2.48q	2.48q	2.49q
	$^3J_{HH}$	7.3Hz	7.1Hz	7.1Hz	7.1Hz
	CH_3	1.02t	0.98t	0.98t	0.98t
	$^3J_{HH}$	7.2Hz	7.1Hz	7.1Hz	7.1Hz
	$Si-(CH_3)_3$	-	0.78	0.78	0.79
^{13}C	CH_2	46.4	46.6	46.6	46.5
	CH_3	11.8	12.1	12.1	11.9
	$Si-(CH_3)_3$	-	5.6	5.7	5.6
^{29}Si	$Si-(CH_3)_3$	-	9.4	10.1	10.3
quantities used:					
Et_3N (mmoles)		2.2	11.0	2.2	0.44
TMSI (mmoles)		-	2.2	2.2	2.2
solvent: CD_2Cl_2, 2.0 ml					

Table 2.26

Variable Temperature N.M.R. Data for a 1:1 mixture of Triethylamine (Et_3N) and Iodotrimethylsilane (TMSI)

δ(ppm)		Et_3N	Temperature (K)	
			300[a]	183
^1H	CH_2	2.52q	2.495q	3.26[b]
	$^3J_{HH}$	7.3Hz	7.3Hz	no[b]
	CH_3	1.02t	0.99	1.40[b]
	$^3J_{HH}$	7.2Hz	7.1Hz	no[b]
	$Si-(CH_3)_3$	-	0.59	0.72
^{13}C	CH_2	46.4	46.6	46.0[c]
	$(CH_2)^*$	-	-	51.1
	CH_3	11.8	11.9	9.7
	$Si-(CH_3)_3$	-	5.6	5.5[c]
	$Si-(CH_3)_3^*$	-	-	0.8
^{29}Si	$Si-(CH_3)_3$	-	9.7[d]	46.0
quantities used: 2.5 mmoles of each component; solvent: CD_2Cl_2, 2.0 ml				

[a] Recorded before lowering temperature and after warming back to ambient temperature.

[b] Broad signals due to solvent viscosity and crystallisation.

[c] Low intensity.

[d] 11.0 ppm at 240K.

spectra at 180 K, attributable to the Et_3N-TMSI salt and the uncomplexed Et_3N and TMSI, shows that exchange between the two species is slow on the n.m.r. time-scale. Despite the use of a lower concentration, there may have been some crystallization at 180 K. This was deduced from the abnormal reduction in the intensity of the deuterium lock signal and the very broad signals observed in the proton spectrum at that temperature. Silicon-29 spectra were only recorded at three temperatures, because the lower concentration combined with the peak intensity reductions resulting from exchange broadening caused accumulation times to lengthen. This combined with the uncertainty in the limiting chemical shift of the Et_3N-TMSI adduct prevent the calculation of reasonably accurate thermodynamic parameters.

N-trimethylsilylimidazole (TMSIm) is a very good silylating agent whose activity can be enhanced by the addition of catalytic quantities of TMSCl[1]. The addition of equimolar quantities of TMSIm and TMSX (X=Br, I, OSO_2CF_3, ClO_4) to hexane produced in each case a colourless crystalline solid, which after purification gave satisfactory elemental analyses consistent with the formation of 1:1 TMSIm-TMSX adducts, although no such adduct could be isolated for X=Cl. The n.m.r. data for each of the solid adducts in various solvents are presented in Tables 4.7 (in chloroform-d_1), 2.27 (in dichloromethane-d_2) and 2.28 (acetonitrile-d_3). Additional data concerning TMSIm/TMSX mixtures are included in Tables 4.1 to 4.6.

The ^1H and ^{13}C chemical shift trends between the isolated TMSIm and the TMSIm-TMSX adduct are analogous to those observed by Pugmire and Grant[82], and also Barlin and Batterham[95] for the protonation of imidazole by HCl. A general decrease in electron density is observed in the imidazolium

Table 2.27

N.M.R. Data for N,N'-Bistrimethylsilylimidazolium salts [$BTMSIm^+X^-$] (X=Br, I, OTf, ClO_4) in Dichloromethane-d_2

[$BTMSIm^+X^-$]

δ(ppm)		BTMSImBr	BTMSImI	BTMSImOTf	BTMSImClO_4	TMSIm
^1H	C_2-H	9.79t	9.34	8.63	8.52	7.55
	$C_{4,5}$-H	7.48d	7.52d	7.42	7.39d	7.03d
	$^4J_{HH}$	1.5Hz	1.2Hz	1.2Hz	nr	0.98Hz
	TMS	0.72	0.75	0.64	0.64	0.42
^{13}C	C_2	144.1	143.0	141.0	143.3	140.2
	CF_3	-	-	121.1q	-	-
	$^1J_{CF}$	-	-	318Hz	-	-
	$C_{4,5}$	124.5	124.7	124.1	124.9	125.5
	TMS	0.0	0.0	-0.81	-0.69	-0.46
^{29}Si	TMS	26.2	26.8	26.9	26.1	13.5
quantities used:						
BTMSImX (mmoles)		0.06	1.45	0.56	0.80	1.5
solvent: CD_2Cl_2, 2.0 ml						

Table 2.28

N.M.R. Data for N,N'-Bistrimethylsilylimidazolium salts [$BTMSIm^+X^-$] (X=Br, I, OTf, ClO_4) in Acetonitrile-d_3

[$BTMSIm^+X^-$]

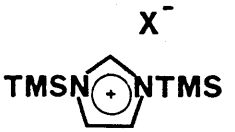

o(ppm)		BTMSImBr	BTMSImI	BTMSImOTf	BTMSImClO_4	TMSIm
^1H	C_2-H	8.91	8.74	8.46	8.33	7.60
	$C_{4,5}$-H	7.59d	7.62d	7.54	7.49d	7.07
	$^4J_{HH}$	1.5Hz	1.2Hz	nr	1.2Hz	no
	TMS	0.63	0.65	0.57	0.59	0.43
^{13}C	C_2	143.4	143.6	142.2	142.3	139.9
	CF_3	-	-	121.9	-	-
	$^1J_{CF}$	-	-	nr	-	-
	$C_{4,5}$	125.3	125.6	125.0	125.0	125.2
	TMS	-0.57	-0.57	-0.97	-0.52	-0.57
^{29}Si	TMS	26.3	26.4	26.7	26.3	14.2
quantities used:						
BTMSImX (mmoles)		0.91	0.67	0.60	0.72	1.5
solvent: CD_3CN, 2.0 ml						

cation with the C_2 position being affected most. The magnitude of this deshielding increases with counterions in the order $X=ClO_4^- < OTf^- < I^- < Br^-$ for the silylated species. Perchlorate and triflate being fairly large, polarizable species are solvated fairly well in non-polar solvents, whilst the bromide and, to a lesser extent, the iodide are relatively small, hard species and thus less well solvated. The imidazolium cation is also affected by these solvation changes, since in the absence of stabilization by solvent, the less solvated ions such as bromide become tight ion pairs (with the imidazolium species acting as the solvent).

Conductivity titrations in dichloromethane between TMSIm and TMSX (X=Cl, Table 2.29; Br, Table 2.30; I, Table 2.31; OTf, Table 2.32) confirm this point, since the maximum conductivity observed (close to 1:1 stoicheiometry) increases in the order Cl << Br < I < OTf. Furthermore it is apparent from the shape of the conductivity titration curves (Figure 2.15) around the point of inflexion that the equilibrium constant for salt formation also increases in the order Cl << Br < I, OTf. Thus the different chemical shifts are not the result of different equilibrium positions for each counterion. The slightly smaller chemical shift changes observed in acetonitrile reflect this solvent's larger dielectric constant, which enables it to solvate the ionic species more effectively. The conductivity of the TMSIm/TMSX (X=I, Br, OTf) solutions decreases gradually after reaching a maximum at approximately 1:1 stoicheiometry. Increasing the proportion of TMSX drives the equilibrium (Scheme 2.19) further over to the side of complex formation and it also changes the nature of the medium. As solvents, the TMSX species are poor at stabilizing ionic species, in comparison to TMSIm, thus increasing the tightness of any ion pairing.

Figure 2.15 Conductivity titration: TMSX (X=Cl, Br, I, OTf) against TMSIm.

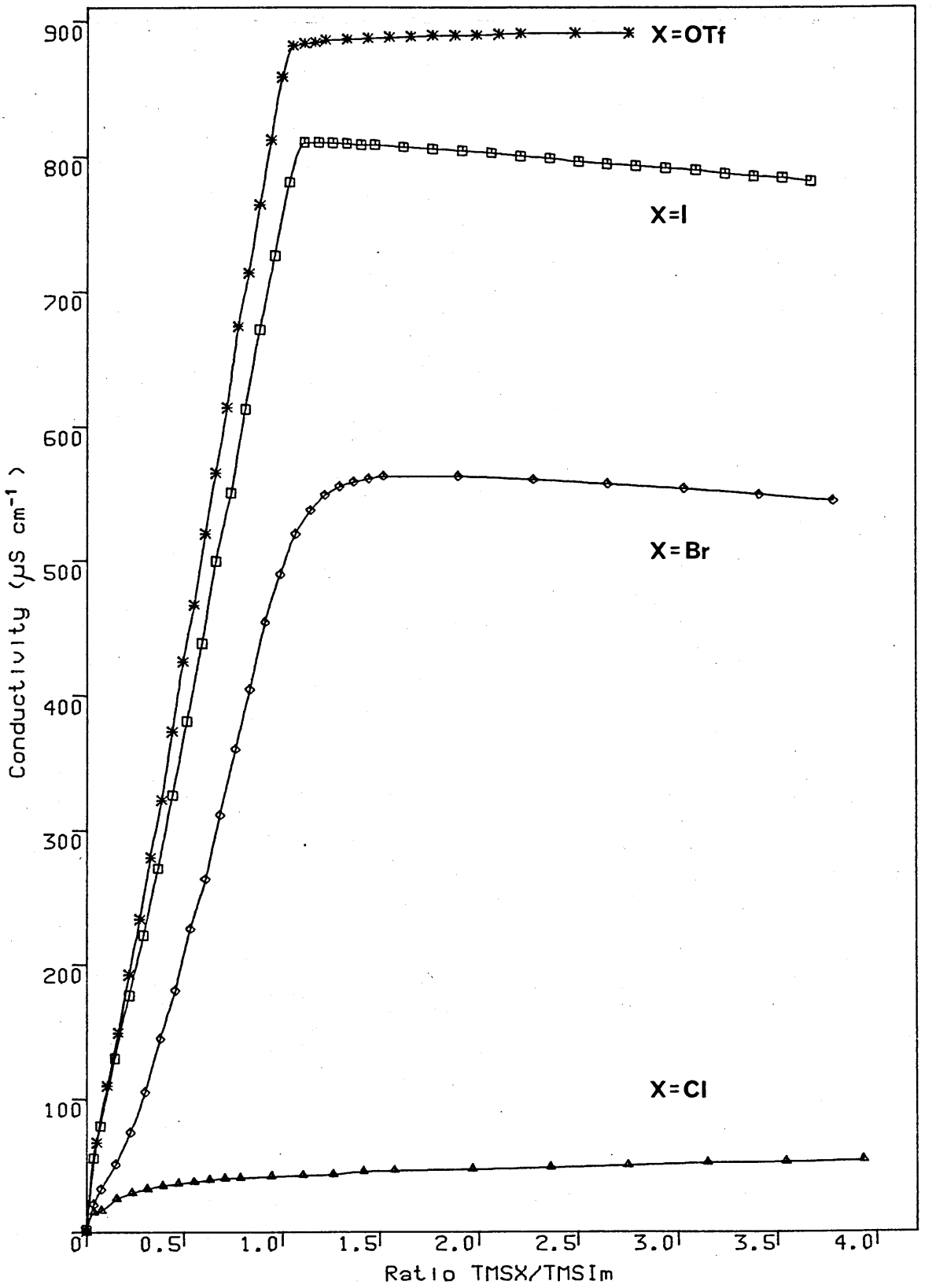

Solvent: dichloromethane. (0.11 molar in TMSIm)

Table 2.29

Conductivity titration: N-Trimethylsilylimidazole (TMSIm) against Chlorotrimethylsilane (TMSCl)

Volume TMSCl (ml)	Ratio TMSIm:TMSCl	Conductivity ($\mu S\ cm^{-1}$)
0.000	0.00 :1	1.4
0.005	25.44 :1	14.2
0.010	12.72 :1	15.7
0.020	6.36 :1	24.2
0.030	4.24 :1	28.5
0.040	3.18 :1	31.6
0.050	2.54 :1	33.8
0.060	2.12 :1	35.2
0.070	1.82 :1	36.4
0.080	1.59 :1	37.9
0.090	1.41 :1	38.7
0.100	1.27 :1	39.2
0.120	1.06 :1	40.2
0.140	1: 1.10	40.8
0.160	1: 1.26	41.4
0.180	1: 1.42	43.4
0.200	1: 1.57	44.0
0.250	1: 1.97	44.8
0.300	1: 2.36	45.9
0.350	1: 2.75	47.1
0.400	1: 3.14	48.6
0.450	1: 3.54	48.8
0.500	1: 3.93	49.8

Solvent: CD_2Cl_2, 10.0 ml; Volume of TMSIm: 0.148 ml (1.1 mmoles)

Initial conductivity of solution: 0.1 $\mu S\ cm^{-1}$; Cell constant: 0.9029

Table 2.30

Conductivity titration: N-Trimethylsilylimidazole (TMSIm) against Bromotrimethylsilane (TMSBr)

Volume TMSBr (ml)	Ratio TMSIm:TMSBr	Conductivity ($\mu S\ cm^{-1}$)
0.000	0.00 :1	0.4
0.005	26.45 :1	19.9
0.010	13.23 :1	31.3
0.020	6.61 :1	49.4
0.030	4.41 :1	72.7
0.040	3.31 :1	101.9
0.050	2.65 :1	140.0
0.060	2.20 :1	174.8
0.070	1.89 :1	219.2
0.080	1.65 :1	254.6
0.090	1.47 :1	300.6
0.100	1.32 :1	347.6
0.110	1.20 :1	389.7
0.120	1.10 :1	437.7
0.130	1.02 :1	471.2
0.140	1: 1.06	499.9
0.150	1: 1.13	516.2
0.160	1: 1.21	526.8
0.170	1: 1.29	532.5
0.180	1: 1.36	535.4
0.190	1: 1.44	536.8
0.200	1: 1.51	538.3
0.250	1: 1.89	535.4
0.300	1: 2.27	530.6
0.350	1: 2.65	524.9
0.400	1: 3.02	519.1
0.450	1: 3.40	512.4
0.500	1: 3.78	505.7

Solvent: CD_2Cl_2, 10.0 ml; Volume of TMSIm: 0.148 ml (1.1 mmoles)

Initial conductivity of solution: 0.3 $\mu S\ cm^{-1}$; Cell constant: 0.9583

Table 2.31

Conductivity titration: N-Trimethylsilylimidazole (TMSIm) against Iodotrimethylsilane (TMSI)

Volume TMSI (ml)	Ratio TMSIm:TMSI	Conductivity ($\mu S\ cm^{-1}$)
0.000	0.00 :1	1.4
0.005	27.28 :1	53.9
0.010	13.64 :1	77.3
0.020	6.82 :1	126.2
0.030	4.55 :1	171.8
0.040	3.41 :1	215.3
0.050	2.73 :1	263.2
0.060	2.27 :1	315.9
0.070	1.95 :1	368.5
0.080	1.71 :1	424.1
0.090	1.52 :1	482.5
0.100	1.36 :1	531.4
0.110	1.24 :1	590.8
0.120	1.14 :1	647.3
0.130	1.05 :1	699.1
0.140	1: 1.03:1	750.8
0.150	1: 1.10:1	778.6
0.160	1: 1.17:1	777.6
0.170	1: 1.25:1	776.7
0.180	1: 1.32:1	775.2
0.190	1: 1.39:1	773.8
0.200	1: 1.47:1	772.8
0.220	1: 1.61:1	769.9
0.240	1: 1.76:1	767.1
0.260	1: 1.91:1	764.2
0.280	1: 2.05:1	761.3
0.300	1: 2.20:1	757.5
0.320	1: 2.35:1	754.6
0.340	1: 2.49:1	750.8
0.360	1: 2.64:1	747.9
0.380	1: 2.79:1	745.0
0.400	1: 2.93:1	742.2
0.420	1: 3.08:1	739.3
0.440	1: 3.23:1	735.5
0.460	1: 3.37:1	732.6
0.480	1: 3.52:1	729.7
0.500	1: 3.67:1	725.9

Solvent: CD_2Cl_2, 10.0 ml; Volume of TMSIm: 0.148 ml (1.1 mmoles)

Initial conductivity of solution: 0.3 $\mu S\ cm^{-1}$; Cell constant: 0.9580

Table 2.32

Conductivity titration: N-Trimethylsilylimidazole (TMSIm) against Trimethylsilyl triflate (TMSOTf)

Volume TMSOTf (ml)	Ratio TMSIm:TMSOTf	Conductivity ($\mu S\ cm^{-1}$)
0.000	0.00 :1	0.7
0.010	18.18 :1	65.5
0.020	9.09 :1	106.6
0.030	6.06 :1	144.8
0.040	4.55 :1	186.7
0.050	3.64 :1	226.8
0.060	3.03 :1	270.8
0.070	2.60 :1	312.0
0.080	2.27 :1	360.9
0.090	2.02 :1	410.7
0.100	1.82 :1	450.9
0.110	1.65 :1	501.7
0.120	1.52 :1	544.8
0.130	1.40 :1	590.8
0.140	1.30 :1	648.3
0.150	1.21 :1	685.6
0.160	1.14 :1	733.5
0.170	1.07 :1	778.6
0.180	1.01 :1	822.6
0.190	1: 1.04	843.7
0.200	1: 1.10	844.7
0.210	1: 1.15	844.7
0.220	1: 1.21	845.6
0.240	1: 1.32	844.7
0.260	1: 1.43	843.7
0.280	1: 1.54	842.8
0.300	1: 1.65	841.8
0.320	1: 1.76	840.8
0.340	1: 1.87	839.4
0.360	1: 1.98	838.0
0.380	1: 2.09	837.0
0.400	1: 2.20	836.0
0.450	1: 2.47	832.2
0.500	1: 2.75	828.4

Solvent: CD_2Cl_2, 10.0 ml; Volume of TMSIm: 0.148 ml (1:1 mmoles)

Initial conductivity of solution: 0.3 $\mu S\ cm^{-1}$; Cell constant: 0.9580

$$Me_3SiIm + Me_3SiX \rightleftharpoons [Me_3SiImSiMe_3]^+X^- \quad (X=Br, I, OTf, ClO_4)$$

Scheme 2.19

In contrast the X=Cl titration displays completely different behaviour. No point of inflexion is observed; the conductivity continues to increase slowly as more TMSCl is added. Addition of 10 μl of water at the end of the TMSIm/TMSCl conductivity titration resulted in an initial increase in conductivity from 55 to 70 μS cm^{-1}, followed by a decrease to 50 μS cm^{-1} some several minutes later. These changes were accompanied by the precipitation of a white solid which was shown by proton n.m.r. to be an imidazolium species (Scheme 2.20).

$$[Me_3SiImSiMe_3]^+Cl^- + H_2O \rightleftharpoons$$ 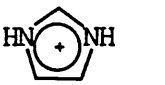 $$Cl^-$$

Scheme 2.20

Similar observations were made after adding water at the end of the other TMSIm/TMSX titrations, although solid precipitates were not always obtained.

The identity of these hydrolysed imidazolium species was confirmed by isolating the products resulting from methanolysis of the $[TMSIm\text{-}TMS]^+X^-$ salts (X=Br, I, OTf). The proton n.m.r. spectra of the imidazolium bromide and triflate in acetonitrile-d_3 show similar chemical shifts to those observed in the corresponding silyl species. However only small differences are observed between the chemical shifts for each counterion,

suggesting that the operation of the anion-dependent C_2-H chemical shift phenomenon is enhanced by the presence of silyl substituents on the imidazolium ring. The low solubility of the imidazolium triflate $[HImH]^+OTf^-$ in dichloromethane prevented the conductivity of this species being measured. Nevertheless this negative result is consistent with the observed decrease in conductivity produced by adding water to the TMSIm/TMSOTf system in CH_2Cl_2.

Comparisons of these conductivity curves with those of Chojnowski[7], for the HMPA/TMSX system (X=Cl, Br, I), show remarkable similarities in both shape and order of maximum conductivity. The dispute over the nature of the HMPA-TMSCl adduct (see discussion above) is thus particularly relevant here. To clarify this point, a low temperature n.m.r. study was carried out for the TMSCl/TMSIm system. Analysis of the results (Table 2.33) clearly indicates a trend towards the ionic chloride salt at lower temperatures. At ambient probe temperature (300K) the silicon-29 n.m.r. chemical shift corresponds to a very fast degenerate exchange (Scheme 2.21) between TMSCl (31.1 ppm) and TMSIm (13.5 ppm) [midpoint is 22.3 ppm].

Scheme 2.21

Fast exchange is maintained down to 183K (rate faster than 76,800 s^{-1} from equation A1.5), but the peak has shifted downfield to 25.4 ppm, consistent with the formation of an ionic adduct, analogous in structure with those observed for TMSIm-TMSX (X=Br, I, OTf, ClO_4) (Scheme 2.19). By

Table 2.33

Variable Temperature N.M.R. Data for a 1:1 mixture of Trimethylsilylimidazole (TMSIm) and Chlorotrimethylsilane (TMSCl)

TMSIm

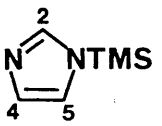

Temperature (K)	δ/ppm ^{1}H			^{29}Si
	C_2-H	$C_{4,5}$-H	Si-$(CH_3)_3$	Si-$(CH_3)_3$
308	7.59	7.03	0.43	22.3
275	7.85	7.10	0.46	22.5
243	9.23	7.49	0.61	23.6
214	10.02	7.75	0.70	25.0
195	-	-	-	25.3
188	10.31	7.87	0.75	25.34
TMSCl	-	-	0.42	31.1
TMSIm	7.55	7.03	0.42	13.5

quantities used: 0.5 mmoles of each component; solvent: CD_2Cl_2, 2.0 ml

analogy with the other TMSIm-TMSX salts it is reasonable to assume that the fully formed chloride complex will have a silicon-29 chemical shift of ca. 26 ppm, although the trend of the silicon-29 chemical shift vs. temperature plot (Figure 2.16) suggests that the limit could be as low as 25.5 ppm. This can be rationalized by examining the silicon-29 chemical shifts of the BTMSImX salts. There is a distinct trend (except X=ClO_4) towards lower shifts for the smaller harder anions i.e. OTf > I > Br (26.9, 26.8 and 26.2 respectively). A $\ln K_{eq}$ vs. 1/T plot, calculated using 25.5 ppm and 22.28 ppm as the limits for complexed and uncomplexed respectively, enables a value of -42 kJ mol^{-1} to be calculated for the enthalpy of complex formation. A value of -170 J K^{-1} mol^{-1} can also be evaluated for the entropy change, although the likely errors in this value are large. The proton n.m.r. chemical shifts for the imidazolium C_2-H can also be used to calculate the thermochemistry of the system. The choice of the upper limit is complicated by the variability of the C_2-H chemical shift. The 10.4 ppm value observed at 183 K for the chloride is consistent with the trend towards higher values for harder, smaller anions. Using limits (Figure 2.17) of 10.45 ppm and 7.55 ppm (TMSIm) gives values of -41 kJ mol^{-1} and -165 J K^{-1} mol^{-1} for the enthalpy and entropy change respectively for salt formation. Similarly the enthalpy and entropy changes can also be calculated from the chemical shifts of the $C_{4,5}$-H and $Si(CH_3)_3$ proton atoms (see Appendix 2 for an evaluation of the errors inherent in the method used to calculate these thermodynamic parameters).

All the data discussed above is consistent with the formation of N,N'-bistrimethylsilylimidazolium X (X=Cl, Br, I, OSO_2CF_3, ClO_4), Figure 2.18A.

Figure 2.16 Variable temperature silicon-29 n.m.r. data for a 1:1 mixture of N-trimethylsilylimidazole and chlorotrimethylsilane

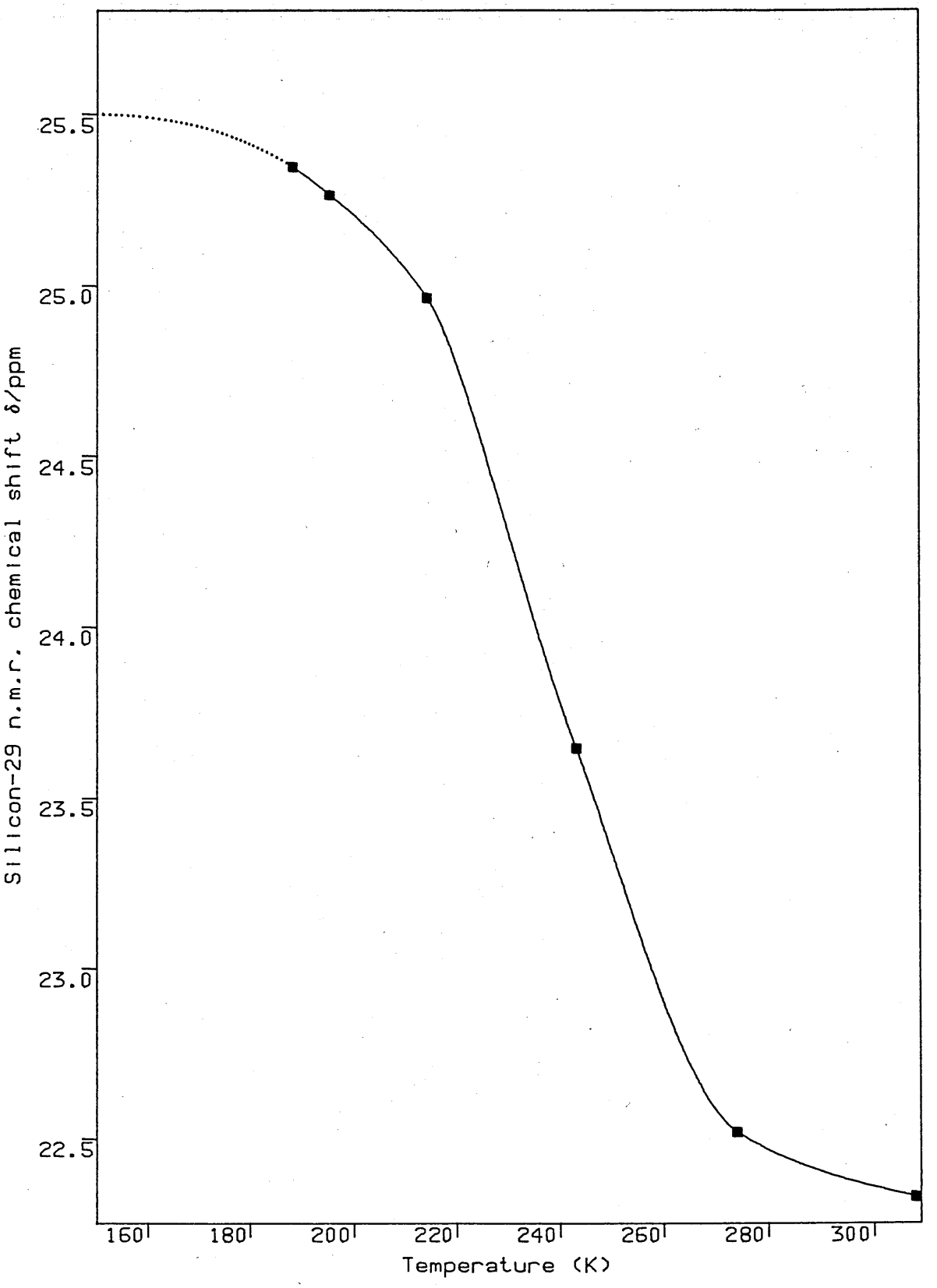

Solvent: dichloromethane-d2

..... Extrapolated curve

Figure 2.17 Variable temperature proton n.m.r. data for a 1:1 mixture of N-trimethylsilylimidazole and chlorotrimethylsilane.

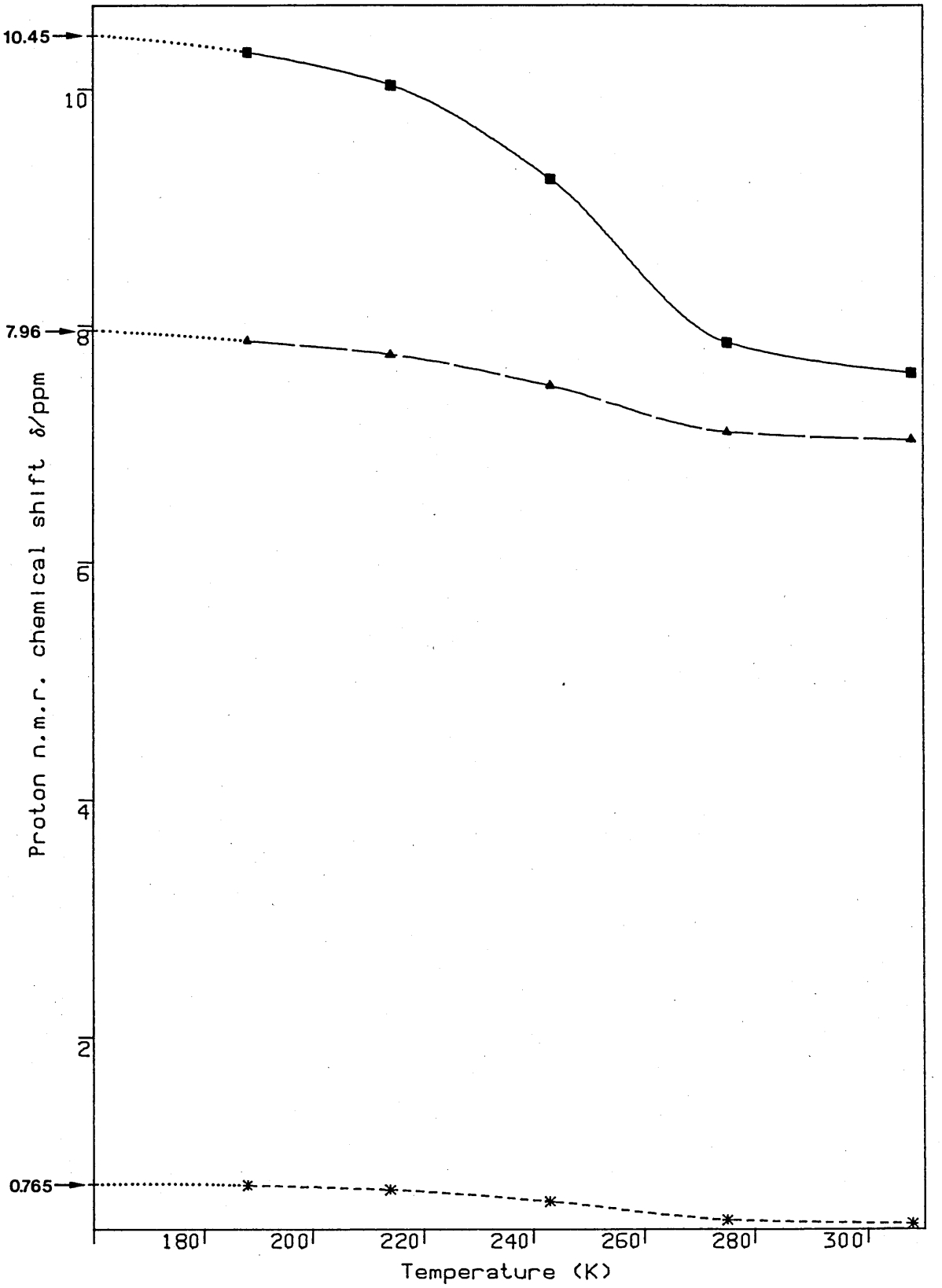

Solvent: dichloromethane-d2, 2.0 ml.

Concentration: 1.05 molar in each component.

..... Extrapolated curve

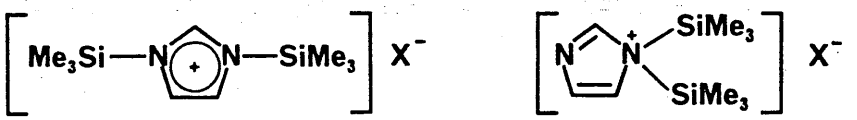

A B

Figure 2.18

The structure 2.18B is conceivable although it is not favoured on steric or electronic grounds. The equilibrium constant for adduct formation increases in the order Cl << Br < I, OTf.

Mixtures of the BTMSImX salts with other TMSX or TMSY species have also been studied. The results and the accompanying discussion are included in Chapter 4.

The n.m.r. data for mixtures of 1-methylimidazole (NMI) and 1,2-dimethylimidazole (DMI) with TMSOTf are shown in Tables 2.34 and 2.35 respectively. The chemical shift assignments for NMI, and by analogy DMI, follow those of Pugmire and Grant[96].

The protonation of imidazoles and histidines (including N-methyl derivatives) has been studied by Pugmire and Grant[96] and others[97]. The effects of silylation by TMSOTf on both NMI and DMI are very similar to the changes induced in TMSIm, allowing for the presence of the methyl groups. The broad nature of the $C_{4,5}$ DMI peaks in the ^{13}C spectra, together with the observation of two distinct peaks in both ^{1}H and ^{29}Si spectra indicate slow exchange between free and silylated DMI (refer to

Table 2.34 Interaction between 1-Methylimidazole (NMI) and Trimethylsilyl triflate (TMSOTf) : N.M.R. Data

NMI 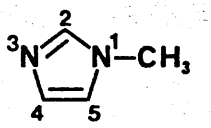

δ(ppm)		Ratio of NMI : TMSOTf 5:0	5:1	1:1[c]	1:5
^{1}H	$N-C_2(H)=N$	7.40	7.77	8.94	9.00
	$C_4(H)=C_5$	7.03	7.05	7.55t	7.50t
	$C_4=C_5(H)$	6.86	7.05	7.41t	7.32t
	$^{3}J_{HH}$	no	no	1.6Hz	1.6Hz
	$N-CH_3$	3.66	3.69	4.02	4.02
	$Si-(CH_3)_3$	-	0.59	0.62	0.62sbr[a]
	$Si-(CH_3)_3$*	-	no	no	0.50sbr[b]
^{13}C	C_2	137.8	138.2	139.8	140.2
	C_4	129.5	127.9	125.0	125.1
	C_5	120.1	121.3	123.7	123.7
	CF_3	-	118.1q	120.8q	118.9q
	$^{1}J_{CF}$	-	318Hz	321Hz	317Hz
	$N-CH_3$	33.3	33.6	36.9	36.1
	$Si-(CH_3)_3$	-	-1.2	-1.1	-1.0[a]
	$Si-(CH_3)_3$*	-	no	no	-0.3[b]
^{29}Si	$Si-(CH_3)_3$	-	26.0	26.8	26.6[a]
	$Si-(CH_3)_3$*	-	no	no	43.7[b]
quantities used:					
NMI (mmoles)		2.2	11.0	2.2	0.44
TMSOTf (mmoles)		-	2.2	2.2	2.2
solvent: $CDCl_3$, 2.0 ml					

Intensity of peak[a] is ca. 20% that of peak[b].

[c] Solution separated into 2 immiscible layers which dissolved on addition of further quantities of NMI.

Table 2.35

Interaction between 1,2-Dimethylimidazole (DMI) and Trimethylsilyl triflate (TMSOTf) : N.M.R. Data

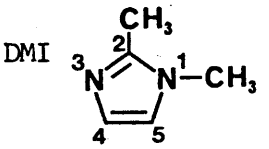

		Ratio of DMI : TMSOTf			
δ(ppm)		5:0	5:1	1:1	1:5
^{1}H	$C_4(H)=C$	6.81d	6.91	7.43d	7.42d
	$^{3}J_{HH}$	1.2Hz	no	2.2Hz	1.2Hz
	$C_4=C_5(H)$	6.73d	6.91	7.16d	7.17d
	$^{3}J_{HH}$	1.2Hz	no	2.2Hz	1.2Hz
	$N-CH_3$	3.48	3.61	3.85	3.84
	C_2-CH_3	2.29	2.41	2.70	2.69
	$Si-(CH_3)_3$	-	0.62	0.63	0.62small
	$Si-(CH_3)_3$*	-	no	no	0.50
^{13}C	C_2	144.7	145.5	148.1	148.6
	C_4	126.7	125.7(br)	122.2(br)	122.5(vbr)
	C_5	120.3	121.3(br)	122.2(br)	122.5(vbr)
	CF_3	-	nr	120.7q	119.3q
	$^{1}J_{CF}$	-	nr	321Hz	318Hz
	$N-CH_3$	32.6	33.1(br)	34.9(br)	35.0(br)
	C_2-CH_3	12.7	12.7(br)	12.2(br)	12.3(br)
	$Si-(CH_3)_3$	-	-0.46	-0.46	0.0(br)
^{29}Si	$Si-(CH_3)_3$	-	25.0	25.1	24.4
	$Si-(CH_3)_3$*	-	no	no	44.2
quantities used:					
DMI (mmoles)		2.93	2.93	2.93	2.93
TMSOTf (mmoles)		-	0.59	2.93	14.65
solvent: $CDCl_3$, 2.0 ml					

Chapter 4 for discussion of dynamic effects). The data is again fully consistent with the formation of a four coordinate silane-nucleophile adduct for NMI and DMI (Figure 2.19).

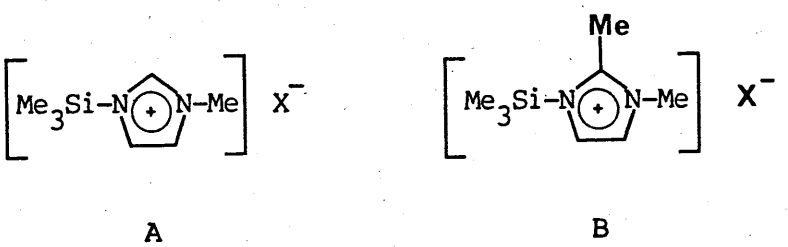

A B

Figure 2.19

The structure of the [NMI-TMS]$^{+}$OTf^{-} adduct (Figure 2.19A) is not a novel one. Maire and co-workers[98] have synthesised the analogous iodide complex by the action of methyl iodide on TMSIm (1 hour reflux in diethyl ether), although the authors did not characterise this species.

2.8 Attempted synthesis of Trimethylsilyltetrafluoroborate (Me_3SiBF_4)

Wenkert et al.[99] recently published a preparation of trimethylsilyl-tetrafluoroborate (Me_3SiBF_4, $TMSBF_4$). This was of considerable interest since it would represent a new highly electrophilic silicon reagent. The authors proposed that the new compound was the product of the reaction between chlorotrimethylsilane and silver tetrafluoroborate ($AgBF_4$) in either acetone or acetonitrile (Scheme 2.22).

$$Me_3SiCl + AgBF_4 \xrightarrow{CH_3CN} Me_3SiN^{+}{\equiv}CCH_3\ BF_4^{-} + AgCl\ (s)$$

Scheme 2.22

However the attempted preparation of this new silyl species failed in acetone or acetonitrile. Fluorotrimethylsilane and the coordinated species between acetone or acetonitrile and BF_3 were found to be produced essentially quantitatively (Scheme 2.23).

$$AgBF_4 + Me_3SiCl \longrightarrow AgCl\ (s) + Me_3SiF + (CH_3)_2C{=}O{:}BF_3$$

Scheme 2.23

The silicon-29 n.m.r. spectrum showed a doublet at 32.9 ppm with J_{Si-F} = 274 Hz; the ^{19}F n.m.r. gave a multiplet at -157 ppm corresponding to TMSF. The presence of BF_3 coordinated to the solvent was confirmed by comparing the ^{19}F resonances with literature values (-147 ppm in acetone-d_6, lit.[100], -148 ppm; -142 ppm in acetonitrile-d_3, lit.[101], -143 ppm). The observation of a resolvable coupling between the fluorine and silicon in TMSF shows that exchange between this species and BF_3 (Scheme 2.24) is slow on the n.m.r. time-scale.

$$BF_3 + Me_3SiF^* \longrightarrow BF_2F^* + Me_3SiF$$

Scheme 2.24

The strength of the Si-F bond in TMSF represents a considerable thermodynamic driving force towards the formation of this product. A similar result was observed by Lawton and Levy[102] who synthesised triphenylfluorosilane during the attempted preparation of triphenylsilyltetrafluoroborate from Ph_3SiCl and $NaBF_4$ (Scheme 2.25).

$$Ph_3SiCl + NaBF_4 + (CH_3)_2C{=}O \longrightarrow Ph_3SiF + BF_3{:}O{=}C(CH_3)_2$$

Scheme 2.25

2.9 Summary

The proton and carbon-13 chemical shift changes induced in the nucleophiles as a result of adduct formation are comparable to those resulting from protonation. Thus the chemical shift changes of these two nuclei were not very useful for verifying whether the observed effects were caused by silylation or by the presence of acidic impurities. Silicon-29 n.m.r. proved to be invaluable for differentiating protonation from silylation, besides being a very sensitive probe for studying the nature of the nucleophile-silane interactions. This underlines the utility of studying donor-acceptor interactions by examining those nuclei that are intimately involved in the adduct formation process, and demonstrates the potential dangers in drawing conclusions from the changes in chemical shifts of peripheral nuclei.

Four coordinate ionic 1:1 adducts were found to be the dominant species in solution for a wide variety of nucleophiles and trimethylsilyl species. No evidence for significant concentration of such adducts could be found in Nu/TMSCl mixtures at ambient temperatures. However evidence gained from the TMSIm/TMSCl low temperature n.m.r. study indicates that this result is owing to a low equilibrium constant for the 1:1 [Nu-TMS]$^{+}$Cl^{-} adduct formation at ambient temperatures.

The similarity between the silicon-29 chemical shifts of a particular [nucleophile-TMS]$^{+}$X^{-} adduct for different counterions (X=Cl, Br, I, OTf, ClO_4) shows that the same type of complex is present in each case. The equilibrium constants for adduct formation for a given nucleophile were found to increase with different counterions in the order:- Cl << Br < I,

OTf. Adduct formation is exothermic in the TMSIm/TMSCl, py/TMSBr and Et_3N/TMSI systems. These three results, together with the qualitative observation of heat evolution during adduct preparation, imply that this type of thermochemistry is a general phenomenon for complex formation between diverse types of nucleophiles and trimethylsilyl species.

The failure to observe stable adduct formation between TMSOTf and three nucleophiles, BIPY, quinoline and 2,6DMP, can be ascribed to low donicity combined with steric effects in BIPY and quinoline, and to a sterically hindered donor site in 2,6DMP. Steric effects may also be responsible for the low concentration of the $[Et_3N\text{-}TMS]^+X^-$ (X=I, OTf) adducts at ambient temperature, but it is conceivable that internal solvation of the counterion in these adducts is also a decisive factor in these systems.

In the absence of stabilization by polar solvents, the anion produced by cleavage of the Si-X bond has to be solvated internally by the cationic charge. The chemical shifts of the N,N'-bistrimethylsilylimidazolium salts with different counterions were attributed to this effect, which was also demonstrated by the lower conductivity readings. Hence, this implies that tighter ion pairing is observed for harder, less easily solvated, anions.

The positive charge resulting from coordination of the Et_3N nitrogen atom to silicon can be dispersed by the inductive effects of the ethyl groups. However the anionic charge cannot be solvated internally with ease, since the cationic nitrogen is shielded by the non-polar alkyl groups on both donor and acceptor sites (Figure 2.20).

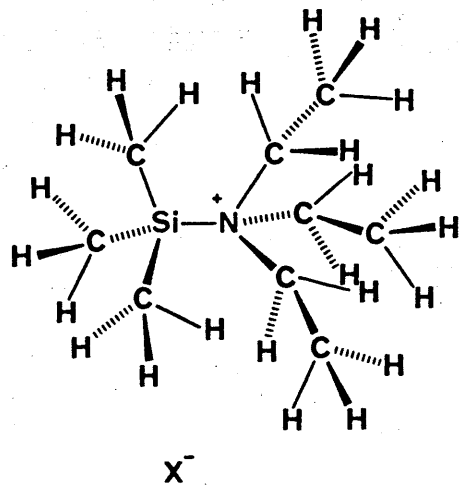

Figure 2.20

In the remaining cases studied here, the donor moiety possesses orbitals which are available to delocalise the induced charge, and could conceivably assist in the solvation of the anion.

No evidence for five coordination was noted except in the BIPY/TMSI system, where the presence of a five coordinate species undergoing fast exchange with a four coordinate adduct was inferred from the silicon-29 chemical shift trends.

Good linear correlations between the donor properties of each nucleophile and the silicon-29 n.m.r. chemical shift of the corresponding $[Nu\text{-}TMS]^{+}OTf^{-}$ complex were found for the amides and pyridines, which can be used to predict the chemical shift of complexes between other nucleophiles and TMSOTf.

A plot of silicon-29 chemical shift of each nucleophile-TMSOTf complex is

shown in Figure 2.21 for all the nucleophiles used in this study. The different classes of nucleophiles fall on separate regression lines, although the correlations involving the phosphine oxides, pyridine N-oxide and the amines are not statistically significant, because the number of points within each class is too small.

This type of behaviour was observed by Taft et al.[60] who described it as "family dependent behaviour". The authors introduced an empirical 'coordinate covalency parameter'; (Xi), to enable the diverse types of functional groups to be related by equation 2.5 (Q = measured quantity).

$$Q_{obs} = Q_o + b\ (Beta) + e\ (Xi) \quad ..... \quad \text{equation 2.5}$$

The separate regression lines, for different types of nucleophiles, can be combined into one correlation (Figure 2.22) using the coordinate covalency parameter (Xi) proposed by Taft[59,60]. The resulting equation $^{29}Si\ (Nu\text{-}TMS)^{+}X^{-} = 79.79 - 53.7\ Beta(Nu) - 2.7\ Xi$ predicts the ^{29}Si chemical shift of each complex to within ± 6 ppm or to ± 2 ppm if the points corresponding to the phosphine oxides and triethylamine are ignored.

Figure 2.21 Silicon-29 chemical shift vs. Beta correlation for all nucleophile-TMSOTf complexes studied.

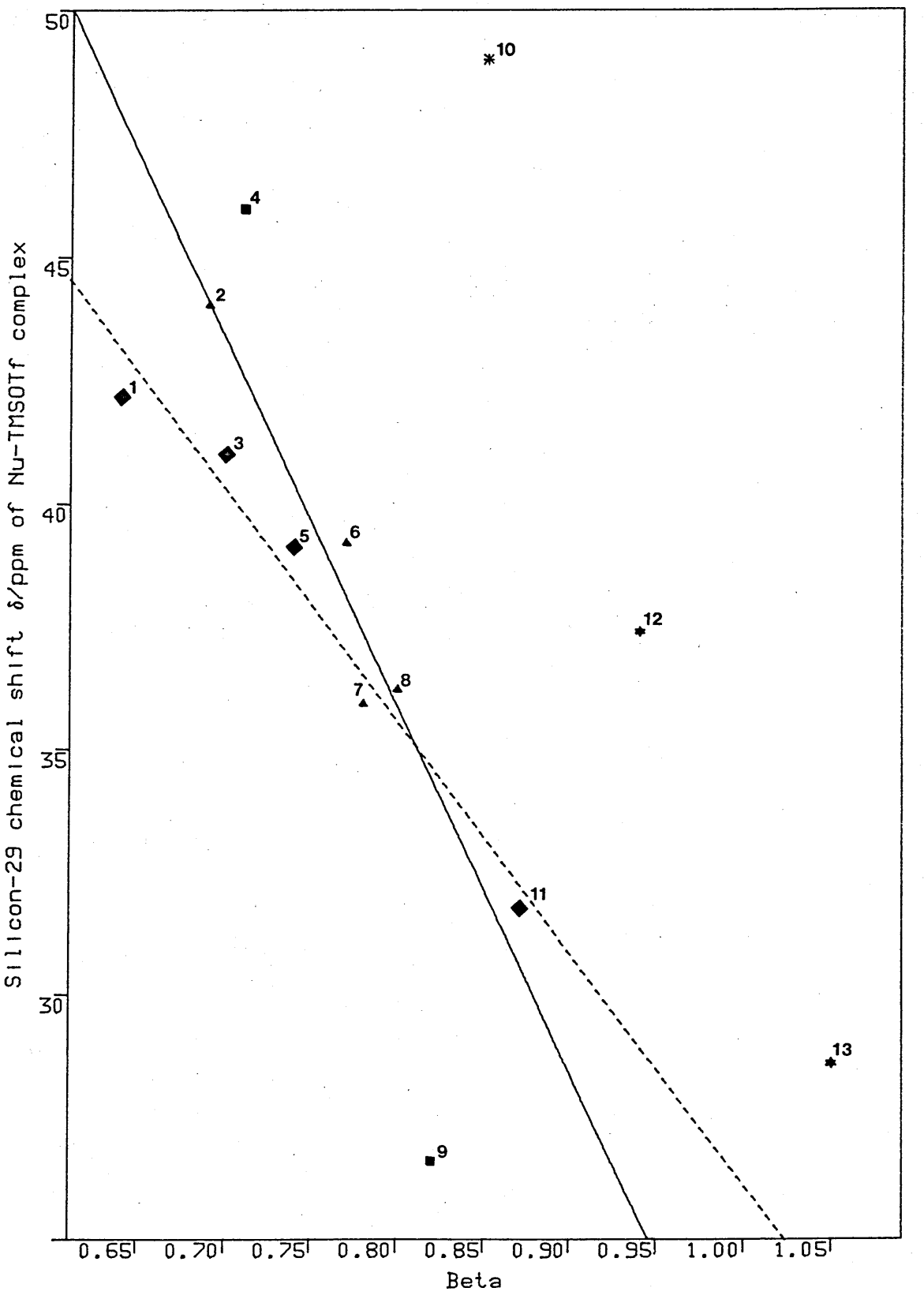

- - - Slope = -47.27, intercept = 73.36 (pyridines)
_____ Slope = -74.61, intercept = 95.52 (amides/ureas)

1, py; 2, DMF; 3, 3,5DMP; 4, Et_3N; 5, 2,4DMP; 6, NMP; 7, NMPO
8, TMU; 9, NMI; 10, PNO; 11, DMAP; 12, TPPO; 13, HMPA

Figure 2.22 Observed vs. calculated silicon-29 chemical shift

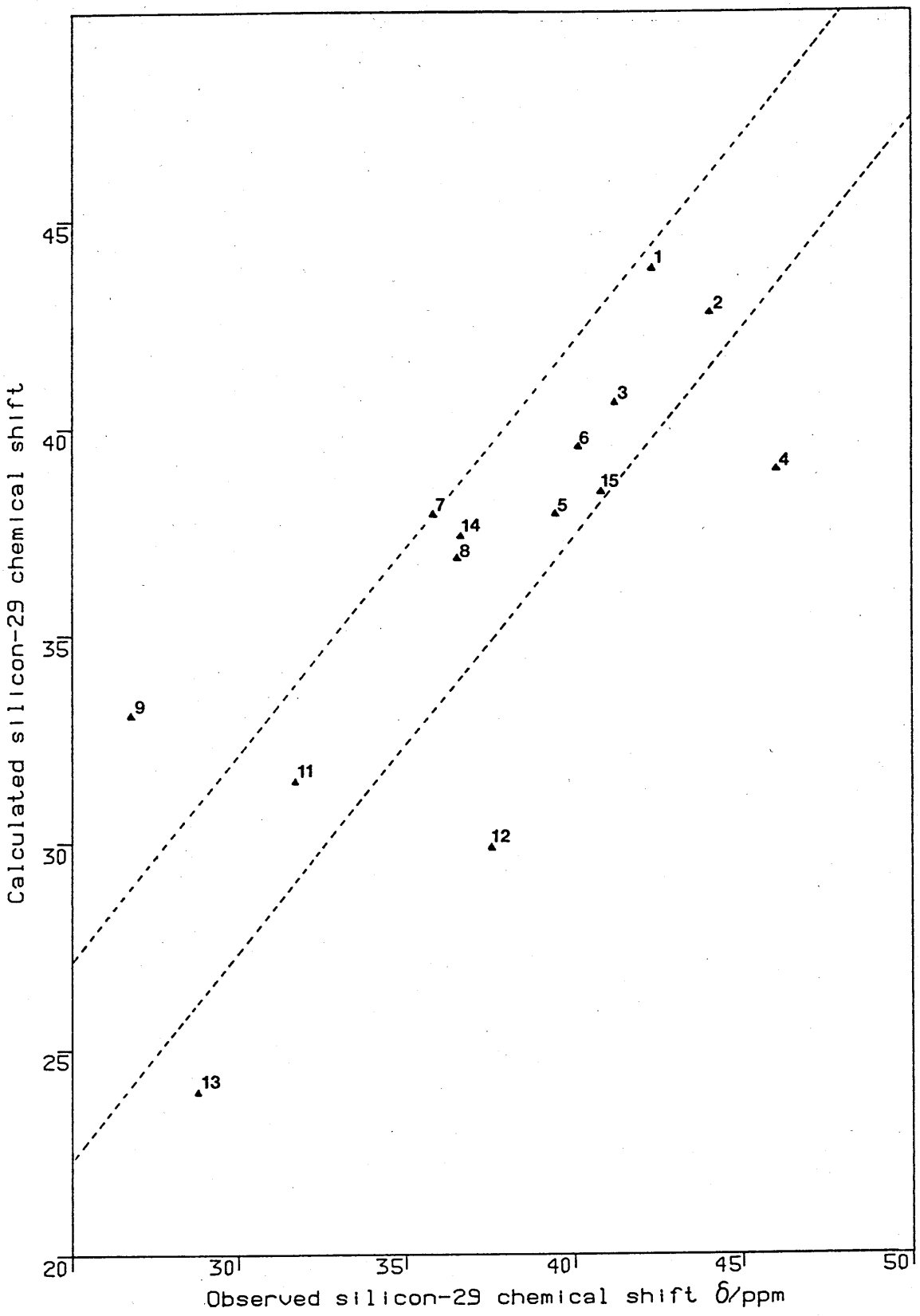

Si-29 chemical shift (calculated) = 79.79 - 53.7(Beta) - 2.7(Xi)
Variance = 11.29 (0.59 for the pyridine/amide points)
The pyridine/amide points are bounded by the dashed lines.
The numbering of the points is the same as in Figure 2.21
14, DMPU; 15, DMEU

CHAPTER 3

COMPETITION REACTIONS BETWEEN NUCLEOPHILES FOR [NUCLEOPHILE-TRIMETHYLSILYL]$^{+}X^{-}$ ADDUCT FORMATION

3.1 Introduction

It is evident from the preceding discussion that the equilibrium constant for formation of ionic 1:1 nucleophile-TMSX complexes is dependent upon the counterion X. Furthermore, the magnitude of the equilibrium constant for a given counterion also depends upon the nucleophile. Thus, for instance, the 1:1 TMSBr/TMSIm mixture shows essentially complete complexation, whereas for the py/TMSBr 1:1 mixture the equilibrium constant for adduct formation is very low at ambient temperatures.

It would, in theory, be possible to determine the relative equilibrium constants by evaluating the equilibrium position for a series of 1:1 Nu/TMSBr mixtures, however this method has some major drawbacks. Those nucleophiles which are effective at forming such complexes display chemical shifts very close to that of the fully formed complexes, because the complexes are already virtually fully formed at this stoicheiometry. Thus comparison of several nucleophiles which all form strong complexes has to rely upon very small differences in chemical shift, which could easily be masked by solvent effects. A similar problem occurs for those nucleophiles exhibiting a low equilibrium constant for adduct formation. Comparison of the relative equilibrium constants of nucleophile/TMSI and nucleophile/TMSOTf mixtures is even more difficult since most of these silane complexes are essentially fully formed at 1:1 stoicheiometry. In order to overcome these difficulties, a different approach was used.

Consider an intimate mixture of two nucleophiles Nu_A and Nu_B with 1:1 stoicheiometry. Addition of an equimolar quantity of TMSX in the mixture of Nu_A and Nu_B results in complex formation with the pair of

nucleophiles. The relative amounts of $[Nu_A\text{-}TMS]^+X^-$ and $[Nu_B\text{-}TMS]^+X^-$ will depend upon the relative magnitudes of each equilibrium constants K_A and K_B (Schemes 3.1 and 3.2).

$$Nu_A + Me_3SiX \rightleftharpoons [Nu_A\text{-}SiMe_3]^+X^-$$

Scheme 3.1

$$Nu_B + Me_3SiX \rightleftharpoons [Nu_B\text{-}SiMe_3]^+X^-$$

Scheme 3.2

The chemical shifts of each complex (v_A and v_B respectively) have already been determined in Chapter 2. Clearly if Nu_A is preferred over Nu_B, the addition of TMSX to the mixture of nucleophiles will produce a chemical shift v_A and vice versa. Therefore v_A and v_B represent the chemical shift limits of the 1:1:1 Nu_A/Nu_B/TMSX mixture. By assuming that exchange is fast for the process shown in Schemes 3.1 and 3.2, for all nucleophiles, it is possible to determine the relative equilibrium constants from the observed chemical shift (v_{obs}) of the aforementioned mixture. This can be rationalised as follows:-

the equilibrium constants for each complex are represented by K_A and K_B.

$$K_A = \frac{[Nu_A\text{-}Me_3SiX]}{[Nu_A]\ [Me_3SiX]} \quad \text{.....} \quad \text{equation 3.1}$$

$$K_B = \frac{[Nu_B\text{-}Me_3SiX]}{[Nu_B]\ [Me_3SiX]} \quad \text{.....} \quad \text{equation 3.2}$$

therefore,

$$\frac{K_A}{K_B} = \frac{[Nu_A\text{-}Me_3SiX]\ \ [Nu_B]}{[Nu_B\text{-}Me_3SiX]\ \ [Nu_A]} \quad \ldots\ldots \quad \text{equation 3.3}$$

In effect the system under study is

$$Nu_A + [Nu_B\text{-}Me_3SiX] \rightleftharpoons Nu_B + [Nu_A\text{-}Me_3SiX]$$

Scheme 3.3

If the initial concentrations of Nu_A, Nu_B, and Me_3SiX are equal, the relative concentration of each species at equilibrium can be represented as follows:

$$[Nu_A] \text{ and } [Nu_B\text{-}SiMe_3] = 1\text{-}x \quad \ldots\ldots \quad \text{equation 3.4}$$

$$[Nu_B] \text{ and } [Nu_A\text{-}SiMe_3] = x \quad \ldots\ldots \quad \text{equation 3.5}$$

thus the equilibrium constant for this process is equal to:

$$\frac{(1\text{-}x)\ \ (1\text{-}x)}{x\ \ \ \ x} = \left[\frac{(1\text{-}x)}{x}\right]^2 = \left[\frac{[Nu_B\text{-}Me_3SiX]}{[Nu_A\text{-}Me_3SiX]}\right]^2 \quad \ldots\ldots \quad \text{equation 3.6}$$

$$\frac{[Nu_A\text{-}Me_3SiX]}{[Nu_B\text{-}Me_3SiX]} = \frac{p_A}{p_B} \quad \ldots\ldots \quad \text{equation 3.7}$$

p_A, p_B = population of A and B.

The observed chemical shift v_{obs} is given by equation A1.1 (see Appendix 1)

$$v_{obs} = p_A v_A + p_B v_B \quad \ldots\ldots \quad \text{equation 3.7}$$

$$p_A + p_B = 1 \quad \ldots\ldots \quad \text{equation 3.8}$$

therefore

$$v_{obs} = p_A v_A + (1 - p_A) v_B \quad \ldots \quad \text{equation 3.9}$$

rearranging this equation gives

$$p_A = \frac{(v_{obs} - v_B)}{(v_A - v_B)} \quad \ldots\ldots \quad \text{equation 3.10}$$

and $$p_B = \frac{(v_A - v_{obs})}{(v_A - v_B)} \quad \ldots\ldots \quad \text{equation 3.11}$$

thus,

$$\frac{p_A}{p_B}^2 = \frac{(v_{obs} - v_B)}{(v_A - v_{obs})}^2 = \frac{K_A}{K_B} = K(Nu_A/Nu_B) \quad \ldots\ldots \quad \text{equation 3.12}$$

Taking the logarithm ($\log_e$) of this ratio enables the values so obtained, $\ln K(Nu_A/Nu_B)$, to be used additively.

3.2 Results and Discussion

In each competition experiment the pair of nucleophiles being investigated were mixed together in chloroform-d_1. Their proton and carbon-13 n.m.r. spectra were recorded to observe any strong nucleophile-nucleophile interactions or medium effects, which might otherwise be misinterpreted in the subsequent competition reaction. The proton and carbon-13 n.m.r. data for the isolated nucleophiles has already been presented in the last chapter. The data for the intimate mixture of the two nucleophiles is displayed in columns 1 and 3 of each competition reaction table (Tables 3.1-3.27). Comparison of the two sets of data shows that the chemical shifts of the nucleophiles are not very susceptible to solvent effects. The chemical shifts (^{1}H, ^{13}C and ^{29}Si) of the 1:1:1 $Nu_A/Nu_B/TMSOTf$ mixtures are shown in column 5, and those of the respective 1:1 $Nu_A/TMSOTf$ and $Nu_B/TMSOTf$ mixtures in columns 2 and 4 to aid comparison.

Apparently anomalous results were produced from those experiments in which a pair of nucleophiles of widely different affinity for adduct formation were studied. For instance the NMP/NMI/TMSOTf mixture gave a silicon-29 chemical shift of 26.6 ppm, indicating greater than 100% complexation - obviously an impossibility. The effect was noted only for those competitions involving NMI (Tables 3.4 and 3.13-3.16). A number of explanations can be advanced to account for these results:-

i) medium effects caused by the presence of the other nucleophile;

ii) extracoordination - no evidence in support of this hypothesis was noted, although it is conceivable that the extra upfield shift could result from a small equilibrium proportion of the five coordinate species (Scheme 3.4).

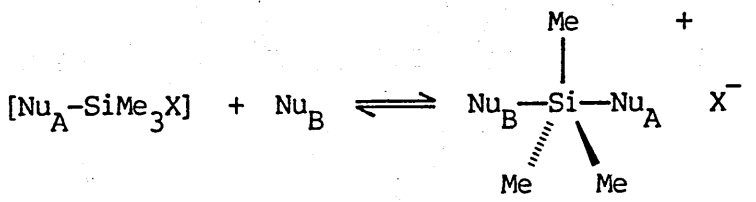

Scheme 3.4

iii) experimental inaccuracies (e.g. relative quantities of material) or hydrolysis; errors resulting from these two effects should be observed for a selection of nucleophiles, not just NMI. The acidic by-products resulting from hydrolysis of TMSOTf would be neutralized by the more basic of the two nucleophiles, thus reducing the availability of that compound for adduct formation. The concentration of the other nucleophile, on the other hand, would increase relative to TMSOTf, since the concentration of the silane would be reduced by hydrolysis. NMI has the higher basicity in most of the Nu/NMI pairs studied here. A more likely explanation is that the NMI-TMSOTf 1:1 value used is not applicable to the competition reaction. At 1:1 stoicheiometry, the Nu-silane complex formed an immiscible layer in chloroform-d_1, which redissolved upon further addition of NMI. Thus the complex is dissolved in a very polar medium, which could easily cause a small solvent shift. The $\ln K(Nu_A/Nu_B)$ values involving NMI shown in Table 3.28 were calculated by assuming a silicon-29 chemical shift of 26.7 ppm for the $[NMI\text{-}TMS]^+OTf^-$ complex.

Reproducibility was checked by repeating the DMPU/DMEU/TMSOTf competition experiment; DMPU and TMSOTf were mixed together prior to the addition of DMEU. The spectral data for all nuclei were identical to the values

Table 3.28 Summary of relative equilibrium constants from silicon-29 n.m.r. data of competition reactions between nucleophiles and trimethylsilyl X species (TMSX X=OTf, I)

Silane	Nu_B		Nu_A	$\ln K[Nu_A/Nu_B(^{29}Si)]$	Table
TMSOTf	py	<	DMF	2.20	3.1
	py	<	NMP	2.78	3.2
	py	<	PNO	7.06	3.3
	py	<<	NMI	a	3.4
	DMEU	<	DMF	1.86	3.5
	DMEU	<	NMP	1.84	3.6
	3,5DMP	<	2,4DMP	1.02	3.7
	3,5DMP	<	DMF	0.58	3.8
	DMF	<	NMP	0.35	3.9
	DMF	<	PNO	4.56	3.10
	NMP	<	DMPU	2.20	3.11
	NMP	<	HMPA	9.30	3.12
	NMP	<<	NMI	9.68[b]	3.13
	2,4DMP	<<	NMI	a	3.14
	DMPU	<<	NMI	9.16[b]	3.15
	TPPO	<	NMI	7.94[b]	3.16
	NMPO	<	DMAP	5.08	3.17
	DMI	<	HMPA	0.76	3.18
	HMPA	<	DMAP	0.98	3.19
	HMPA	<	NMI	1.24 (0.96[b])	3.20
	DMAP	<	NMI	0.08 (0.16[b])	3.21
	DMEU	<	DMPU	4.74	3.22
TMSI	py	<	NMI	-	3.23
	py	<	NMP	-	3.24
	NMP	<	HMPA	-	3.25
	NMP	<	NMI	-	3.26
	HMPA	<	NMI	-	3.27

[a] infinity

[b] Calculated using 26.7 ppm for the chemical shift of $[NMI\text{-}TMS]^+OTf^-$.

obtained from the existing DMPU/DMEU/TMSOTf competition reaction (Table 3.22). Furthermore, this experiment demonstrates that the observed behaviour of this and (by analogy) other competition experiments is not the result of a kinetic effect. The occurrence of a sharp single resonance with approximately natural linewidth justifies the previous assumption that fast exchange occurs between salt and uncomplexed nucleophile.

The silicon-29 chemical shifts were used for determining the $\ln K(Nu_A/Nu_B)$ values. Those pairs of nucleophiles which exhibited anomalous values were not used in the calculation. The calculated values are shown in Table 3.28. A scale incorporating all of the $\ln K(Nu_A/Nu_B)$ values was built up in the following manner:-

i) NMP was chosen, arbitrarily, as the reference point ($\ln K_{rel} = 0.0$);

ii) $\ln K_{rel}$ values for those nucleophiles which have been studied in competition with NMP (py, DMEU, DMF, DMPU and HMPA) were calculated by addition if the nucleophile was better than NMP, and by subtraction for nucleophiles worse than NMP;

iii) $\ln K_{rel}$ values for the remaining nucleophiles were obtained using the values calculated from ii) and so on, until each nucleophile had been assigned a value;

iv) the consistency of each $\ln K_{rel}$ value was judged by cross referencing the experimental $\ln K(Nu_A/Nu_B)$ values. For example, the py/DMF/PNO system was checked by adding the $\ln K(Nu_A/Nu_B)$ value of py/DMF (2.2) to that of DMF/PNO (4.16). Thus the predicted py/PNO $\ln K(Nu_A/Nu_B)$ value is 6.36. A discrepancy is found between this value and the experimental one (7.06, a difference of 0.70). In cases such as

Table 3.29

^{29}Si N.M.R. chemical shifts and relative equilibrium constants for salt formation, from the reaction of nucleophiles with TMSOTf in dichloromethane-d_2

Nucleophile	Abbreviation	$\delta^{29}Si$[a]	K_{rel}[b]	$\ln K_{rel}$	Beta[c]
Pyridine	py	42.3	0.10	-2.3	0.64
Dimethylethylene urea[d]	DMEU	40.1	0.11	-2.2	0.75[e]
3,5-Dimethylpyridine	3,5DMP	41.2	0.55	-0.6	0.70[f]
Dimethylformamide	DMF	44.0	0.81	-0.2	0.69
1-Methyl-2-pyrrolidone	NMP	39.4	1.0	0.0	0.78
2,4-Dimethylpyridine	2,4DMP	40.8	1.2	0.2	0.74
Dimethylpropylene urea[g]	DMPU	36.6	9.0	2.2	0.79[e]
Triphenylphosphine oxide	TPPO	37.5	11.0	2.4	0.94
Pyridine N-oxide	PNO	49.4	66	4.2	0.85
N-methyl-2-pyridone	NMPO	35.8	182	5.2	0.78
1,2-Dimethylimidazole	DMI	25.1	5430	8.6	-
Hexamethylphosphoramide	HMPA	28.8	9900	9.2	1.05
4-N,N-dimethylaminopyridine	DMAP	31.7	32800	10.4	0.87
N-methylimidazole	NMI	26.8	32800	10.4	0.82

a ^{29}Si n.m.r. chemical shift of 1:1 $[Nu\text{-}SiMe_3]^+OTf^-$ (ppm) relative to internal Me_4Si in $CDCl_3$ (in CD_3CN for py).

b K_{eq} for reaction [NMP-TMSX] + Nu^* $\rightleftharpoons$ [Nu^*-TMSX] + NMP

c From reference 60.

d Also referred to as 1,3-dimethyl-2-imidazolidinone.

e Calculated from equation 2.1.

f Calculated from equation 2.2.

g Also referred to as 1,3-dimethyl-3,4,5,6-tetrahydro-2(1H)-pyrimidinone.

this, the existing $\ln K_{rel}$ values for each nucleophile were judged to have equal significance and the error limits on each value were increased accordingly. The $\ln K_{rel}$ values presented in Table 3.29 represent the midpoint of the error limits of each nucleophile's $\ln K_{rel}$ value. The estimated error limit for each $\ln K_{rel}$ value is ± 1 unit. The K_{rel} values presented in the table are a measure of the equilibrium constants for the reaction shown in Scheme 3.5 with different nucleophiles.

$$Nu_x + [NMP\text{-}SiMe_3]^+OTf^- \rightleftharpoons [Nu_x\text{-}SiMe_3]^+OTf^- + NMP$$

Scheme 3.5

The overall order was found to be:
NMI, DMAP > HMPA > DMI > NMPO > PNO > TPPO > DMPU > 2,4DMP > NMP > DMF > 3,5DMP > DMEU > py (by inference py > 2,6DMP, quinoline, BIPY and Et_3N).

Correlations of the $\ln K_{rel}$ values with Beta and ^{29}Si [(Nu-TMS)$^+OTf^-$] are presented in Figures 3.1 and 3.2. Deviation of the points corresponding to PNO and the phosphine oxides - TPPO and HMPA from the other data points, as illustrated in Figure 3.1, suggests that the spread of points reflects the different functional groups involved ('Family dependent behaviour'[59,60]). This behaviour is analogous to that observed previously in the Beta vs. ^{29}Si (Nu-TMSOTf) correlations (Figure 2.21). The correlation improves significantly if the TPPO, HMPA and PNO points are ignored (pyridine and amide points bounded by dashed lines).

The silicon-29 chemical shift (Nu-TMSOTf)/$\ln K_{rel}$ correlation (Figure 3.2) is somewhat better than the previous one, although again the PNO point is

Figure 3.1 Correlation of Beta value against ln Krel for 1:1 nucleophile-silane adduct formation.

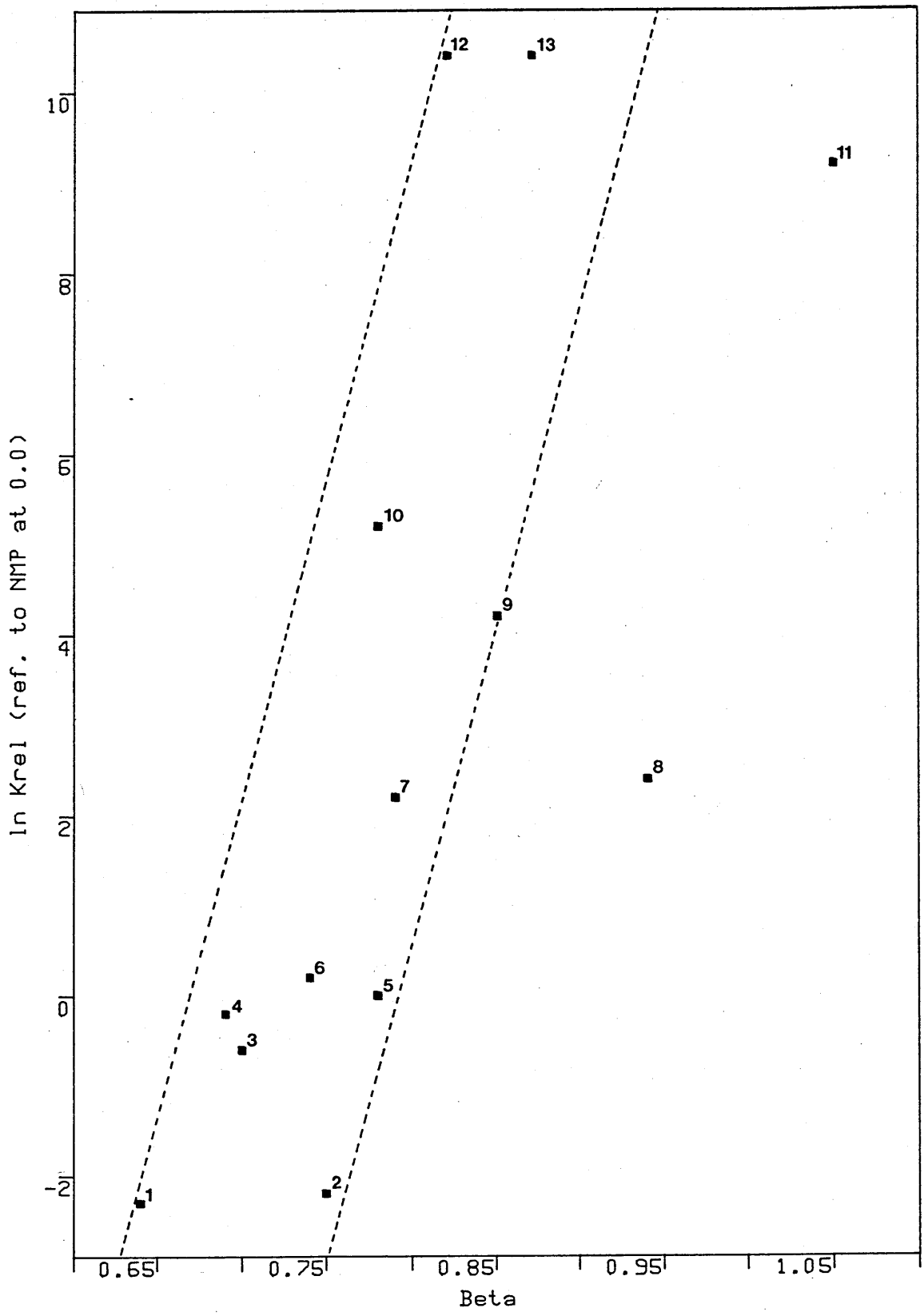

1, py; 2, DMEU; 3, 3,5DMP; 4, DMF; 5, NMP; 6, 2,4DMP; 7, DMPU 8, TPPO; 9, PNO; 10, NMPO; 11, HMPA; 12, DMAP; 13, NMI.

Solvent: chloroform-d1, except py (acetonitrile-d3)

Figure 3.2 Correlation of silicon-29 chemical shift against ln Krel for 1:1 nucleophile-TMSOTf adduct formation.

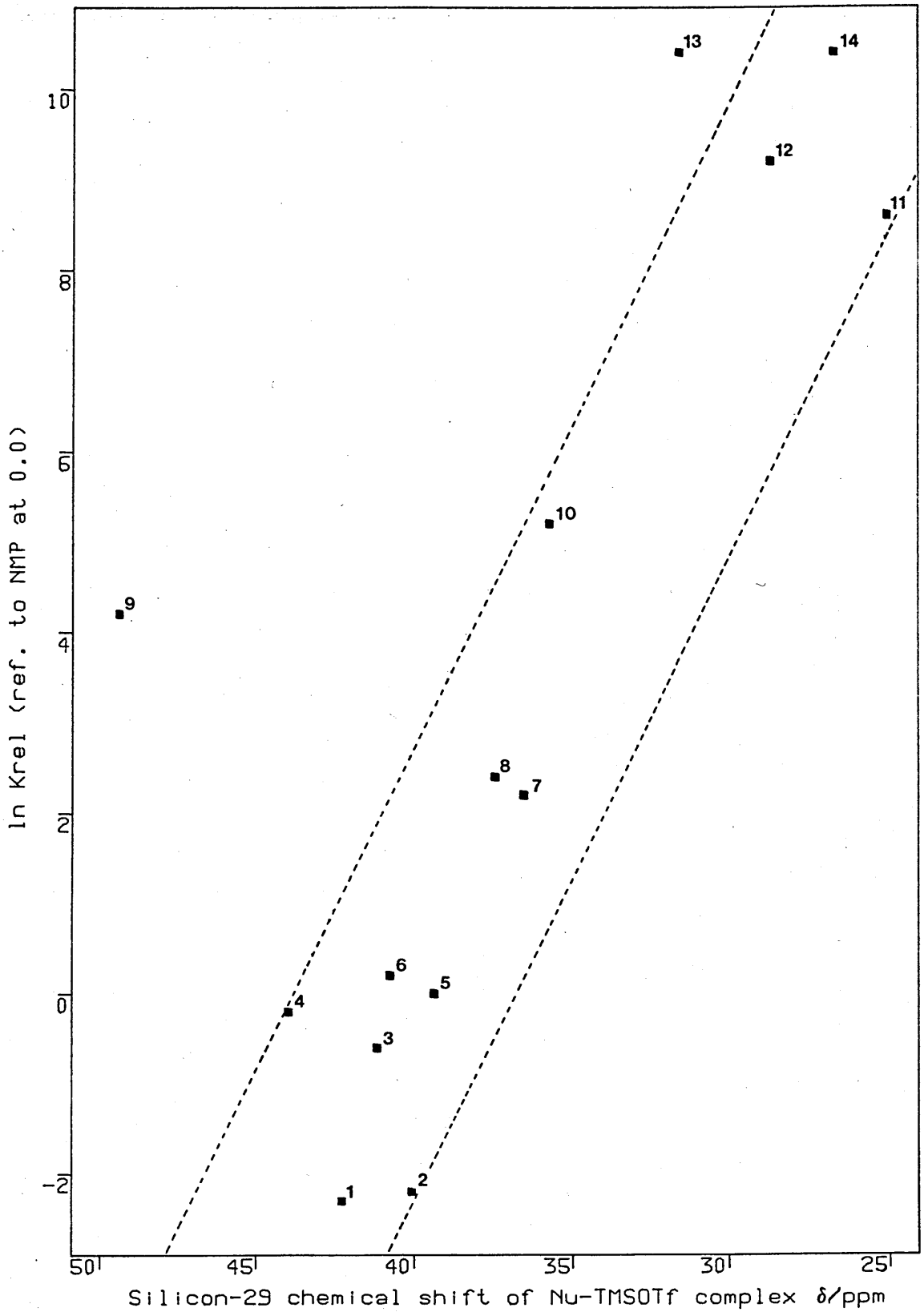

1, py; 2, DMEU; 3, 3,5DMP; 4, DMF; 5, NMP; 6, 2,4DMP; 7, DMPU 8, TPPO; 9, PNO; 10, NMPO; 11, DMI; 12, HMPA; 13, DMAP; 14, NMI.

a deviant one. These correlations are particularly interesting, because they show that the factors controlling silicon-29 chemical shifts of each adduct are also important in determining the stability of that complex. These complexes can be regarded as donor-acceptor interactions, thus stronger donor species, such as DMAP, HMPA, NMI etc., are better in donating the electrons required to form the donor-silicon bond. This effect is revealed by the various strengths of the Nu-silane bond and the increased shielding around silicon, demonstrated by the lower frequency chemical shifts of the complexes involving better donor ligands.

Several competition experiments were performed using TMSI (Tables 3.23 to 3.27) instead of TMSOTf. The same trends were observed for each silane which suggests that the relative order of K_{eq} is essentially the same irrespective of counterion.

3.3 Summary

The equilibrium constants are related to the free energy change by $\Delta G = -RT\ln K_{eq}$, and hence to the enthalpy change, since $\Delta G^{o} = \Delta H^{o} - T\Delta S$. Therefore at constant temperature, assuming a constant entropy change, the equilibrium constant is proportional to the enthalpy change.

Adduct formation involves cleavage of the Si-X bond and formation of the nucleophile-Si bond. Therefore, for a given silane e.g. TMSOTf, the Si-X bond energy term is constant so the overall enthalpy change reflects the

strength of the donor-acceptor bond[103]. This bond is essentially a dative one (Nu:⟶ Si), thus those nucleophiles that can easily donate an electron pair will stabilise the silicon atom, which is severely deshielded by the departure of the negatively charged leaving group.

Table 3.1

Competition between N,N-Dimethylformamide (DMF) and Pyridine (py) for Trimethylsilyl triflate (TMSOTf) : N.M.R. Data

		DMF	DMF + TMSOTf (1:1)	py	py* + TMSOTf (1:1)	DMF + py + TMSOTf (1:1:1)
δ(ppm)						
^{1}H	H-C=O	8.00	8.45	-	-	8.39
	$N-(CH_3)^a$	2.93	3.45	-	-	3.35d
	$^{4}J_{HH}$	no	no	-	-	0.73Hz
	$N-(CH_3)^b$	2.85d	3.23d	-	-	3.14d
	$^{4}J_{HH}$	0.49Hz	0.75Hz	-	-	0.97Hz
	(a-b)	6.8Hz	19.8Hz	-	-	18.1Hz
	aromatic C-H	-	-	8.58-8.62m	8.51-8.90m	8.65-8.74m
		-	-	7.59-7.76m	8.00-8.17m	7.83-7.96m
		-	-	7.20-7.35m	-	7.44-7.59m
	$Si-(CH_3)_3$	-	0.50	-	0.73	0.56
^{13}C	C=O	162.5	163.4	-	-	163.2
	$N-(CH_3)^a$	36.4	41.1	-	-	40.0
	$N-(CH_3)^b$	31.3	35.8	-	-	34.8
	(a-b)	113.9Hz	120.4Hz	-	-	117.8Hz
	$C_{2,6}$	-	-	149.8	148.8	148.6
	C_4	-	-	135.9	146.7	138.8
	$C_{3,5}$	-	-	123.7	129.8	125.1
	$Si-(CH_3)_3$	-	-0.63	-	0.98	-0.75
^{29}Si	$Si-(CH_3)_3$	-	44.0	-	42.4	43.6
quantities used: 2.2 mmoles of each component; solvent: $CDCl_3$, 2.0 ml						

* Recorded in acetonitrile-d_3.

Table 3.2 Competition between 1-Methyl-2-pyrrolidone (NMP) and Pyridine (py) for Trimethylsilyl triflate (TMSOTf) : N.M.R. Data

		NMP	NMP + TMSOTf (1:1)	py	py[a] + TMSOTf (1:1)	NMP + py + TMSOTf (1:1:1)
δ(ppm)						
^{1}H	$C_3(H)-C=O$	3.35t	3.89t	-	-	3.81t
	$^{3}J_{HH}$	7.3Hz	7.8Hz	-	-	7.6Hz
	$N-CH_3$	2.82	3.11	-	-	3.07
	$C_5(H)-N$	1.80-2.45m	2.97t	-	-	2.79-3.07m
	C_4-H	1.80-2.45m	2.32qn	-	-	2.27qn
	$^{3}J_{HH}$	obsc	7.1Hz	-	-	7.5Hz
	aromatic C-H	-	-	8.58-8.65m	8.51-8.90m	8.66-8.73m
		-	-	7.59-7.69m	8.00-8.17m	7.79-7.93m
		-	-	7.19-7.35m	-	7.41-7.56m
	$Si-(CH_3)_3$	-	0.60	-	0.73	0.55
^{13}C	C=O	174.9	175.8	-	-	175.8
	$N-CH_3$	49.3	52.9	-	-	52.5
	C_3	30.6	32.2	-	-	31.9
	C_5	29.5	31.4	-	-	31.5
	C_4	17.6	17.1	-	-	17.3
	$C_{2,6}$	-	-	149.8	148.8	148.9
	C_4	-	-	135.9	146.7	138.4
	$C_{3,5}$	-	-	123.7	129.8	124.9
	$Si-(CH_3)_3$	-	0.0	-	0.98	0.0
^{29}Si	$Si-(CH_3)_3$	-	39.4	-	42.4	40.0

quantities used: 2.2 mmoles of each component; solvent: $CDCl_3$, 2.0 ml

[a] Recorded in acetonitrile-d_3.

Table 3.3

Competition between Pyridine N-oxide (PNO) and Pyridine (py) for Trimethylsilyl triflate (TMSOTf) : N.M.R. Data

		PNO	PNO + TMSOTf (1:1)	py	py[a] + TMSOTf (1:1)	PNO + py + TMSOTf (1:1:1)
δ(ppm)						
^{1}H	aromatic C-H	8.23-8.33m	9.03-9.10m	-	-	8.23-8.70m
		7.18-7.23m	8.15-8.63m	-	-	7.27-7.43m
		-	-	8.58-8.65m	8.51-8.90m	9.11-9.20m
		-	-	7.37-7.74m	8.00-8.17m	7.66-8.16m
	$Si-(CH_3)_3$	-	0.50	-	0.73	0.50
^{13}C	$C_{2,6}$	139.2	141.6	-	-	141.7
	$C_{3,5}$	126.3	129.8	-	-	129.9
	C_4	125.5	143.3	-	-	143.3
	$C_{2,6}$	-	-	149.8	148.8	149.5
	C_4	-	-	135.9	146.7	136.7
	$C_{3,5}$	-	-	123.7	129.8	124.2
	$Si-(CH_3)_3$	-	-1.4	-	0.98	-1.4
^{29}Si	$Si-(CH_3)_3$	-	49.4	-	42.4	49.2

quantities used: 2.2 mmoles of each component; solvent: $CDCl_3$, 2.0 ml

[a] Recorded in acetonitrile-d_3.

Table 3.4

Competition between 1-Methylimidazole (NMI) and Pyridine (py) for Trimethylsilyl triflate (TMSOTf) : N.M.R. Data

δ(ppm)		NMI	NMI + TMSOTf (1:1)	py	py[a] + TMSOTf (1:1)	NMI + py + TMSOTf (1:1:1)
^1H	$N-C_2(H)=N$	7.39	8.94	-	-	8.96
	$C_4(H)=C_5$	7.03	7.55t	-	-	7.58t
	$^3J_{HH}$	no	1.6Hz	-	-	1.6Hz
	$C_4=C_5(H)$	6.85	7.41t	-	-	7.42t
	$^3J_{HH}$	no	1.6Hz	-	-	1.7Hz
	$N-CH_3$	3.62	4.02	-	-	4.01
	aromatic C-H	-	-	8.55-8.63m	8.51-8.90m	8.50-8.60m
		-	-	7.16-7.75m	8.00-8.17m	7.25-7.78m
	$Si-(CH_3)_3$	-	0.62	-	0.73	0.61
^{13}C	C_2	137.8	139.8	-	-	139.7
	C_4	129.5	125.0	-	-	125.0
	C_5	120.1	123.7	-	-	123.7
	$N-CH_3$	33.1	36.9	-	-	35.8
	$C_{2,6}$	-	-	149.8	148.8	149.6
	C_4	-	-	135.9	146.7	136.3
	$C_{3,5}$	-	-	123.7	129.8	124.0
	$Si-(CH_3)_3$	-	-1.1	-	0.98	-1.2
^{29}Si	$Si-(CH_3)_3$	-	26.8	-	42.4	26.7
quantities used: 2.2 mmoles of each component; solvent: $CDCl_3$, 2.0 ml						

[a] Recorded in acetonitrile-d_3.

Table 3.5

Competition between 1,3-Dimethyl-2-imidazolidinone (DMEU) and N,N-Dimethylformamide (DMF) for Trimethylsilyl triflate (TMSOTf) : N.M.R. Data

		DMEU	DMEU + TMSOTf (1:1)	DMF	DMF + TMSOTf (1:1)	DMF + DMEU + TMSOTf (1:1:1)
δ(ppm)						
^{1}H	$N-CH_3$	3.28	3.84	-	-	3.45
	$C_{4,5}-H$	2.78	2.96	-	-	2.82
	H-C=O	-	-	8.01	8.45	8.39
	$N-(CH_3)^a$	-	-	2.98	3.45	3.35d
	$^{4}J_{HH}$	-	-	no	no	0.74Hz
	$N-(CH_3)^b$	-	-	2.88	3.23	3.15d
	$^{4}J_{HH}$	-	-	no	0.75Hz	1.0Hz
	(a-b)	-	-	8.8Hz	19.8Hz	18.1Hz
	$Si-(CH_3)_3$	-	0.51	-	0.50	0.51
^{13}C	C=O	162.1	159.0	-	-	161.3
	$N-CH_3$	45.0	46.3	-	-	45.4
	$C_{4,5}$	31.4	32.2	-	-	31.6
	C=O	-	-	162.5	163.4	163.2
	$N-(CH_3)^a$	-	-	36.4	41.1	39.9
	$N-(CH_3)^b$	-	-	31.4	35.8	34.6
	(a-b)	-	-	112.6Hz	120.4Hz	117.8Hz
	$Si-(CH_3)_3$	-	0.69	-	-0.63	-0.40
^{29}Si	$Si-(CH_3)_3$	-	40.1	-	44.0	42.9

quantities used: 2.2 mmoles of each component; solvent: $CDCl_3$, 2.0 ml

Table 3.6

Competition between 1-Methyl-2-pyrrolidone (NMP) and 1,3-Dimethyl-2-imidazolidinone (DMEU) for Trimethylsilyl triflate (TMSOTf) : N.M.R. Data

		NMP	NMP + TMSOTf (1:1)	DMEU	DMEU + TMSOTf (1:1)	NMP + DMEU + TMSOTf (1:1:1)
δ(ppm)						
^{1}H	$C_3(H)-C=O$	3.40t	3.89t	-	-	3.79t
	$^{3}J_{HH}$	6.0Hz	7.8Hz	-	-	7.3Hz
	$N-CH_3$	2.84	3.11	-	-	3.06
	$C_5(H)-N$	2.03-2.54m	2.97t	-	-	2.18-2.57m
	C_4-H	2.03-2.54m	2.32qn	-	-	2.18-2.57m
	$^{3}J_{HH}$	obsc	7.1Hz	-	-	obsc
	$N-CH_3$	-	-	3.29	3.84	3.41
	$C_{4,5}-H$	-	-	2.78	2.96	2.81
	$Si-(CH_3)_3$	-	0.49	-	0.51	0.50
^{13}C	C=O	174.9	175.8	-	-	175.8
	$N-CH_3$	49.3	52.9	-	-	52.2
	C_3	30.6	32.2	-	-	31.6
	C_5	29.5	31.4	-	-	31.4
	C_4	17.6	17.1	-	-	17.3
	C=O	-	-	162.0	159.0	161.5
	$N-CH_3$	-	-	45.0	46.3	45.3
	$C_{4,5}$	-	-	31.4	32.2	32.5
	$Si-(CH_3)_3$	-	0.0	-	0.69	0.23
^{29}Si	$Si-(CH_3)_3$	-	39.4	-	40.1	39.6

quantities used: 2.2 mmoles of each component; solvent: $CDCl_3$, 2.0 ml

Table 3.7 Competition between 2,4-Dimethylpyridine (2,4DMP) and 3,5-Dimethylpyridine (3,5DMP) for Trimethylsilyl triflate (TMSOTf) : N.M.R. Data

δ(ppm)		2,4DMP	2,4DMP + TMSOTF (1:1)	3,5DMP	3,5DMP + TMSOTF (1:1)	2,4DMP + 3,5DMP + TMSOTF (1:1:1)
^{1}H	C_6-H	8.33d	8.49d	-	-	8.34d
	$^{3}J_{56}$	5.1Hz	5.6Hz	-	-	5.1Hz
	C_3-H	6.93	7.43	-	-	7.10
	C_5-H	6.87d	7.39d	-	-	7.06d
	$^{3}J_{56}$	5.1Hz	5.6Hz	-	-	5.5Hz
	C_2-CH_3	2.49	2.72	-	-	2.54
	C_4-CH_3	2.25	2.47	-	-	2.34
	$C_{2,6}$-H	-	-	8.23	8.53	8.59
	C_4-H	-	-	7.24	8.11	8.16
	$C_{3,5}$-CH_3	-	-	2.26	2.56	2.57
	Si-$(CH_3)_3$	-	0.70	-	0.77	0.78
^{13}C	C_2	158.0	154.9	-	-	157.6
	C_6	148.8	147.1	-	-	148.0
	C_4	147.1	157.4	-	-	149.3
	C_3	124.1	128.2	-	-	125.1
	C_5	121.7	124.5	-	-	122.5
	C_2-$\underline{C}H_3$	24.2	23.3	-	-	23.8
	C_4-$\underline{C}H_3$	20.9	21.4	-	-	21.0
	$C_{2,6}$	-	-	147.4	142.9	142.8
	C_4	-	-	137.0	147.3	147.7
	$C_{3,5}$	-	-	132.4	138.7	138.9
	$C_{3,5}$-$\underline{C}H_3$	-	-	18.2	18.3	18.3
	Si-$(CH_3)_3$	-	0.69	-	-0.92	-0.80
^{29}Si	Si-$(CH_3)_3$	-	40.8	-	41.2	40.95

quantities used: 2.2 mmoles of each component; solvent: $CDCl_3$, 2.0 ml

Table 3.8

Competition between N,N-Dimethylformamide (DMF) and 3,5-Dimethylpyridine (3,5DMP) for Trimethylsilyl triflate (TMSOTf) : N.M.R. Data

δ(ppm)		DMF	DMF + TMSOTf (1:1)	3,5DMP	3,5DMP + TMSOTf (1:1)	DMF + 3,5DMP + TMSOTf (1:1:1)
^{1}H	H-C=O	8.00	8.45	-	-	8.22[a]
	$N-(CH_3)^a$	2.94	3.45	-	-	3.18
	$N-(CH_3)^b$	2.85	3.23	-	-	3.02
	$^{4}J_{HH}$	no	0.75Hz	-	-	0.74Hz
	(a-b)	8.7Hz	19.8Hz	-	-	14.3Hz
	$C_{2,6}-H$	-	-	8.22	8.53	8.37[a]
	C_4-H	-	-	7.28	8.11	7.65
	$C_{3,5}-CH_3$	-	-	2.27	2.56	2.40
	$Si-(CH_3)_3$	-	0.50	-	0.77	0.60
^{13}C	C=O	162.5	163.4	-	-	162.4
	$N-(CH_3)^a$	36.4	41.1	-	-	38.4
	$N-(CH_3)^b$	31.3	35.8	-	-	33.2
	(a-b)	115.2Hz	120.4Hz	-	-	116.5Hz
	$C_{2,6}$	-	-	147.4	142.9	145.3
	C_4	-	-	137.1	147.3	141.3
	$C_{3,5}$	-	-	132.5	138.7	135.0
	$C_{3,5}-CH_3$	-	-	18.2	18.3	18.2
	$Si-(CH_3)_3$	-	-0.63	-	-0.92	-0.75
^{29}Si	$Si-(CH_3)_3$	-	44.0	-	41.2	42.8

quantities used: 2.2 mmoles of each component; solvent: $CDCl_3$, 2.0 ml

[a] assignment uncertain

Table 3.9 Competition between 1-Methyl-2-pyrrolidone (NMP) and N,N-Dimethylformamide (DMF) for Trimethylsilyl triflate (TMSOTf) : N.M.R. Data

δ(ppm)		NMP	NMP + TMSOTf (1:1)	DMF	DMF + TMSOTf (1:1)	NMP + DMF + TMSOTf (1:1:1)
^{1}H	$N-CH_3$	2.83	3.11	-	-	2.99
	$C_5(H)-N$	2.02-2.99m	2.97t	-	-	2.11-2.71m
	C_4-H	2.02-2.99m	2.32qn	-	-	2.11-2.71m
	$^{3}J_{HH}$	obsc	7.8Hz	-	-	obsc
	$C_3(H)-C=O$	3.40t	3.89t	-	-	3.69t
	$^{3}J_{HH}$	7.4Hz	7.8Hz	-	-	7.3Hz
	$H-C=O$	-	-	8.01	8.45	8.26
	$N-(CH_3)^a$	-	-	2.98	3.45	3.23d
	$^{4}J_{HH}$	-	-	no	no	0.49Hz
	$N-(CH_3)^b$	-	-	2.87d	3.23d	3.05d
	$^{4}J_{HH}$	-	-	0.49Hz	0.75Hz	0.97Hz
	(a-b)	-	-	10.0Hz	19.8Hz	15.4Hz
	$Si-(CH_3)_3$	-	0.60	-	0.5	0.5
^{13}C	C=O	174.8	175.8	-	-	175.7
	$N-CH_3$	49.3	52.9	-	-	51.5
	C_3	30.7	32.2	-	-	34.8
	C_5	29.4	31.4	-	-	31.2
	C_4	17.7	17.1	-	-	17.5
	$H-C=O$	-	-	162.4	163.4	163.1
	$N-(CH_3)^a$	-	-	31.2	35.8	33.5
	$N-(CH_3)^b$	-	-	36.4	41.1	38.7
	(a-b)	-	-	115.2Hz	120.4Hz	116.5Hz
	$Si-(CH_3)_3$	-	0.0	-	-0.63	-0.29
^{29}Si	$Si-(CH_3)_3$	-	39.4	-	44.0	41.5

quantities used: 2.2 mmoles of each component; solvent: $CDCl_3$, 2.0 ml

Table 3.10

Competition between Pyridine N-oxide (PNO) and N,N-Dimethylformamide (DMF) for Trimethylsilyl triflate (TMSOTf) : N.M.R. Data

		PNO	PNO + TMSOTf (1:1)	DMF	DMF + TMSOTf (1:1)	PNO + DMF + TMSOTf (1:1:1)
δ(ppm)						
^{1}H	aromatic C-H	7.77-7.87m	9.03-9.10m	-	-	9.04-9.12m
		6.85-6.99m	8.15-8.63m	-	-	8.07-8.66m
	H-C=O	-	-	7.60	8.45	obscured
	$N-(CH_3)^a$	-	-	2.53	3.45	3.05
	$N-(CH_3)^b$	-	-	2.42	3.23	2.90
	$^{4}J_{HH}$	-	-	no	0.75Hz	0.73Hz
	(a-b)	-	-	10.0Hz	19.8Hz	13.2Hz
	$Si-(CH_3)_3$	-	0.50	-	0.50	0.50
^{13}C	$C_{2,6}$	139.2	141.6	-	-	142.6
	$C_{3,5}$	126.4	129.8	-	-	129.8
	C_4	125.8	143.3	-	-	141.6
	C=O	-	-	162.4	163.4	162.7
	$N-(CH_3)^a$	-	-	36.3	41.1	36.8
	$N-(CH_3)^b$	-	-	31.2	35.8	31.6
	(a-b)	-	-	115.2Hz	120.4Hz	116.5Hz
	$Si-(CH_3)_3$	-	-1.4	-	-0.63	-1.3
^{29}Si	$Si-(CH_3)_3$	-	49.4	-	44.0	48.8

quantities used: 2.2 mmoles of each component; solvent: $CDCl_3$, 2.0 ml

Table 3.11 Competition between 1-Methyl-2-pyrrolidone (NMP) and 1,3-Dimethyl-3,4,5,6-tetrahydro-2(1H)-pyrimidinone (DMPU) for Trimethylsilyl triflate (TMSOTf) : N.M.R. Data

δ(ppm)		NMP	NMP + TMSOTf (1:1)	DMPU	DMPU + TMSOTf (1:1)	NMP + DMPU + TMSOTf (1:1:1)
^{1}H	$C_3(H)-C=O$	3.40t	3.89t	-	-	3.51m
	$^{3}J_{HH}$	6.0Hz	7.8Hz	-	-	6.1Hz
	$N-CH_3$	2.84	3.11	-	-	2.91
	$C_5(H)-N$	1.85-2.43m	2.97t	-	-	2.02-2.50m
	$^{3}J_{HH}$	obsc	7.8Hz	-	-	obsc
	C_4-H	1.85-2.43m	2.32qn	-	-	2.02-2.50m
	$^{3}J_{HH}$	obsc	7.1Hz	-	-	obsc
	$C_{4,6}-H$	-	-	3.26t	3.60t	3.51m
	$^{2}J_{HH}$	-	-	6.0Hz	6.0Hz	6.1Hz
	$N-CH_3$	-	-	2.91	3.11	3.06
	C_5-H	-	-	1.85-2.43m	2.13qn[a]	2.02-2.50m
	$Si-(CH_3)_3$	-	0.49	-	0.48	0.50
^{13}C	C=O	174.9	175.8	-	-	175.1
	$N-CH_3$	49.3	52.9	-	-	50.3
	C_3	30.7	32.2	-	-	30.9
	C_5	29.5	31.4	-	-	30.2
	C_4	17.6	17.1	-	-	17.5
	C=O	-	-	156.8	154.0	155.0
	$N-CH_3$	-	-	47.9	47.9	48.1
	$C_{4,6}$	-	-	35.6	37.7	37.4
	C_5	-	-	22.2	19.3	20.3
	$Si-(CH_3)_3$	-	0.0	-	-0.4	0.29
^{29}Si	$Si-(CH_3)_3$	-	39.4	-	36.6	37.3

quantities used: 2.2 mmoles of each component; solvent: $CDCl_3$, 2.0 ml

a $^{3}J_{HH}$ 5.9Hz

Table 3.12

Competition between 1-Methyl-2-pyrrolidone (NMP) and Hexamethylphosphoramide (HMPA) for Trimethylsilyl triflate (TMSOTf) : N.M.R. Data

		NMP	NMP + TMSOTf (1:1)	HMPA	HMPA + TMSOTf (1:1)	NMP + HMPA + TMSOTf (1:1:1)
δ(ppm)						
^{1}H	$C_3(H)-C=O$	3.40t	3.89t	-	-	3.44t
	$^{3}J_{HH}$	7.1Hz	7.8Hz	-	-	7.3Hz
	$N-CH_3$	2.84	3.11	-	-	2.84
	$C_5(H)-N$	2.03-2.50m	2.97t	-	-	2.05-2.53m
	C_4-H	2.03-2.50m	2.32qn	-	-	2.05-2.53m
	$^{3}J_{HH}$	obsc	7.1Hz	-	-	obsc
	$O=P(N-CH_3)_3$	-	-	2.66d	2.77d	2.78d
	$^{3}J_{PH}$	-	-	9.3Hz	9.8Hz	10.5Hz
	$Si-(CH_3)_3$	-	0.49	-	0.43	0.43
^{13}C	C=O	174.9	175.8	-	-	175.3
	$N-CH_3$	49.4	52.9	-	-	49.6
	C_3	30.7	32.2	-	-	30.7
	C_5	29.5	31.4	-	-	29.6
	C_4	17.7	17.1	-	-	17.6
	$O=P(N-CH_3)_3$	-	-	36.9d	36.6d	36.6d
	$^{2}J_{PC}$	-	-	3.9Hz	5.2Hz	5.2Hz
	$Si-(CH_3)_3$	-	0.0	-	0.69	0.69
^{29}Si	$Si-(CH_3)_3$	-	39.4	-	28.8d	28.9d
	$^{3}J_{PSi}$	-	-	-	10.2Hz	no

quantities used: 2.2 mmoles of each component; solvent: $CDCl_3$, 2.0 ml

Table 3.13 Competition between 1-Methylimidazole (NMI) and 1-Methyl-2-pyrrolidone (NMP) for Trimethylsilyl triflate (TMSOTf) : N.M.R. Data

δ(ppm)		NMI	NMI + TMSOTf (1:1)	NMP	NMP + TMSOTf (1:1)	NMI + NMP + TMSOTf (1:1:1)
^{1}H	$N-C_2(H)=N$	7.42[a]	8.94	-	-	8.99[a]
	$C_4(H)=C_5$	7.02[a]	7.55t	-	-	7.60[a]
	$C_4=C_5(H)$	6.90[a]	7.41t	-	-	7.45[a]
	$^{3}J_{HH}$	no	1.6Hz	-	-	no
	$N-CH_3$	3.68	4.02	-	-	4.03
	$C_3(H)-C=O$	-	-	3.37t	3.89t	3.42t
	$^{3}J_{HH}$	-	-	7.3Hz	7.8Hz	7.1Hz
	$N-CH_3$	-	-	2.82	3.11	2.84
	$C_5(H)-N$	-	-	1.92-2.34m	2.97t	1.96-2.44m
	C_4-H	-	-	1.92-2.34m	2.32qn	1.96-2.44m
	$^{3}J_{HH}$	-	-	obsc	7.1Hz	obsc
	$Si-(CH_3)_3$	-	0.62	-	0.49	0.63
^{13}C	C_2	137.9(br)	139.8	-	-	139.8
	C_4	129.4	125.0	-	-	125.1
	C_5	120.3(br)	123.7	-	-	123.7
	$N-CH_3$	33.3	36.9	-	-	35.9
	$C=O$	-	-	174.9	175.8	175.0
	$N-CH_3$	-	-	49.4	52.9	49.5
	C_3	-	-	30.7	32.2	30.8
	C_5	-	-	29.5	31.4	29.5
	C_4	-	-	17.6	17.1	17.6
	$Si-(CH_3)_3$	-	-1.1	-	0.0	-1.1
^{29}Si	$Si-(CH_3)_3$	-	26.8	-	39.4	26.8

quantities used: 2.2 mmoles of each component; solvent: $CDCl_3$, 2.0 ml

[a] slightly broadened signals.

Table 3.14

Competition between 1-Methylimidazole (NMI) and 2,4-Dimethylpyridine (2,4DMP) for Trimethylsilyl triflate (TMSOTf) : N.M.R. Data

δ(ppm)		NMI	NMI + TMSOTf (1:1)	2,4DMP	2,4DMP + TMSOTf (1:1)	NMI+2,4DMP + TMSOTf (1:1:1)
^{1}H	$N-C_2(H)=N$	7.38	8.94	-	-	8.91
	$C_4(H)=C_5$	7.02	7.55t	-	-	7.56t
	$C_4=C_5(H)$	6.85	7.41t	-	-	7.42t
	$^{3}J_{HH}$	no	1.6Hz	-	-	1.5Hz
	$N-CH_3$	3.62	4.02	-	-	4.01
	C_6-H	-	-	8.32d	8.49d	8.32d
	C_3-H	-	-	6.93	7.43	7.00
	C_5-H	-	-	6.85d	7.39d	6.96d
	$^{3}J_{56}$	-	-	4.9Hz	5.6Hz	4.9Hz
	C_2-CH_3	-	-	2.48	2.72	2.50
	C_4-CH_3	-	-	2.26	2.47	2.30
	$Si-(CH_3)_3$	-	0.62	-	0.70	0.62
^{13}C	C_2	137.8	139.8	-	-	139.7
	C_4	129.4	125.0	-	-	124.9
	C_5	120.0	123.7	-	-	124.0
	$N-CH_3$	33.1	36.9	-	-	35.8
	C_2	-	-	158.0	154.9	157.8
	C_6	-	-	148.8	147.1	148.4
	C_4	-	-	147.2	157.4	147.9
	C_3	-	-	124.1	128.2	124.4
	C_5	-	-	121.7	124.5	122.0
	$C_2-\underline{C}H_3$	-	-	24.2	23.3	24.0
	$C_4-\underline{C}H_3$	-	-	20.8	21.4	20.9
	$Si-(CH_3)_3$	-	-1.1	-	0.69	-1.15
^{29}Si	$Si-(CH_3)_3$	-	26.8	-	40.8	26.7

quantities used: 2.2 mmoles of each component; solvent: $CDCl_3$, 2.0 ml

Table 3.15

Competition between 1-Methylimidazole (NMI) and 1,3-Dimethyl-3,4,5,6-tetrahydro-2(1H)-pyrimidinone (DMPU) for Trimethylsilyl triflate (TMSOTf): N.M.R. Data

δ(ppm)		NMI	NMI + TMSOTf (1:1)	DMPU	DMPU + TMSOTf (1:1)	NMI + DMPU + TMSOTf (1:1:1)
^{1}H	$N-C_2(H)=N$	7.41	8.94	-	-	8.96(vbr)
	$C_4(H)=C_5$	7.01	7.55t	-	-	7.60(vbr)
	$^{3}J_{HH}$	no	1.6Hz	-	-	no
	$C_4=C_5(H)$	6.89	7.41t	-	-	7.47(br)
	$^{3}J_{HH}$	no	1.6Hz	-	-	no
	$N-CH_3$	3.68	4.02	-	-	4.02
	$C_{4,6}-H$	-	-	3.23t	3.60t	3.27t
	$^{2}J_{HH}$	-	-	6.0Hz	6.0Hz	5.98Hz
	$N-CH_3$	-	-	2.90	3.11	2.91
	C_5-H	-	-	1.95qn	2.13qn	1.99qn
	$^{3}J_{HH}$	-	-	5.9Hz	5.9Hz	4.6Hz
	$Si-(CH_3)_3$	-	0.62	-	0.48	0.63
^{13}C	C_2	137.8	139.8	-	-	139.6
	C_4	129.4	125.0	-	-	124.7(br)
	C_5	120.1	123.7	-	-	123.9(br)
	$N-CH_3$	33.2	36.9	-	-	35.7
	C=O	-	-	156.8	154.0	156.8
	$N-CH_3$	-	-	47.9	47.9	47.9
	$C_{4,6}$	-	-	35.6	37.7	35.6
	C_5	-	-	22.2	19.3	22.1
	$Si-(CH_3)_3$	-	-1.1	-	-0.4	-1.2
^{29}Si	$Si-(CH_3)_3$	-	26.8	-	36.6	26.8
quantities used : 2.2 mmoles of each component; solvent: $CDCl_3$, 2.0 ml						

Table 3.16

Competition between N-Methylimidazole (NMI) and Triphenylphosphine oxide (TPPO) for Trimethylsilyl triflate (TMSOTf) : N.M.R. Data

δ(ppm)		NMI	NMI + TMSOTf (1:1)	TPPO	TPPO + TMSOTf (1:1)	NMI + TPPO + TMSOTf (1:1:1)
^{1}H	$N-C_2(H)=N$	obsc	8.94	-	-	8.98
	$C_4(H)=C_5$	7.02(sbr)	7.55t	-	-	7.10(sbr)
	$C_4=C_5(H)$	6.85(sbr)	7.41t	-	-	7.35(sbr)
	$^{3}J_{HH}$	no	1.6Hz	-	-	nr
	$N-CH_3$	3.63	4.02	-	-	3.98
	aromatic C-H	-	-	7.46-7.80m	7.37-7.8m	7.77-7.45m
	$Si-(CH_3)_3$	-	0.62	-	0.35	0.60
^{13}C	C_2	137.8(sbr)	139.8	-	-	140.6
	C_4	obsc	125.0	-	-	125.9
	C_5	120.0(sbr)	123.7	-	-	124.6
	$N-CH_3$	33.2	36.9	-	-	36.9
	C_{para}	-	-	131.9d	136.2d	133.3
	$^{4}J_{PC}$	-	-	3.9Hz	2.3Hz	no
	C_{meta}	-	-	132.1d	132.6d	133.1d
	$^{3}J_{PC}$	-	-	10.4Hz	12.9Hz	obsc
	C_{ortho}	-	-	128.5d	130.4d	129.7d
	$^{2}J_{PC}$	-	-	12.9Hz	12.9Hz	obsc
	C_{ipso}	-	-	obsc	133.0d	133.3d
	$^{1}J_{PC}$	-	-	obsc	104.6Hz	104.7Hz
	$Si-(CH_3)_3$	-	-1.1	-	1.1	1.09
^{29}Si	$Si-(CH_3)_3$	-	26.8	-	37.5	26.9

quantities used: 2.2 mmoles of each component; solvent: $CDCl_3$, 2.0 ml

Table 3.17 Competition between 1-Methyl-2-pyridinone (NMPO) and 4-Dimethylaminopyridine (DMAP) for Trimethylsilyl triflate (TMSOTf): N.M.R. Data

δ(ppm)		NMPO	NMPO + TMSOTf (1:1)	DMAP	DMAP + TMSOTf (1:1)	NMPO + DMAP + TMSOTf (1:1:1)
^{1}H	$C_{5,6}$-H	7.25-7.44m	8.32-8.56m	-	-	7.36-7.54m
	C_3-H	6.55d,d	7.33-7.50m	-	-	6.58d
	J_{HH}	9.8,1.4Hz	obsc	-	-	8.79Hz
	C_4-H	6.15t,d	7.33-7.50m	-	-	6.28t,d
	J_{HH}	6.8,1.4Hz	obsc	-	-	8.0,1.2Hz
	N-CH_3	3.54	4.07	-	-	3.59
	$C_{2,6}$-H	-	-	8.20d,d	8.15d	8.12d
	$^{3}J_{HH}$	-	-	5.1,1.7Hz	7.8Hz	7.6Hz
	$C_{3,5}$-H	-	-	6.70d,d	7.05	7.02d
	$^{3}J_{HH}$	-	-	5.4,1.5Hz	7.8Hz	7.8Hz
	N-CH_3	-	-	3.03	3.28	3.27
	Si-$(CH_3)_3$	-	0.54	-	0.63	0.59
^{13}C	C=O	163.1	157.2	-	-	162.7
	C_a	139.6	148.1	-	-	140.5
	C_b	138.5	144.0	-	-	193.2
	C_c	120.5	119.0	-	-	119.9
	C_d	105.9	116.0	-	-	107.0
	N-CH_3	37.6	41.6	-	-	37.9
	C_4	-	-	154.7	156.9	157.1
	$C_{2,6}$	-	-	147.9	143.3(br)	142.2
	$C_{3,5}$	-	-	106.7	108.4(br)	108.4
	N-CH_3	-	-	39.2	40.0	40.0
	Si-$(CH_3)_3$	-	-0.23	-	-1.1	-0.34
^{29}Si	Si-$(CH_3)_3$	-	35.8	-	31.7	32.0

quantities used: 2.2 mmoles of each component; solvent: $CDCl_3$, 2.0 ml

Table 3.18

Competition between 1,2-Dimethylimidazole (DMI) and Hexamethylphosphoramide (HMPA) for Trimethylsilyl triflate (TMSOTf) : N.M.R. Data

δ(ppm)		DMI	DMI + TMSOTf (1:1)	HMPA	HMPA + TMSOTf (1:1)	DMI + HMPA + TMSOTf (1:1:1)
^{1}H	$C_4(H)=C_5$	6.77	7.43d	-	-	7.12
	$^{3}J_{HH}$	no	2.2Hz	-	-	no
	$C_4=C_5(H)$	6.77	7.16d	-	-	6.93
	$^{3}J_{HH}$	no	2.2Hz	-	-	no
	$N-CH_3$	3.52	3.85	-	-	3.67
	C_2-CH_3	2.30	2.70	-	-	2.46
	$N-CH_3$	-	-	2.60d	2.77d	2.73d
	$^{3}J_{PH}$	-	-	9.3Hz	9.8Hz	10.0Hz
	$Si-(CH_3)_3$	-	0.63	-	0.43	0.49
^{13}C	C_2	144.5	148.1	-	-	145.9
	C_4	126.6	122.2(br)	-	-	124.5
	C_5	120.3	122.2(br)	-	-	122.0
	$N-CH_3$	32.6	34.9(br)	-	-	33.3
	C_2-CH_3	12.7	12.2(br)	-	-	12.3
	$N-CH_3$	-	-	36.7d	36.6d	36.6d
	$^{2}J_{PC}$	-	-	3.9Hz	5.2Hz	5.2Hz
	$Si-(CH_3)_3$	-	-0.46	-	0.69	0.0
^{29}Si	$Si-(CH_3)_3$	-	25.1	-	28.8d	27.3
	$^{3}J_{PSi}$	-	-	-	10.2Hz	no

quantities used: 2.2 mmoles of each component; solvent: $CDCl_3$, 2.0 ml

Table 3.19

Competition between 4-Dimethylaminopyridine (DMAP) and Hexamethylphosphoramide (HMPA) for Trimethylsilyl triflate (TMSOTf) : N.M.R. Data

		DMAP	DMAP + TMSOTf (1:1)	HMPA	HMPA + TMSOTf (1:1)	DMAP + HMPA + TMSOTf (1:1:1)
δ(ppm)						
^{1}H	$C_{2,6}$-H	8.17d	8.15d	-	-	8.16d
	$^{3}J_{HH}$	5.4Hz	7.8Hz	-	-	5.5Hz
	$C_{3,5}$-H	6.44d	7.05d	-	-	6.84d
	$^{3}J_{HH}$	6.6Hz	7.8Hz	-	-	6.6Hz
	N-CH_3	2.94	3.28	-	-	3.15
	N-CH_3	-	-	2.61d	2.77d	2.70d
	$^{3}J_{PH}$	-	-	9.3Hz	9.8Hz	9.5Hz
	Si-$(CH_3)_3$	-	0.63	-	0.43	0.55
^{13}C	C_4	154.0	156.9	-	-	155.8
	$C_{2,6}$	149.5	143.3(br)	-	-	145.5
	$C_{3,5}$	106.5	108.4(br)	-	-	107.8
	N-CH_3	38.8	40.0	-	-	39.4
	N-CH_3	-	-	36.7d	36.6d	36.6d
	$^{2}J_{PC}$	-	-	3.9Hz	5.2Hz	3.9Hz
	Si-$(CH_3)_3$	-	-1.1	-	0.69	-0.52
^{29}Si	Si-$(CH_3)_3$	-	31.7	-	28.8d	30.6
	$^{3}J_{PSi}$	-	no	-	10.2Hz	no

quantities used: 2.51 mmoles of each component; solvent: $CDCl_3$, 2.0 ml

Table 3.20

Competition between 1-Methylimidazole (NMI) and Hexamethylphosphoramide (HMPA) for Trimethylsilyl triflate (TMSOTf) : N.M.R. Data

		NMI	NMI + TMSOTf (1:1)	HMPA	HMPA + TMSOTf (1:1)	NMI + HMPA + TMSOTf (1:1:1)
δ(ppm)						
^{1}H	$N-C_2(H)=N$	7.41	8.94	-	-	8.39
	$C_4(H)=C_5$	7.00t	7.55t	-	-	7.36t
	$^{3}J_{HH}$	1.0Hz	1.6Hz	-	-	1.5Hz
	$C_4=C_5(H)$	6.90t	7.41t	-	-	7.27t
	$^{3}J_{HH}$	1.0Hz	1.6Hz	-	-	1.2Hz
	$N-CH_3$	3.68	4.02	-	-	3.90
	$O=P(N-CH_3)_3$	-	-	2.64d	2.77d	2.70d
	$^{3}J_{PC}$	-	-	9.3Hz	9.8Hz	10.0Hz
	$Si-(CH_3)_3$	-	0.62	-	0.43	0.54
^{13}C	C_2	137.8	139.8	-	-	139.4
	C_4	129.3	125.0	-	-	126.3
	C_5	120.1	123.7	-	-	123.5
	$N-CH_3$	33.2	36.9	-	-	35.1
	$O=P(N-CH_3)_3$	-	-	36.8d	36.6d	37.1d
	$^{2}J_{PC}$	-	-	3.9Hz	5.2Hz	3.9Hz
	$Si-(CH_3)_3$	-	-1.1	-	0.69	0.4
^{29}Si	$Si-(CH_3)_3$	-	26.8	-	28.8d	27.5
	$^{3}J_{PSi}$	-	no	-	10.2Hz	no

quantities used: 2.2 mmoles of each component; solvent: $CDCl_3$, 2.0 ml

Table 3.21

Competition between 1-Methylimidazole (NMI) and 4-Dimethylaminopyridine (DMAP) for Trimethylsilyl triflate (TMSOTf) : N.M.R. Data

δ(ppm)		NMI	NMI + TMSOTf (1:1)	DMAP	DMAP + TMSOTf (1:1)	NMI + DMAP + TMSOTf (1:1:1)
^{1}H	$N-C_2(H)=N$	7.41	8.94	-	-	8.09
	$C_4(H)=C_5$	7.02	7.55t	-	-	7.22d
	$^{3}J_{HH}$	no	1.6Hz	-	-	1.0Hz
	$C_4=C_5(H)$	6.87	7.41t	-	-	7.18
	$^{3}J_{HH}$	no	1.6Hz	-	-	no
	$N-CH_3$	3.66	4.02	-	-	3.85
	$C_{2,6}-H$	-	-	8.17d,d	8.15d	8.19d
	$^{3}J_{HH}$	-	-	5.4,1.5Hz	7.8Hz	5.6Hz
	$C_{3,5}-H$	-	-	6.52d,d	7.05d	6.83d
	$^{3}J_{HH}$	-	-	5.1,1.5Hz	7.8Hz	7.0Hz
	$N-CH_3$	-	-	3.01	3.28	3.17
	$Si-(CH_3)_3$	-	0.62	-	0.63	0.60
^{13}C	C_2	137.8	139.8	-	-	138.8
	C_4	129.1	125.0	-	-	126.6
	C_5	120.1	123.7	-	-	122.5
	$N-CH_3$	33.2	36.9	-	-	34.5
	C_4	-	-	154.7	156.9	156.3
	$C_{2,6}$	-	-	147.5	143.3(br)	144.2
	$C_{3,5}$	-	-	106.6	108.4(br)	107.8
	$N-CH_3$	-	-	39.1	40.0	39.7
	$Si-(CH_3)_3$	-	-1.1	-	-1.1	-0.80
^{29}Si	$Si-(CH_3)_3$	-	26.8	-	31.7	29.3
quantities used: 2.2 mmoles of each component; solvent: $CDCl_3$, 2.0 ml						

Table 3.22

Competition between 1,3-dimethyl-2-imidazolidinone (DMEU) and 1,3-dimethyl-3,4,5,6-tetrahydro-2(1H)-pyrimidinone (DMPU) for Trimethylsilyl triflate (TMSOTf) : N.M.R. Data

		DMEU	DMEU + TMSOTf (1:1)	DMPU	DMPU + TMSOTf (1:1)	DMEU + DMPU + TMSOTf (1:1:1)
δ(ppm)						
^{1}H	$N-CH_3$	3.28	3.84	-	-	3.35
	$C_{4,5}-H$	2.77	2.96	-	-	2.78
	$C_{4,6}-H$	-	-	3.25t	3.60t	3.57t
	$^{2}J_{HH}$	-	-	6.0Hz	6.0Hz	5.9Hz
	$N-CH_3$	-	-	2.91	3.11	3.10
	C_5-H	-	-	2.03qn	2.13qn	2.12qn
	$^{3}J_{HH}$	-	-	5.25Hz	5.9Hz	6.3Hz
	$Si-(CH_3)_3$	-	0.51	-	0.48	0.50
^{13}C	C=O	161.9	159.0	-	-	161.8
	$N-CH_3$	45.0	46.3	-	-	45.1
	$C_{4,5}$	31.4	32.2	-	-	31.5
	C=O	-	-	156.7	154.4	154.7
	$N-CH_3$	-	-	47.9	48.3	48.2
	$C_{4,6}$	-	-	35.6	38.1	37.9
	C_5	-	-	22.2	19.7	19.9
	$Si-(CH_3)_3$	-	0.69	-	0.40	0.40
^{29}Si	$Si-(CH_3)_3$	-	40.1	-	36.6	36.9

quantities used: 2.2 mmoles of each component; solvent: $CDCl_3$, 2.0 ml

Table 3.23

Competition between 1-Methylimidazole (NMI) and Pyridine (py) for Iodotrimethylsilane (TMSI) : N.M.R. Data

δ(ppm)		NMI	NMI + TMSOTf (1:1)	py	py[a] + TMSOTf (1:1)	NMI + py + TMSI (1:1:1)
^{1}H	$N-C_2(H)=N$	7.39	8.94	-	-	9.78
	$C_4(H)=C_5$	7.03	7.55t	-	-	7.82t
	$^{3}J_{HH}$	no	1.6Hz	-	-	1.5Hz
	$C_4=C_5(H)$	6.85	7.41t	-	-	7.53t
	$^{3}J_{HH}$	no	1.6Hz	-	-	1.5Hz
	$N-CH_3$	3.62	4.02	-	-	4.20
	aromatic C-H	-	-	8.55-8.63m	8.51-8.90m	8.55-8.62m
		-	-	7.16-7.75m	8.00-8.17m	7.23-7.75m
	$Si-(CH_3)_3$	-	0.62	-	0.73	0.72
^{13}C	C_2	137.8	139.8	-	-	139.9
	C_4	129.5	125.0	-	-	125.1
	C_5	120.1	123.7	-	-	123.9
	$N-CH_3$	33.1	36.9	-	-	36.7
	$C_{2,6}$	-	-	149.8	148.8	149.6
	C_4	-	-	135.9	146.7	136.1
	$C_{3,5}$	-	-	123.7	129.8	123.9
	$Si-(CH_3)_3$	-	-1.1	-	0.98	-0.17
^{29}Si	$Si-(CH_3)_3$	-	26.8	-	42.3	26.8

quantities used: 2.2 mmoles of each component; solvent: $CDCl_3$, 2.0 ml

[a] Recorded in acetonitrile-d_3.

Table 3.24

Competition between 1-Methyl-2-pyrrolidone (NMP) and Pyridine (py) for Iodotrimethylsilane (TMSI) : N.M.R. Data

		NMP	NMP + TMSI (1:1)	py	py[a] + TMSOTf (1:1)	NMP + py + TMSI (1:1:1)
δ(ppm)						
^{1}H	$C_3(H)-C=O$	3.35t	4.11t	-	-	3.94t
	$^{3}J_{HH}$	7.3Hz	7.6Hz	-	-	7.8Hz
	$N-CH_3$	2.82	3.23	-	-	3.13
	$C_5(H)-N$	1.80-2.45m	3.3m[b]	-	-	2.90-3.20m
	C_4-H	1.80-2.45m	2.45qn	-	-	2.36qn
	$^{3}J_{HH}$	obsc	7.0Hz	-	-	7.6Hz
	aromatic C-H	-	-	8.58-8.65m	8.51-8.90m	8.75-8.82m
		-	-	7.59-7.78m	8.00-8.17m	7.85-8.07m
		-	-	7.19-7.35m	-	7.47-7.62m
	$Si-(CH_3)_3$	-	0.60	-	0.73	0.66
^{13}C	C=O	174.9	176.0	-	-	175.8
	$N-CH_3$	49.3	53.9	-	-	52.9
	C_3	30.6	33.8	-	-	32.8
	C_5	29.5	33.1	-	-	32.6
	C_4	17.6	17.3	-	-	17.5
	$C_{2,6}$	-	-	149.8	148.8	148.8
	C_4	-	-	135.9	146.7	138.4
	$C_{3,5}$	-	-	123.7	129.8	124.8
	$Si-(CH_3)_3$	-	1.3	-	0.98	0.92
^{29}Si	$Si-(CH_3)_3$	-	38.9(sbr)	-	42.4	40.3
quantities used: 2.2 mmoles of each component; solvent: $CDCl_3$, 2.0 ml						

[a] Recorded in acetonitrile-d_3.

[b] partially obscured by the $N-CH_3$ peak.

Table 3.25

Competition between 1-Methyl-2-pyrrolidone (NMP) and Hexamethylphosphoramide (HMPA) for Iodotrimethylsilane (TMSI) : N.M.R. Data

		NMP	NMP + TMSI (1:1)	HMPA	HMPA + TMSOTf (1:1)	NMP + HMPA + TMSI (1:1:1)
δ(ppm)						
^{1}H	$C_3(H)-C=O$	3.40t	4.11t	-	-	3.46t
	$^{3}J_{HH}$	7.1Hz	7.6Hz	-	-	7.3Hz
	$N-CH_3$	2.84	3.23	-	-	2.85
	$C_5(H)-N$	2.03-2.50m	3.3m[a]	-	-	2.07-2.65m
	C_4-H	2.03-2.50m	2.45qn	-	-	2.07-2.65m
	$^{3}J_{HH}$	obsc	7.0Hz	-	-	obsc
	$O=P(N-CH_3)_3$	-	-	2.66d	2.77d	2.87d
	$^{3}J_{PH}$	-	-	9.3Hz	9.8Hz	10.5Hz
	$Si-(CH_3)_3$	-	0.60	-	0.43	0.48
^{13}C	C=O	174.9	176.0	-	-	173.5
	$N-CH_3$	49.4	53.9	-	-	48.1
	C_3	30.7	33.8	-	-	29.4
	C_5	29.5	33.1	-	-	28.3
	C_4	17.7	17.3	-	-	16.4
	$O=P(N-CH_3)_3$	-	-	36.9d	36.6d	36.1d
	$^{2}J_{PC}$	-	-	3.9Hz	5.2Hz	5.2Hz
	$Si-(CH_3)_3$	-	1.3	-	0.69	0.0
^{29}Si	$Si-(CH_3)_3$	-	38.9(sbr)	-	28.8d	28.7
	$^{3}J_{PSi}$	-	no	-	10.2Hz	no
quantities used: 2.2 mmoles of each component; solvent: $CDCl_3$, 2.0 ml						

[a] obscured by the $N-CH_3$ peak.

Table 3.26

Competition between 1-Methylimidazole (NMI) and 1-Methyl-2-pyrrolidone (NMP) for Iodotrimethylsilane (TMSI) : N.M.R. Data

δ(ppm)		NMI	NMI + TMSOTf (1:1)	NMP	NMP + TMSI (1:1)	NMI + NMP + TMSI (1:1:1)
^{1}H	$N-C_2(H)=N$	7.42(sbr)	8.94	-	-	9.74
	$C_4(H)=C_5$	7.02(sbr)	7.55t	-	-	7.83t
	$C_4=C_5(H)$	6.90(sbr)	7.41t	-	-	7.56t
	$^{3}J_{HH}$	no	1.6Hz	-	-	1.7Hz
	$N-CH_3$	3.68	4.02	-	-	4.20
	$C_3(H)-C=O$	-	-	3.37t	4.11t	3.43t
	$^{3}J_{HH}$	-	-	7.3Hz	7.6Hz	7.3Hz
	$N-CH_3$	-	-	2.82	3.23	2.85
	$C_5(H)-N$	-	-	1.92-2.34m	3.3m[a]	1.97-2.36m
	C_4-H	-	-	1.92-2.34m	2.45qn	1.97-2.36m
	$^{3}J_{HH}$	-	-	obsc	7.0Hz	obsc
	$Si-(CH_3)_3$	-	0.62	-	0.60	0.73
^{13}C	C_2	137.9(br)	139.8	-	-	140.0
	C_4	129.4	125.0	-	-	125.1
	C_5	120.3(br)	123.7	-	-	123.9
	$N-CH_3$	33.3	36.9	-	-	36.5
	$C=O$	-	-	174.9	176.0	174.9
	$N-CH_3$	-	-	49.4	53.9	49.4
	C_3	-	-	30.7	33.8	30.7
	C_5	-	-	29.5	33.1	29.5
	C_4	-	-	17.6	17.3	17.6
	$Si-(CH_3)_3$	-	-1.1	-	1.3	-0.17
^{29}Si	$Si-(CH_3)_3$	-	26.8	-	38.9(sbr)	26.7

quantities used: 2.2 mmoles of each component; solvent: $CDCl_3$, 2.0 ml

[a] obscured by the $N-CH_3$ peak.

Table 3.27

Competition between 1-Methylimidazole (NMI) and Hexamethylphosphoramide (HMPA) for Iodotrimethylsilane (TMSI) : N.M.R. Data

		NMI	NMI + TMSOTf (1:1)	HMPA	HMPA + TMSOTf (1:1)	NMI + HMPA + TMSI (1:1:1)
δ(ppm)						
^{1}H	$N-C_2(H)=N$	7.41	8.94	-	-	8.87
	$C_4(H)=C_5$	7.00t	7.55t	-	-	7.53(sbr)
	$^{3}J_{HH}$	1.0Hz	1.6Hz	-	-	no
	$C_4=C_5(H)$	6.90t	7.41t	-	-	7.34
	$^{3}J_{HH}$	1.0Hz	1.6Hz	-	-	no
	$N-CH_3$	3.68	4.02	-	-	4.02
	$O=P(N-CH_3)_3$	-	-	2.64d	2.77d	2.73d
	$^{3}J_{PH}$	-	-	9.3Hz	9.8Hz	9.8Hz
	$Si-(CH_3)_3$	-	0.62	-	0.43	0.62
^{13}C	C_2	137.8	139.8	-	-	139.1(sbr)
	C_4	129.3	125.0	-	-	126.1
	C_5	120.1	123.7	-	-	123.2(sbr)
	$N-CH_3$	33.2	36.9	-	-	35.4
	$O=P(N-CH_3)_3$	-	-	36.8d	36.6d	37.0d
	$^{2}J_{PC}$	-	-	3.9Hz	5.2Hz	3.9Hz
	$Si-(CH_3)_3$	-	-1.1	-	0.69	0.4
^{29}Si	$Si-(CH_3)_3$	-	26.8	-	28.8d	27.5
	$^{3}J_{PSi}$	-	no	-	10.2Hz	no

quantities used: 2.2 mmoles of each component; solvent: $CDCl_3$, 2.0 ml

CHAPTER 4

THE DYNAMIC BEHAVIOUR OF NUCLEOPHILE / TRIMETHYLSILYL X MIXTURES (TMSX, X=Br, I, OTf, Cl, ClO_4, Im)

4.1 Introduction

Some aspects of the kinetic behaviour of nucleophile/TMSX mixtures have already been discussed in previous chapters, although the rationale behind the observed differences has not been established. For instance, DMF/TMSBr mixtures (Table 2.1) show fast exchange at all stoicheiometries, whereas similar DMF/TMSI solutions (Table 2.2) show significantly slower exchange, even after allowing for the various energy difference between exchanging sites. To interpret and explain such results, the dynamic behaviour of mixtures of N,N'-bistrimethylsilylimidazolium X salts (BTMSImX where X=Br, I, OTf, ClO_4, Cl) with various trimethylsilyl species (TMSY where Y=Cl, Br, I, OTf, ClO_4, Im) was investigated (Scheme 4.1).

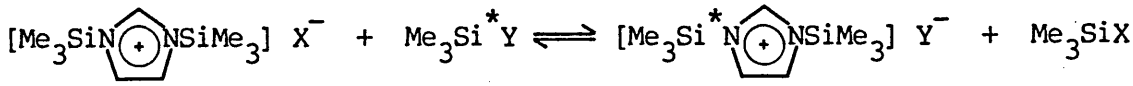

Scheme 4.1

These systems have the advantage that both exchanging sites (BTMSImX and TMSY) can be observed by n.m.r. spectroscopy (^1H, ^{13}C and ^{29}Si), and the chemical shifts of each isolated species have already been determined (Chapter 2.7). The BTMSImX salts were established as being the major species present in solution for a 1:1 mixture of TMSX (X=Br, I, OTf, ClO_4) and TMSIm.

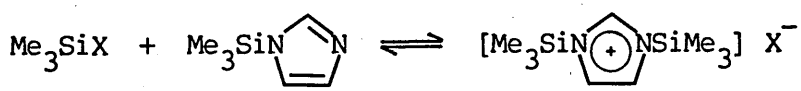

Scheme 4.2

The position of this equilibrium and that of Scheme 4.1 can be readily deduced from the chemical shifts of each BTMSImX/TMSY mixture, and the relative rates of exchange between the various species assessed from the lineshapes.

4.2 Results and Discussion

A comprehensive series of experiments were performed in acetonitrile-d_3 for N,N'-bistrimethylsilylimidazolium X salts (BTMSImX); X=Br (Table 4.1); X=I (Table 4.2); X=OTf (Table 4.3); X=ClO_4 (Table 4.4). The results can be interpreted as follows:-

a) BTMSImBr and TMSY (Y=Br, I, OTf, Im)

Fast exchange is illustrated by the presence of a single silyl peak for each mixture. The bromide counterion of BTMSImBr is displaced by iodide or triflate, indicating that the equilibrium constant for salt formation is greater for iodide and triflate (Scheme 4.3). This is deduced from the absence of isolated TMSY (Y=OTf, I) resonances.

Scheme 4.3

b) BTMSImI and TMSY (Y=Cl, Br, I, OTf)

The rate of exchange between BTMSImI and TMSY (Y=Cl, Br, I, OTf) can be summarised in the following order:- Cl > Br >> OTf > I. The exchange between BTMSImI and TMSCl is slightly faster compared with TMSBr, which in turn is much faster than TMSOTf and TMSI.

Table 4.1

Exchange reactions between N,N'-Bistrimethylsilylimidazolium bromide (BTMSImBr) and Trimethylsilyl X (TMSX) : N.M.R. Data

		BTMSImBr	BTMSImBr + TMSBr 1:1	BTMSImBr + TMSI 1:1	BTMSImBr + TMSOTf 1:1	BTMSImBr + TMSIm 1:1
δ(ppm)						
^{1}H	C_2-H	8.91	8.96	8.75	8.55	9.15
	$C_{4,5}$-H	7.59d	7.60d	7.63d	7.54d	7.50
	$^{4}J_{HH}$	1.5Hz	1.2Hz	1.2Hz	1.2Hz	no
	TMS	0.63	0.61	0.63(sbr)	0.60	0.71
	TMSX	-	0.57	0.79	0.48	0.42
^{13}C	C_2	143.4	143.3	143.1	142.7	142.7
	$C_{4,5}$	125.3	125.1	125.2	125.2	125.2
	CF_3	-	-	-	nr	-
	$^{1}J_{CF}$	-	-	-	nr	-
	TMS	-0.57	-0.46	2.01	0.40	-0.17
	TMSX	-	4.1	5.6	0.29	-0.57
^{29}Si	TMS	26.3	27.5(sbr)	27.2(br)	27.2	23.7
	TMSX	-	28.7	12.1	46.1	14.2
quantities used:						
BTMSImBr (mmoles)		0.67	0.67	0.905	0.68	0.56
TMSX (mmoles)		-	0.67	0.905	0.68	0.11
solvent: CD_3CN, 2.0 ml						

Table 4.2

Exchange reactions between N,N'-Bistrimethylsilylimidazolium iodide (BTMSImI) and Trimethylsilyl X (TMSX) : N.M.R. Data

		BTMSImI	BTMSImI + TMSCl	BTMSImI + TMSBr	BTMSImI + TMSI	BTMSImI + TMSOTf	BTMSImI + TMSIm
δ(ppm)			1:2	1:1	1:1	1:1	1:1
^{1}H	C_2-H	8.74	8.65	8.60	8.80	8.54	8.05
	$C_{4,5}$-H	7.62d	7.48	7.60d	7.62	7.52d	7.28d
	$^{4}J_{HH}$	1.2Hz	nr	1.2Hz	nr	1.2Hz	1.2Hz
	TMS	0.65	0.43	0.60sbr	0.65	0.67	0.55
	TMS*	-	-	-	0.79	0.60[a]	-
	TMSX	-	0.42	0.57	0.79	0.48	0.43
^{13}C	C_2	143.6	134.9(br)	141.3(br)	-	143.3	-
	$C_{4,5}$	125.6	120.2(br)	124.1(br)	-	125.7	-
	TMS	-0.57	2.3	2.1sbr	-	3.1	-
	TMS*	-	-	-	-	-0.92	-
	TMSX	-	3.2	4.1	5.6	0.29	-
^{29}Si	TMS	26.3	31.9(br)	26.6(br)	26.4	26.4	20.2
	TMS*	-	-	28.9(br)	12.1	22.4	-
	TMSX	-	32.0	28.7	12.1	46.1	14.2
quantities used:							
BTMSImX (mmoles)		0.67	0.54	0.29	0.67	0.36	0.71
TMSX (mmoles)		-	0.54	0.29	0.67	0.36	0.71
solvent: CD_3CN, 2.0 ml							

[a] slightly broadened signal

Table 4.3

Exchange reactions between N,N'-Bistrimethylsilylimidazolium triflate (BTMSImOTf) and Trimethylsilyl X (TMSX) : N.M.R. Data

δ(ppm)		BTMSImOTf	BTMSImOTf + TMSCl 1:1	BTMSImOTf + TMSI 1:1	BTMSImOTf + TMSOTf 1:1	BTMSImOTf + TMSIm 1:1
^{1}H	C_2-H	8.46	-	8.57	8.47	8.09
	$C_{4,5}$-H	7.54	-	7.59d	7.58d	7.34d
	$^{4}J_{HH}$	nr	-	1.2Hz	1.2Hz	1.2Hz
	TMS	0.57	-	0.62	0.61	0.53
	TMS*	-	-	0.71	0.49	-
	TMSX	-	-	0.79	0.48	0.43
^{13}C	C_1	142.2	nr	143.5	143.1	nr
	$C_{4,5}$	125.0	-	125.6	125.5	-
	CF_3	121.9	-	nr	122.0	-
	$^{1}J_{CF}$	321Hz	-	nr	321Hz	-
	TMS	-0.97	-	-0.80	-1.2	-
	TMS*	-	-	4.2	-0.92	-
	TMSX	-	-	5.6	0.29	-
^{29}Si	TMS	26.7	26.8(br)	26.5	26.5	22.1
	TMS*	-	-	21.6[a]	46.4	-
	TMSX	-	32.0	12.1	46.1	14.2
quantities used:						
BTMSImOTf (mmoles)		0.60	0.69	1.45	0.60	0.72
TMSX (mmoles)		-	0.69	1.45	0.62	0.72
solvent: CD_3CN, 2.0 ml						

[a] After leaving the solution for 2 days, this peak shifted to 23.7 ppm.

Table 4.4

Exchange reactions between N,N'-Bistrimethylsilylimidazolium perchlorate (BTMSImP) and Trimethylsilyl X (TMSX) : N.M.R. Data

δ(ppm)		BTMSImP	BTMSImP + TMSBr 1:1	BTMSImP + TMSI 1:1	BTMSImP + TMSOTf 1:1	BTMSImP + $TMSClO_4$ 1:1
^1H	C_2-H	8.33	8.38	8.34	8.33	8.62
	$C_{4,5}$-H	7.49d	7.50d	7.51d	7.51d	7.46
	$^4J_{HH}$	1.2Hz	1.3Hz	1.2Hz	1.2Hz	nr
	TMS	0.59	0.59	0.59	0.59	0.43
	TMS*	no	no	0.78	0.49	0.15[a]
	TMSX	-	0.57	0.79	0.48	nr
^{13}C	C_2	142.3	142.2(sbr)	143.3	143.3	-
	$C_{4,5}$	125.0	125.1(sbr)	125.7	125.7	-
	CF_3	-	-	-	nr	-
	$^1J_{CF}$	-	-	-	nr	-
	TMS	-0.52	-0.92(sbr)	-0.98	-0.98	-
	TMS*	no	no	2.2	0.30	-
	TMSX	-	4.1	5.6	0.29	-
^{29}Si	TMS	26.3	26.7(sbr)	26.4	26.5	32.1(br)[a]
	TMS*	-	-	12.9	46.5	10.1(br)[a]
	TMSX	-	28.7	12.1	46.1	46.0
quantities used:						
BTMSImP (mmoles)		0.41	0.48	0.41	0.39	0.78
TMSX (mmoles)		-	0.48	0.41	0.39	0.78
solvent: CD_3CN, 2.0 ml						

[a] Peak assignment uncertain, possibly the product of a $TMSClO_4/CD_3CN$ reaction.

For the BTMSImI/TMSOTf mixture, the presence of a new peak in the spectra of all nuclei can be attributed to an exchange between the isolated trimethylsilyl species, TMSI and TMSOTf. The position of this peak at 20.8 ppm in the silicon-29 n.m.r. spectrum indicates that the population of uncomplexed TMSI is slightly higher than that of TMSOTf (the midpoint between the chemical shifts of TMSOTf and TMSI is 29.1), which in turn implies that the triflate counterion is more strongly bound to BTMSImX. The relative magnitudes of the equilibrium constants for formation of the respective BTMSImX salts can be calculated using the same reasoning as was employed for determining the relative order of K_{eq} for complex formation for a series of nucleophiles (Chapter 3.1); thus K_{rel}(OTf/I) = 8.4.

c) BTMSImOTf and TMSY (Y=Cl, Br, I, OTf, Im, ClO_4)

Moderately fast exchange is observed between the salt and TMSCl, whereas very slow exchange occurs with TMSI and TMSOTf.

The BTMSImOTf/TMSI mixture shows a new peak at 21.6 ppm in the ^{29}Si n.m.r. spectrum, which can be attributed to the exchange between TMSI and TMSOTf, analogous to that observed for the BTMSImI/TMSOTf system. The value of K_{rel}(OTf/I) (6.6) obtained from this chemical shift value is slightly lower than that obtained above. This may reflect a measurement error, but it is more likely to be the result of incomplete equilibration. The latter hypothesis was confirmed by recording a second silicon-29 spectrum of the BTMSImOTf/TMSI mixture, after a time lapse of two days. The resonance shifted 2.1 ppm upfrequency to 23.7 ppm during this period, which is consistent with a shift of the equilibrium in favour of the N,N'-bistrimethylsilylimidazolium iodide salt. The K_{rel}(OTf/I) value calculated from this fully equilibrated system is 3.7.

d) BTMSImP and TMSY (Y=Cl, Br, I, OTf, Im, ClO_4)

The interpretation of the n.m.r. data indicates a moderately fast exchange for TMSBr and very slow exchange for TMSOTf and TMSI.

The BTMSImP/$TMSClO_4$ system shows apparently anomalous chemical shifts which are consistent with a reaction between $TMSClO_4$ and acetonitrile-d_3. This was also noted for isolated $TMSClO_4$ in acetonitrile-d_3. The exact nature of this reaction has not been elucidated in this study, but the products are likely to be analogous to those observed by Simchen[13] (see discussion in Chapter 2.4).

The rate of exchange deduced from each spectrum reflects, to some extent, the energy difference between the exchanging sites, nevertheless, some trends are clearly apparent. A summary of the relative rates of exchange, together with the spectral separation (in Hertz) between exchanging sites, are presented in Table 4.5. A detailed examination of the data shows that the rates of exchange between BTMSImX salts and TMSY depend upon the nature of the counterions X and Y. In general, the rates increase in the following order:-

i) for X (Cl) > Br >> I > OTf > ClO_4;

ii) for Y Im >> Cl > Br >> I, OTf.

Iodide tends to show slightly faster exchange rates for a given X or Y species than triflate, but the differences are not very significant. The exchange between BTMSImX and TMSIm was found to be fast in all cases.

Two mechanisms can be proposed for these exchanges between the imidazolium salts and various trimethylsilyl species.

Table 4.5

Summary of rates of exchange and peak separation between N,N'-Bistrimethylsilylimidazolium X (BTMSImX) and Trimethylsilyl Y (TMSY)

BTMSImX	N.M.R. Nucleus	TMSY				
		Im	Cl	Br	I	OTf
X=Br	^{1}H	38(vf)	-	5(vf)	14(f)	13(vf)
	^{13}C	-	-	40(vf)	19(vf)	19(vf)
	^{29}Si	222(vf)	-	43(f)	252,43[a](vf)	352,43[a](vf)
X=I	^{1}H	13(vf)	21(vf)	7(f)	13(vs)	15(s)
	^{13}C	-	85(vf)	40(f)	139(vs)	-
	^{29}Si	222(vf)	99(f)	41(s)	350(vs)	254(s)
X=OTf	^{1}H	19(vf)	-	-	11(vs)	8(vs)
	^{13}C	-	-	-	148(vs)	28(vs)
	^{29}Si	217(vf)	94(f)	-	259(vs)	344(vs)
X=ClO_4	^{1}H	-	-	2(vf)	18(vs)	10(vs)
	^{13}C	-	-	39(f)	138(vs)	18(vs)
	^{29}Si	-	-	(f)	252(vs)	348(vs)
Solvent: acetonitrile-d_3						

vs: two sharp resonances, of approximately natural linewidth.

s: two resonances, slightly broadened

f: one resonance, slightly broadened.

vf: one resonance, of approximately natural linewidth.

[a] BTMSImY/TMSX exchange.

A) a mechanism involving molecular attack on the N,N'-bistrimethylsilyl imidazolium salt.

i) for nucleophilic attack by Nu

Scheme 4.4

ii) nucleophilic attack by imidazolium nitrogen on Si

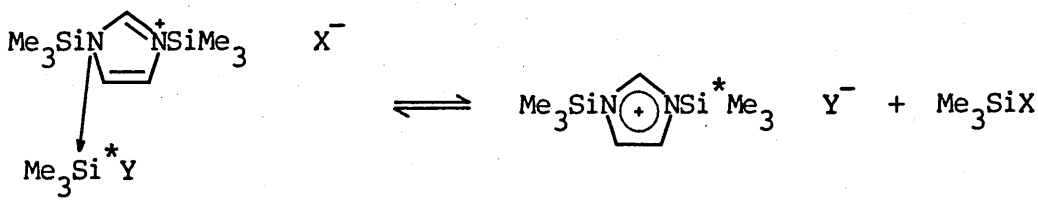

Scheme 4.5

B) a dissociation-reassociation process, nucleophilic attack by X^-.

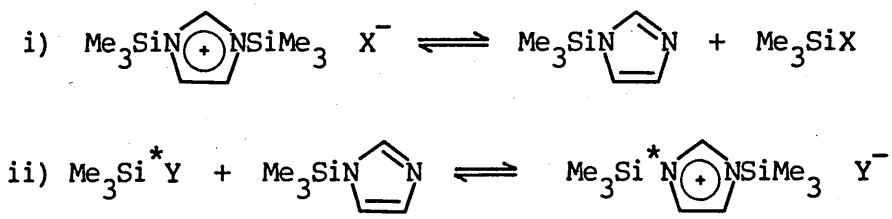

Scheme 4.6

For mechanism B, the second step is likely to be very fast since the nitrogen of TMSIm is a very good nucleophile, therefore the rate determining step will be k_{diss}.

Unlike the other TMSX (X=Cl, Br, I, OTf, ClO_4) species, TMSIm is a very powerful nucleophile, therefore direct attack onto the silyl group of the BTMSImX species is likely to be the first step, leading to rapid dissociation of the complex and exchange. Nucleophilic attack by either of the BTMSImX imidazolium nitrogen atoms is conceivable, although both atoms are fairly sterically hindered, besides being poor nucleophiles. If the mechanism A ii) is the dominant one, the rate should be essentially the same for all counterions, since the rate determining step involves attack of the bistrimethylsilylimidazolium nitrogen atom on the silane. The nucleophilicity of the imidazolium nitrogen atoms is low, irrespective of the counterion X. Furthermore, the degree of deshielding in the individual imidazolium species, determined above (Chapter 2.7), was found to be slightly greater when X=Cl. Therefore, the faster exchange observed for X=Cl is inconsistent with the rate determining step being the attack of an imidazolium nitrogen onto TMSY, since the BTMSImCl nitrogen atoms are the weakest nucleophiles.

In the alternative dissociation-reassociation mechanism, the rate determining step is the dissociation of the BTMSImX adduct, because the reassociation process involves rapid attack by TMSIm, which is a good nucleophile, onto TMSY. Assuming that there are no competing reactions, the dissociation step must be slower than the reassociation step, since the equilibrium constant for salt formation is high. The dissociation process will be controlled by the nucleophilicity of the counterion, so large diffuse ions such as iodide, triflate and perchlorate, which are poor nucleophiles, should not exchange so rapidly; as is indeed observed. This hypothesis is confirmed by the increasing rate of exchange in the order: I < Br < Cl, which also parallels that of increasing nucleophilicity.

The dependence of exchange rates upon the counterion X may also reflect the ability of each anion to be solvated by acetonitrile. Large diffuse species such as triflate or perchlorate, which are well solvated, must break through their solvation shell before attacking the silicon atom. Conversely, tight ion paired species such as chloride or bromide, are already in close vicinity to the silicon centre, thus nucleophilic attack will be facilitated. If this reasoning is correct, a rate acceleration should be observed by decreasing the polarity of the solvent, since charged species will be better solvated in a medium with a low dielectric constant. Therefore additional exchange experiments were performed in dichloromethane-d_2 (Table 4.6) and chloroform-d_1 (Table 4.7) to investigate whether the solvent, and hence the counterions, play a vital role in these processes.

In general, the rates of exchange between BTMSImX and TMSY in acetonitrile and the chlorinated solvents are similar; nonetheless some significant differences are apparent. For instance, the BTMSImOTf/TMSOTf exchange in dichloromethane-d_2 shows two slightly broadened silyl peaks in all three n.m.r. nuclei, whereas the same system in acetonitrile-d_3 gave sharp resonances, indicative of very slow exchange. The trend towards increased rate in this system is enhanced in chloroform-d_1, which shows slightly broadened peaks in the silicon-29 spectrum, but coalesced peaks in the proton n.m.r. spectrum.

The presence of exchange between the isolated TMSX and TMSY species was confirmed by examining several TMSX/TMSY mixtures in a variety of solvents (Table 4.8). Only those mixtures containing ClO_4, OTf or I showed exchange.

Table 4.6 Exchange reactions between N,N'-Bistrimethylsilylimidazolium salts (BTMSImX) and Trimethylsilyl X (TMSX) : N.M.R. Data

		BTMSImBr + TMSBr		BTMSImI + TMSI		BTMSImOTf + TMSOTf		BTMSImClO$_4$ + TMSClO$_4$[a]	
δ(ppm)		1:0	1:1	1:0	1:1	1:0	1:1	1:0	1:1
^{1}H	C_2-H	9.79t	9.98	9.34	9.48	8.63	8.66	8.52	-
	$C_{4,5}$-H	7.48d	7.54d	7.52d	7.53d	7.42	7.44	7.39d	-
	$^4J_{HH}$	1.5Hz	1.5Hz	1.2Hz	1.2Hz	1.2Hz	-	nr	-
	TMS	0.72	0.62	0.75	0.75	0.64	0.63[b]	0.64	-
	TMS*	-	-	-	0.79	-	0.52[b]	-	-
	TMSX	-	0.57	-	0.79	-	0.49	-	0.35
^{13}C	C_2	144.1	144.6	143.0	144.0	141.0	142.7	143.3	-
	CF_3	-	-	-	-	121.1q	120.0q	-	-
	$^1J_{CF}$	-	-	-	-	318Hz	318Hz	-	-
	$C_{4,5}$	124.5	124.5	124.7	124.9	124.1	125.2	124.9	-
	TMS	0.0	3.1	0.0	0.2	-0.81	-0.75	-0.69	-
	TMS*	-	-	-	5.6	-	0.0	-	-
	TMSX	-	4.2	-	5.6	-	0.29	-	0.80
^{29}Si	TMS	26.2	27.5	26.8	26.9	26.9	26.6[c]	26.1	26.6
	TMS*	-	-	-	10.7	-	44.3[c]	-	45.3
	TMSX	-	27.6	-	10.2	-	43.9	-	46.0
quantities used:									
BTMSImX (mmoles)		0.66	0.66	1.45	1.45	0.56	0.56	1.95	1.95
TMSX (mmoles)		-	0.66	-	1.45	-	0.56	-	1.95
solvent: CD_2Cl_2, 2.0 ml									

[a] solvent: CD_2Cl_2 (1.0 ml) and toluene/TMSClO$_4$ (2.0 ml).

[b] broad signals.

[c] slightly broadened signals.

Table 4.7

Exchange reactions between N,N'-Bistrimethylsilylimidazolium salts (BTMSImX) and Trimethylsilyl species (TMSY) : N.M.R. Data

δ/ppm		BTMSImOTf[a]	BTMSImOTf + TMSOTf	BTMSImOTf + TMSIm	BTMSImBr[b]	BTMSImBr + TMSBr	BTMSImBr + TMSIm
^1H	C_2H	8.77	8.80	7.80	9.93(br)	9.95(br)	9.1(br)
	$C_{4,5}$-H	7.39d	7.46d	7.12d	7.78d	7.73d	7.5(br)
	$^4J_{HH}$	1.1Hz	0.73Hz	0.98Hz	1.2Hz	1.2Hz	no
	TMS	0.62	0.65(br)	0.50	0.79	0.74	0.71
^{13}C	C_2	142.0	-	-	142.6	143.9	142.6
	$C_{4,5}$	124.5	-	-	123.7	124.9	125.2
	CF_3	119.1q	-	-	-	-	-
	$^1J_{CF}$	-	-	-	-		-
	TMS	-0.92	-	-	-1.3	-0.80	0.17
^{29}Si	TMS	26.8	26.7(sbr)	16.1[c]	26.5	26.8	23.8
	TMS*	-	43.6(sbr)	-	-	-	-
quantities used:							
BTMSImX (mmoles)		0.71	0.60	1.3	b	0.92	0.56
TMSX (mmoles)		-	0.60	5.2	b	0.92	0.11
solvent: $CDCl_3$, 2.0 ml							

[a] Reaction with BTMSImI not possible since it is only sparingly soluble in $CDCl_3$.

[b] Prepared by adding 0.4 ml of TMSBr into 0.447 ml of TMSIm in 2.0 ml $CDCl_3$.

[c] No change in chemical shift when diluted 4 fold.

Table 4.8

Exchange reactions between Trimethylsilyl X species (TMSX) and Trimethylsilyl Y species (TMSY)

solvent	X	Y	^{1}H $Si-(CH_3)_3$	^{13}C [a] $Si-(CH_3)_3$	^{29}Si $Si-(CH_3)_3$
$CDCl_3$	I	Br	0.80	5.6	9.6
			0.60	4.1	27.8
	I	OSO_2CF_3	0.80	5.6	9.7
			0.50	0.34	43.3
	OAc	Cl	0.27	0.23	23.0
			0.42	3.50	30.6
CD_2Cl_2 [b]	ClO_4	OSO_2CF_3	0.40	-0.34	44.1
CD_2Cl_2	ClO_4	Br	0.40	-0.69	45.0
			0.52	4.8	27.2
	ClO_4	I	0.43	-0.63	45.3
			0.75	5.6	9.8
CD_3CN	OSO_2CF_3	I	0.63	2.75	no

[a] No significant shift of CF_3 peak observed.

[b] Mixture of 1.0 ml dichloromethane-d_2 and 1.0 ml toluene.

It is interesting that exchange is only observed between TMSOTf and other very powerful silylating agents such as TMSI. This implies that the mechanism of the exchange process may involve initial silylation of the sulphonyl oxygen of the trifluoromethanesulphonate group, followed by dissociation, which leads to exchange averaging of the two trimethylsilyl resonances.

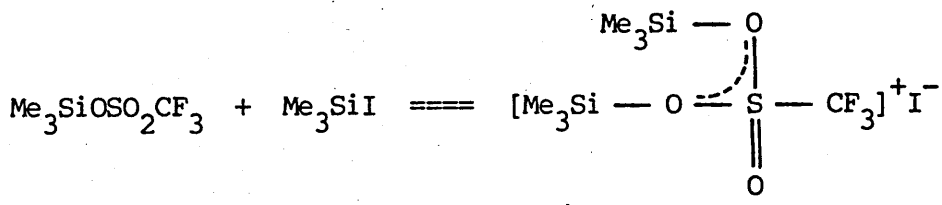

Scheme 4.7

The absence of exchange in chloroform-d_1 and its presence in acetonitrile-d_3 imply that the latter solvent may be involved in the exchange process, although the difference may be caused by polarity effects.

The oxygen-17 n.m.r. spectrum of TMSOTf alone in chloroform-d_1 shows only one resonance, indicating that rapid exchange of the silyl group is taking place between the oxygen atoms of the sulphonate group, but it is not possible, solely on the basis of this observation, to distinguish between an inter- or an intra-molecular exchange process.

The position of the exchanging peak in the TMSI/TMSOTf system in acetonitrile-d_3 is, as expected, at the midpoint between the chemical shifts of the two isolated trimethylsilyl species. The separation between

exchanging sites is 606 Hz which is very similar to that used for calculating the lineshapes presented above in Figures A1.1 and A1.2, therefore a rate of ca. 20,000 s^{-1} can be estimated by comparison of the very broad experimental peaks with the theoretical bandshapes.

Addition of NMI to an exchanging mixture of TMSI and TMSOTf in chloroform-d_1 caused the rate of exchange to increase and a peak characteristic of $[NMI\text{-}TMS]^+X^-$ to be observed in the spectra of all nuclei. The K_{rel}(OTf/I) calculated from the peak position at 30.1 is 0.26.

4.3 Summary

In conclusion, the interpretation of the results in this chapter shows that exchange processes involving $[Nu\text{-}TMS]^+X^-$ adducts occur by two different mechanisms depending upon the exchanging species.

The first mechanism is applicable to exchange between the 1:1 adduct and nucleophilic species. The initial step is the direct nucleophilic attack on the silicon centre, this process is facilitated by the positive charge of Nu^+-Si which results in a neutral leaving group.

The second mechanism concerns exchange between ionic $[Nu\text{-}TMS]^+X^-$ salts and electrophilic species, such as TMSX. Rate determining nucleophilic attack by the counterion X on the silicon centre precedes dissociation of the complex into isolated nucleophile and TMSX. The nucleophile then becomes free to interact with the electrophilic TMSY species. Solvation of the counterion by polar media slows down the dissociation step.

The conclusions reached here are consistent with the behaviour noted in Chapter 2 for the DMF/TMSX and HMPA/TMSOTf mixtures, indicating that the the exchange mechanisms deduced here are not specific to the TMSIm/TMSX systems.

PART I EXPERIMENTAL

Purification of starting reagents

Chemicals were purified by either distillation, sublimation or, in some cases, simply storing over molecular sieves under nitrogen prior to use. Distillations were carried out at reduced pressure in most cases. The pressure was adjusted to achieve a distillation temperature of between 50-100 ^{o}C if possible.

Chloroform:- BDH Chemicals Ltd., 'AnalaR'. It was washed several times with water to remove the ethanol stabilizer, dried with potassium carbonate and distilled in the dark from calcium chloride, and finally stored under nitrogen in a light proof container, over 4A molecular sieves.

Hexane:- Rathburn Chemicals Ltd., HPLC grade, distilled from sodium wire.

Hexamethylphosphoramide:- Aldrich Chemical Co. Ltd., distilled from phosphorus pentoxide (P_2O_5) and stored over 4A sieves.

Toluene:- BDH Chemicals Ltd., 'AnalaR', distilled from sodium wire.

Iodotrimethylsilane:- Aldrich Chemical Co. Ltd., distilled in the dark from copper powder and stored over copper beads.

a) The following compounds were allowed to stand for at least two days over 4A molecular sieves, distilled and stored over 4A molecular sieves under nitrogen:-

1-methylimidazole (Aldrich Chemical Co. Ltd.)

1-methyl-2-pyrrolidinone (Aldrich Chemical Co. Ltd.)

1-methyl-2-pyridone (Aldrich Chemical Co. Ltd.)

1,3-dimethyl-3,4,5,6-tetrahydro-2(1H)-pyrimidinone (Fluka AG, purum)

1,2-dimethyl-2-imidazolidinone (Fluka AG, purum)

1,1,3,3-tetramethylurea (Aldrich Chemical Co. Ltd., 99%)

b) Reagent grade solvents and the chemicals listed below were stored over 4A molecular sieves and used without further purification:-

dichloromethane-d_2 (Aldrich Chemical Co. Ltd., GOLD LABEL, 99.6 atom % D)

acetonitrile-d_3 (Aldrich Chemical Co. Ltd., GOLD LABEL, 99 atom % D)

acetone-d_6 (Aldrich Chemical Co. Ltd., GOLD LABEL, 99.5 atom % D)

chloroform-d_1 (Aldrich Chemical Co. Ltd., GOLD LABEL, 99.8 atom % D)

dichloromethane (Aldrich Chemical Co. Ltd., GOLD LABEL, spectroscopic grade 99+%)

diphenylmethylsilane (Aldrich Chemical Co. Ltd.)

silver perchlorate (BDH Chemicals Ltd., 98%)

silver tetrafluoroborate (BDH Chemicals Ltd., 98%)

chlorotriphenylsilane (Aldrich Chemical Co. Ltd.)

triphenylsilanol (Aldrich Chemical Co. Ltd.)

potassium chloride (BDH Chemicals Ltd., 'AnalaR')

potassium hydroxide (BDH Chemicals Ltd., 'AnalaR')

benzoic acid (Aldrich Chemical Co. Ltd., 99%)

acetic acid glacial (BDH Chemicals Ltd., 'AnalaR')

N-bromosuccinimide (Aldrich Chemical Co. Ltd., 99%)

phenyl-lithium (Aldrich Chemical Co. Ltd., 2 M in cyclohexane-ether)

c) The following compounds were sublimed twice under vacuum:-

2,2-bipyridyl (BDH Chemicals Ltd., spot test reagent or Aldrich Chemical Co. Ltd., 99.5%)

imidazole (Aldrich Chemical Co. Ltd., 99%)

triphenylphosphine oxide (Aldrich Chemical Co. Ltd.)

4-dimethylaminopyridine (Aldrich Chemical Co. Ltd., 99%)

d) The following compounds were distilled from potassium hydroxide (KOH) and 4A molecular sieves:-

pyridine (Aldrich Chemical Co. Ltd.)

2,6-dimethylpyridine (Aldrich Chemical Co. Ltd., 99%)

3,5-dimethylpyridine (Aldrich Chemical Co. Ltd., 98+%)

2,4-dimethylpyridine (Aldrich Chemical Co. Ltd., 96+%)

triethylamine (Aldrich Chemical Co. Ltd.)

quinoline (Aldrich Chemical Co. Ltd.)

e) Since some of the chemicals were very reactive, e.g. chlorotrimethylsilane reacts with molecular sieves, therefore distillations were carried out in the absence of any drying agents in these cases.

chlorodimethylsilane (Aldrich Chemical Co. Ltd., 98%)

chlorotrimethylsilane (Aldrich Chemical Co. Ltd.)

bromotrimethylsilane (Aldrich Chemical Co. Ltd., 98%)

trifluoromethanesulphonic acid (Aldrich Chemical Co. Ltd.)

trimethylsilyl triflate (Fluka AG, purum)

phenyltrichlorosilane (Fluka AG, purum)

f) Straightforward distillation was carried out for the following compounds:-

phenylsilane (Marshalton or Silar Laboratories Inc.)

triethylsilane (Silar Laboratories Inc.)

1,2-dimethylimidazole (Aldrich Chemical Co. Ltd., 98%)

N-trimethylsilylimidazole (Aldrich Chemical Co. Ltd., 98%)

pyridine N-oxide (Halewood Chemicals Ltd., supplied as a liquid, solidified after distillation)

bromomethyldiphenylsilane (Silar Laboratories Inc.)

N.M.R. Parameters

All spectral measurements were made on a Jeol FX90Q n.m.r. spectrometer, equipped with a tunable, multinuclear probe. The spectral parameters were generally as follows:-

^{1}H: spectral width, 89.56 MHz, 1000 Hz or 1500 Hz; pulse width, 22 μS; pulse delay, 0.1 s.

^{13}C: spectral width, 22.50 MHz, 5302 Hz (-16 ppm to 219 ppm); pulse width, 22 μS; pulse delay, 2.0 s; completely decoupled, exponential window, 1.24 Hz.

^{29}Si: spectral width, 17.76 MHz, 4000 Hz (+65 to -160 ppm) or 2000 Hz (-55 to +57 ppm); pulse width, 14 μS; pulse delay, 10 to 25 seconds; proton decoupled, no nuclear Overhauser enhancement, exponential window, 3.09 Hz.

^{29}Si INEPT: this technique was used mainly for trimethylsilyl species. Pulse width, pulse interval and predelay settings were dependent on the magnitude of J_{SiH}[44,45], values of 13 mS, 13 μS and 13 mS respectively were found to be suitable for most trimethylsilyl compounds. The use of similar parameters for Me_2HSiX compounds produced negative signals with respect to the reference or trimethylsilyl compounds.

Sources of error

Extensive precautions were taken to exclude moisture, when handling moisture sensitive compounds, but the possibility of a small percentage of hydrolysis cannot be entirely discounted.

All compounds including both silanes and nucleophiles were handled under nitrogen (air products - high purity grade). The normal techniques used for handling moisture sensitive compounds were employed i.e. transfer in dry nitrogen glove box or via stainless steel needles etc. In addition the highly reactive nature of electrophilic species, such as CF_3SO_3H, $R_3SiOSO_2CF_3$, R_3SiX ($X=OSO_2CF_3$, I, ClO_4, Br), meant that PTFE/rubber septa valves (Pierce Mininert valves) had to be used for storing these species. Silicon rubber was dissolved quickly by the more reactive species e.g. the silyltriflates, but the more stable butyl rubber septa suffered from poor resealability after being punctured by needles. The use of a combination of both types of septa (reactive species contaminated by PTFE/butyl rubber/PTFE/silicone rubber) or the use of septa together with teflon valves was found to be necessary in many cases for effective protection. In addition, reagent bottles were stored in a silica gel dessicator or used entirely in a nitrogen glove box. Fine gauge (27 gauge) stainless steel needles with a non-coring tip were used to minimise the damage to septa.

Weighings were done on a Sartorius 2000 MP digital balance. Hamilton all-glass/teflon, gas tight syringes of the appropriate size were used for measuring quantities of reagents. Accuracy of these syringes was determined by weighing measured volumes of distilled water. The maximum deviation from the indicated volume was found to be $\pm$0.7%.

Infrared

Spectra were recorded on a Pye Unicam SP1050 (polystyrene reference). All reported data were obtained from Nujol mulls, which were made up under dry nitrogen for all moisture sensitive or hydroscopic compounds.

Melting points

These were determined on a Buchi 510 melting point apparatus.

Microanalysis

Elemental analyses were carried out by Butterworth Laboratories or on a Perkin Elmer 240C.

Syntheses

Compounds were generally synthesised by standard literature methods except in cases mentioned below.

General procedure for studying the interaction between nucleophiles and silanes in various stoicheiometries

Three successive aliquots (x/5, 4x/5 and 4x mmoles) of nucleophile were added to the silane (x mmoles) in chloroform-d_1 (2.0 ml), under nitrogen, in a n.m.r. tube (10 mm), to give nucleophile:silane ratios of 1:5, 1:1 and 5:1. ^{1}H, ^{13}C and ^{29}Si n.m.r. spectra were recorded after each addition. Dichloromethane-d_2 or acetonitrile-d_3 were used as solvents if the solubility of the nucleophile/silane system was low. The spectral data, solvent, the quantities of silanes and nucleophiles used are given in the appropriate table as summarized below:- Tables 2.1-2.6, 2.8, 2.9, 2.13-2.16, 2.18-2.22, 2.24 and 2.25.

In the following systems, successive aliquots of silane (x/5, 4x/5 and 4x mmoles) were added to the nucleophile (x mmoles):- PNO (Table 2.21), DMAP (Table 2.17), BIPY (Table 2.19), TMU (Table 2.7), TPPO (Table 2.23).

Preparation of Trimethylsilyl perchlorate (Me_3SiClO_4)

Chlorotrimethylsilane (Me_3SiCl; 0.64 ml, 5.55 mmoles) was added to a solution of silver perchlorate ($AgClO_4$; 1.048 g, 5.05 mmoles) in toluene (1 ml). The resulting white precipitate was centrifuged down and the clear supernatant solution decanted off. The precipitate was washed with a further aliquot of toluene (1 ml) and the combined solution of trimethylsilyl perchlorate in toluene was used immediately.

Synthesis of Trimethylsilylacetate [$Me_3SiOC(O)CH_3$]

Acetic acid (5.2 g, 0.086 mole) in sodium dried diethylether was added slowly to a stirred solution of chlorotrimethylsilane (10 ml, 8.59 g, 0.09 mole) and triethylamine (9.1 g, 0.09 mole) in sodium dried diethylether (2 dm^3). The resulting white precipitate was filtered off under nitrogen after stirring for 2 hours. When removal of the ether by distillation was complete, the product was distilled to give a colourless, moisture sensitive liquid.

b.p. 101° C

N.M.R. δ/ppm ($CDCl_3$, Me_4Si)

^1H 0.28 (9H, s, $SiMe_3$); 2.04 ($CO-CH_3$)

^{13}C 0.29 ($Si-CH_3$); 23.0 ($CO-CH_3$); 172.1 (C=O)

^{29}Si 21.8

General procedure for the preparation of Trimethylsilyl(nucleophile)$^+$ X^- complexes

The trimethylsilyl species (2 mmoles) was added to a stirred solution of nucleophile (2 mmoles) in n-hexane (5 ml), under dry nitrogen. The resulting precipitate was filtered off, washed with fresh n-hexane (2 ml) and dried under vacuum to yield a colourless crystalline solid.

Preparation of N,N'-Bistrimethylsilylimidazolium X salts (BTMSIm$^+X^-$)

X = Br, I, OSO_2CF_3

The salts were made using the same procedure as for the syntheses of trimethylsilyl(nucleophile)$^+X^-$adducts.

X = ClO_4

A solution of trimethylsilyl perchlorate in toluene was used.

X = Cl

No precipitation occurred using the previously mentioned method or by addition of equimolar quantities of chlorotrimethylsilane and trimethylsilylimidazole in the absence of solvent.

Analyses (a) X=Br

Found : C, 36.50; H, 7.19; N, 10.00%.

$C_9H_{21}N_2Si_2Br$ requires C, 36.85; H, 7.22; N, 9.55%.

(b) X=I

Found: C, 31.66; H, 6.22; N, 8.95%.

$C_9H_{21}N_2Si_2I$ requires C, 31.76; H, 6.22; N, 8.23%.

(c) $X=OSO_2CF_3$

Found: C, 33.15; H, 5.98; N, 7.91%.

$C_{10}H_{21}N_2Si_2O_3SF_3$ requires C, 33.13; H, 5.84; N, 7.73%.

(d) $X=ClO_4$

Found: C, 34.20; H, 6.31; N, 9.22%.

$C_9H_{21}N_2Si_2ClO_4$ requires C, 34.55; H, 6.77; N, 8.95%.

Reaction between Silver tetrafluoroborate and Chlorotrimethylsilane

$$AgBF_4 + Me_3SiCl \xrightarrow{(CD_3)CO \text{ or } CD_3CN} Me_3SiF + BF_3{-}O{=}C(CD_3)_2 + AgCl$$

Chlorotrimethylsilane (0.4 ml, 3.15 mmoles) was added slowly to a solution of silver tetrafluoroborate (0.614 g, 3.15 mmoles) in acetonitrile-d_3 (2.0 ml) under nitrogen. The resulting white precipitate of silver chloride was centrifuged down and the clear supernatant solution (1.5 ml) decanted off into a n.m.r. tube. The experiment was repeated using acetone-d_6 as the solvent.

N.M.R. δ/ppm (CD_3CN, Me_4Si, ^{19}F n.m.r. spectrum referenced to $CFCl_3$)

^1H 0.21 (d, $^3J_{HF}$ 7.57Hz, F-Si$(CH_3)_3$)

^{13}C 0.34 ($SiMe_3$); 118.38 (d, $^2J_{CF}$ 332.7Hz, $CFCl_3$)

^{29}Si 33.9 (d, $^1J_{SiF}$ 273.9Hz)

^{19}F -141.8 (BF_3, Lit.[101], -143); -156.5 (Me_3SiF, decet, $^3J_{FH}$ 7.3Hz, Lit.[105], -158); ($AgBF_3$ -150.2)

δ/ppm [$(CD_3)_2CO$, Me_4Si]

^1H 0.20 (d, $^3J_{HF}$ 7.33Hz, F-Si$(CH_3)_3$)

^{29}Si 32.9 (d, $^1J_{SiF}$ 273.9Hz, F-Si$(CH_3)_3$)

^{19}F -147.5 (Lit.[100], 148);

-156.6 (decet, $^3J_{FH}$ 7.3Hz, F-Si$(CH_3)_3$)

Conductivity

Conductivity measurements were carried out using a PTI-10 digital conductivity meter (quoted accuracy $\pm$0.5%, repeatability $\pm$1 digit); all experiments were performed under nitrogen. Calibration of the meter was checked frequently using standard solutions of potassium chloride.

Successive aliquots of the silane were added via a microlitre syringe to a solution of the nucleophile (generally 0.1 molar) in dichloromethane (10 ml). The conductivity readings are illustrated in Tables 2.29-2.32 and 5.4-5.6. The conductivity of the following solutions was measured:-

$^nBu_4NBr$ (0.3577 g, 10 ml CD_2Cl_2, 0.11 molar) 1255 $\mu S\ cm^{-1}$

$^nBu_4NI$ (0.4064 g, 10 ml CD_2Cl_2, 0.11 molar) 1353 $\mu S\ cm^{-1}$

Imidazolium triflate (0.2410 g, 10 ml CD_2Cl_2, 0.11 molar)
0.7 $\mu S\ cm^{-1}$ (not fully dissolved)

Trimethylsilyl trifluoromethanesulphonate (0.2 ml, 1.1 mmoles, 10 ml CD_2Cl_2, 0.11 molar) 0.80 $\mu S\ cm^{-1}$

$^nBu_4NBr$ (0.3535 g, 10 ml CH_3CN, 0.11 molar) 8820 $\mu S\ cm^{-1}$

$^nBu_4NI$ (0.4074 g, 10 ml CH_3CN, 0.11 molar) 9220 $\mu S\ cm^{-1}$

Imidazolium triflate (0.2417 g, 10 ml CH_3CN, 0.11 molar)
7560 $\mu S\ cm^{-1}$

Variable temperature n.m.r. study of the interactions between various nucleophiles and silanes: general method

Equimolar quantities of silane and nucleophile were added together in dichloromethane-d_2 (2.0 ml). Temperatures were set using a Jeol temperature controller which was not calibrated (quoted temperature accuracy ± 2 ^{o}C). In general the silicon-29 n.m.r. spectra were recorded first, then at progressively lower temperatures down to 180 K (CD_2Cl_2 freezes at 176 K). Other nuclei n.m.r. spectra were recorded, if necessary, upon warming up to ambient temperature. Two minutes were allowed, after each readjustment of temperature, for the solution to reach thermal equilibrium.

A second silicon-29 n.m.r. was recorded after the solution had returned to ambient probe temperature (300 K). Solubility of the components under study was investigated, prior to the experiment, by cooling the sample in a carbon dioxide/acetone bath (-78 ^{o}C). The quantities of each species used and the spectral results are shown in the appropriate tables.

Table 2.11

Pyridine (py) and bromotrimethylsilane (Me_3SiBr)

Table 2.12

Pyridine (py) and chlorotrimethylsilane (Me_3SiCl)

Table 2.20

2,2-Bipyridyl (BIPY) and iodotrimethylsilane (Me_3SiI)

Table 2.26

Triethylamine (Et_3N) and iodotrimethylsilane (Me_3SiI)

Table 2.33

N-trimethylsilylimidazole (TMSIm) and chlorotrimethylsilane (Me_3SiCl)

Methanolysis of N,N'-Bistrimethylsilylimidazolium X salts ($BTMSIm^+X^-$): synthesis of Imidazolium salts

N,N'-bistrimethylsilylimidazolium X (2.2 mmoles) was dissolved in methanol (5 ml). Removal of the solvent by evaporation and subsequent recrystallisation from acetone gave colourless crystals.

X = OSO_2CF_3

m.p. 191-193 °C

N.M.R. δ/ppm (CD_3CN, Me_4Si)

^1H 7.43 (2H, $C_{4,5}$-H); 8.58 (1H, s, C_2-H);

^{13}C 121.9 (q, $^1J_{CF}$ 320Hz, CF_3); 120.4 (s, $C_{4,5}$); 135.1

Analysis Found: C, 22.10; H, 2.35; N, 13.2%.

$C_4H_5N_2O_3F_3S$ requires C, 22.02; H, 2.31; N, 12.84%.

X = Br

m.p. 221-222 °C

N.M.R. δ/ppm (CD_3CN, Me_4Si)

^1H 7.42 (2H, s, $C_{4,5}$-H); 8.58 (1H, s, C_2-H)

11.74 (2H, s, br, N-H)

^{13}C 119.9 (s, $C_{4,5}$); 134.2 (C_2)

Analysis Found: C, 24.17; H, 3.38; N, 18.80%.

$C_3H_5N_2Br$ requires C, 24.17; H, 3.31; N, 18.09%.

X = I

m.p. 226-227 °C

N.M.R. δ/ppm (CD_3CN, Me_4Si)

^1H 7.43 (2H, s, $C_{4,5}$-H); 8.59 (1H, s, C_2-H);

(15.1 or 5.6)

Analysis Found: C, 18.37; H, 2.61; N, 13.34%.

$C_3H_5N_2I$ requires C, 18.38; H, 2.57; N, 14.29%.

General method for studying the competition of a pair of nucleophiles for a given Trimethylsilyl X species (X = I, OSO_2CF_3)

Equimolar amounts (generally 2.2 mmoles) of nucleophile A and nucleophile B were added to chloroform-d_1 (2.0 ml). ^1H and ^{13}C n.m.r. spectra were recorded, followed by the addition of a stoicheiometric quantity of the trimethylsilyl species to the solution of the two nucleophiles. ^1H, ^{13}C and ^{29}Si n.m.r. spectra were again recorded.

The spectral results are presented in Table 3.1 to 3.27. The n.m.r. data of a 1:1 mixture of each nucleophile with the respective silane are also illustrated in the tables for comparison in columns 2 and 4 (these nucleophile-silane data have already been presented in Chapter 2). The various combinations of nucleophiles and silanes are outlined in Table 3.28.

Exchange between N,N'-Bistrimethylsilylimidazolium X ($BTMSIm^+X^-$) and Trimethylsilyl species (TMSY)

A quantity of N,N'-bistrimethylsilylimidazolium X was weighed into a n.m.r. tube, dissolved in solvent (2.0 ml) and an equimolar amount of trimethylsilyl species was then added to this solution. The ^1H, ^{13}C and ^{29}Si n.m.r. data were recorded (see Tables 4.1-4.4, 4.6 and 4.7).

Exchange Reaction between Iodotrimethylsilane (Me_3SiI) and Trimethylsilyl triflate ($Me_3SiOSO_2CF_3$)

Iodotrimethylsilane (0.3 ml, 2.2 mmoles) was added to a solution of trimethylsilyl triflate (0.4 ml, 2.2 mmoles) in chloroform-d_1 (2.0 ml). ^1H, ^{13}C and ^{29}Si n.m.r. spectra were recorded before and after the addition of N-methylimidazole (0.175 ml, 2.2 mmoles). A further aliquot of trimethylsilyl triflate (0.4 ml, 2.2 mmoles) was then added to the mixture and the ^{29}Si n.m.r. spectrum taken.

N.M.R. δ/ppm ($CDCl_3$, Me_4Si)

(i) mixture of Me_3SiI and $Me_3SiOSO_2CF_3$

^1H 0.795 (9H, s, Me_3SiI); 0.498 (9H, s, $Me_3SiOS_2CF_3$)

^{13}C 5.57 (Me_3SiI); 0.34 ($Me_3SiOSO_2CF_3$);
118.4 (q, $^1J_{CF}$ 317Hz, CF_3)

^{29}Si 9.74 (Me_3SiI, 9.6, $CDCl_3$)
34.6 (unknown, low intensity)
43.34 ($Me_3SiOSO_2CF_3$, 43.9, $CDCl_3$)

(ii) mixture of Me_3SiI, $Me_3SiOSO_2CF_3$ and N-methylimidazole

^1H 9.43 (1H, H_2); 7.72 (1H, t, J 1.5Hz, H_4); 7.49 (1H, t, J_{HH} 1.7Hz, H_5); 4.13 (3H, Me-N); 0.68 (9H, salt); 0.61 (9H, Me_3SiI/Me_3SiOTf exchange)

^{13}C 140.0 (C_2); 125.2, 123.7 ($C_{4,5}$); 36.4 (Me-N); 2.53 (Me_3SiI/Me_3SiOTf exchange); -0.63 (salt)

^{29}Si 26.80 [$(NMISiMe_3)^+(I^-$ or $OSO_2CF_3^-)$]

30.2 (br, midpoint between Me_3SiI and $Me_3SiOSO_2CF_3$ in $CDCl_3$ is 26.5)

(iii) Addition of further aliquot of $Me_3SiOSO_2CF_3$

^{29}Si 26.8, 35.0

The addition of same quantities of $Me_3SiOSO_2CF_3$ to Me_3SiI was repeated in acetonitrile-d_3 (2.0 ml).

N.M.R. δ/ppm (CD_3CN, Me_4Si)

^1H 0.63 (midpoint between Me_3SiI and $Me_3SiOSO_2CF_3$ in CD_3CN is 0.635)

^{13}C 2.75 (midpoint for Me_3Si species is 2.93 in CD_3CN) species)

^{29}Si 29.8 very broad

A very small amount of a pale yellow solid was precipitated upon addition of TMSI to TMSOTf/CD_3CN/TMS mixture. Additional exchange experiments were performed, the n.m.r. data are shown in Table 4.8.

N.M.R. Data for a 1:1 mixture of Trimethylsilylacetate (Me_3SiOAc) and Chlorotrimethylsilane (TMSCl)

Trimethylsilylacetate	0.75 ml
Chlorotrimethylsilane	0.6 ml

δ/ppm ($CDCl_3$, Me_4Si)

^1H 0.27 (9H, s, Me_3SiOAc); 0.42 (9H, s, TMSCl);
2.02 (3H, s, $CH_3C{=}O$); 2.04 (AcOH, low intensity)

^{13}C 171.9 (s, C=O); 23.0 (s, CH_3); 3.5 (s, Me_3SiCl);
0.23 (s, Me_3SiOAc)

^{29}Si 30.6 (Me_3SiCl); 23.0 (Me_3SiOAc); 7.1 (HMDSO, low intensity)

PART I SUMMARY AND CONCLUSIONS

Part I - Summary and Conclusions

It is clear from the accumulated data presented in this section that adducts between TMSX species (X=Br, I, OTf, ClO_4) and a diverse range of nucleophiles $[Nu\text{-}TMS]^+X^-$ are the dominant species present in solution. Similar adducts with chloride as the counterion are less stable in solution at ambient temperatures, but they can be observed at low temperatures with strongly donating nucleophiles. Their lower stability reflects the poor leaving group ability of the chloride ion, together with the rapid dissociation of the resulting $[Nu\text{-}TMS]^+Cl^-$ adduct, which in turn results from the greater nucleophilicity of the chloride anion. Similar principles apply to other counterions, but in these species the dissociation step is increasingly slower in the series

$$Cl > Br > I, OTf > ClO_4.$$

Solvation of the counterion by polar solvents decreases the rate of attack of the anion onto the silicon centre. For a given counterion the equilibrium constant for salt formation increases in the following order:-

2,6DMP, quinoline, BIPY, Et_3N < py < DMEU < 3,5DMP << DMF < NMP < 2,4DMP < DMPU < TPPO < PNO < NMPO < DMI < HMPA < NMI, DMAP.

This order reflects the relative concentration of each $[Nu\text{-}TMS]^+X^-$ adduct in solution, which has important implications for the mechanism of nucleophilically assisted silylation reactions.

If the first step in such process involves a rapid pre-equilibrium formation of a $[Nu\text{-}TMS]^+X^-$ complex, then the overall rate should depend upon the equilibrium constant, in addition to the concentration of the species being silylated e.g. ROH.

$$Nu + R_3SiX \rightleftharpoons [Nu\text{-}Si]^+X^- \xrightarrow{R'OH} R'OSiR_3 + Nu^+H\ X^-$$

$$\text{Rate} \propto K_{eq}\ k_2\ [Nu]\,[TMSX]\,[R'OH]$$

Scheme I.1

It is conceivable that the adducts are merely the products from side reactions and are not involved in the reaction pathway (Scheme I.2).

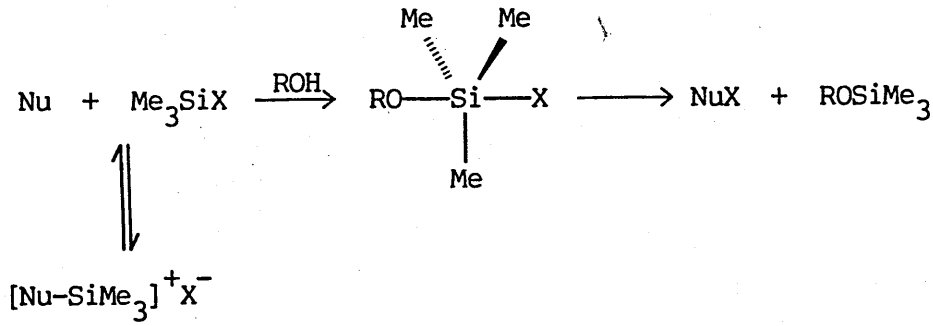

Scheme I.2

If this were the case, then a smaller rate increase for the powerful nucleophiles, such as HMPA, DMAP or NMI, would be expected since they form very stable $[Nu\text{-}TMS]^+X^-$ adducts, and therefore in these systems, the equilibrium concentration of the isolated nucleophile and TMSX is very low. Attack of the alcohol onto TMSX would be preceded by rate limiting dissociation of the complex, which was shown in Chapter 4 to be

considerably slower than nucleophilic attack onto the $[Nu\text{-}TMS]^+X^-$ complex. This is clearly inconsistent with the rate accelerations produced by the better nucleophiles. Furthermore, the attack by nucleophiles on the $[Nu^+\text{-}TMS]^+X^-$ adduct is facilitated with respect to the isolated TMSX because the nucleophiles$^+$ in $[Nu^+\text{-}TMS]X^-$ are excellent, neutral, leaving groups. The observed rate acceleration produced by each nucleophile should therefore be proportional to the equilibrium constant for salt formation for that particular nucleophile.

The observations by Chaudhary and Hernandez[6] concerning the rate of solvolyses assisted by DMAP, and the results of Corriu[104] who originally demonstrated a rate acceleration by HMPA and DMF, agree qualitatively with this hypothesis, nevertheless, a detailed kinetic study is definitely required to further elucidate this mechanism.

The negative enthalpy of formation found for py/TMSBr, Et_3N/TMSI and TMSIm/TMSCl can probably be applied to the majority of $[Nu\text{-}TMS]^+X^-$ adducts. This explains the low or negative value obtained for the racemisation and hydrolysis of chlorosilanes[104]. The equilibrium concentrations of the adducts decrease at higher temperatures, which should therefore lead to a rate retardation with increasing temperature. Thus the apparent activation enthalpy will be negative, although each step in the process may actually have a positive activation enthalpy (Figure I.1). The failure to observe any evidence for five coordinate acyclic nucleophile-silane adducts indicates that the stability of the intermediate I.1(ii) (Figure I.1) is low, if it exists at all.

The applicability of this mechanism to silanes other than trimethyl will be discussed in the following section.

Figure I.1

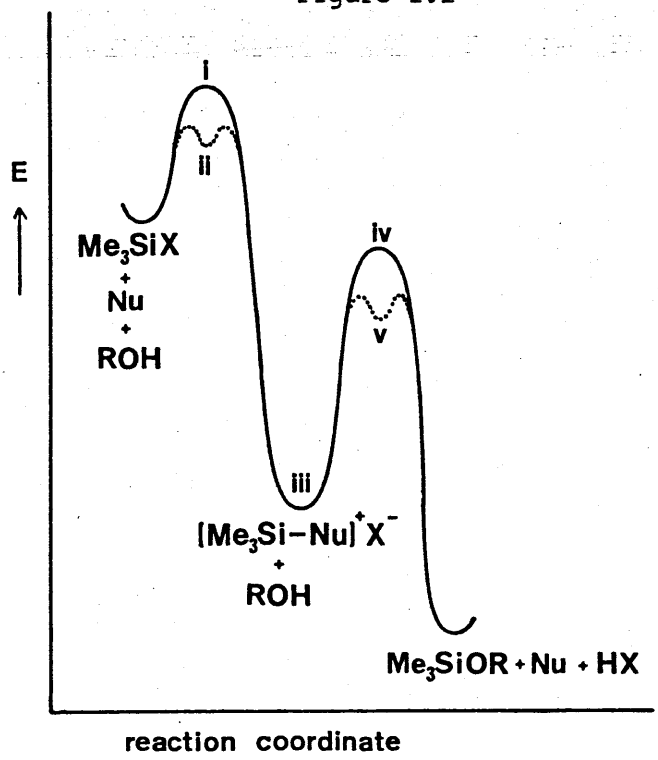

(i) 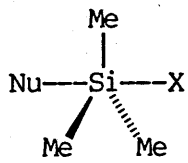 transition state

(ii) 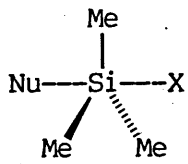 five coordinate intermediate

(iii) $[Nu\text{-}SiMe_3]^+X^-$ four coordinate ionic intermediate

(iv) 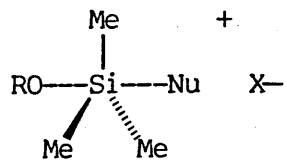 five coordinate transition state

(v) 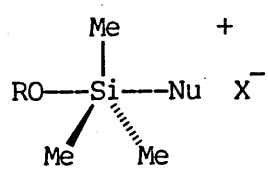 five coordinate intermediate

PART II

CHAPTER 5

THE INTERACTIONS BETWEEN NUCLEOPHILES AND ALKYL OR ARYL SUBSTITUTED SILANES

5.1 Introduction

In the preceding section, formation of ionic adducts between nucleophiles and the highly electrophilic trimethylsilyl species was strongly implicated as being the first step in the mechanism of nucleophile assisted silylation. Therefore it is very important to determine whether analogous complexes are produced by the interactions of nucleophiles with other silyl species, or whether they are a phenomenon specific to trimethylsilyl species.

The trends deduced above indicate that a combination of NMI as the nucleophile and triflate as the counterion should provide near optimum conditions for the observation of stable $[R_3Si\text{-}Nu]^+X^-$ adducts. However only a few silyltriflates are available commercially, so it was necessary to synthesise a number of functionalised silyltriflates, prior to investigating their behaviour with nucleophiles.

Silyltriflates that have been reported in the literature are mainly those with alkyl or phenyl[13,14,106,107] substituents. The latter were synthesised by reaction of the appropriate chlorosilane with silver triflate (Scheme 5.1).

$$R_3SiCl + CF_3SO_3Ag \longrightarrow R_3SiOSO_2CF_3 + AgCl(s)$$

Scheme 5.1

However the most common and economic route to silyltriflates involves the direct reaction between halosilanes (R_3SiX) and trifluoromethanesulphonic acid[107,108] (triflic acid, TfOH).

$$R_3SiX + CF_3SO_3H \longrightarrow R_3SiOSO_2CF_3 + HX$$

(X=Cl[109], H[110], Ph[110], allyl[110], CH_3[110]; R=alkyl)

Scheme 5.2

This method has a number of advantages; in particular it avoids the use of the expensive and inconvenient silver triflate and it gives HX co-products that can be separated easily in the majority of cases.

5.2 Syntheses of Silyltriflates

A summary of the silyltriflates synthesised in this study, together with the reaction conditions used, is given in Table 5.1.

The attempted synthesis of $^tBuPh_2SiOTf$ from $^tBuPh_2SiCl$ and triflic acid failed because the acid cleaved the phenyl group in preference to the chloride, yielding $^tBuPhClSiOTf$ and benzene. Selective cleavage of phenyl in preference to hydride or alkyl was also noted in Ph_2MeHSi, although naphthalene was cleaved instead of the phenyl group in 1-NpPhMeSiH. It can be inferred from the data presented in Table 5.1 that the relative ease of cleavage is:-

$$Np > Ph > Cl > H >> Me, Et, {}^tBu.$$

Table 5.1

The Syntheses of Silyltriflates, $R_2SiXOTf$, from R_2SiXY and Triflic acid

R_2SiXY	$R_2SiXOTf$	Isolated yield (%)[a]	B.p. (°/mmHg)	Reaction conditions[b]
Me_2SiHCl	$Me_2SiHOTf$[c]	95	123/760	stirred 5 mins
Me_2SiHPh	$Me_2SiHOTf$[c]	86	123/760	stirred 5 mins
H_3SiPh	H_3SiOTf	d	nr	instantaneous
$^tBuPhSiClPh$	$^tBuPhSiClOTf$[c]	92	70/0.01	stirred 30 mins
Ph_3Si^tBu	Ph_2Si^tBuOTf[c]	73	115/0.02	silane in $CHCl_3$, 30 mins reflux
Cl_3SiPh	Cl_3SiOTf[c]	85	32/25	60° for 3 h
(+)-1-NpPhMeSiH	PhMeSiHOTf	e		silane in $CHCl_3$, stirred 10 mins
Ph_2MeSiH	PhMeSiHOTf[c]	93	67/0.8	stirred 5 mins

a All reactions essentially quantitative by ^1H N.M.R..

b Unless otherwise stated, equimolar quantities of reagents used, triflic acid added dropwise to neat silane at ambient temperature, distilled after stirring.

c Satisfactory microanalytical data were obtained .

d product not isolated pure.

e All spectral properties identical to the product obtained from Ph_2MeSiH, not isolated.

The cleavage of aryl groups from silicon is thought to involve charged intermediates (Scheme 5.3).

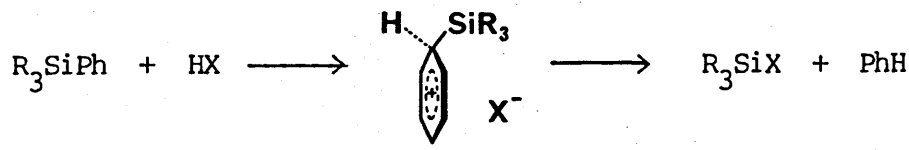

Scheme 5.3

The preferential cleavage of the naphthyl rather than the phenyl is in accord with the expected behaviour if this mechanism is in operation, because the naphthyl group is better at stabilizing the positively charged intermediate.

Protodesilylation reactions similar to these have been extensively studied by Eaborn et al.[111,112,113] and others[114].

The formation of a novel optically active silyltriflate may be possible since the cleavage of the naphthyl group is from the optically active (+)-1-NpPhMeSiH. However the results of a preliminary optical rotation study of this reaction indicated that the product had lost its optical activity.

In the preparation of silyltriflate ($H_3SiOSO_2CF_3$), the first fraction collected from distillation of the crude H_3SiPh/CF_3SO_3H mixture was a clear mobile liquid with b.p. 79-80 ^{o}C at atmospheric pressure. Attempted removal of this fraction using a previously oven dried, stainless steel needle and glass/teflon syringe, via a teflon/silicon rubber septum, resulted in a violent explosion. The black sooty deposits and white powdery residue (assumed to be silica) left from the incident can be

taken as evidence for the presence of a product, or products, containing both silicon and carbon. This suggests that the silyltriflate distilled with the benzene co-product. The explosion may have been initiated by the presence of a pyrophoric gas, probably silane, which was observed in the remainder of the apparatus, although the exact cause of such behaviour was not further examined. Disproportionation may have occurred to give the silane and an unidentified co-product, probably silylditriflate [$H_2Si(OSO_2CF_3)_2$] (Scheme 5.4).

$$2\ H_3SiPh + 2\ CF_3SO_3H \longrightarrow 2\ H_3SiOTf + 2\ PhH$$

$$\Downarrow$$

$$H_4Si + H_2Si(OSO_2CF_3)_2$$

Scheme 5.4

Since silyltriflate ($H_3SiOSO_2CF_3$) could not be isolated pure by distillation, it was characterised from the crude product using ^1H, ^{13}C and ^{29}Si n.m.r.. In subsequent reactions the silyltriflate was used in chloroform solution, in the presence of the benzene co-product.

With the phenylsilanes, except in the case of $PhSiH_3$, a transitory red colour was observed upon addition of triflic acid to the silane. The red colour became permanent when a 10% molar excess of triflic acid was syringed into a solution of $^tBuPh_3Si$ in chloroform. A very strong but unresolved electron paramagnetic resonance (e.s.r.) signal was observed for this solution. Biphenyl was isolated from the distillation residue of the Et_3SiPh/CF_3SO_3H reaction in approximately 25% yield (% of possible

product). These two observations provide some evidence for a mechanism involving the intervention of radicals, at least as a competitive route, although it is conceivable that the red colouration was the result of contamination by metal ions dissolved from the stainless steel transfer needle. To eliminate such a possibility, the $^{t}BuPh_2SiOTf$ reaction was repeated using all-glass apparatus, which had previously been washed with 'AnalaR' concentrated hydrochloric acid and oven dried. The triflic acid used for the reaction was also distilled and transferred in similarly cleansed, all-glass apparatus. The red colouration and strong e.s.r. signal were again observed, undiminished by this treatment. A transitory blue-green colour was also noted during addition of triflic acid to a chloroform solution of 1-NpPhMeSiH. The intensity of these colours indicates that the molar absorption coefficient (ϵ) values for these intermediates are very high. This may be produced by a charge transfer process, although the precise nature of the transition involved cannot be assessed without further information.

5.3 Interactions with nucleophiles

a) Silyltriflate (H_3SiOTf)

Addition of a stoicheiometric quantity of NMI to a solution of silyltriflate in chloroform/benzene resulted in a vigorous exothermic reaction, accompanied by the precipitation of a colourless solid and the evolution of a pyrophoric gas. In view of the previous explosion encountered with this silane and the evolution of the gas, n.m.r. studies were not carried out. Therefore, no firm conclusions can be reached from these observations, though it seems likely that disproportionation was occurring to give silane and an unidentified adduct with NMI.

An equimolar mixture of silyltriflate and triethylamine in chloroform/benzene exhibited silicon-29 chemical shifts of -74.1 ppm (quintet, J_{SiH} = 267 Hz) and -82.1 ppm (quintet, J_{SiH} = 286 Hz). The low frequency silicon-29 chemical shifts indicate that two different, probably, five coordinate silicon adducts have been formed (Figure 5.1).

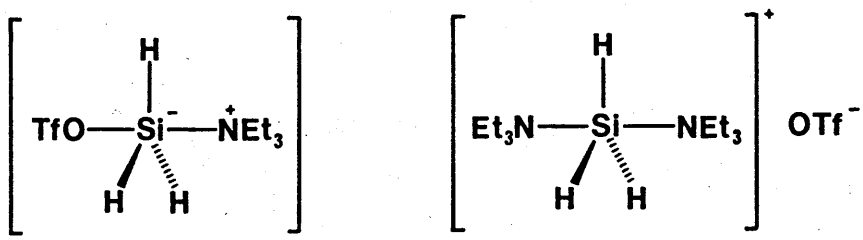

Figure 5.1

A six coordinate silicon species cannot be ruled out on the basis of these data alone, although the silicon-29 chemical shifts are typical of five rather than six coordination. A small ^{29}Si resonance was noted at -96.1 ppm (triplet, J_{SiH} = 364 Hz). The multiplicity of this peak indicated that it was a SiH_2 species and therefore the product of a disproportionation reaction. The proton and carbon-13 n.m.r. data were consistent with quarternized triethylamine.

b) Dimethylsilyl derivatives

Titration of N-methylimidazole (NMI) on chlorodimethylsilane (DMSCl) (Table 5.2) caused the silicon-29 resonance to move steadily downfrequency from an initial value of 11.6 ppm (corresponding to isolated DMSCl) to a chemical shift of -80 ppm, at a NMI:DMSCl ratio of 2.5:1. No significant change in the chemical shift was observed upon further addition of NMI up to a 5:1 ratio.

Table 5.2

Silicon-29 N.M.R. chemical shift titration: Chlorodimethylsilane (DMSCl) against N-methylimidazole (NMI)

Volume NMI (ml)	Ratio DMSCl:NMI	^{29}Si $Si(CH_3)_2$
0.020	18.04:1	11.5
0.050	7.23:1	10.6
0.100	3.61:1	6.5
0.150	2.40:1	1.4
0.200	1.80:1	-4.0
0.250	1.44:1	-10.0
0.300	1.20:1	-15.7
0.350	1.03:1	-21.5
0.360	1.00:1	-22.8
0.380	1:1.05	-25.4
0.400	1:1.11	-27.6
0.420	1:1.16	-30.4
0.430	1:1.19	-31.4
0.440	1:1.22	-32.8
0.450	1:1.25	-33.6
0.450	1:1.25	-34.2
0.460	1:1.27	-35.3
0.470	1:1.30	-36.6
0.480	1:1.33	-37.8
0.490	1:1.36	-39.2
0.500	1:1.39	-40.0
0.600	1:1.66	-52.6
0.700	1:1.94	-64.1
0.800	1:2.22	-72.0
0.900	1:2.49	-76.0
1.000	1:2.77	-78.0
1.100	1:3.05	-78.8
1.500	1:4.16	-80.3

Solvent: chloroform-d_1

Table 5.3

Silicon-29 N.M.R. chemical shift titration: Dimethylsilyl triflate (DMSOTf) against 1-Methylimidazole (NMI)

Volume DMSOTf (ml)	Ratio NMI: DMSOTf	^{29}Si Si	Volume DMSOTf (ml)	Ratio NMI: DMSOTf	^{29}Si Si	^{29}Si Si*
0.10	22.39:1	-80.2	1.75	1.28:1	-8.0	-
0.20	11.19:1	-80.1	1.80	1.24:1	-4.8	-
0.40	5.60:1	-79.9	1.85	1.21:1	-1.7	-
0.60	3.73:1	-79.4	1.90	1.18:1	1.4	-
0.80	2.80:1	-78.8	1.95	1.15:1	4.3	-
1.00	2.24:1	-74.6	2.00	1.12:1	7.1	-
1.20	1.87:1	-56.5	2.05	1.09:1	9.3	-
1.30	1.72:1	-46.2	2.10	1.07:1	9.3	-
1.35	1.66:1	-39.9	2.20	1.02:1	9.3	24.3
1.40	1.60:1	-36.2	2.30	1:1.03	9.3	24.3
1.45	1.54:1	-31.5	2.40	1:1.07	9.3	24.3
1.50	1.50:1	-26.1	2.50	1:1.12	9.3	24.3
1.55	1.44:1	-23.4	2.60	1:1.16	9.3	24.3
1.60	1.40:1	-19.5	2.80	1:1.25	9.3	24.3
1.65	1.36:1	-14.8	3.00	1:1.34	9.3	24.3
1.70	1.32:1	-11.8	4.00	1:1.79	9.3	24.3

Solvent: dichloromethane-d_2

* new silicon-29 peak

Addition of NMI to a solution of dimethylsilyl triflate (DMSOTf) in chloroform resulted in the precipitation of a white solid. Therefore the silicon-29 chemical shift titration of NMI against DMSOTf was carried out by adding DMSOTf to NMI in chloroform-d_1 (Table 5.3). In the presence of a 5 fold excess of NMI, the dimethylsilyl resonance was observed at very low frequency (-81 ppm), indicating that similar types of complex were being formed between NMI and the dimethylsilyl derivatives irrespective of counterion. Successive additions of aliquots of DMSOTf to NMI enabled a steady upfrequency shift to be observed at NMI:DMSOTf ratios of lower than ca. 2.5, this trend continued until 1:1 stoicheiometry was reached, where a very sharp point of inflexion occurred (9.5 ppm), suggesting that a second type of complex had been formed. Further titration of the DMSOTf onto NMI resulted in a new resonance being observed at 24 ppm (corresponding to isolated DMSOTf), which gradually became more intense as the concentration of DMSOTf increased. The shape of this titration curve (Figure 5.2) and the exchange behaviour at low NMI:DMSOTf ratios are consistent with the formation of a $(NMI)_2$-DMSOTf complex, which is undergoing fast exchange with a 1:1 NMI-DMSOTf complex, whereas the latter is exchanging relatively slowly, on the n.m.r. time-scale, with isolated DMSOTf. The sharp point of inflexion at 1:1 shows that the equilibrium constant for the formation of this complex is very high. Extrapolation of the straight line regions of the curve between 1:1 and 2:1, as well as, 3:1 and 5:1, confirms that the NMI-DMSOTf complex has an essentially 2:1 stoicheiometry (see Appendix 2). Extrapolation of the NMI/DMSCl titration curve indicates that this complex has a similar stoicheiometry, and the equilibrium constant for 2:1 complex formation is slightly higher in the DMSOTf system .

Figure 5.2 Silicon-29 chemical shift titration: N-methylimidazole against (a) dimethylsilyl triflate and (b) chlorodimethylsilane.

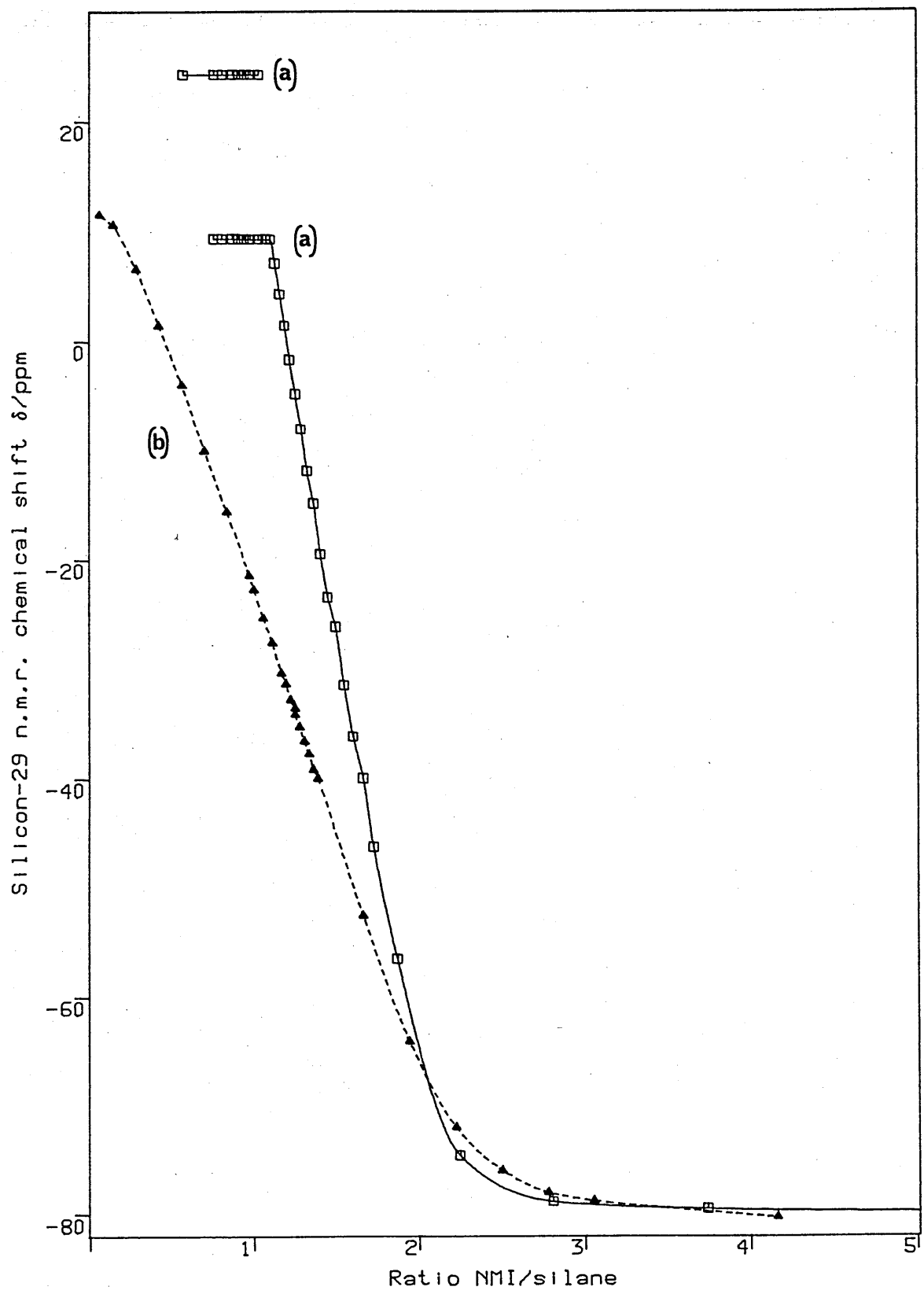

Solvent: chloroform-d1

Table 5.4 Conductivity titration between Chlorodimethylsilane (DMSCl) and N-Methylimidazole (NMI)

Volume DMSCl (ml)	Ratio NMI:DMSCl	Conductivity ($\mu S\ cm^{-1}$)
0.000	0.00:1	0.0
0.005	38.06:1	12.3
0.010	19.03:1	15.1
0.020	9.52:1	21.9
0.030	6.34:1	28.5
0.040	4.76:1	34.4
0.050	3.81:1	38.1
0.060	3.17:1	41.8
0.070	2.72:1	45.4
0.080	2.38:1	48.3
0.090	2.11:1	51.1
0.100	1.90:1	53.7
0.110	1.73:1	56.3
0.120	1.59:1	58.4
0.130	1.46:1	60.5
0.140	1.36:1	62.3
0.150	1.27:1	64.2
0.160	1.19:1	65.9
0.170	1.12:1	67.6
0.180	1.06:1	69.2
0.190	1: 1.00	70.7
0.200	1: 1.05	72.2
0.210	1: 1.10	73.6
0.220	1: 1.16	74.9
0.230	1: 1.21	75.9
0.240	1: 1.26	77.0
0.250	1: 1.31	77.8
0.260	1: 1.37	78.7
0.270	1: 1.42	79.6
0.280	1: 1.47	80.4
0.290	1: 1.52	81.3
0.300	1: 1.58	82.1
0.310	1: 1.63	82.8
0.320	1: 1.68	83.6
0.330	1: 1.73	84.2
0.340	1: 1.79	84.7
0.350	1: 1.84	85.2
0.360	1: 1.89	85.8
0.370	1: 1.94	86.3
0.380	1: 2.00	86.8
0.390	1: 2.05	87.1
0.400	1: 2.10	87.6
0.410	1: 2.15	88.0
0.420	1: 2.21	88.4
0.430	1: 2.26	88.8
0.440	1: 2.31	89.1
0.450	1: 2.36	89.5
0.460	1: 2.42	89.8
0.470	1: 2.47	90.1
0.480	1: 2.52	90.3
0.490	1: 2.57	90.7
0.500	1: 2.63	91.0

Solvent: CD_2Cl_2, 10.0 ml; Volume of NMI: 0.085 ml (1.1 mmoles)

Initial conductivity of solution: 0.0 $\mu S\ cm^{-1}$; Cell constant: 0.9162

Table 5.5 Conductivity titration between N-Methylimidazole (NMI) and Dimethylsilyl triflate (DMSOTf)

Volume DMSOTf (ml)	Ratio NMI:DMSOTf	Conductivity ($\mu S\ cm^{-1}$)
0.000	0.00:1	2.0
0.005	38.06:1	57.5
0.010	19.03:1	84.3
0.015	12.69:1	109.6
0.020	9.52:1	128.5
0.025	7.61:1	179.0
0.030	6.34:1	227.2
0.035	5.44:1	280.4
0.040	4.76:1	326.2
0.045	4.23:1	375.6
0.050	3.81:1	425.1
0.055	3.46:1	465.4
0.060	3.17:1	511.2
0.065	2.93:1	550.6
0.070	2.72:1	588.2
0.075	2.54:1	618.4
0.080	2.38:1	657.8
0.085	2.24:1	676.2
0.090	2.11:1	696.3
0.095	2.00:1	711.0
0.100	1.90:1	717.4
0.105	1.81:1	717.4
0.110	1.73:1	712.8
0.115	1.65:1	702.7
0.120	1.59:1	692.6
0.125	1.52:1	672.5
0.130	1.46:1	652.3
0.135	1.41:1	634.0
0.140	1.36:1	610.2
0.145	1.31:1	588.2
0.150	1.27:1	559.8
0.155	1.23:1	536.0
0.160	1.19:1	510.3
0.165	1.15:1	484.7
0.170	1.12:1	483.8
0.175	1.09:1	485.6
0.180	1.06:1	485.6
0.190	1:1.00	486.5
0.200	1:1.05	487.4
0.210	1:1.10	488.3
0.220	1:1.16	488.3
0.230	1:1.21	489.3
0.240	1:1.26	490.2
0.250	1:1.31	491.1

Solvent: CD_2Cl_2, 10.0 ml; Volume of NMI: 0.085 ml (1.1 mmoles)

Initial conductivity of solution: 0.0 $\mu S\ cm^{-1}$; Cell constant: 0.9162

Table 5.6 Conductivity titration: Dimethylsilyl triflate (DMSOTf) against N-Methylimidazole (NMI)

Volume NMI (ml)	Ratio DMSOTf:NMI	Conductivity ($\mu s\ cm^{-1}$)
0.000	0.00:1	2.2
0.005	21.79:1	14.3
0.010	10.90:1	17.4
0.015	7.26:1	30.1
0.020	5.45:1	62.7
0.025	4.36:1	91.1
0.030	3.63:1	115.2
0.035	3.11:1	146.4
0.040	2.72:1	180.8
0.045	2.42:1	212.7
0.050	2.18:1	247.5
0.055	1.98:1	280.5
0.060	1.82:1	320.9
0.065	1.68:1	356.6
0.070	1.56:1	398.8
0.075	1.45:1	438.2
0.080	1.36:1	476.7
0.085	1.28:1	518.0
0.090	1.21:1	556.5
0.095	1.15:1	600.5
0.100	1.09:1	641.8
0.105	1.04:1	684.8
0.110	1: 1.01	729.8
0.115	1: 1.06	792.1
0.120	1: 1.10	884.7
0.125	1: 1.15	995.6
0.130	1: 1.19	1081.8
0.135	1: 1.24	1163.4
0.140	1: 1.28	1252.3
0.145	1: 1.33	1345.9
0.150	1: 1.38	1435.7
0.155	1: 1.42	1520.1
0.160	1: 1.47	1621.8
0.165	1: 1.51	1695.2
0.170	1: 1.56	1771.3
0.175	1: 1.61	1842.8
0.180	1: 1.65	1916.1
0.185	1: 1.70	1989.5
0.190	1: 1.74	2053.6
0.195	1: 1.79	2117.8
0.200	1: 1.84	2163.6
0.205	1: 1.88	2227.8
0.210	1: 1.93	2273.7
0.215	1: 1.97	2328.7
0.220	1: 2.02	2374.5
0.225	1: 2.06	2411.2
0.230	1: 2.11	2447.9
0.235	1: 2.16	2475.4
0.240	1: 2.20	2512.0
0.245	1: 2.25	2539.5
0.250	1: 2.29	2567.0

Solvent: CD_2Cl_2, 10.0 ml; Volume of DMSOTf: 0.244 ml

Initial conductivity of solution: 0.0 $\mu S\ cm^{-1}$; Cell constant: 0.9168

Conductivity titrations between NMI and DMSX were performed for X=Cl (Table 5.4) and X=OTf (Table 5.5) (Figure 5.3). In the titration of DMSCl into NMI, a gradual increase in the conductivity readings up to a maximum of about 100 $\mu S\ cm^{-1}$ was recorded, whereas in the NMI/DMSOTf system the conductivity data increased up to a maximum of 750 $\mu S\ cm^{-1}$ at 2:1, and then decreased to 500 $\mu S\ cm^{-1}$ at 1:1 stoicheiometry. The behaviour in the NMI/DMSOTf case is consistent with the formation of 2:1 Nu-silane adduct, followed by the formation of an adduct with a 1:1 stoicheiometry. The lower conductivity reading for the 1:1 NMI/DMSOTf complex indicates that ion pairing is significantly greater in this species.

The behaviour of the NMI/DMSCl mixture is very similar to that observed in the TMSIm/TMSX (X=Cl) conductivity titrations (Table 2.29), where the low conductivity was attributed to a small equilibrium constant for salt formation. However in this case the large negative Si-29 chemical shift change is very good evidence for complexation; therefore it can be inferred that the system consists of very tightly bound ion pairs. This is in accord with the observation in the preceding section concerning the proton chemical shifts of the imidazolium C_2-H proton with different counterions, where it was shown that the degree of ion pairing could be arranged in the ascending series OTf < I < Br < Cl.

A second conductivity titration was performed for the NMI/DMSCl system, although in this experiment NMI was titrated on DMSCl in dichloromethane-d_2 (Table 5.6). Markedly different behaviour was observed in this case. The shape of the conductivity titration curve (Figure 5.4) provides a great deal of information on the nature of the adduct; extrapolation of the straight line sections of the curve shows that two

Figure 5.3 Conductivity titration between N-methylimidazole and (a) dimethylsilyl triflate and (b) chlorodimethylsilane.

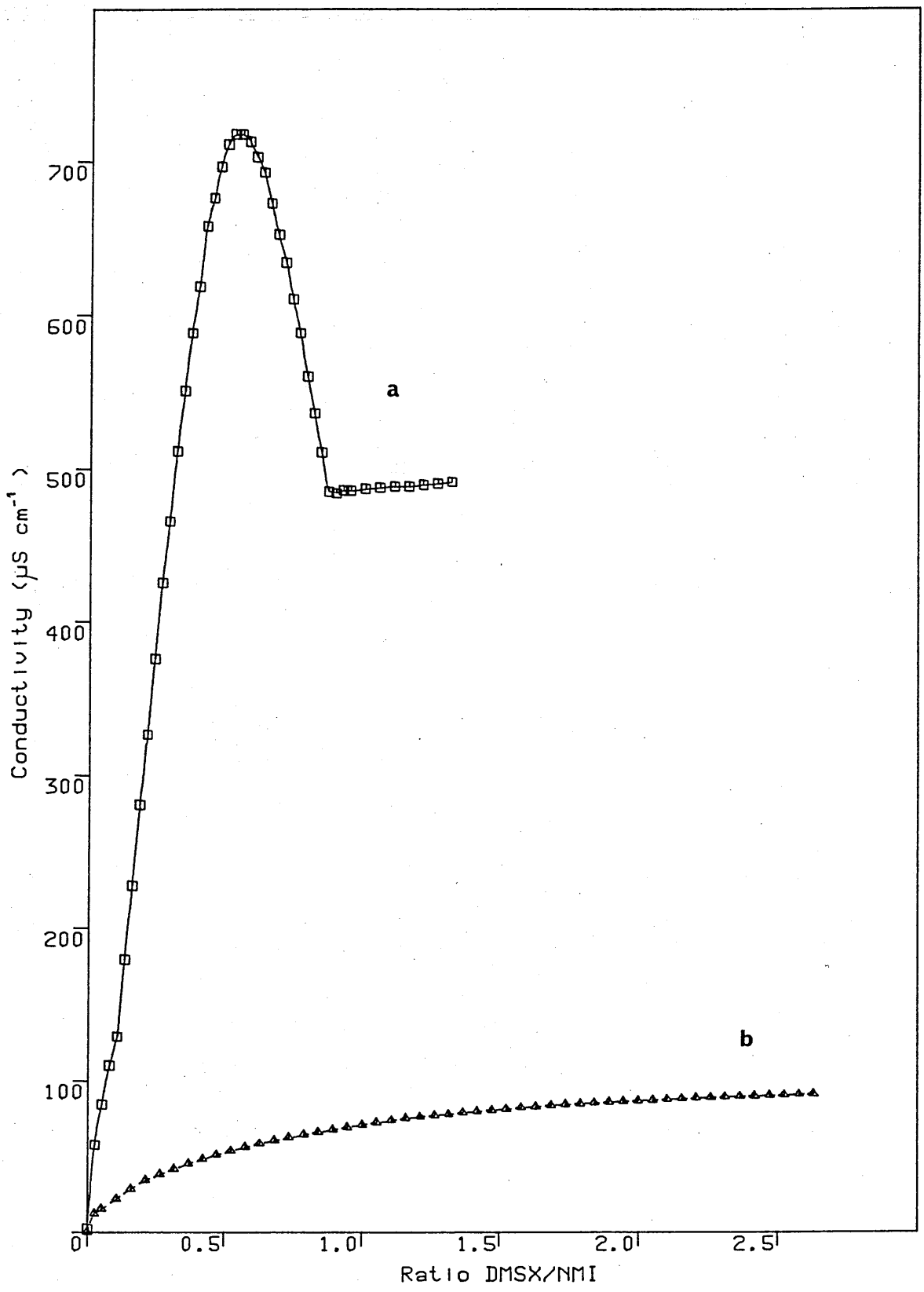

Solvent: dichloromethane-d2

Figure 5.4 Conductivity titration: NMI against DMSCl.

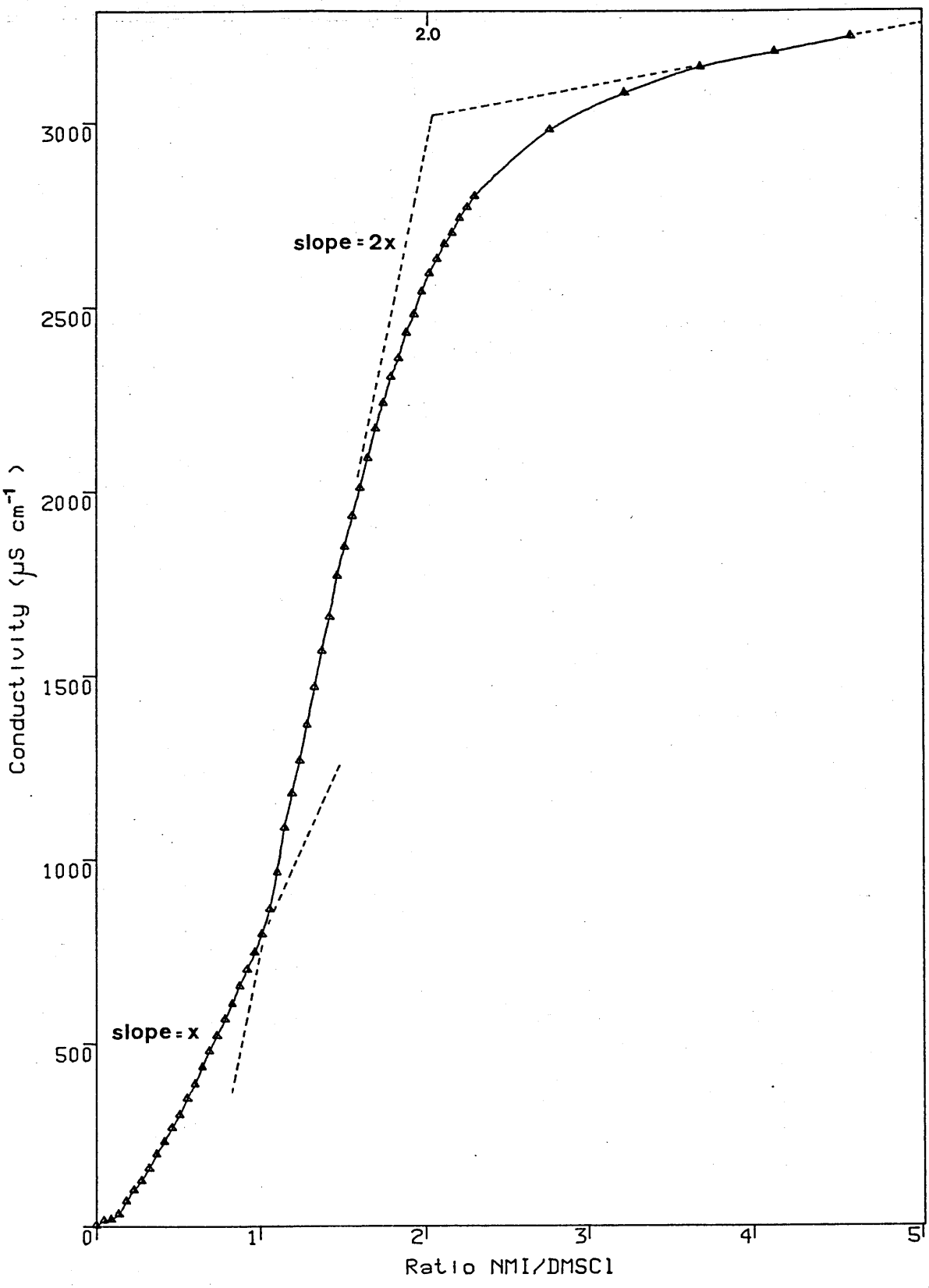

Solvent: dichloromethane-d2 (0.11 molar in the silane)

complexes are being formed. A point of inflexion is observed at 1:1 and the extrapolation indicates that a second complex is formed at 2:1. The precise nature of the 1:1 complex cannot be determined from the available results, but two likely structures can be proposed (Figure 5.5A,B).

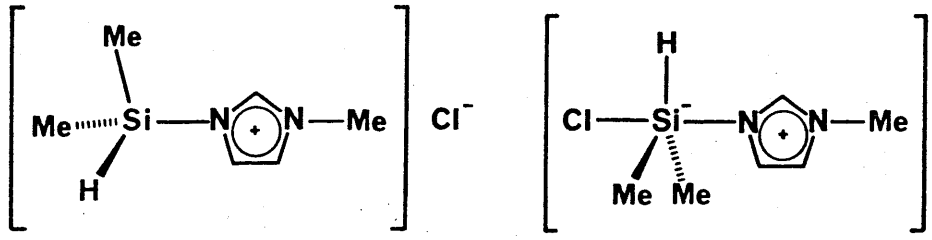

A B

Figure 5.5

Structure A is less likely on two accounts:-

i) The conductivity value observed in the first experiment is low enough to be attributable, in theory, to hydrolysis but the second experiment proves that some kind of ionic species is present in significant quantities. The different behaviour of these two experiments can be rationalised if the ionic species formed in the first experiment are ion paired in the relatively non-polar medium, whilst in the second experiment this ionic species can be solvated by the increasing amounts of the very polar NMI.

ii) The ^{29}Si chemical shift of the trialkyl substituted, five coordinate compound observed by Yoder[73] (see Scheme 2.3) is -30 ppm[74]. Therefore, given the generally lower chemical shifts of the dimethylsilyl derivatives, it is likely that A would have a chemical shift substantially lower than -30 ppm. The chemical shift of B should be very

similar to that of $[DMS\text{-}NMI]^+OTf^-$ i.e. at 9.5 ppm. Thus the small shoulder at low ratios of NMI/DMSCl ^{29}Si n.m.r. titration curve may indicate the presence of small amounts of B, although this is only circumstantial evidence.

Thus it can be concluded that for X=Cl the five coordinate complex is strongly favoured over the four coordinate complex. This was verified by the synthesis of the five coordinate $[DMS\text{-}NMI]^+Cl^-$ adduct which was prepared by adding a deficiency of NMI to neat DMSCl i.e. with DMSCl acting as the solvent. After removal of the solvent under vacuum, the resulting white solid gave an elemental microanalysis consistent with $[(NMI)_2\text{-}DMS]^+Cl^-$, hydridodimethyl-bis(3-methyl-1-imidazolio) silicon (IV) chloride.

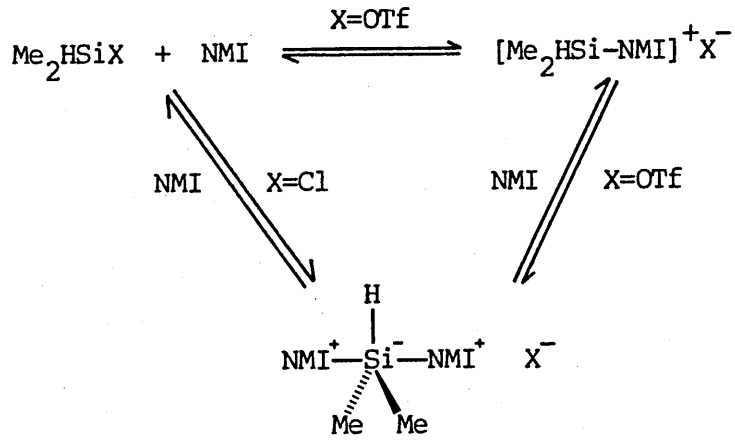

Scheme 5.5

The analogous triflate species, hydridodimethyl-bis(3-methyl-1-imidazolio) silicon (IV) triflate $[(NMI)_2\text{-}DMS]^+OTf^-$, was isolated as an analytically pure oil from a hexane/chloroform mixture; whereas the 1:1 ionic $[NMI\text{-}DMS]^+OTf^-$ adduct was an analytically pure solid. The relative

stability of the four coordinate DMSX/NMI adducts (X=Cl, OTf) is similar to that observed with the trimethylsilyl X/NMI adducts (X=Cl, OTf). In view of this, it is somewhat surprising that the 5-coordinate $[(NMI)_2$-DMS$]^+Cl^-$ adduct is so stable.

The ^{29}Si chemical shift of the 5-coordinate chloro- adduct was found to be highly concentration dependent. A single peak was observed at -59.5 ppm (0.83 M) for the dissolved adduct, which moved to high frequency (-23.0 ppm at 0.29 M) on dilution with chloroform-d_1 (Figure 5.6). This behaviour results from dissociation of the 5-coordinate complex at higher dilutions, as expected from the stoicheiometry. Line broadening is also observed at lower concentrations, indicating a slower rate of exchange, which is consistent with the rate limiting step being an intermolecular process (Scheme 5.6).

Rate limiting attack of uncomplexed NMI on the five coordinate $(NMI)_2$-DMSCl adduct:

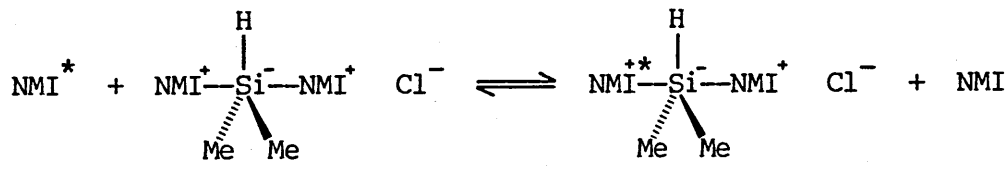

Scheme 5.6

It is conceivable that a hexacoordinate silicon intermediate could be involved in this process, although no evidence for such a species was noted. A scan from +60 to -250 ppm (silicon-29) for a solution of DMSCl

Figure 5.6 Concentration dependence of the silicon-29 chemical shift of [(NMI_2)-DMSCl].

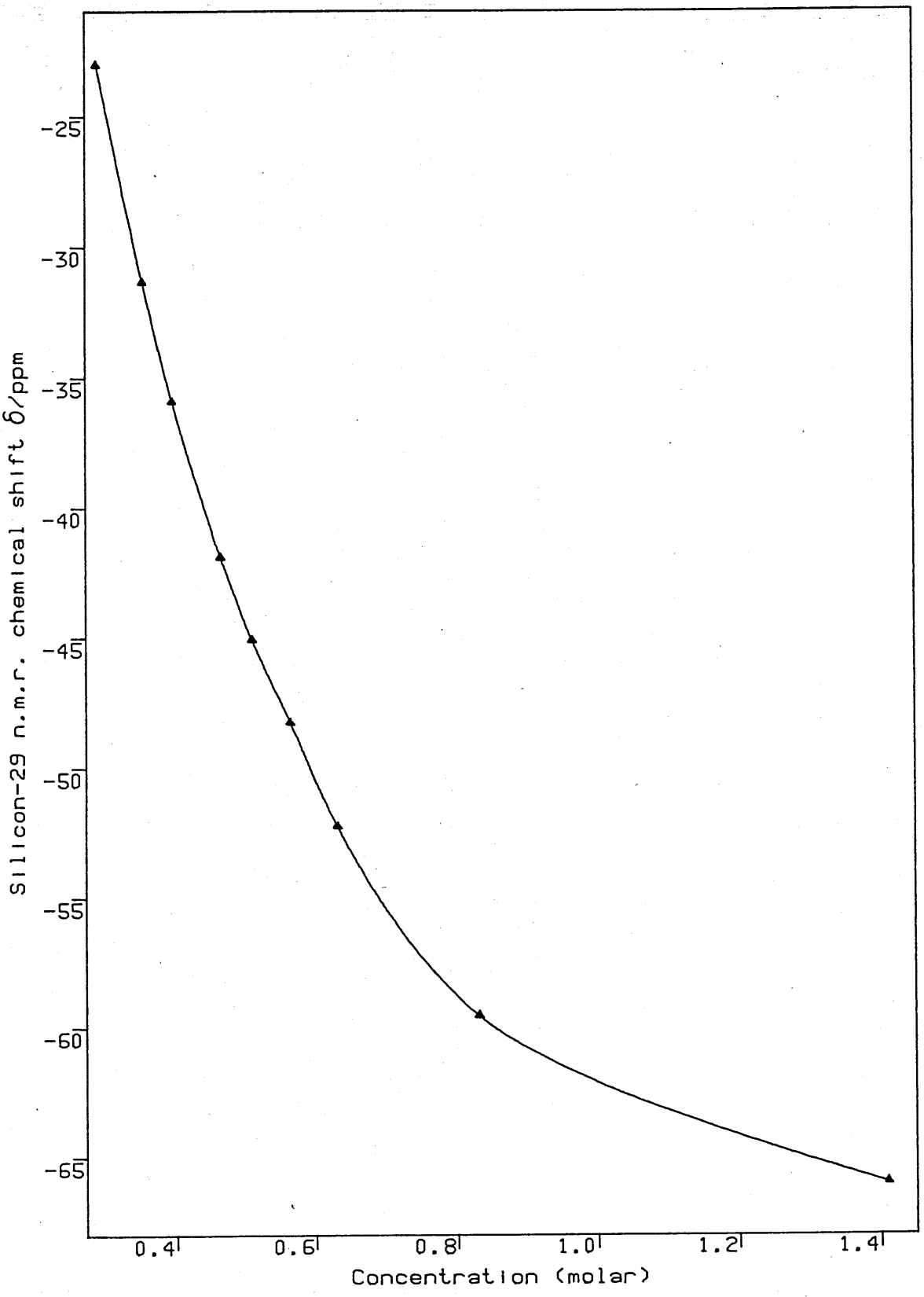

The concentration of [(NMI_2)-DMSCl] adduct was evaluated assuming no dissociation of the complex.

Solvent: chloroform-d1

in neat NMI (very large excess) revealed only one peak at -80 ppm, of approximately natural linewidth, showing that the concentration of any hexacoordinate silicon species is not significant under these conditions.

No chemical shift changes were noted in either donor or acceptor for DMSOBz/NMI mixtures (Table 5.7), indicating that under the conditions of the experiment, no significant quantities of any complex were formed.

Silicon-29 n.m.r. titrations were also performed for the following systems:- DMAP/DMSCl (Table 5.8), DMAP/DMSOTf (Table 5.9), py/DMSCl (Table 5.10) and py/DMSOTf (Table 5.11). A marked line broadening was observed in the DMAP/DMSOTf system at higher Nu:silane ratios. This effect eventually caused the signal to disappear into the spectral noise, which prevented observation of the limiting chemical shift of the 5-coordinate species, though the lower limit observed for the DMAP/DMSCl system at -52 ppm is consistent with the trend of the DMAP/DMSOTf titration curve (Figure 5.7). The behaviour at lower Nu:silane ratios was analogous to that observed for the NMI/DMSX systems (X=Cl, OTf), the chloride showed fast exchange at all ratios, whilst the triflate exhibited slow exchange between the 4-coordinate DMAP-DMSOTf salt (18 ppm) and the isolated DMSOTf (Scheme 5.7, X=OTf).

$$\text{DMAP} + \text{Me}_2\text{HSiX} \underset{\text{exchange}}{\overset{\text{slow}}{\rightleftharpoons}} [\text{DMAP-SiMe}_2\text{H}]^+\text{X}^- \underset{\text{exchange}}{\overset{\text{fast}}{\rightleftharpoons}} [\text{DMAP-SiMe}_2\text{H-DMAP}]^+\text{X}^-$$

Scheme 5.7

Table 5.7

Interaction between N-Methylimidazole (NMI) and Dimethylsilylbenzoate (DMSOBz) : N.M.R. Data

				Ratio of NMI : DMSOBz		
δ(ppm)		NMI	DMSOBz	1:5	1:1	5:1
^1H	$N-C_2(H)=N$	7.41	-	obsc	7.39	7.36
	$C_4(H)=C_5$	7.00t	-	7.05	7.03	6.98
	$^3J_{HH}$	0.9Hz	-	no	no	no
	$C_4=C_5(H)$	6.90	-	6.55	6.85	6.83
	$^3J_{HH}$	1.0Hz	-	no	no	no
	$N-CH_3$	3.68	-	3.63	3.62	3.55
	aromatic C-H	-	8.00-8.11m	8.00-8.1m	8.02-8.10m	7.97-8.08m
		-	7.30-7.56m	7.30-7.6m	7.39-7.48m	7.48-(obsc)
	Si-H	-	4.99qn	4.98qn	4.97qn	4.97qn
	$Si-(CH_3)_2$	-	0.465d	0.465	0.46	0.446
	$^3J_{HH}$	-	2.9Hz	2.8Hz	2.7Hz	2.9Hz
^{13}C	C_2	137.8	-	137.8	137.8	137.8
	C_4	129.3	-	129.6	129.4	129.2
	C_5	120.1	-	120.1	120.1	120.2
	$N-CH_3$	33.2	-	33.2	33.2	33.0
	C_{para}	-	133.1	133.2	133.2	133.2
	C_{ortho}	-	130.2	130.2	130.2	130.2
	C_{meta}	-	128.3	128.3	128.3	128.4
	C_{ipso}	-	obsc	167.1	167.0	166.8
	$Si-(CH_3)_2$	-	-1.95	-1.95	-1.95	-2.01
^{29}Si	$Si-(CH_3)_2$	-	7.65	7.625	7.625	7.49
quantities used:						
NMI (mmoles)		2.2	-	11.0	2.2	0.44
DMSOBz (mmoles)		-	2.2	2.2	2.2	2.2
solvent: $CDCl_3$, 2.0 ml						

Table 5.8

Silicon-29 N.M.R. chemical shift titration: Chlorodimethylsilane (DMSCl) against 4-Dimethylaminopyridine (DMAP)

Volume DMSCl (ml)	Ratio DMAP:DMSCl	^{29}Si $Si(CH_3)_2$
0.065	4.98:1	-52.3
0.100	3.28:1	-46.9
0.200	1.64:1	-23.3
0.300	1.09:1	-11.7
0.310	1.06:1	-11.1
0.320	1.03:1	-10.5
0.330	1:1.00	-9.9
0.340	1:1.03	-9.6
0.350	1:1.06	-9.0
0.360	1:1.10	-8.7
0.380	1:1.16	-7.9
0.400	1:1.22	-7.0
0.450	1:1.37	-5.1
0.550	1:1.67	-1.7
0.650	1:1.98	0.6
0.700	1:2.13	1.4
0.800	1:2.43	2.8
0.900	1:2.74	3.8
1.000	1:3.04	4.6
1.200	1:3.65	5.9
1.400	1:4.26	6.8
1.600	1:4.87	7.4
1.800	1:5.48	7.9
2.000	1:6.09	8.3
2.200	1:6.70	8.8

Solvent: chloroform-d_1

Table 5.9

Silicon-29 N.M.R. chemical shift titration: Dimethylsilyl triflate (DMSOTf) against 4-Dimethylaminopyridine (DMAP)

Volume DMSOTf (ml)	Ratio DMAP: DMSOTf	^{29}Si $Si(CH_3)_2$	^{29}Si $Si(CH_3)_2$*
0.07	3.10:1	-40.4	-
0.10	2.17:1	-24.9	-
0.15	1.45:1	0.0	-
0.20	1.09:1	18.9	-
0.25	1:1.15	19.0	24.5
0.50	1:2.30	19.0	24.5
0.75	1:3.45	19.1	24.5
1.00	1:4.60	19.1	24.5
1.25	1:5.75	19.2	24.5

Solvent: chloroform-d_1

Table 5.10

Silicon-29 N.M.R. chemical shift titration: Chlorodimethylsilane (DMSCl) against Pyridine (py)

Volume DMSCl (ml)	Ratio py:DMSCl	^{29}Si $Si(CH_3)_2$
0.10	3.41:1	12.2
0.30	1.14:1	12.0
0.32	1.07:1	12.0
0.34	1.00:1	12.0
0.40	1:1.17	12.0
0.60	1:1.76	12.0
0.80	1:2.34	11.9
1.00	1:2.93	11.8
1.20	1:3.51	11.8
1.40	1:4.10	11.7

Solvent: dichloromethane-d_2

Table 5.11

Silicon-29 N.M.R. chemical shift titration: Dimethylsilyl triflate (DMSOTf) against Pyridine (py)

Volume DMSOTf (ml)	Ratio py:DMSOTf	^{29}Si	
		$Si(CH_3)_2$	$Si(CH_3)_2$*
0.10	5.52:1	-43.4	-
0.20	2.76:1	-43.1	-
0.30	1.85:1	-31.5	-
0.40	1.38:1	-3.3	-
0.50	1.10:1	11.5	-
0.55	1.00:1	15.3	-
0.60	1:1.09	17.8	-
0.80	1:1.45	22.0	-
1.00	1:1.81	23.1	-
1.20	1:2.17	23.7	-
1.40	1:2.54	23.7	29.8
1.90	1:3.44	24.1	30.2

Solvent: dichloromethane-d_2

* New silicon-29 peak.

Figure 5.7 Silicon-29 chemical shift titration: 4-dimethylamino-pyridine against dimethylsilyl X (X=Cl, OTf)

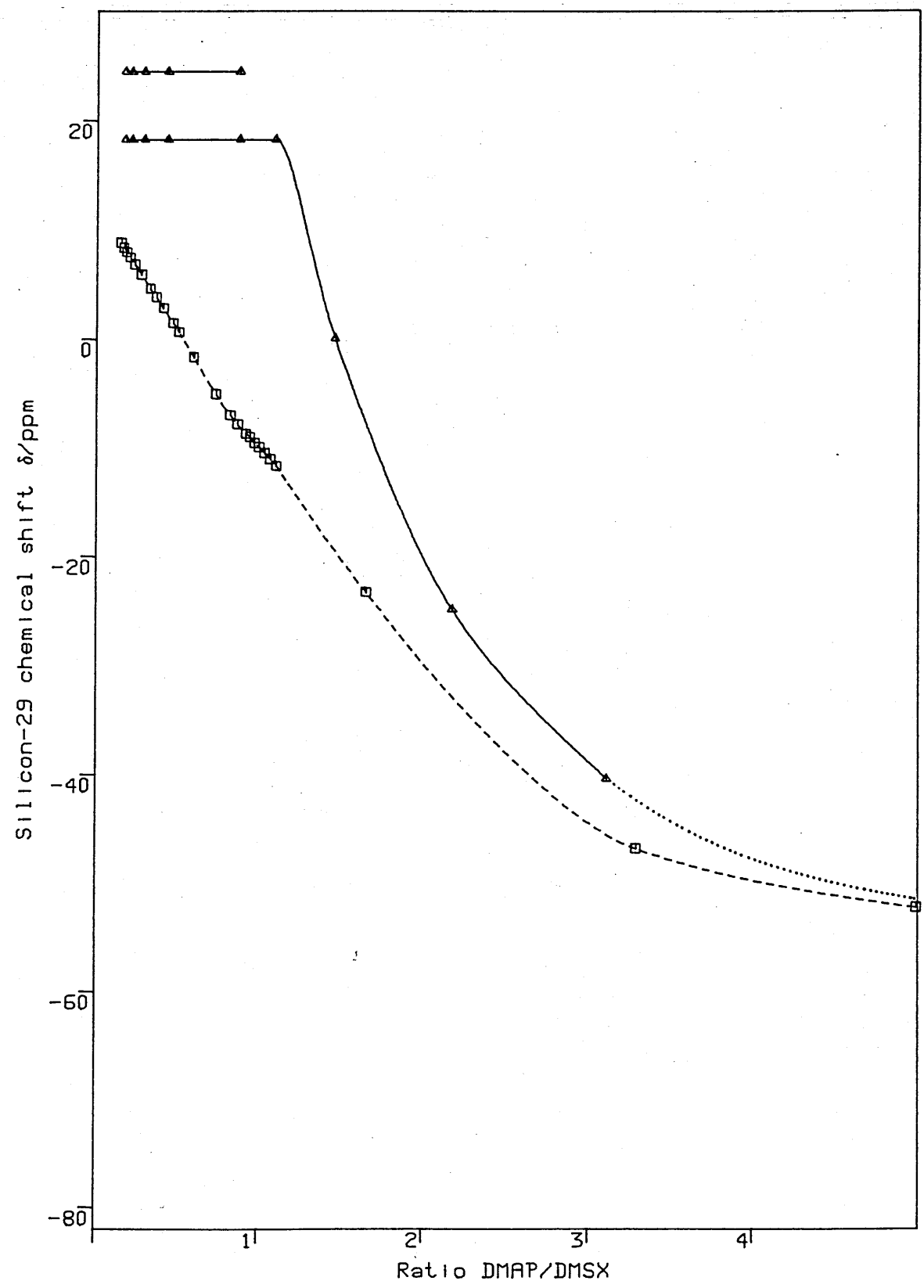

Solvent: chloroform-d1

---□---, X=Cl; ——△——, X=OTf

..... Extrapolated curve

Addition of a large excess of pyridine to DMSCl failed to induce any significant chemical shift changes in the silane, though the chemical shifts changes of the DMSOTf/py titration (Figure 5.8) are comparable to those observed for DMAP or NMI with dimethylsilyl triflate. A small equilibrium constant for the formation of the four coordinate 1:1 adduct can be deduced from the broad nature of the resonance at 30 ppm, observed at a py:DMSOTf ratio of 1:3. The py/DMSOTf titration also indicates that the py-DMSOTf complex is not fully formed even in the presence of a 5 fold excess of nucleophile. The smaller equilibrium constant of the $[py\text{-}DMS]^{+}OTf^{-}$ adduct in comparison to that of the $[py\text{-}TMS]^{+}OTf^{-}$ adduct may reflect the greater inductive stabilization of the highly deshielded nucleophile-silane complexes in the trimethylsilyl cases.

An equimolar mixture of HMPA and DMSOTf gave a silicon-29 resonance at 12.9 ppm which is split into a doublet by coupling to phosphorus. Addition of a second aliquot of HMPA to this system destroyed the silicon-phosphorus coupling but it caused only a 1.4 ppm low frequency shift. Increasing the HMPA:DMSOTf ratio to 5:1 caused the resonance to disappear completely, presumably due to a moderately fast chemical exchange with a 5-coordinate adduct at lower frequency. The behaviour of the 4-coordinate HMPA-DMSOTf adduct is consistent with that of the HMPA/TMSOTf system. However, despite the considerable nucleophilic strength of HMPA, it appears that the equilibrium constant for the formation of $[Me_2HSi\text{-}(HMPA)_2]^{+}OTf^{-}$ adduct (Scheme 5.8) is small.

$$HMPA + Me_2HSiOTf \underset{k_{-1}}{\overset{k_1}{\rightleftharpoons}} [HMPA\text{-}SiMe_2H]^{+}OTf^{-} \underset{k_{-2}}{\overset{k_2}{\rightleftharpoons}} [HMPA\text{-}SiMe_2H\text{-}HMPA]^{+}OTf^{-}$$

$$k_1 >> k_{-1} \qquad\qquad k_{-2} >> k_2$$

Scheme 5.8

Figure 5.8 Silicon-29 n.m.r. chemical shift titration: pyridine against dimethylsilyl X (X=Cl, OTf)

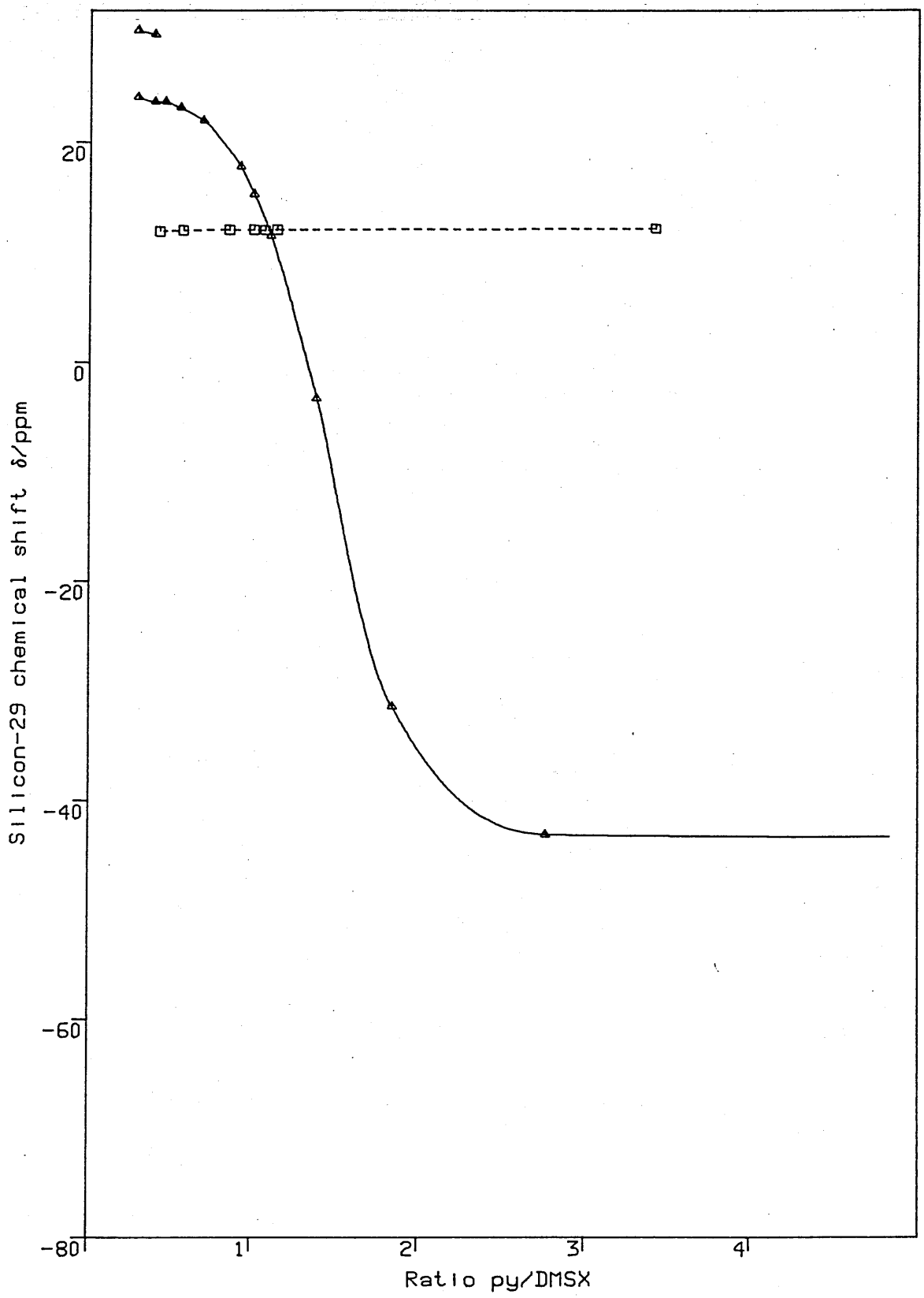

Solvent: chloroform-d1

---□---, X=Cl, ——△——, X=OTf

The interactions of DMSOTf with nucleophiles to give 1:1 complexes are comparable to those observed in the analogous TMSOTf/Nu systems. This implies that the stability of 4-coordinate nucleophile-dimethylsilyl triflate adducts is related to the donor properties, in a similar manner to that found for trimethylsilyl derivatives.

The very good correlation between the silicon-29 chemical shifts of HMPA, DMAP and NMI with DMSOTf and with TMSOTf (Figure 5.9) indicates that nuclear shielding of silicon is affected by the donor strength in each case. The interpretation of the slope indicates a greater susceptibility of the silicon-29 chemical shift of the dimethylsilyl species to donicity changes in the nucleophile.

The point for py deviates from the line because the equilibrium constant for py/DMSOTf system is low, in contrast to the py/TMSOTf case. This difference may be caused by the electron releasing (+I) effect of the methyl ligands if the silicon bears a positive charge in the py-TMSOTf adduct. The chemical shift of the py-TMSOTf or py-DMSOTf adduct is indicative of a highly deshielded silicon, thus the presence of electron donating substituents, such as methyl, may contribute to the stability of $[Nu\text{-}SiR_3]^+X^-$.

c) Methylphenylsilyl triflate ($MePhHSiOSO_2CF_3$)

The behaviour of this silane with NMI is in accord with that observed in the dimethylsilyl system. In the presence of an excess of silane, two silicon-29 n.m.r. resonances were observed, one at 12 ppm corresponding to the isolated silane; and a second peak at 1.4 ppm, probably a $[NMI\text{-}SiMePhH]^+OTf^-$ salt (Table 5.12). The lower frequency peak shifted

Figure 5.9 Correlation between the silicon-29 chemical shifts of dimethylsilyl- and trimethylsilyl triflate-Nu complexes.

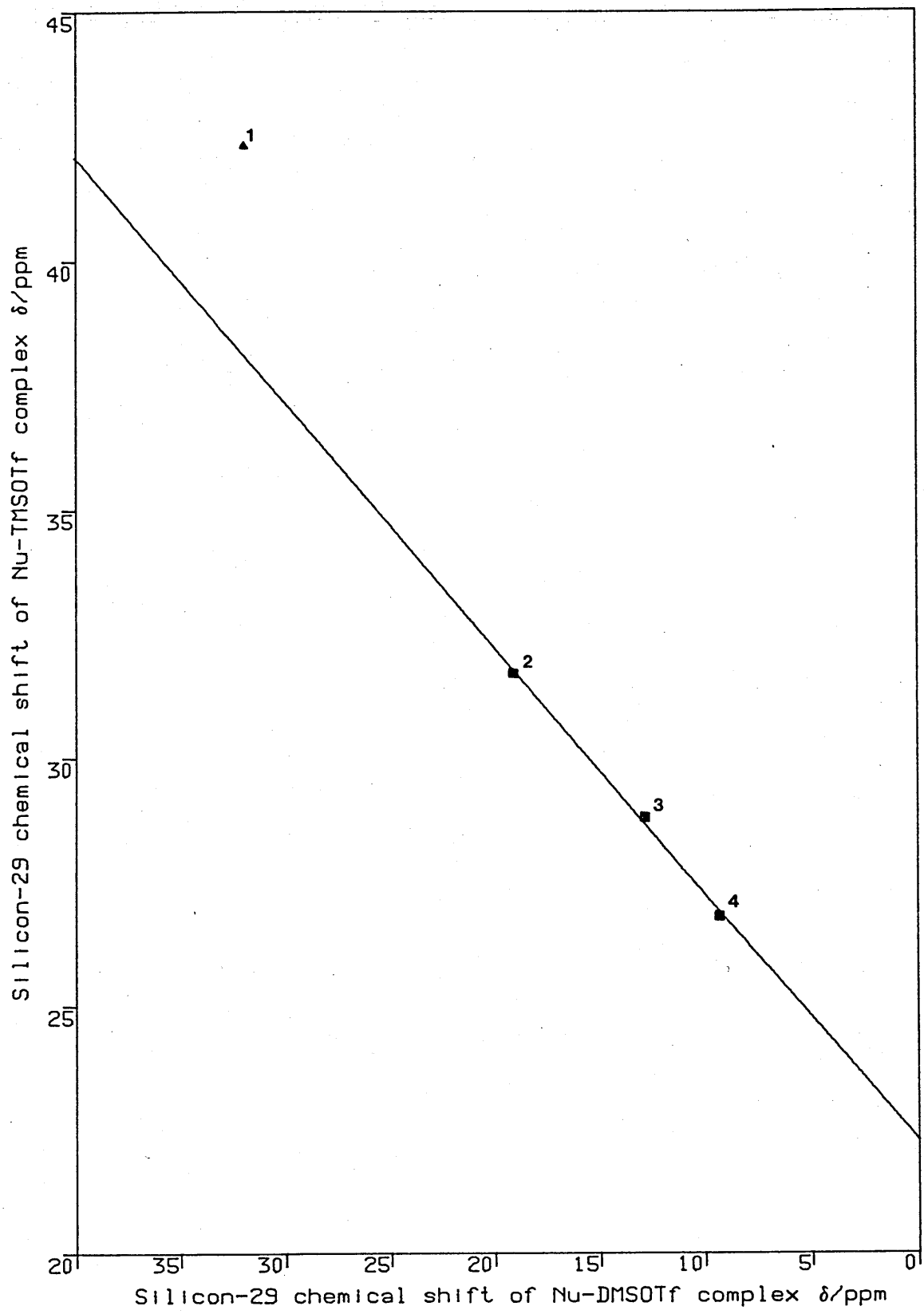

1, py; 2, DMAP; 3, HMPA; 4, NMI.

Slope = 0.49 (s.d. = 0.018), intercept = 22.28 (s.d. = 0.26)

Variance = 0.016 (excluding the point for py)

Table 5.12

Interaction between Methylphenylsilyl triflate (MePhHSiOTf) and N-Methylimidazole (NMI) : N.M.R. Data

		Ratio of NMI : MePhHSiOTf			
δ(ppm)		5:0[a]	5:1	1:1	1:5
^{1}H	$N-C_2(H)=N$	7.40	7.66(sbr)	8.89	8.99
	$C_4(H)=C_5$	7.03	7.96	7.50	obscured
	$C_4=C_5(H)$	6.86	6.91	7.25	7.33
	$N-CH_3$	3.66	3.64	3.94	3.94
	aromatic C-H	-	7.00-7.65m	7.25-7.73m	7.35-7.73m
	Si-H	-	5.50q	5.49q	5.39q
	$Si-CH_3$	-	0.77d	1.00d	0.96(vbr)
	$^{3}J_{HH}$	-	1.8Hz	3.3Hz	no
^{13}C	C_{phenyl}	-	134.4	134.9	130.3
	C_{phenyl}	-	132.5	132.6	126.5
	C_{phenyl}	-	128.7	129.0	125.3[a]
	C_2	137.8	140.8	140.2	135.8
	C_4	129.5	125.2	127.9	119.5
	C_5	120.1	124.4	127.6	119.5
	$N-CH_3$	33.3	36.2	36.0	31.9
	$Si-CH_3$	-	-3.2	-5.0	-1.8
^{29}Si	$Si-CH_3$	-	no	no	12.0
	$Si-CH_3$*	-	-84.5	0.33	1.4small
quantities used:					
NMI (mmoles)		2.2	11.0	2.2	0.44
MePhHSiOTf (mmoles)		-	2.2	2.2	2.2
solvent: $CDCl_3$, 2.0 ml					

[a] N.m.r. data for MePhHSiOTf are shown in the experimental section.

slightly to lower frequency upon addition of more NMI, whilst the MePhHSiOTf peak disappeared. A large upfield shift to -52 ppm, consistent with formation of a five coordinate adduct, hydridomethylphenyl-bis-(3-methyl-1-imidazolium) silicon (IV) trifluoromethanesulphonate (Scheme 5.9), was produced by adding a five fold excess of NMI.

$$\text{NMI} + \text{MePhHSiOTf} \underset{k_{-1}}{\overset{k_1}{\rightleftharpoons}} [\text{NMI-SiMePhH}]^+\text{OTf}^- \underset{k_{-2}}{\overset{k_2}{\rightleftharpoons}} [\text{NMI-MePhHSi-NMI}]^+\text{OTf}^-$$

$$k_1 >> k_{-1} \qquad\qquad k_{-2} >> k_2$$

Scheme 5.9

d) Triphenylsilyl derivatives (Ph_3SiX, X=I, Br)

Mixtures of Ph_3SiI or Ph_3SiBr with BIPY did not show any chemical shift differences from the isolated species. This result is consistent with the behaviour of the TMSX/BIPY systems (X=I, OTf) at ambient temperature, indicating that the triphenylsilyl species are not significantly better at stabilizing adducts than the trimethylsilyl species. This finding is inconsistent with that of Corey and West[91] who proposed a five coordinate ionic structure (Scheme 5.10) for the adduct between Ph_3SiI and BIPY.

$$Ph_3SiI + \text{BIPY} \rightleftharpoons$$

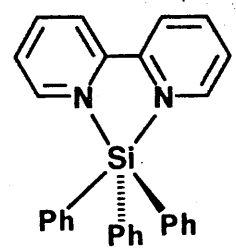

Scheme 5.10

Considering the much quoted importance of this work, the species was not exceptionally well characterised as regards the structure around silicon. The existence of a BIPY adduct is not disputed, from the analytical data, and the presence of an ionic species is demonstrated by the conductivity measurements. However the remaining evidence is not so conclusive; the indication of a cis-bipyridyl species in the U.V. spectra does not mean, a priori, that a five coordinate species has been formed. Moreover, the authors made no attempt to distinguish a fully formed 5-coordinate species from a 4-coordinate one, in which the silicon was rapidly interchanging between the two bipyridyl nitrogen atoms (see above). The colour change from pink to yellow attributed to complex formation is irrelevant, since a similar result can be produced simply by adding pure bipyridyl to a pink solution of iodine in dichloromethane; complexes between iodine and a variety of nucleophiles, including the pyridines, are well known[115].

It is conceivable that a BIPY-Ph_3SiI adduct might be stable in the solid state, but in the solution phase, if the complex exists, it may be regarded as a four coordinate species, in which the silicon centre is rapidly exchanging between the two bipyridyl nitrogen atoms.

A five fold excess of NMI caused the Ph_3SiI resonance to move downfrequency from -8 to -18 ppm (broad), suggesting the formation of a complex which is undergoing exchange with another species. The relatively small chemical shift change implies that the resulting adduct between NMI and Ph_3SiI is four coordinate. However it is not possible to be unequivocal about this, since the broad nature of the peak may also indicate that it is the result of an exchange with a five coordinate species at very low frequency (Scheme 5.11).

$$Ph_3SiI + NMI \rightleftharpoons [Ph_3Si\text{-}NMI]^+I^- \overset{NMI}{\rightleftharpoons} [NMI\text{-}Ph_3Si\text{-}NMI]^+I^-$$

Scheme 5.11

e) Bromomethyldiphenylsilane ($MePh_2SiBr$)

Successive additions of aliquots of NMI to $MePh_2SiBr$ induced a gradual downfrequency shift of the silicon-29 resonance of this silane from 8 to -10 ppm, in the presence of a ten fold excess of NMI (Table 5.13). The chemical shift changes in the proton and carbon nuclei are consistent with adduct formation at 1:1 stoicheiometry but they are uninformative about the coordination number of silicon. Bromotrimethylsilane was found to have a low equilibrium constant for 1:1 ionic salt formation; a high concentration of nucleophile being required in order to observe the fully formed complex in some cases (e.g. the DMF/TMSBr system, Chapter 2.2). The behaviour of the silicon-29 resonance is similar in the $MePh_2SiBr$/NMI system, although it is not feasible to rule out the presence of exchange with a second low frequency resonance, as was proposed for the Ph_3SiI/NMI mixture.

f) Trialkylsilyl triflates ($R^1R^2R^3SiOSO_2CF_3$)

The silicon-29 chemical shifts of triethyl-, tri-isopropyl- or tert-butyldimethylsilyl triflates in the presence of a five molar excess of NMI are 28.3, 23.9 and 28.8 ppm respectively. These shifts are comparable with that at 26.6 ppm observed for the NMI/TMSOTf system, which shows that the electronic differences between the various trialkylsilyl species are relatively small.

Table 5.13

Interaction between 1-Methylimidazole (NMI) and Bromodiphenylmethylsilane ($Ph_2MeSiBr$)

δ (ppm)		NMI	$Ph_2MeSiBr$	Ratio NMI : $Ph_2MeSiBr$ 10:1	5:1	1:1
^1H	$N-C_2(H)=N$	7.41	-	7.63	7.87	9.53
	$C_4(H)=C_5$	7.00t	-	7.00	7.12	7.88
	$^3J_{HH}$	0.9Hz	-	no	no	no
	$C_4=C_5(H)$	6.90	-	6.94	6.95	7.02
	$^3J_{HH}$	1.0Hz	-	no	no	no
	$N-CH_3$	3.68	-	3.60	3.70	4.1
	aromatic C-H	-	7.34-7.7m	7.46m	7.48-7.57m	7.55-7.77m
	$Si-CH_3$	-	1.06	1.23	1.26	1.3
^{13}C	C_2	137.8	-	138.0	138.2	140.5
	C_4	129.3	-	128.7[a]	128.7[a]	128.9
	C_5	120.1	-	120.8	121.3	124.9
	$N-CH_3$	33.2	-	33.4	33.9	35.96
	C_{ortho}[b]	-	134.3	134.6	134.7	134.8
	C_{para}	-	130.6	131.4	131.7	132.0
	C_{meta}	-	128.1	128.3[a]	128.7[a]	128.5
	$Si-CH_3$	-	1.78	-2.24	-2.53	-2.87
^{29}Si	$Si-CH_3$	-	8.01	-10.07	-4.09	4.31
quantities used:						
NMI (mmoles)		2.2	-	23.2	11.6	2.32
$Ph_2MeSiBr$ (mmoles)		-	2.32	2.32	2.32	2.32
solvent: $CDCl_3$, 2.0 ml						

[a] Assignment uncertain.

[b] ipso carbon resonance obscured.

PART II EXPERIMENTAL

Purification of starting reagents

See Part I experimental for the purification of chemicals.

General method for the preparation of Trialkylphenylsilanes ($R^1R^2R^3PhSi$)

Phenyl-lithium (PhLi) in diethyl ether/benzene was added slowly to a stirred solution of the chlorosilane ($R^1R^2R^3SiCl$, equimolar with PhLi) in diethyl ether under dry nitrogen. Reaction mixtures were left to stir overnight, extracted with ether, washed with saturated ammonium chloride solution and finally dried over anhydrous magnesium sulphate. Subsequent removal of ether gave crude products which were purified either by distillation or by recrystallisation from methanol/ether mixture.

Tert-butyltriphenylsilane ($^tBuPh_3Si$)[116]

Phenyl-lithium	13.1 mmoles
^{t}Butylchlorodiphenylsilane	3.61 g, 13.1 mmoles

Yield 2.85 g, 68.6%

N.M.R. δ/ppm ($CDCl_3$, Me_4Si)

^1H 1.12 (9H, s, ^tBu)

^{13}C 19.2, 29.3, 128.2, 129.6, 135.3, 137.0

^{29}Si -6.00

Tert-butyldimethylphenylsilane ($^tBuMe_2PhSi$)[117]

Phenyl-lithium	35.5 mmoles
^{t}Butylchlorodimethylsilane	5.35 g, 35.5 mmoles

b.p. 68 °C/4.8 mm Hg

N.M.R. δ/ppm (CD_3CN, external Me_4Si)

^{13}C -4.7, 18.2, 27.25, 135.8 (C_{ortho}), 130.2 (C_{para}), 129.0 (C_{meta})

^{29}Si 3.13

Triethylphenylsilane (Et_3PhSi)

Phenyl-lithium	15 mmoles
Triethylchlorosilane	15 mmoles

b.p. 82-84 °C/35 mm Hg

N.M.R. δ/ppm ($CDCl_3$, Me_4Si)

^{1}H 7.74-7.13 (5H, m, Ph)

^{13}C 141.7 (C_1, Lit.[118], 141.7);
129.2 (C_2, Lit.[118], 129.2);
127.6 ($C_{2,4}$, Lit.[118], 127.7)

Synthesis of Dimethylsilylbenzoate (DMSOBz)

The preparation was the same as for the synthesis of trimethylsilyl-acetate in Part I Experimental. Acetic acid and chlorotrimethylsilane were replaced by benzoic acid and chlorodimethylsilane respectively.

Yield 65%

b.p. 55 °C/0.5 mm Hg (Lit.[119], 146-147 °C/35 mm Hg)

N.M.R. δ/ppm ($CDCl_3$, Me_4Si)

^{1}H 0.47 (d, J_{HH} 2.9Hz, $SiMe_2$);

4.99 (q, J_{HH} 2.9Hz, Si-H);

7.30-7.60, 7.98-8.13 (m, Ph)

^{13}C -1.95 ($SiMe_2$)

128.3, 130.2 and 133.1 (Ph)

167.0 (C=O)

^{29}Si 7.65 (tetramethyldisiloxane, -4.7)

General method for the preparation of Silyltriflates ($R^1R^2XSiOSO_2CF_3$)

Stoicheiometric quantities of trifluoromethanesulphonic acid (triflic acid, CF_3SO_3H) were added dropwise to the respective silanes, with stirring, under an atmosphere of dry nitrogen. Distillation of the resulting solution yielded moisture sensitive, colourless liquids. ^1H n.m.r. of the reaction mixtures, prior to distillation, indicated essentially quantitative formation of the products.

Silyltriflate ($H_3SiOSO_2CF_3$)

Phenylsilane	0.70 ml, 5.65 mmoles
Trifluoromethanesulphonic acid	0.5 ml, 0.848 g, 5.65 mmoles

Exothermic reaction, distillation resulted in a clear mobile liquid that was violently explosive on contact with air.

b.p. 79-81 °C

N.M.R. (crude product) δ/ppm ($CDCl_3$, external Me_4Si)

^1H 4.2 (3H, s, SiH); 7.18 (6H, benzene)

^{13}C 118.2 (benzene); 122.0 (q, J 25Hz, CF_3)

^{29}Si -23.2 (q, J 254Hz, SiH)

Trichlorosilyl trifluoromethanesulphonate ($Cl_3SiOSO_2CF_3$)

Trifluoromethanesulphonic acid	3.12 ml, 35.3 mmoles
Trichlorophenylsilane	5.65 ml, 35.3 mmoles

The reaction mixture was refluxed at 60 °C for 3 hours prior to distillation.

Yield	5.1 g, 84%
b.p.	35 °C/25 mm Hg
N.M.R.	δ/ppm (CD_3CN, Me_4Si)
	^1H no phenyl resonances
	^{13}C 119 (q, J 315Hz, CF_3)
	^{29}Si -18.3
	^{17}O one peak (no reference)
Analysis	Found: C, 4.00%. $CF_3O_3Cl_3SSi$ requires C, 4.25%.

Dimethylsilyl trifluoromethanesulphonate ($HMe_2SiOSO_2CF_3$)

Trifluoromethanesulphonic acid	10 ml, 16.96 g, 0.113 M
Chlorodimethylsilane	15 ml, 12.78 g, 0.135 M

An endothermic reaction occurred, with the evolution of HCl gas (as indicated by moist pH paper and the formation of a white precipitate with aqueous silver nitrate solution).

Yield	86%
b.p.	123-124 °C/760 mm Hg

N.M.R. δ/ppm (CD_2Cl_2, Me_4Si)

^1H 0.57 (6H, d, $^3J_{HH}$ 2.9Hz, Me_2)

4.98 (1H, qn, $^3J_{HH}$ 2.9Hz, SiH)

^{13}C 1.4 (Me_2); 119.2 (q, $^1J_{CF}$ 317Hz, CF_3)

^{29}Si 24.8 (d, septet, $^1J_{SiH}$ 232.9Hz, $^2J_{SiCH}$ 7.3Hz)

^{17}O one peak (not referenced)

Analysis Found: C, 17.25; H, 3.3%. $C_3H_7F_3O_3SSi$ requires C, 17.3; H, 3.4%.

Tert-butylchlorophenylsilyl trifluoromethanesulphonate ($^tBuClPhSiOSO_2CF_3$)

Trifluoromethanesulphonic acid	3.64 g, 24.2 mmoles
Tert-butylchlorodiphenylsilane	7.34 g, 26.7 mmoles

The reaction was exothermic. After stirring for 30 minutes, benzene was isolated from the product by collecting in a carbon dioxide/acetone cold trap during distllation.

Yield 8.3 g, 92%

b.p. 70 °C/0.01 mm Hg

N.M.R. δ/ppm (CD_3CN, Me_4Si)

^1H 1.14 (9H, s, ^tBu); 7.54-7.77 (5H, m, Ph)

^{13}C 22.0 (C-Me); 24.3; 24.7 (C-CH_3);

127.3; 129.7; 133.9; 135.3 (Ph)

^{29}Si 10.2

I.R. ν_{max} (liquid film) 2965, 2950, 2905, 2870 (CMe_3), 1595 (Ph), 1475, 1465, 1430, 1410 (intense), 1370, 1320, 1250, 1200 (very intense, Si-O), 1150, 1120, 1090, 940 (broad), 845, 820, 770, 748, 712, 689, 645, 615 cm^{-1}

Analysis Found: C, 38.0; H, 4.12%. $C_{10}H_{10}ClF_3SO_3Si$ requires C, 38.07; H, 4.07%.

Tert-butyldimethylsilyl trifluoromethanesulphonate ($^tBuMe_2SiOSO_2CF_3$)

Trifluoromethanesulphonic acid	2.48 g, 16.5 mmoles
Tert-butyldimethylphenylsilane	3.18 g, 16.5 mmoles

A transitory red colour was observed upon addition of triflic acid to the silane. The solution remained a pale orange colour after addition was complete. Benzene was isolated from the product by distillation (b.p. 80 ^oC at 760 mm Hg). Biphenyl was separated from the distillation residue and recrystallised from ethanol/chloroform mixture to give colourless leaf shaped crystals (approximate yield 20%; m.p. 69-70 ^oC, Lit.[120], 71 ^oC).

Yield 4.0 g, 91%

b.p. 40 ^oC/2 mm Hg (Lit.[121], 65-67 ^oC/12 mm Hg)

N.M.R. δ/ppm (CD_3CN, external Me_4Si)

^1H 0.48 (6H, s, Me); 1.00 (9H, s, ^tBu)

^{13}C -4.22 (Me_2); 18.7; 25.0;
119.4 (q, $^1J_{CF}$ 316Hz, CF_3)

^{29}Si 45.6

^1H, ^{13}C n.m.r. data identical to literature values.

N.M.R. data for the interactions between Dimethylsilyl triflate (DMSOTf) and nucleophiles

δ/ppm ($CDCl_3$, 2.0 ml; Me_4Si)

a) DMSOTf (2.2 mmoles) and HMPA (2.2 mmoles)

^1H 0.53 (d, J_{HH} 2.9Hz, $SiMe_2$); 2.79 (d, J_{PH} 10.5Hz, HMPA); 5.00 (m, Si-H)

^{13}C -0.92 (CH_3); 38.4 (d, J_{PC} 5.2Hz, HMPA); 121.7 (q, J_{CF} 321Hz, CF_3)

^{29}Si 12.9 (d, J_{SiP} 8.3Hz)

b) DMSOTf (2.2 mmoles) and HMPA (4.4 mmoles)

^1H 0.53 (d, J_{HH} 2.7Hz, $SiMe_2$); 2.72 (d, J_{PH} 10.0Hz, HMPA); 4.95 (q, J_{HH} 2.7Hz, Si-H)

^{13}C -0.69 ($SiMe_2$); 36.6 (d, J_{PC} 5.2Hz, HMPA); 121.8 (q, J_{CF} 320Hz, CF_3)

^{29}Si 11.5

c) DMSOTf (2.2 mmoles) and HMPA (11.0 mmoles)

^{29}Si no resonances observed between +60 and -120

d) DMSOTf (0.4 ml) and NMI (2 ml)

^{29}Si -79.3 (scanned from +65 to -272)

N.M.R. data for interaction between Tri-isopropylsilyl triflate[109] ($^{i}Pr_3SiOTf$, 2.2 mmoles) and 1-Methylimidazole (NMI, 10.1 mmoles)

δ/ppm ($CDCl_3$, 2.0 ml; Me_4Si)

^{1}H 1.08 (d, J 6.2Hz, Me_2CSi); 1.51 (septet, J 6.2Hz, HCSi); 3.59 (MeN, NMI); 6.88 (C_5-H, NMI); 6.97 (C_4-H, NMI); 7.39 (C_2-H, NMI)

^{13}C 10.5 (CH_3, ^{i}Pr); 16.3 (C, ^{i}Pr); 31.7 (Me, NMI); 115.0 (C_5, NMI); 123.2 (C_4, NMI); 131.7 (C_2, NMI)

^{29}Si 23.9

N.M.R. data for interaction between ^{t}Butyldimethylsilyl triflate ($^{t}BuMe_2SiOTf$, 2.2 mmoles) and 1-Methylimidazole (NMI, 11.0 mmoles)

^{29}Si δ/ppm ($CDCl_3$, 2.0 ml; Me_4Si) 28.8

N.M.R. data for the interaction between Triethylsilyl triflate (Et_3SiOTf, 2.2 mmoles) and 1-Methylimidazole (NMI, 11.0 mmoles)

^{29}Si δ/ppm ($CDCl_3$, 2.0 ml; Me_4Si) 28.3

(+)-Methyl-1-naphthylphenylsilane [(+)-MeNpPhSiH] and Trifluoromethanesulphonic acid (CF_3SO_3H) : Optical Rotation Study

(+)-MeNpPhSiH 1.2848 g, 4.13 mmoles

CF_3SO_3H 0.366 ml, 4.13 mmoles

(+)-Methyl-1-naphthylphenylsilane[123] was dissolved in chloroform (10.0 cm^3). 8.0 cm^3 of this solution was introduced into a 5 cm cell under nitrogen, and the optical rotation measured. Triflic acid was added dropwise to this solution, which produced a transitory blue-green colour. A further measurement of the optical rotation was taken, after mixing the solution.

Optical Rotation (Na lamp)

(i)	chloroform only	0.0 °
(ii)	(+)-MeNpPhSiH in chloroform	3.85 °
(iii)	after addition of triflic acid to (ii)	0.0 °
(iv)	0.366 ml triflic acid in 8.0 ml chloroform	0.0 °

^1H, ^{13}C and ^{29}Si n.m.r. data for the product from (iii) were consistent with the formation of methylphenylsilyl triflate and naphthalene.

Reaction between Silyltriflate ($H_3SiOSO_2CF_3$) and Triethylamine (Et_3N)

Triethylamine (0.99 g, 9.78 mmoles) was added slowly to a solution of silyltriflate (9.32 mmoles) in benzene (9.32 mmoles), resulting in the production of heat and a pale yellow viscous liquid. The product was pumped under high vacuum (0.005 mm Hg) overnight to give a pale yellow oil.

N.M.R. δ/ppm ($CDCl_3$, Me_4Si)

^1H 0.97 (t, br, J 2.6Hz); 1.19 (t, J 7.3Hz, CH_3); 2.51 (q, br, J 6.97Hz); 2.82 (q, J 7.3Hz, CH_2); 3.70 (vbr); 4.03 (br, Si-H); 4.08 (vbr); 7.28 (benzene)

^{13}C 8.3 (CH_3); 47.6 (CH_2); 120.1 (q, J_{CF} 320Hz)

^{29}Si -74.1 (sbr, q, J 267Hz, SiH_3); -82.1 (sbr, q, J 286Hz, SiH_3); -96.1 (low intensity, t, J 364Hz, SiH_2)

Analysis Found: C, 35.87; H, 7.33; N, 5.27%. $SiH_3O_3SCF_3(C_6H_5N)_{1.4}$ requires C, 35.08; H, 7.52; N, 6.09%.

Synthesis of Bromotriphenylsilane (Ph_3SiBr)

N-Bromosuccinimide (3.7 g, 0.02 mole) was refluxed for an hour with triphenylsilane (5.4 g, 0.02 mole) in carbon tetrachloride (30 ml). After cooling, succinimide was filtered off from the pale orange reaction mixture under dry nitrogen. The solvent was removed by distillation under reduced pressure and the off-white solid residue recrystallised from acetonitrile to yield a colourless crystalline product.

m.p. 119-120 °C (Lit.[124], 120 °C; Lit.[125], 120-121 °C)

N.M.R. δ/ppm (CD_2Cl_2, Me_4Si)

^1H 7.7-7.6 (m, Ph) (Ph_3SiH, 7.98-7.87); 7.5-7.4 (m, Ph) (Ph_3SiH, 7.71-7.60)

^{13}C 128.5 (Ph_3SiH, 128.61); 131.2 (Ph_3SiH, 130.34); 135.8 (Ph_3SiH, 136.30)

^{29}Si 0.77 (Ph_3SiH, -17.7)

N.M.R. data for interaction between Bromotriphenylsilane (Ph_3SiBr) and nucleophiles in chloroform-d_1 (2 ml)

δ/ppm ($CDCl_3$, 2.0 ml; Me_4Si)

a) Ph_3SiBr (0.4 mmoles) and N,N-dimethylformamide (DMF, 0.4 mmoles)

^{29}Si 0.8 (Ph_3SiBr at 0.8)

b) Ph_3SiBr (0.78 mmoles) and HMPA (0.78 mmoles)

^{29}Si 0.5

Synthesis of Iodotriphenylsilane (Ph_3SiI)

Iodine (4.87 g, 19.2 mmoles) was added to a stirred solution of triphenylsilane (10 g, 38.4 mmoles) in ethyl iodide (40 ml) and the mixture was refluxed overnight. After cooling, the resulting solid was filtered off and recrystallised from dichloromethane to give off-white crystals.

m.p. 154-155 °C (Lit.[126], 154-156 °C)

N.M.R. δ/ppm (0.159 g in 1.5 ml CD_2Cl_2)

^1H 7.32-7.69 (m, Ph)

^{13}C 128.5, 131.2, 136.0 (Ph)

^{29}Si -8.9

N.M.R. data for interaction between Iodotriphenylsilane (Ph_3SiI) and nucleophiles

δ/ppm ($CDCl_3$, 2.0 ml; Me_4Si)

a) Ph_3SiI (3.40 mmoles) and 2,2-bipyridyl (BIPY, 3.40 mmoles)

^{29}Si -8.9

b) Ph_3SiI (2.59 mmoles) and 1-methylimidazole (NMI; 12.95 mmoles)

^{29}Si -18.3 (very broad); -18.5 (sharp, low intensity, may be $Ph_3SiOSiPh_3$)

N.M.R. Data for a 1:1 mixture of Dimethylsilyl triflate ($Me_2HSiOSO_2CF_3$) and Trimethylsilyl triflate (TMSOTf)

δ/ppm (CD_2Cl_2, Me_4Si)

^1H 0.49 (9H, s, TMS); 0.57 (6H, d, $^3J_{HH}$ 2.95Hz, Me_2Si); 5.0 (1H, qn, $^3J_{HH}$ 2.95Hz, SiH)

^{13}C -1.4 (SiMe); 0.34 (SiMe); 169.0 (q, $^1J_{CF}$ 317.1Hz, CF_3)

^{29}Si 43.9; 24.4

Synthesis of Hydridodimethyl-bis(3-methyl-1-imidazolio) silicon (IV) chloride $[NMI_2\text{-}DMS]^+Cl^-$

1-Methylimidazole (9.5 mmoles) was added to stirred chlorodimethylsilane (5 ml) resulting in the precipitation of a white semi-solid. After stirring overnight, the product was filtered off under nitrogen and dried under vacuum to give a white solid.

m.p. 90 °C (decomposition occurred)

Analysis Found: C, 45.96; H, 7.27; N, 22.96%.

$SiC_{10}H_{19}N_4$ requires C, 46.41; H, 7.40; N, 21.65%.

N.M.R. δ/ppm ($CDCl_3$, Me_4Si)

^1H 0.52 (d, J_{HH} 2.5Hz); 3.82 (s, N-CH_3); 4.94 (q, J_{HH} 2.5Hz); 7.04; 7.58 (br)

^{13}C -3.0, 31.6, 118.8, 122.8, 134.5

^{29}Si -61.1 (d, J_{SiH} 266Hz) (-80.1 with NMI:DMSCl ratio at 5:1)

Synthesis of Hydrido-bis(3-methyl-1-imidazolio) silicon (IV) triflate $[NMI_2\text{-}DMS]^+OTf^-$

Dimethylsilyl triflate (5.2 mmoles) was added to 1-methylimidazole (10.4 mmoles) in hexane/chloroform mixture (chloroform was added dropwise to 20 ml hexane until NMI dissolved); causing an oil to separate out from the mixture. After decanting off the upper chloroform/hexane layer, the oil was held under vacuum for several hours to give a colourless oil.

N.M.R. δ/ppm (5.2 mmoles in 2 ml $CDCl_3$, Me_4Si)

^1H 0.52 (d, J_{HH} 2.4Hz); 3.81; 4.96 (q, J_{HH} 2.4Hz); 7.25 (br); 8.24 (br)

^{13}C 0.2, 35.38, 124.0 (br), 125.2, 138.9

^{29}Si -60.7

Analysis Found: C, 34.54; H, 4.93; N, 15.16%.

$SiC_{11}H_{19}N_4O_3SF_3$ requires C, 35.47; H, 5.14; N, 15.04%.

Synthesis of Hydridodimethyl-(3-methyl-1-imidazolio) silicon (IV) triflate

This was prepared from equimolar amounts of dimethylsilyl triflate and 1-methylimidazole by the same procedure used for synthesising the $[Nu\text{-}TMS]^+X^-$ salts.

m.p. 50-54 °C

N.M.R. δ/ppm (CD_3CN, Me_4Si)

^1H 0.65 (d, J_{HH} 3.2Hz); 3.89; 4.94 (q, J_{HH} 3.2Hz); 7.49; 8.65

^{13}C -3.2; 36.0; 120.8 (q, J_{CF} 320Hz); 124.1; 125.1; 139.9

^{29}Si 9.3 (9.0 in $CDCl_3$)

Table EII.1

Dilution Study on Hydridodimethyl-bis(3-methyl-1-imidazolio) silicon (IV) chloride $[(NMI)_2\text{-}DMS]^+Cl^-$

Volume chloroform-d_1 (ml)	Concentration (mol dm^{-3}, molar)	^{29}Si chemical shift (ppm)
a	1.41	-66.0
2.5	0.83	-59.5
3.5	0.63	-52.3 (sbr)
4.0	0.56	-48.3 (sbr)
4.5	0.51	-45.1 (sbr)
5.0	0.46	-41.9 (br)
6.0	0.39	-35.9 (br)
6.8	0.35	-31.4 (br)
8.5	0.29	-23.0 (br)
quantities used: 0.683 g $[(NMI)_2DMS]^+Cl^-$		

a Extrapolation from the NMI/DMSCl titration (Table 5.2).

N.M.R. data for the interactions between Dimethylsilyl triflate (DMSOTf) and nucleophiles

δ/ppm ($CDCl_3$, 2.0 ml; Me_4Si)

a) DMSOTf (2.2 mmoles) and HMPA (2.2 mmoles)

^1H 0.53 (d, J_{HH} 2.9Hz, $SiMe_2$); 2.79 (d, J_{PH} 10.5Hz, HMPA); 5.00 (m, Si-H)

^{13}C -0.92 (CH_3); 38.4 (d, J_{PC} 5.2Hz, HMPA); 121.7 (q, J_{CF} 321Hz, CF_3)

^{29}Si 12.9 (d, J_{SiP} 8.3Hz)

b) DMSOTf (2.2 mmoles) and HMPA (4.4 mmoles)

^1H 0.53 (d, J_{HH} 2.7Hz, $SiMe_2$); 2.72 (d, J_{PH} 10.0Hz, HMPA); 4.95 (q, J_{HH} 2.7Hz, Si-H)

^{13}C -0.69 ($SiMe_2$); 36.6 (d, J_{PC} 5.2Hz, HMPA); 121.8 (q, J_{CF} 320Hz, CF_3)

^{29}Si 11.5

c) DMSOTf (2.2 mmoles) and HMPA (11.0 mmoles)

^{29}Si no resonances observed between +60 and -120

d) DMSOTf (0.4 ml) and NMI (2 ml)

^{29}Si -79.3 (scanned from +65 to -272)

N.M.R. data for interaction between Tri-isopropylsilyl triflate[109] ($^{i}Pr_3SiOTf$, 2.2 mmoles) and 1-Methylimidazole (NMI, 10.1 mmoles)

δ/ppm ($CDCl_3$, 2.0 ml; Me_4Si)

^{1}H 1.08 (d, J 6.2Hz, Me_2CSi); 1.51 (septet, J 6.2Hz, HCSi); 3.59 (MeN, NMI); 6.88 (C_5-H, NMI); 6.97 (C_4-H, NMI); 7.39 (C_2-H, NMI)

^{13}C 10.5 (CH_3, ^{i}Pr); 16.3 (C, ^{i}Pr); 31.7 (Me, NMI); 115.0 (C_5, NMI); 123.2 (C_4, NMI); 131.7 (C_2, NMI)

^{29}Si 23.9

N.M.R. data for interaction between ^{t}Butyldimethylsilyl triflate ($^{t}BuMe_2SiOTf$, 2.2 mmoles) and 1-Methylimidazole (NMI, 11.0 mmoles)

^{29}Si δ/ppm ($CDCl_3$, 2.0 ml; Me_4Si) 28.8

N.M.R. data for the interaction between Triethylsilyl triflate (Et_3SiOTf, 2.2 mmoles) and 1-Methylimidazole (NMI, 11.0 mmoles)

^{29}Si δ/ppm ($CDCl_3$, 2.0 ml; Me_4Si) 28.3

PART II SUMMARY AND CONCLUSIONS

Part II - Summary and conclusions

The stability of [nucleophile-TMS]$^{+}X^{-}$ adducts is controlled by a combination of thermodynamic and kinetic factors as summarised below:-

a) The equilibrium constant is related to the electron donating properties of the nucleophile. The stronger the donor, the higher the equilibrium constant.

b) Adduct formation is exothermic.

c) Exchange processes involving the adducts take place by two mechanisms:-

i) Fast exchange occurs with good nucleophiles via direct rate determining nucleophilic attack at the silicon centre.

ii) Slower exchange occurs with powerful electrophilic species such as TMSX. Rate limiting dissociation of the complex is followed by rapid reassociation. The rate of the initial dissociation step is governed by the nucleophilicity of the counterion, which decreases in the following order:-

$$Cl > Br > I, OTf > ClO_4.$$

This rate is also influenced by solvation of the counterion in different solvents:-

$$CDCl_3 > CD_2Cl_2 > CD_3CN.$$

d) The low conductivity of TMSCl/Nu solutions results from a combination of ion pairing and a low equilibrium constant for ionic adduct formation.

e) Physical properties:- the silicon-29 chemical shift of each [Nu-TMS]$^{+}X^{-}$ adduct reflects the donor strength of the nucleophiles.

It appears from the preliminary studies on the Nu/DMSX systems that these rationalizations can be applied to other silanes, although in some cases, the situation is complicated by the presence of five coordinate adducts. The facility of a given nucleophile for forming five coordinate adducts decreases in the following order:-

H_3SiOTf > HMe_2SiX (X=OTf > X=Cl), $PhMeHSiOTf$ >> Ph_3SiX (X=I,Br), $Ph_2MeSiBr$ > Me_3SiX (X=Cl, Br, I, OTf, ClO_4), Et_3SiOTf, $^{t}BuMe_2SiOTf$, $^{i}Pr_3SiOTf$.

Although a trend towards five coordination in the less sterically hindered species is apparent, the contribution of electronic effects cannot be ruled out as factors affecting the stability of five coordinate species. The silicon-29 chemical shifts of the dimethylsilyl triflate-nucleophile adducts are more susceptible to donicity changes in the nucleophiles.

In conclusion, it is clear from the accumulated results that ionic 1:1 [nucleophile-silane]$^{+}X^{-}$ adducts are formed as a result of the interactions between a wide range of nucleophiles and silanes. Furthermore, these complexes undergo rapid exchange with other nucleophiles, and with their parent silanes at a rate which is controlled by the initial dissociation of the complex. These findings support the mechanism of nucleophile assisted alcoholysis proposed by Chojnowski[7] (see Section 1.7).

This mechanism, involving initial formation of four coordinate ionic Nu-silane adducts, recently received additional support from Frye et al.[127], whose paper was received after the first draft of this thesis had been written. The authors carried out a detailed kinetic study on the tertiary alcoholysis of chlorosilanes. On the basis of their results, they proposed that initial formation of a four coordinate ionic Nu-silane adduct was followed by alcoholysis (Scheme II.1), a mechanism essentially the same as that proposed by Chojnowski[7]. The rate of the process (k_1) was monitored in the presence of a series of nucleophiles.

$$Nu + Ph_2SiCl_2 \rightleftharpoons [Nu\text{-}Ph_2SiCl]^+Cl^- \xrightarrow{ROH} ROSiPh_2Cl + HCl$$

Scheme II.1

A plot of $\ln K(Nu_A/Nu_B)$ vs. $\ln k_1$ (from the data presented by Frye[127]) (Figure II.1) shows an excellent correlation between the observed rate and the equilibrium constant for salt formation for the pyridines, although the point for HMPA deviates from the main trend.

The implications of this correlation are very important. The K_{rel} values determined in this study are a measure of the relative quantities of each Nu-silane complex in solution, thus the correlation shows that the rate is dependent upon this concentration, indicating that the first step in the nucleophilic catalysed alcoholysis of silanes is the formation of a Nu-silane complex. The essentially zero rate increase observed by Frye for 2,6-lutidine and triethylamine is consistent with the low equilibrium constant for salt formation observed for these species in this study. Frye suggests that the apparent inability of triethylamine to assist in

the alcoholysis of Ph_2SiCl_2 is due to steric constraints in that nucleophile. A similar but less marked effect is likely to be observed with HMPA, since the donor site in this nucleophile is also sterically hindered, though to a lesser extent than triethylamine. This may help to explain why the rate enhancement by HMPA is slower than expected from its lnK_{rel} value, and hence why the point for this nucleophile lies outside the main correlation in Figure II.1. The very small rate enhancement produced by 2,6-dimethylpyridine is consistent with the observation made in this study that the equilibrium constant for 1:1 $[2,6DMP\text{-}TMS]^+X^-$ (X= I, OTf) formation is very low.

The facile exchange observed with the five coordinate $[bis\ nucleophile\text{-}DMS]^+X^-$ adduct shows that it is not necessary to invoke the formation of a six coordinate intermediate to explain the racemisation of halosilanes by nucleophiles (see Scheme 1.7).

Figure II.1 Correlation between the rates of nucleophile assisted alcoholysis and Keq for Nu-TMSOTf adduct formation.

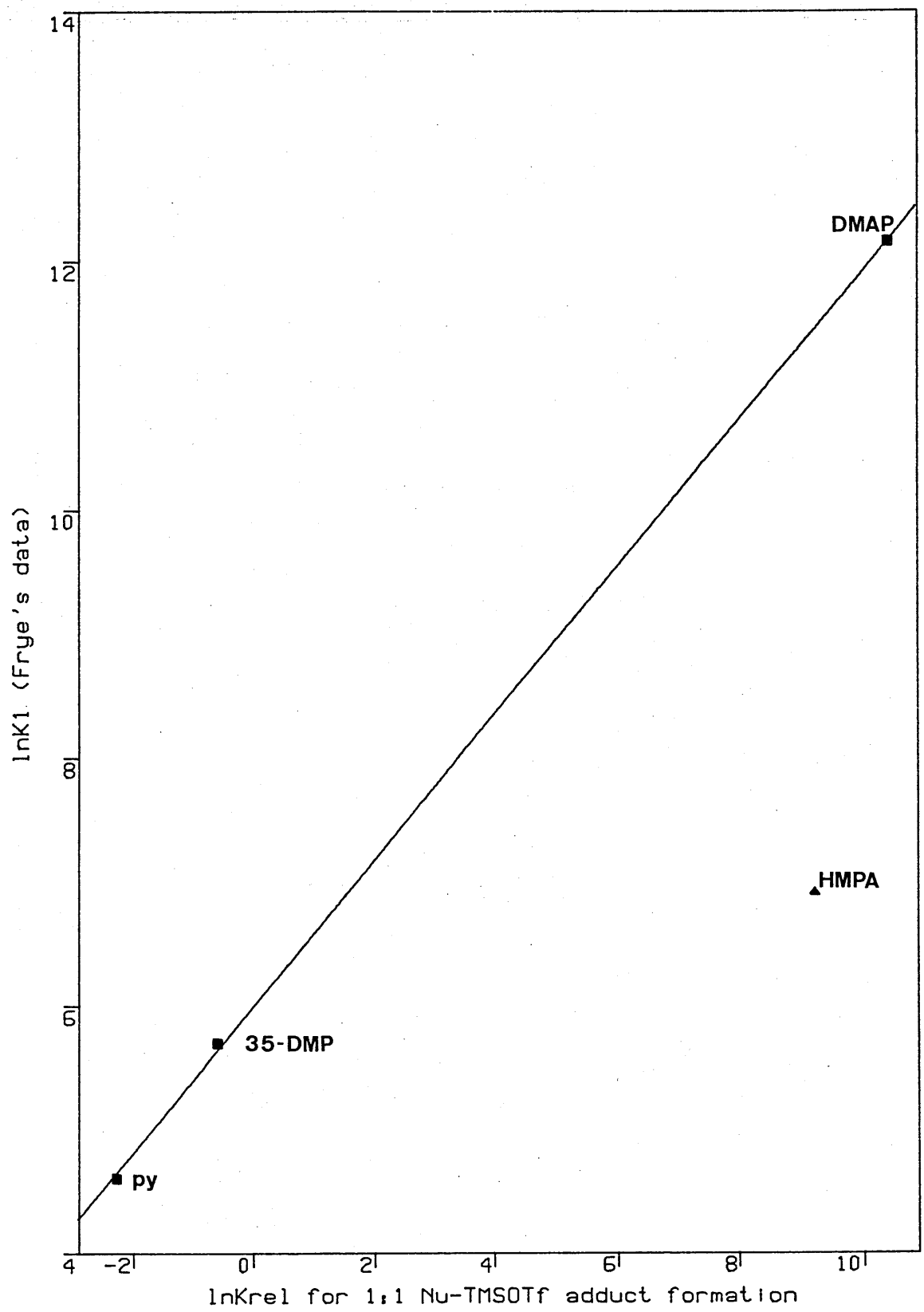

Variance = 0.0026 (excluding the point for HMPA)

Slope = 0.591 (s.d. = 0.0052)

Intercept = 6.0 (s.d. = 0.032)

APPENDICES

Appendix 1 Dynamic N.M.R. processes

The n.m.r. spectrum of a non-exchanging chemical system can be represented by:

i) the chemical shifts of each magnetic environment or site (v_i);

ii) the relative population of each site (p_i);

iii) any coupling constants (J_{ij});

iv) the natural bandwidth (W_i).

Thus we can imagine a 2-spin system which would consist of 2 lines, each with linewidth W_i. A gradual increase in the rate of exchange is accompanied by slight line broadening of each species, followed by progressively more broadening until the two signals merge. Further increases in the exchange rate result in an increasingly sharp signal until finally an averaged signal, of linewidth W_i, is observed. The position of this signal is determined by the relative populations and chemical shifts of the two species (A and B) by equations A1.1 and A1.2.

$$v_{observed} = v_A p_A + v_B p_B \quad ..... \quad \text{equation A1.1}$$

$$p_A + p_B = 1 \quad ..... \quad \text{equation A1.2}$$

The bandshape changes resulting from exchange between two equally populated, uncoupled sites are shown in Figures A1.1 and A1.2.

In this case equal populations of the two species cause the signals to change in a symmetric fashion. Unequal populations however cause the less intense signal to broaden more quickly and to be shifted more strongly by exchange. This situation could occur, for example, in a silicon spectrum,

Figure A1.1

Calculated line shapes for an uncoupled, two sites exchange system with equal populations ($p_A = p_B$, $T_2 = 0.2$, $\delta\nu = 600$ Hz).

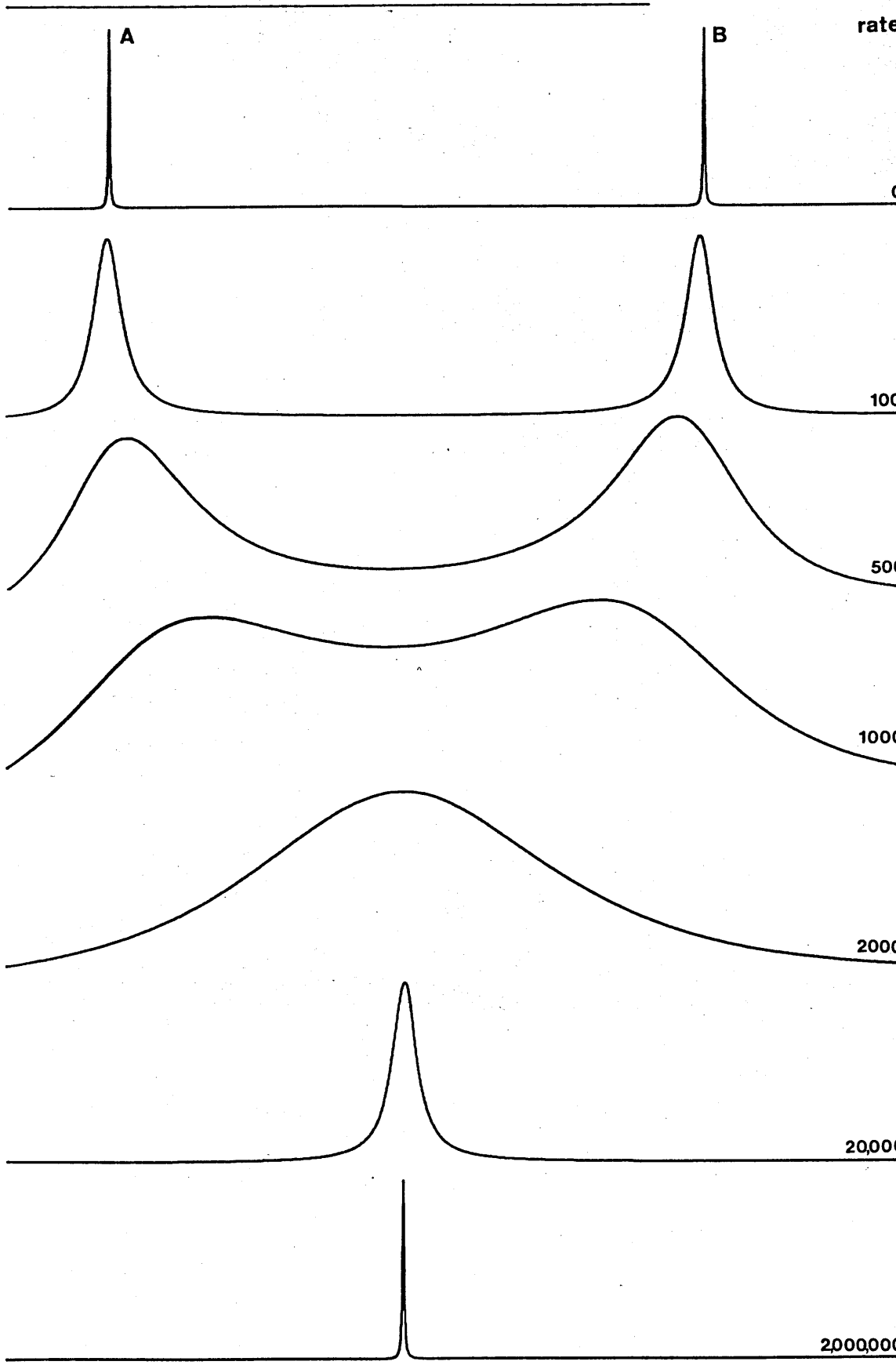

Figure A1.2

Calculated bandshapes for an uncoupled, two site exchange system with equal populations ($p_A = p_B$, $T_2 = 0.2$, $\delta\nu = 600$ Hz), scaled to the height of the reference peak C.

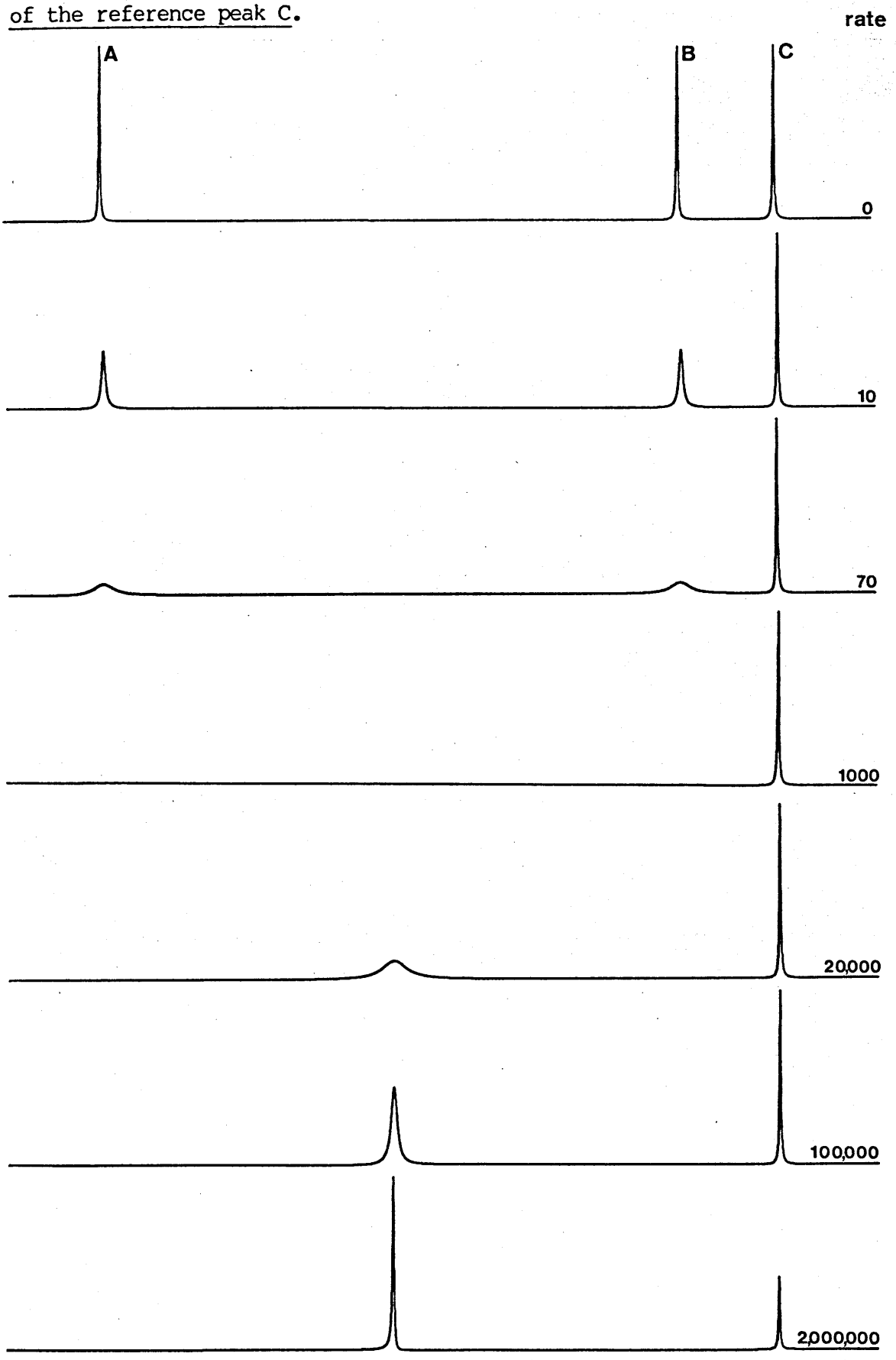

when a dominant 4-coordinate species was exchanging with a small proportion of, say, a 5-coordinate species at a lower frequency. A relative population of 100:1 and a shift difference between the two sites of 300 Hz (approximately 15 ppm for ^{29}Si) will cause the strong peak to be shifted by only 3 Hz, but the maximum broadening may reduce its intensity to 25% or below[92].

Three equations can be derived[128] to give the approximate rate at slow exchange, coalescence and fast exchange as a function of exchange broadening (ΔW_e) and the separation of exchanging sites ($\delta\nu$).

Slow exchange	$k = \pi \Delta W_e$	.....	equation A1.3
Coalescence	$k = \frac{\pi \delta\nu}{\sqrt{2}}$	.....	equation A1.4
Fast exchange	$k = \frac{\pi(\delta\nu)^2}{2(\Delta W_e)}$	.....	equation A1.5

Total line shape analysis[53] enables accurate rate constants to be determined for the full range of line shapes. The mathematical basis for this theory is complex and it will not be discussed here, however computer programs are available to suit specific requirements[53]. At its most sophisticated level the technique is a very powerful one, but extreme care must be taken to minimise errors. An excellent discussion on DNMR has been presented by Sandstrom[129] who provides the basic theoretical background together with the experimental and statistical treatment necessary to minimise errors.

Considerable problems can arise due to the poor signal-to-noise ratio around the coalescence region. This is apparent in the line shapes presented in Figure A1.2, which were calculated using the same parameters as those used for producing Figure A1.1, except that the peak heights were scaled to the height of a non-exchanging reference nucleus (v_C, $p_A=p_B=p_C$). Clearly, for a system undergoing fast exchanging, the equilibrium population of two species can be determined from the observed line position provided that the chemical shifts of each species in the absence of exchange are known.

Appendix 2 Equilibrium constants from Chemical Shift Titrations and Variable Temperature N.M.R.

Consider the case of a donor(D)/acceptor(A) system, undergoing fast exchange with a D-A complex(C).

$$dD + aA \rightleftharpoons cC$$

(populations: p_d, p_a, p_c; chemical shifts: v_d, v_a, v_c)

Scheme A2.1

The composition of the complex C can be determined by titration of either donor on acceptor or vice versa, and plotting the measured quantity (Q) e.g. chemical shift or conductivity, as a function of the concentration of D ($[D]_o$) or A ($[A]_o$), or the ratio $[D]_o:[A]_o$ (the concentrations and ratios are calculated from the amounts added, rather than from the equilibrium values). Idealised titration curves for such a system are shown in Figure A2.1.

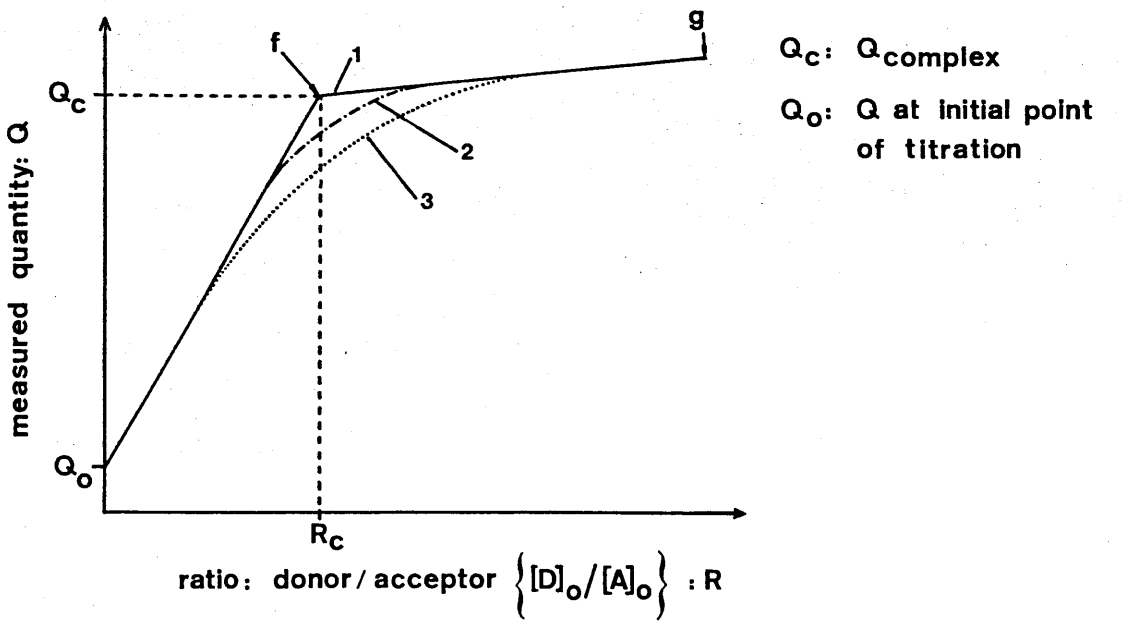

Figure A2.1

Curve 1 (the solid line) represents an ideal case for a system having a very high equilibrium constant for formation of C. At f the complex is fully formed and thus the equilibrium concentrations of A and D are zero. Therefore it follows that the stoicheiometry of the complex at this point can be found from $R_c = d/a$, and the chemical shift of the complex from $Q_c = v_c$. Following the arguments of Guryanova et al.[130], it can be shown that

$$v_{observed} = \frac{[D]_o \, d \, (v_c - v_a)}{[A]_o \, a} + v_a \quad \ldots\ldots \quad \text{equation A2.1}$$

Thus the slope of the initial linear section of the titration curve is equal to $(v_c - v_a)d/a$ and the intercept v_a.

The broken curves 2 and 3 represent progressively greater amounts of dissociation of the complex C. Extrapolation of the linear sections of the curve allows the point f to be determined, although this may not be possible for weakly associated complexes.

The equilibrium concentration of the complex and thus the equilbrium constant can be determined from equation A2.2 or A2.3, depending on whether the donor or the acceptor is the n.m.r. active species, if the uncomplexed (v_a or v_d) and complexed limits are known.

$$[C]_e = \frac{(v_{obs} - v_a) \, [A]_o}{(v_c - v_a)} \quad \ldots\ldots \quad \text{equation A2.2}$$

$$[C]_e = \frac{(v_{obs} - v_d) \, [D]_o}{(v_c - v_a)} \quad \ldots\ldots \quad \text{equation A2.3}$$

Determination of these values is relatively easy from the titration curve, although the situation is frequently complicated by medium dependent chemical shifts, which are represented in Figure A2.1 by the sloping section (f-g) of the curve (in other situations the slope may be zero or negative). The problem of defining the chemical shift limits is particularly acute in, for example, low temperature studies, where for experimental reasons it is not always possible to lower the temperature sufficiently to permit observation of the fully formed adduct. In such cases the complexed limit (v_c) has to be extrapolated from the existing data or in favourable cases, estimated from the chemical shift of a structurally analogous complex. The errors resulting from an incorrect choice of v_c can be quite significant, especially for values close to this limit. The severity of this problem is demonstrated with respect to particular experimental systems in 2.3 and 2.5 (see below).

If the equilibrium composition of a given donor/acceptor system can be determined over a range of temperatures, it is possible to determine the enthalpy and entropy changes resulting from complex formation using the integrated form of the Van't Hoff Isochore.

$$\ln K_{eq} = \frac{-\Delta H}{RT} + \frac{\Delta S}{R} \qquad \text{.....} \qquad \text{equation A2.4}$$

Hence a plot of $\ln K_{eq}$ vs. $1/T$ should give a straight line with slope $-\Delta H/R$ and intercept $\Delta S/R$, assuming that the enthalpy and entropy changes are themselves independent of temperature. The latter assumption is normally a valid one over the relatively narrow range of temperatures in which the experiment is performed.

It was not the primary objective of this study to determine the thermochemistry of each system; nevertheless estimates of the enthalpy and entropy changes were calculated for each variable temperature n.m.r. system studied. The errors in these values may be fairly significant since no attempt was made to quantify contributions to the overall enthalpy change, from factors such as donor-solvent, acceptor-solvent or complex-solvent interactions.

The most significant source of error is the choice of the limits for the complexed and uncomplexed species. This is demonstrated by an analysis of the silicon-29 chemical shift data for the py/TMSBr system at various temperatures (Table 2.11). The thermochemical data calculated using various values for the complexed limit are shown below (uncomplexed limit = 27.6 ppm, TMSBr):-

Complexed limit (ppm)	Variance	Slope (s.d.)	Intercept (s.d.)	ΔH (kJ mol^{-1})
41.0	0.74	5180 (441)	-21.4 (1.9)	43
41.5	0.36	4480 (310)	-18.8 (1.3)	37
42.0	0.28	4120 (270)	-17.5 (1.2)	34
42.5	0.25	3880 (255)	-16.6 (1.1)	32
43.0	0.23	3695 (250)	-16.0 (1.1)	31
43.5	0.22	3550 (240)	-15.5 (1.05)	30

Extrapolation of the curve shown in Figure 2.6 yields a chemical shift of approximately 41.4 ppm for the py-TMSBr adduct. The enthalpy and entropy changes calculated from this value are -38 kJ mol^{-1} and -160 J K^{-1} mol^{-1}

with error limits of $\pm$10 kJ mol^{-1} and $\pm$40 J K^{-1} mol^{-1} respectively. Clearly the values obtained from these calculations should only be regarded as estimates. Nonetheless they clearly show that adduct formation is substantially exothermic in this case.

Similar considerations can be applied to the TMSIm/TMSCl system, although in this system the chemical shifts of the imidazolium protons, the methyl protons and the silicon atom can each be used to calculate the thermodynamic parameters. Reasonable agreement is found between the calculated values for each nuclei if the following limits are chosen:

Nucleus	Complexed limit (ppm)	Uncomplexed limit (ppm)	Slope (s.d.)	Intercept (s.d.)
^{29}Si	25.5	22.28	5028 (136)	-20.7 (0.6)
^{1}H (C_2-H)	10.45	7.55	4942 (306)	-20.0 (1.3)
^{1}H ($C_{4,5}$-H)	7.96	7.03	5015 (628)	-21.3 (2.7)
^{1}H (CH_3)	0.765	0.42	5069 (168)	-20.4 (0.7)
		average values:-	4957 (309)	-20.6 (1.3)

A ln K_{eq} *vs.* 1/T plot for all four sets of data are shown in Figure A2.2. Values of -42 ($\pm$5) kJ mol^{-1} and -171 ($\pm$30) J K^{-1} mol^{-1} for the enthalpy and entropy changes respectively are obtained by taking the mean of the four sets of data.

Figure A2.2 lnKeq vs. 1/T plots calculated from Si-29 and proton n.m.r. data for a 1:1 mixture of TMSIm and TMSCl.

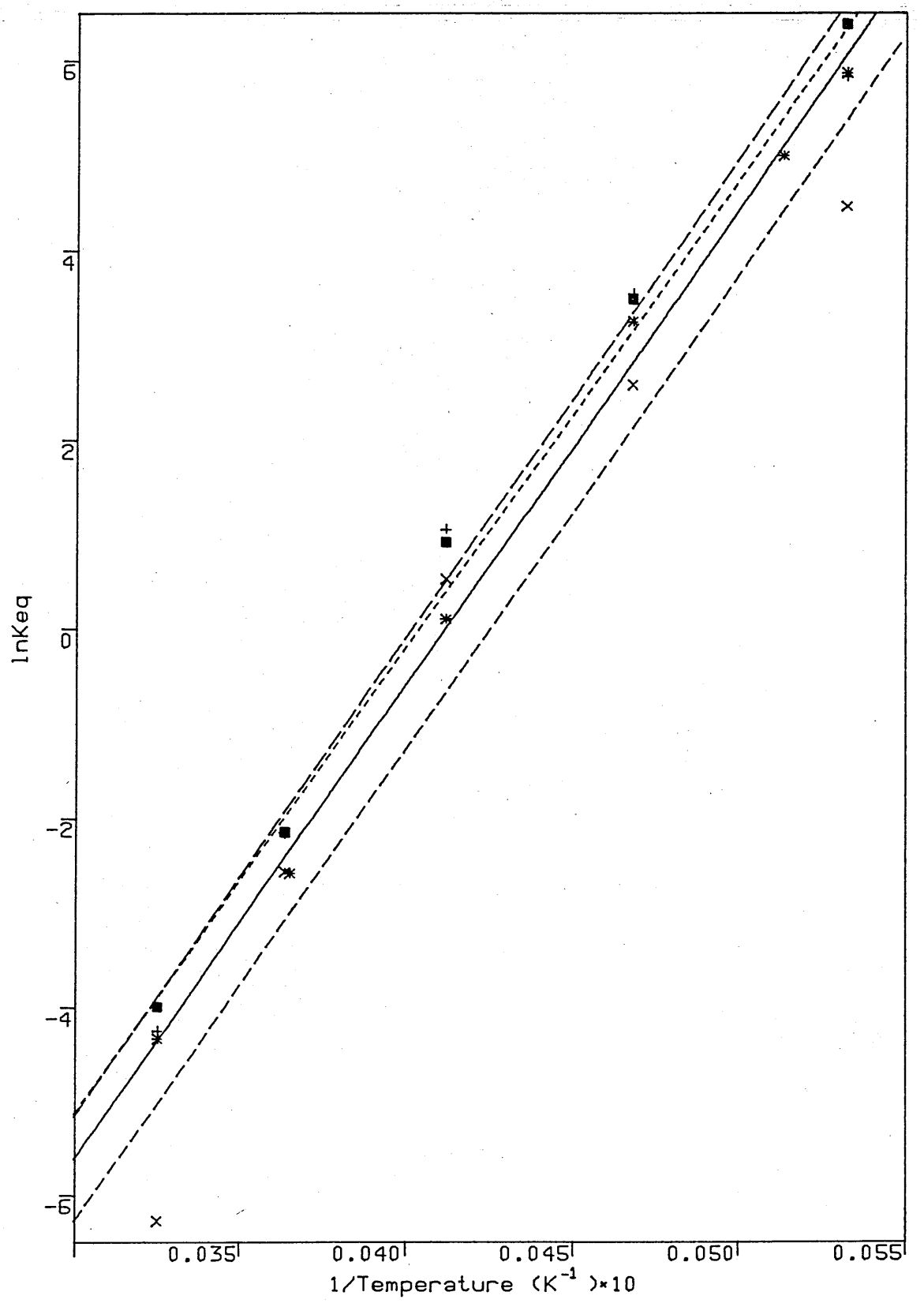

Solvent: dichloromethane-d2, 2.0 ml.

The data were calculated using the following limits:
✱ 22.28, 25.5 (Silicon-29); + 7.55, 10.45 (C_2-H),
× 7.03, 7.96 ($C_{4,5}$-H); ■ 0.42, 0.765 ($Si(CH_3)_3$).

Appendix 3 Summary of N.M.R. Data of Trimethylsilyl species (TMSX)

solvent		^1H	^{13}C			^{29}Si
		$Si-(CH_3)_3$	CF_3	$^1J_{CF}$	$Si-(CH_3)_3$	$Si-(CH_3)_3$
$CDCl_3$	$(CH_3)_3SiCl$	0.43	-	-	3.3	31.0
	$(CH_3)_3SiBr$	0.58	-	-	4.1	nr
	$(CH_3)_3SiI$	0.80	-	-	5.6	9.6
	$(CH_3)_3SiOTf$	0.50	nr	nr	0.34	43.4
	$(CH_3)_3SiClO_4$	nr	-	-	nr	nr
	$[(CH_3)_3Si]_2O$	0.06	-	-	1.9	7.4
CD_2Cl_2	$(CH_3)_3SiCl$	0.42	-	-	3.3	31.1
	$(CH_3)_3SiBr$	0.57	-	-	4.2	27.6
	$(CH_3)_3SiI$	0.79	-	-	5.6	10.3
	$(CH_3)_3SiOTf$	0.49	nr	nr	0.29	43.9
	$(CH_3)_3SiClO_4$ [a]	0.35	-	-	0.80	45.1
CD_3CN	$(CH_3)_3SiCl$	0.42	-	-	3.2	32.0
	$(CH_3)_3SiBr$	0.57	-	-	4.1	28.7
	$(CH_3)_3SiI$	0.79	-	-	5.6	12.1
	$(CH_3)_3SiOTf$	0.48	118.11q	323.14Hz	0.29	46.1
	$(CH_3)_3SiClO_4$	0.09	-	-	nr	32.6
quantities used: 2.2 mmoles of silane; solvent: 2.0 ml						

[a] solvent: 1 ml toluene and 1 ml CD_2Cl_2.

Summary of the physical properties of solvents and nucleophiles

Nucleophile	^{29}Si[a]	β[b]	pKa[c]	DN[d]	AN[d]	ϵ	π^*[b]	D[e]	lnK_{rel}[f]
DMF	44.0	0.69	...	26.6	16.0	36.5	...	...	-0.2
NMP	39.4	0.77	...	27.3	13.3	...	0.92	...	0.0
DMEU	40.1	0.75[g]	...	...	...	...	...	...	-2.2
DMPU	36.6	0.79[g]	...	...	...	...	...	...	2.2
TMU	36.5	0.80	...	...	...	...	...	...	-
NMPO	35.8	0.78	...	...	...	...	...	...	5.2
py	42.3	0.64	5.20	33.1	14.2	12.3	...	2.19	-2.3
2,6DMP	-	0.76	6.77	...	...	...	...	...	-
2,4DMP	40.8	0.74	6.72	...	...	...	...	...	0.2
3,5DMP	41.2	0.70[g]	6.14	...	...	...	...	...	-0.6
quinoline	-	0.64	4.90	...	...	9.0	...	2.29	-
DMAP	31.7	0.87	9.61	...	...	...	...	...	10.4
BIPY	-	-	4.44	...	...	...	...	...	-
PNO	49.0	0.85	...	...	...	...	...	...	4.2
HMPA	28.8	1.05	...	38.8	10.6	30.0	0.87	...	9.2
TPPO	37.4	0.94	...	...	...	...	...	...	2.4
NMI	26.7	0.82	7.3	...	...	...	...	...	10.4
DMI	25.1	-	...	...	...	...	...	...	8.6
TMSIm	26.5	-	...	...	...	...	...	...	-
Et_3N	46.0	0.71	10.65	61.0	...	2.4	0.14	0.66	-
CH_3CN	...	...	...	14.1	18.9	38.0	...	3.51	-
CH_2Cl_2	...	...	...	...	20.4	...	...	...	-
$CHCl_3$	...	...	...	...	...	4.8	...	1.11	-

[a] $[Nu\text{-}TMS]^+OTf^-$ complex.

[b] from reference 60.

[c] from reference 120.

[d] from reference 50.

[e] Dipole moment in Debyes (1 Debye = 3.335×10^{-30} C m^{-1}).

[f] see Chapter 3.

[g] calculated (see Chapter 2).

REFERENCES

References

1. A.E. Pierce
'Silylation of Organic Compounds', Pierce Chemical Co., Rockford, Illinois, 1968.

2. W.P. Weber
'Silicon Reagents for Organic Synthesis', Springer-Verlag, Berlin, 1983

3. E.W. Colvin
'Silicon in Organic Synthesis', Butterworths Monographs in Chem. and Chem. Eng., Butterworths, 1981

4a. Pierce and Warriner
Preview - Protein Digest No. 1, 1984.

4b. 'Handbook and General Catalog', Pierce Chem. Co. Ltd., 1983, 110-119

5. Aldrich Technical Information Bulletin on Tert-butylchlorodimethylsilane and references therein

6. S.K. Chaudhary and O. Hernandez
Tetrahedron Letters, 1979, 2, 99-102

7. J. Chojnowski, M. Cypryk and J. Michalski
Journal of Organometallic Chemistry, 1978, 161, C31-C35

8. R.J.P. Corriu, G. Dabosi and M. Martineau
Journal of Organometallic Chemistry, 1980, 186, 25-37

9. A.D. Allen, J.C. Charlton, C. Eaborn and G. Modena
J. Chem. Soc., 1957, 3668-3670

10. A.D. Allen and G. Modena
J. Chem. Soc., 1957, 3671-3678

11. C. Eaborn
'Organosilicon Compounds', Butterworths, London, 1960

12. L.H. Sommer

'Sterochemistry, Mechanism and Silicon', McGraw-Hill, New York, 1965

13. H. Emde, D. Domsch, H. Feger, U. Frick, A. Gotz, H.H. Hergott, K. Hofmann, W. Kober, K. Krageloh, T. Oesterle, W. Steppan, W. West, G. Simchen
Synthesis, 1982, 1-25

14. R. Noyori, S. Murata and M. Suzuki
Tetrahedron, 1981, Vol. 37, No. 23, 3899-3910

15. Aldrich Technical Information Bulletin on Trimethylsilyl triflate and references therein

16. G.A. Olah and S.C. Narang
Tetrahedron, 1982, Vol. 38, No. 15, 2225-2277

17. A.H. Schmidt
Aldrichimica Acta, 1981, Vol. 14, No. 2, 31-38

18. E.A. Williams and J.D. Cargioli
'Annual Reports on NMR Spectroscopy', Vol. 9, Academic Press, 1979, p. 221 and references therein

19. E.A. Williams
'Recent Advances in Silicon-29 NMR Spectroscopy', 235-289

20. E.A.V. Ebsworth
'Physical Basis of the Chemistry of the Group IV Elements'

21. M.J.S. Dewar and E. Healy
Organometallics, 1982, Vol. 1, No. 12, 1705-1708

22. G.A. Olah and G.K.S. Prakash
Chemistry in Britain, November 1983, 916-926

23. T.R. Forbus Jr. and J.C. Martin
J. Amer. Chem. Soc., 1979, Vol. 101, No. 17, 5057-5059

24. J.C. Martin
Science, 1983, Vol. 221, No. 4610, 509-514

25. R.R. Holmes, R.O. Day, J.J. Harland, A.C. Sau and J.M. Holmes
Organometallics, 1984, Vol. 3, No. 3, 341-353 and references therein

26. C.G. Pitt
Chem. Commun., 1971, 816

27. C.G. Pitt
Journal of Organometallic Chemistry, 1973, 61, 49-70

28. M.J.S. Dewar
'Hyperconjugation', The Ronald Press Company, New York, 1962

29a. T.G. Traylor et al.
J. Amer. Chem. Soc., 1971, 93, 5715

29b. T.G. Traylor
Pure Appl. Chem., 1972, 30, 599

30. V. Chvalovsky and J.M. Bellama
'Carbon Functional Organosilicon Compounds', Modern Inorganic Chemistry, Plenum Press, New York and London, 1984, p. 233

31. D.A. Armitage
'Comprehensive Organometallic Chemistry', Vol. 2, Peramon, 1982, p. 1

32a. G.A. Olah
J. Amer. Chem. Soc., 1972, 94, 808

32b. G.A. Olah and Y.K. Mo
J. Amer. Chem. Soc., 1971, 93, 4942

33. A.G. MacDiarmid
Intra-Science Chem. Rept., 1973, Vol. 7, No. 4, 83-95 and references therein

34. M. Zeldin, P. Mehta and W.D. Vernon
Inorganic Chemistry, 1979, Vol. 18, No. 2, 463-466

35. T.J. Barton and C.R. Tully

J. Org. Chem., 1978, Vol. 43, No. 19, 3649-3653

36. K. Hensen, T. Zengerly, P. Pickel and G. Klebe
Angew. Chem. Int. Ed. Engl., 1983, 22, 725

37. J. Schraml, V. Chvalovsky, V. Bazant and M.Horak
'Handbook of Organosilicon Compounds Advances since 1961', Marcel Dekker inc., New York, 1973, Volume 1

38. S.J. Berry
J. Chem. Phys., 1960, 32, 933

39. G.R. Holzman, P.C. Lauterbur, J.H. Anderson and W. Koth
J. Chem. Phys., 1956, 25, 172

40. J. Schraml and J.M. Bellama
'Determination of Organic Structure by Physical Methods', Academic Press, New York, 1976, Vol. 6, 203-269

41. H. Marsmann
'NMR Basic Principles and Progress Grundlagen und Fortschritte 17 Oxygen-17 and Silicon-29', Springer-Verlag Berlin Heidelberg, New York, 1981, p. 65

42. R. Bennn and H. Gunther
Angew. Chem. Int. Ed. Engl., 1983, Vol. 22, No. 5, 350-380

43. G.A. Morris and R. Freeman
J. Amer. Chem. Soc., 1979, Vol. 101, No. 3, 760-762

44. D.M. Doddrell, D.T. Pegg, W. Brooks and M.R. Bendall
J. Amer. Chem. Soc., 1981, 103, 727-728

45. B.J. Helmer and R. West
Organometallics, 1982, 1, 877-879

46. W. McFarlane and J.M. Seaby
J. Chem. Soc., Perkin II, 1972, 1561-1564

47. C.R. Ernst, L. Spialter, G.R. Buell and D.L. Wilhite
J. Amer. Chem. Soc., 1974, Vol. 96, No. 17, 5375-5381

48. E.A. Williams, J.D. Cargioli and R.W. Larochelle
Journal of Organometallic Chemistry, 1976, 108, 153-158

49. V. Gutmann
Angew. Chem. Internat. Edit., 1970, Vol. 9, No. 11, 843-860

50. V. Gutmann
'Coordination Chemistry Reviews', 1976, 18, 225-255

51. G. Klebe, K. Hensen and J.V. Jouanne
Journal of Organometallic Chemistry, 1983, 258, 137-146

52. G.A. Olah and L.D. Field
Organometallics, 1982, Vol. 1, No. 11, 1485-1487

53. G. Binsch and H. Kessler
Angew. Chem. Int. Ed. Engl., 1980, Vol. 19, No. 6, 411-428

54. C. Eaborn and D.R.M. Walton
Journal of Organometallic Chemistry, 1965, 4, 217

55. F.K. Cartledge
Organometallics, 1983, 2, 425-430

56a. R.J.P. Corriu and C. Guerin
Journal of Organometallic Chemistry, 1980, 198, 231-320

56b. R.J.P. Corriu and C. Guerin
Adv. Organomet. Chem., 1982, Vol. 20, p.265, Academic Press

56c. R.J.P. Corriu, C. Guerin and J. Moreau
'Topics in Stereochemistry', Wiley Interscience, 1984, Vol. 15, p. 43 and references therein

57. R.S. Drago and B.B. Wayland
J. Amer. Chem. Soc., 1965, 87, 3571

58. A.P. Marks and R.S. Drago
Inorganic Chemistry, 1976, Vol. 15, No. 8, 1800-1807

59. R.W. Taft, T. Gramstad and M.J. Kamlet
J. Org. Chem., 1982, Vol. 47, No. 23, 4557-4563

60. M.J. Kamlet, J.-L.M. Abboud, M. Abraham and R.W. Taft
J. Org. Chem., 1983, Vol. 48, No. 17, 2877-2887

61. R.H. Prince
'Nucleophilic Displacement at Some Main Group Elements 9', p. 353-393

62. I. Fleming
'Comprehensive Organic Chemistry', 1979, Vol. 3, Part 13, p. 541-686

63. L.H. Sommer
Intra-Science Chemistry Reports, 1973, Vol. 7, No. 4, 1-44

64. M.J. Gallagher and I.D. Jenkins
'Topics in Stereochemistry', Interscience Publishers, 1968, Vol. 3, p. 1

65. F. Klanberg and E.L. Muetterties
Inorganic Chemistry, 1968, 7, 155

66. A.F. Janzen, J.A. Gibson and D.G. Ibott
Inorganic Chemistry, 1972, 11, 2853

67. W.B. Farnham and R.L. Harlow
J. Amer. Chem. Soc., 1981, Vol. 103, No. 15, 4608-4610

68. W.H. Stevenson III and J.C. Martin
J. Amer. Chem. Soc., 1982, 104, 309-310

69. E.F. Perozzi and J.C. Martin
J. Amer. Chem. Soc., 1979, Vol. 101, No. 6, 1591-1593

70. N.T. Anh and C.J. Minot
J. Amer. Chem. Soc., 1980, 102, 103

71. K. Fukui
Accts. Chem. Res., 1971, 4, 57

72. A.R. Bassindale, C. Eaborn and D.R.M. Walton
Journal of Organometallic Chemistry, 1970, 25, 57

73. C.H. Yoder, C.M. Ryan, G.F. Martin and P.S. Ho
Journal of Organometallic Chemistry, 1980, 190, 1

74. A.R. Bassindale, Personal communication

75. T.L. Ho
'Hard and Soft Acids and Bases Principle in Organic Chemistry', Academic Press Inc. Ltd., London, 1977, p. 39-42 and references therein

76. N. Kornblum, R.A. Smiley, R.K. Blackwood and D.C. Iffland
J. Amer. Chem. Soc., 1955, 77, 6269

77. R.B. Homer and C.D. Johnson
'The Chemistry of Amides', Interscience Publishers (John Wiley & Sons), 1970, p. 187-244 and references therein

78. M.R. Robin, F.A. Bovey and H. Basch
'The Chemistry of Amides', Interscience Publishers (John Wiley & Sons), 1970, p.1-72 and references therein

79. C.H. Yoder and C.L. Hausman
Journal of Organometallic Chemistry, 1978, 161, 313-317

80. W.E. Stewart and T.H. Siddall III
Chemical Reviews, 1970, Vol. 70, No. 5, 517-551

81. W.F. Reynolds and R.A. McClelland
Chem. Commun., 1974, 824-825

82. R.J. Pugmire and D.M. Grant
J. Amer. Chem. Soc., 1968, Vol. 90, No. 16, 4232-4238

83. D. H. Williams and I. Fleming
'Spectroscopic methods in organic chemistry', McGraw Hill Book Co. (UK) Ltd., 1973

84. J.P. Kintzinger
see reference 41, p. 1 and references therein

85. T.J. Batterham

'NMR Spectra of Simple Heterocycles', Wiley-Interscience, 1973

86. E. Breitmaier and K.H. Spohn
Tetrahedron, 1973, 29, 1145

87. H. Gunther
'NMR Spectroscopy', John Wiley & Sons, 1980

88. Perkampus and Kruger
see reference 85, p.22

89. E.N. Guryanova, I.P. Gol'dshtein and I.P. Romm
'Donor-Acceptor Bond', John Wiley & Sons (Halsted Press), 1975, p. 315

90. H.C. Brown and D.C. Gintis
J. Amer. Chem. Soc., 1956, 78, 5378

91. J.Y. Corey and R. West
J. Amer. Chem. Soc., 1963, 85, 4043

92. J. Sandstrom
'Dynamic NMR Spectroscopy', Academic Press, 1982, 14-18

93. T. Tanaka, G. Matsubayashi, A. Shimizu and S. Matsuo
Inorganic Chimica Acta., 1969, 3, 187-190

94. J.A. Joule and G.F. Smith
'Heterocyclic Chemistry', Van Nostrand Reinhold Co., London, 1978, p. 71

95. G.B. Barlin and T.J. Batterham
J. Chem. Soc. (B), 1967, 516-518

96. R.J. Pugmire, D.M. Grant, L.B.Townsend and R.K. Robins
J. Amer. Chem. Soc., 1973, Vol. 95, No. 9, 2791-2794

97. R.E. Wasylishen and G. Tomlinson
J. Biochem., 1975, 147, 605-607

98. J.P. Gasparini, R. Gassend, J.C. Maire and J. Elgners
Journal of Organometallic Chemistry, 1980, 188, 141-150

99. R. Caputo, C. Ferreri, G. Palumbo and E. Wenkert
Tetrahedron Letters, 1984, Vol. 25, No. 5, 577-578

100. see reference 89, p.220

101. Y.A. Basulaev, V.V. Eusikov and Y.V. Kokunov
Koord. Khim., 1979, 5, 637

102. E.A. Lawton and A. Levy
J. Amer. Chem. Soc., 1955, 77, 6083

103. see reference 89

104. R.J. Corriu, G. Dabosi and M. Martineau
Journal of Organometallic Chemistry, 1978, 154, 33-43

105. G. Englehardt and K. Licht
Z. Chem., 1970, 10, 266

106. E.J. Corey and P.B. Hopkins
Tetrahedron Letters, 1982, 23, 4871

107. P.J. Stang, M. Hanack and L.R. Subramanian
Synthesis, 1982, 85

108. P.J. Stang and M.R. White
Aldrichimica Acta, 1983, Vol. 16, No. 1, 15-22

109. E.J. Corey, H. Chi, C. Rucker and D.H. Hua
Tetrahedron Letters, 1981, Vol. 22, No. 36, 3455

110. G.A. Olah, A. Hussain, B.F.B. Gupta, G.F. Salem and S.C. Narang
J. Org. Chem., 1981, 46, 5212

111. R.W. Bott, C. Eaborn and K. Leyshon
J. Chem. Soc., 1964, p. 1974

112. A.R. Bassindale, C. Eaborn, D.R.M. Walton and D.J. Young
Journal Organometallic Chemistry, 1969, 20, 49

113. see reference 11, 146-152

114. D.R.M. Walton
Journal of Organometallic Chemistry, 1965, 3, 438

115. see reference 89, p.171-182 and 211-213

116. see reference 37, Volume 2, p. 54

117. see reference 37, Volume 3, p. 116

118. Chem. Abs., 1963, 59, 15303

119. Chem. Abs., 75, 88682F

120. 'Handbook of Chemistry and Physics', The Chemical Rubber Co., Ohio, 1975

121. M. Riediker and W. Graf
Helv. Chim. Acta, 1979, 62, 205

122. Advertisement of Fluka AG, Synthesis, December 1980

123. see reference 37, Volume 3, p. 446

124. W. Gee, R.A. Shaw and B.C. Smith
J. Chem. Soc., 1964, 2845

125. McCusker and Reilly
J. Amer. Chem. Soc., 1953, 75, 1583

126. see reference 37, Volume 3, p. 488

127. H.K. Chu, M.D. Johnson and C.L. Frye
Journal of Organometallic Chemistry, 1984, 271, 327-336

128. see reference 92, p. 116

129. see reference 92

130. see reference 89, p. 53-58